ELECTRONIC ENGINEERING

VOL. 38 No. 458

APRIL 1966

Commentary

AS we already know, the electronic industry in this country has, for a number of reasons, been going through a bad period and the position was made clear in a recent Economic Review issued by the National Institute of Economic and Social Research which showed that while the British electronic industry is the second largest in the world, closely followed by France, West Germany and Japan, it is, by comparison with the American electronic industry the leader, a very poor second indeed.

Various propositions have been put forward to help solve not only the present difficulties of the electronic industry but the economic problems of the country as a whole, and many—far too many—words have been uttered on this subject during the recent electioneering period.

However, by the time this issue appears in print, the election campaign will be over and the country will have decided which of the two main political parties is to form the next Government.

It is to be hoped therefore that the party leaders will have had time to take account of the 21st Annual Report issued by the Electronic Engineering Association and in particular the address by Mr. R. Telford, the retiring Chairman of the Association at its recent Annual Lunch, for it is here, in the Chairman's Foreword to the Report and in his Address that the present difficulties and possible solutions are admirably summarized.

Our electronic industry, declares Mr. Telford, "is a growth industry with a proven performance and with tremendous potential, not only for providing employment for those of high skill, whether manual or technical, not only for exporting equipment embodying little imported material, not only for producing significant equipment for Defence, Education, Medicine, Broadcasting and Television, but also providing the means of increasing productivity dramatically over the whole range of British industry and commerce. The industrial strength of this country was built on technology. The leadership in technology has resulted up to today in substantial exports of, in the field of electronics for example, broadcasting, communications and navigational equipment."

All of this is undoubtedly true.

"But what is the picture today?" asks Mr. Telford.

"It is a sombre one" he replies and continues that, "Somehow by decision or by default we have missed the technological challenge of the past decade" quoting as an example the world-wide communications by satellites, originally developed by the U.S.A. and now being actively exploited by them, and he quotes as a further example that a significant proportion of defence equipment is purchased from abroad in the radar, communication and navigational field and he feels that there must be a British "Buy American" act on the Statute Book.

What, then, are the reasons for what appears to be a depressing situation?

First it seems to be the vast American development in the technology of electronics to meet the Defence and Space requirements combined with the enormous home market for the secondary products derived from these new techniques.

Next it is due to the lack of appreciation here of the importance of advanced technology and the absence of clear-cut programmes and objectives to stimulate product developments and, in addition, policies where we have had them—presumably from the Government—have often been hesitant and decisions have frequently been changed.

Finally, the Industry itself is accused of being too inward looking, too conscious of its technology and not dynamic enough in attacking the markets at home and abroad.

If this, then, is the present position of the British electronic industry, although we believe it is by no means as black as it is painted, what steps have already been taken and what are the plans for the immediate future if the industry is to recover?

It is known, of course, that there has been considerable re-organization and a great deal of new thinking in the industry itself together with much closer co-operation with the various ministries.

But as regards to the future one can do no better than quote from the Address of the Association's Chairman whose remarks are directed mainly to the new Government.

He gives the headlines, as he says, "without embroidery" as follows:

(1) An urgent necessity for the announcement of policy and plans for broadcasting and television for the next decade. The promise to start colour television in the autumn of 1967 is a welcome augury.

(2) The immediate initiation of an independent British Space programme covering the next four years.

(3) The closest co-operation with the Government in joint international aviation projects such as the Anglo/French one.

(4) In other joint projects, particularly with the United States, truly joint co-operation and not master/servant relationships. If American aircraft are to be bought, the electronic equipment must be British.

(5) Policies must continue to be developed for the use of Public Purchasing power to stimulate our advanced techniques.

Correction of the Phase Error of a PAL Colour Television Transmission

By W. Bruch*

This article describes a new method for correcting faults in a PAL colour television signal. A correcting colour phasor is added into the composite colour picture, blanking and sync signal which compensates the unwanted phase modulation. This compensating voltage is derived from the difference between two colour signals, one of them obtained through the direct channel and the other through a 'colour carrier modifier' combined with a delaying device. Additional amplitude correction removes the resulting cosine error. The form of compensation chosen does not affect the luminance signal.

(Voir page 272 pour le résumé en français: Zusammenfassung in deutscher Sprache auf Seite 279)

HUE errors caused in an NTSC colour television receiver by various phase distortions on the transmission path are compensated for by the PAL system, a variant of the NTSC system. The tolerable amount of these distortions as well as the completeness of the compensation depend on the decoding method employed. In the Simple-PAL receiver without a delay line excessive phase errors cannot be tolerated, whereas the so-called Standard-PAL decoder with delay line and together with a crystal-controlled subcarrier regenerator does compensate for serious distortions[1]. Through new methods of synchronizing the reference carrier, which are only possible in a PAL delay line receiver, the reference carrier phase can be locked to the fluctuating signal. Receivers employing a circuit of this kind display a picture of correct hues even in the presence of extreme transmission phase errors. In these receivers, the phase of the picture modulation becomes so uncritical in respect of the burst phase that electronic fade-over and cutting techniques in a studio are facilitated[2]. The advantages of this demodulation principle, referred to as New-PAL, should be made use of by all colour television receivers, even by those using Simple-PAL demodulation. It is desirable, therefore, to install the error compensating circuit at the studio output, or even better at the transmitter input. The receivers will then be supplied with a signal which contains distortions only if they have occurred on the radio path or because of misaligned circuits in the receiver itself. Such errors are often sufficiently removed through Simple-PAL demodulation, but will always be overcome by the Standard-PAL principle.

In a recent publication on transcoders[3] two of these compensators, called PAL/PAL transcoders, have been described. Both have been realized and were shown on various occasions. Thence it has been established that receivers using Simple-PAL demodulation can profit by all the advantages of PAL even when tape recording and fade-over techniques are concerned. Both methods of

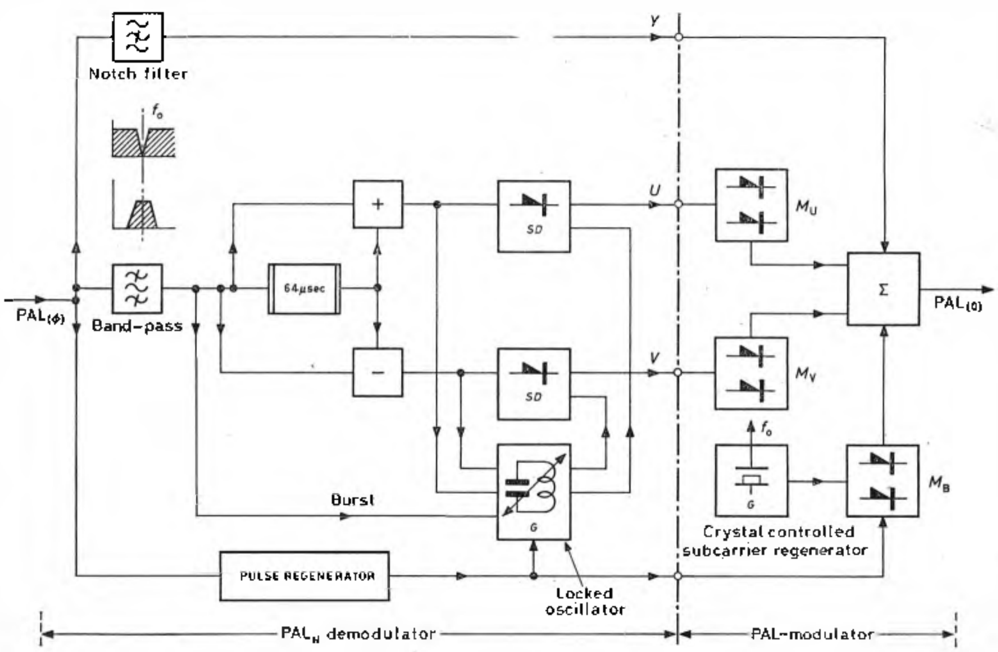

Fig. 1. PAL error corrector, which demodulates the incoming phase-displaced PAL signal with respect to U and V axes, employing New-PAL demodulation and featuring lock-in control of the reference carrier regenerator by the colour signal. Re-modulation of U and V signals supplies a faultless PAL signal

compensation are based on removing the distorted colour information from the composite video signal and substituting for it an undistorted modulation. In doing so a particular procedure proved to be favourable where the colour information is separated from the composite signal and demodulated by means of the so-called New-PAL demodulator which features a subcarrier regenerator locked to the colour signal itself. The demodulation retrieves the two colour difference signals, e.g. $(R\text{-}Y)$ and $(B\text{-}Y)$, which are afterwards re-modulated in a PAL modulator. A so-called notch filter will then suffice to suppress the colour signal in the luminance channel. This filter will not remove more information from the Y-channel than similar filters do in the colour receiver where they are used to suppress subcarrier interferences on the picture screen. Fig. 1 shows the block diagram of the error corrector just outlined which can also be used as a transcoder PAL/NTSC, provided the modulator is

* *Telefunken AG, Germany.*

connected for NTSC modulation. Two individual sub-carrier regenerators are employed. The first is used for demodulation purposes and is phase controlled by the phase error of the PAL signal[1], whereas the second unit is of common design with crystal control and integrating a.p.c. loop and supplies the constant-phase carrier to be re-modulated by the correctly retrieved signals* (R-Y) and (B-Y). The error compensation in this case is brought about by averaging the contrarily distorted signals of two consecutive lines by means of an ultrasonic delay line.

This article describes a new approach to a PAL error corrector which features the averaging of two lines to derive a correcting signal. The phase of the chrominance signal proper within the composite video signal is then shifted to the correct value by means of the correcting signal, but separation of chrominance and luminance is not necessary. To correct linear transmission errors within the subcarrier frequency range an automatic chroma control has been designed in addition. By means of this device a certain amount of the chrominance signal is phase-correctly added to the composite video signal in such a way that the attenuated parts of the subcarrier spectrum are restored[4]. The unit performed so well that the same principle will now be applied to eliminate also phase errors from the PAL signal. The first problem to be dealt with is, therefore, how to derive a signal which, when added to the composite video signal, returns the phase of the chrominance signal to the corect value.

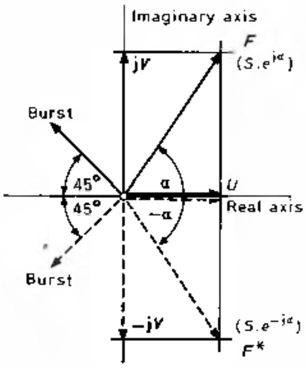

Fig. 2. Vector diagram of PAL modulation

Obtaining a Phase Correcting Signal

The PAL signal of every other line is NTSC-modulated and may be written as[5]

$$F = \mathrm{Re}\,[S\,.\,\exp\,(\mathrm{j}\alpha)\,.\,\exp\,(\mathrm{j}\omega_0 t)\,] \quad \ldots\ldots\ldots \quad (1)$$

This notation of both the phase and amplitude modulated signal is facilitated by applying the complex modulation phasor $\mathbf{F}$

$$\mathbf{F} = S\,.\,\mathrm{e}^{\mathrm{j}\alpha} \quad \ldots\ldots\ldots\ldots\ldots\ldots \quad (2)$$

In this equation S approximately equals the gamma-corrected saturation and indicates the amplitude modulation. The angle α denotes the hue and describes the phase modulation. Thus expressed in terms of two arbitrary colour difference signals U and V, equation (2) may also be written as†

$$\mathbf{F} = U + \mathrm{j}V \quad \ldots\ldots\ldots\ldots\ldots\ldots \quad (3)$$

with $S = \mathbf{F} = \sqrt{(U^2 + V^2)}$

$\alpha = \arctan V/U$

Each line following an NTSC-modulated one features a commutation of $+\mathrm{j}V$ to $-\mathrm{j}V$. Thus the resulting chrominance signal is then modulated by the conjugate complex signal $\mathbf{F}^*$. Hence equation (2) reads

$$\mathbf{F}^* = S\,.\,\mathrm{e}^{-\mathrm{j}\alpha} \quad \ldots\ldots\ldots\ldots\ldots\ldots \quad (4)$$

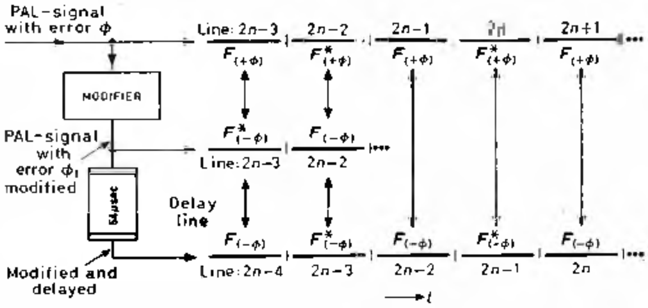

Fig. 3. Line-sequential order of PAL-modulation colour-carrier vectors in the presence of a phase error ϕ (upper sequence).

Changing the signal to the conjugate complex form with negative ϕ, by means of a modifier (middle sequence). Signal delay for the duration of one line (64µsec) yields lower sequence where in coincidence with the upper sequence the same signal appears but with error ϕ of opposite sign

To synchronize the line-sequential commutation switch at the receiver end the burst is transmitted with its phase angle alternating in consecutive lines (Alternating Burst, $\mathrm{PAL_{AB}}$), (Fig. 2).

The upper part of Fig. 3 shows the line-sequential order of PAL signals. As an example, let an unwanted phase error ϕ be introduced by a faulty transmission path or by speed fluctuations of a magnetic tape during playback (with ϕ depending on t or Y). Equation (1) will then be:

$$F_{(\phi)} = \mathrm{Re}\,[S\,.\,\exp\,(\mathrm{j}\alpha)\,.\,\exp\,(\mathrm{j}\phi)\,.\,\exp\,(\mathrm{j}\omega_0 t)] \quad \ldots\ldots \quad (5)$$

or $\mathbf{F}_{(\phi)} = \mathbf{F}\,.\,\mathrm{e}^{\mathrm{j}\phi}$

and correspondingly:

$$\mathbf{F}^*_{(\phi)} = \mathbf{F}^*\,\mathrm{e}^{\mathrm{j}\phi}$$

This phase displacement of the modulation phasor can be cancelled if another phasor of appropriate amplitude is added with 90° phase shift. To obtain this second phasor the chrominance signal has to be modified, first of all, in a so-called colour signal modifier[3], the principle of which is illustrated in Fig. 4.

In a balanced modulator the carrier $f_{(2\omega(0)t)}$ of twice the subcarrier frequency is modulated by the signal $\mathbf{F}\,.\,\exp\,(\mathrm{j}\omega_0 t)$. This procedure gives rise to an upper sideband of triple frequency and a lower sideband of the form $\mathbf{F}^*\exp\,(\mathrm{j}\omega_0 t)$, as will be shown mathematically. By filtering the upper sideband is suppressed, leaving only $\mathbf{F}^*\,.\,\exp\,(\mathrm{j}\omega_0 t)$. If, however, $\mathbf{F}^*\,.\,\exp\,(\mathrm{j}\omega_0 t)$ is fed into the modifier, $\mathbf{F}\,.\,\exp\,(\mathrm{j}\omega_0 t)$ will appear at the output provided the modulator is well balanced in respect of the modulating $\mathbf{F}^*\,.\,\exp\,(\mathrm{j}\omega_0 t)$.

If the chrominance signal contains a phase error, the situation will be as follows:

Let the reference carrier which is fed into the modifier for modification purposes have the null-phase ϕ_M and be of the form:

$$f_{(\phi)(M)} = \mathrm{Re}\,[\exp\,(\mathrm{j}\phi_M)\,.\,\exp\,(\mathrm{j}\omega_0 t)] \quad \ldots\ldots \quad (6)$$

and after frequency doubling:

$$f_{(2\phi(M);2\omega(0)t)} = \mathrm{Re}\,[\exp\,(\mathrm{j}2\phi_M)\,.\,\exp\,(\mathrm{j}2\omega_0 t)] \quad \ldots\ldots \quad (7)$$

The signal of equation (7) is now modulated by:

$$\mathrm{Re}\,[\mathbf{F}_{(\phi)}\,.\,\exp\,(\mathrm{j}\omega_0 t)] = F_{(\phi)}$$

Fig. 4. Basic modifier circuit using a frequency doubled reference carrier

(a) Arrangement of modifier

(b) Frequency-band allocation

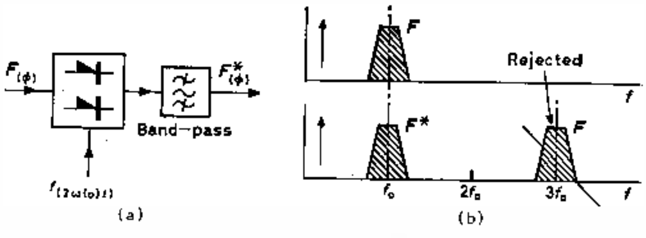

---

* *To exploit the equipment fully a crystal controlled sub-carrier regenerator of rather narrow noise bandwidth (and hence a slow-speed regulation) should be used since only then all phase fluctuations are totally eliminated.*

† *During the first PAL tests the quantities were $U = Q$ and $V = I$, with I and Q obeying the original NTSC equations. The performance of the PAL system is not affected, of course, when substituting U for Q and V for I in the calculations.*

The PAL standard now commonly used according to an agreement of the competent EBU study group defines the quantities U and V as $U = 0{\cdot}493(B\text{-}Y)$ and $V = 0{\cdot}877(R\text{-}Y)$.

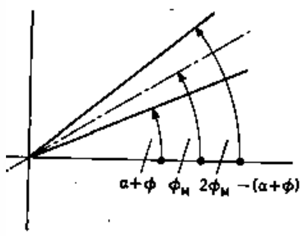

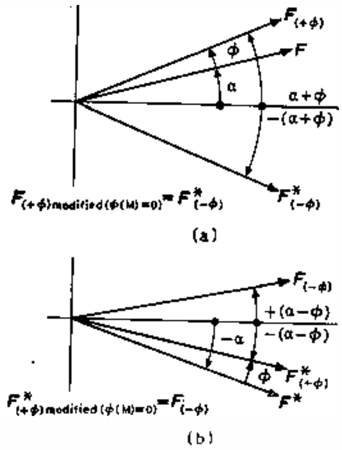

Fig. 5 (left). Common vector diagram of modification
Fig. 6 (right). Vector diagram of modification with the modifying carrier at zero-phase. Mirroring of $(\pm\alpha+\phi)$ against zero axis; e.g.
(a) $F_{(\phi)}$ turned into $F^*_{(-\phi)}$
(b) $F^*_{(\phi)}$ turned into $F_{(-\phi)}$

This procedure corresponds to a multiplication of two quantities:

$$F_{(\phi)} \cdot f_{(2\phi(M);2\omega(0)t)} = \{\mathrm{Re}[S \cdot \exp(j\alpha) \cdot \exp(j\phi) \cdot \exp(j\omega_0 t)]\} \cdot \{\mathrm{Re}\,[\exp\,(j2\phi_M) \cdot \exp\,(j2\omega_0 t)]\}$$
$$= \mathrm{Re}\,[S \cdot \exp(j\alpha) \cdot \exp(j\phi) \cdot \exp(j2\phi_M) \cdot \exp(j3\omega_0 t)] + \mathrm{Re}\,[S \cdot \exp(-j\alpha) \cdot \exp(-j\phi) \cdot \exp(j2\phi_M) \cdot \exp(j\omega_0 t)] \quad \ldots\ldots\ldots\ldots (8a)$$

The term containing $3\omega_0 t$ is suppressed by a band-pass filter to retain the $\omega_0 t$-term:

$$[\mathbf{F}_{(\phi)}]_{(\mathrm{modif.}2\phi(M))} = S \cdot \exp(-j\alpha) \cdot \exp(-j\phi) \cdot \exp(j2\phi_M) \quad \ldots\ldots\ldots\ldots (8b)$$

The original signal has thus been mirrored with respect to the ϕ_M-axis (Fig. 5). Let the reference carrier of $2\omega_0$-frequency be fed into the modifier via a phase shifter and let the null-phase ϕ_M be set to zero. The mirroring axis will then be the U-axis and hence (Fig. 6(a)):

$$[\mathbf{F}_{(\phi)}]_{(\mathrm{modif.}2\phi(M)=0)} = \mathbf{F}^*_{(-\phi)} \quad \ldots\ldots\ldots\ldots (9a)$$

and in reverse from the same modifier (Fig. 6(b)):

$$[\mathbf{F}^*_{(\phi)}]_{(\mathrm{modif.}2\phi(M)=0)} = \mathbf{F}_{(-\phi)} \quad \ldots\ldots\ldots\ldots (9b)$$

The modifier (Fig. 4) mirrors the incoming chrominance signal phasor with respect to the U-axis and simultaneously commutates the error ϕ as well, according to equation (9).

At the modifier output the signals **F** and **F*** are interchanged in chronological sequence. By means of an ultrasonic delay line the whole sequence can be delayed for the duration of one line (approximately 64μsec). The carrier signals of two lines, the direct and the modified plus delayed one, must precisely be phased, with correlation assumed. Fig. 3 (right-hand side) shows the two sequences in their time relationship. The signals now coinciding are:

$\mathbf{F}_{(+\phi)}$ and $\mathbf{F}_{(-\phi)}$ or

$\mathbf{F}^*_{(+\phi)}$ and $\mathbf{F}^*_{(-\phi)}$, respectively.

By subtraction, a suitable signal for the phase correction can be obtained (Fig. 7):

$$\tfrac{1}{2}\{\mathbf{F}_{(-\phi)} - \mathbf{F}_{(+\phi)}\} = \mathbf{F}\,\frac{e^{-j\phi} - e^{j\phi}}{2} = -j\mathbf{F}\sin\phi \quad \ldots\ldots (10a)$$

and

$$\tfrac{1}{2}\{\mathbf{F}^*_{(-\phi)} - \mathbf{F}^*_{(+\phi)}\} = \quad = -j\mathbf{F}^*\sin\phi \quad \ldots\ldots (10b)$$

Adding this correction signal to the composite video signal (Fig. 8), that is to the distorted signal $\mathbf{F}_{(+\phi)}$, yields:

$$\mathbf{F} \cdot e^{j\phi} - j\mathbf{F}\sin\phi = \mathbf{F}\cos\phi \quad \ldots\ldots\ldots\ldots (11a)$$

and

$$\mathbf{F}^* \cdot e^{j\phi} - j\mathbf{F}^*\sin\phi = \mathbf{F}^*\cos\phi \quad \ldots\ldots\ldots (11b)$$

during the subsequent line.

Thus the phase modulation of equation (5) is removed, but the original carrier amplitude S is now changed to $S \cdot \cos\phi$. As in the case with the phase error correcting demodulation in the Standard-PAL receiver which substitutes for the hue error a less visible saturation error $\Delta S = S(1 - \cos\phi)$, this error correcting principle generates a subcarrier amplitude modulation which gives rise to similar saturation errors in the receiver. Therefore, additional measures must be provided to restore the correct subcarrier amplitude in the presence of phase errors.

To begin with the phase compensation will be illustrated by a number of vectorscope displays. Fig. 9(a) shows the vectorscope picture of an undistorted PAL signal of horizontal colour bars, each bar represented by a luminous dot. If now an interfering phase modulation $\phi(t)$ is introduced to the chrominance signal, and hence to each bar, in such a way that ϕ increases linearly as a line frequency sawtooth function along each line and beginning at the left side of the colour picture, then the result is the vectorscope display of Fig. 9(b). The dots, marking the extreme points of the colour carrier phasors, has been changed to circular arcs. Application of the phase correction cancels the phase modulation and the circular arcs vanish. The radial lines which appear instead correspond to an amplitude modulation $S(1 - \cos\phi)$, (Fig. 9(c)). This vectorscope display, by the way, is also suitable to illustrate the performance of the Standard-PAL demodulator.

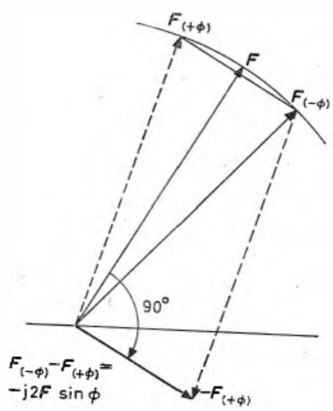

Fig. 7. Obtaining $(-j\mathbf{F} \cdot \sin\phi)$ by saturation

Fig. 8. Phase correction by adding $(-j\mathbf{F} \cdot \sin\phi)$ to the faulty $\mathbf{F}_{(\phi)}$-signal, and $(-j\mathbf{F}^* \cdot \sin\phi)$ to the faulty $\mathbf{F}^*_{(\phi)}$-signal

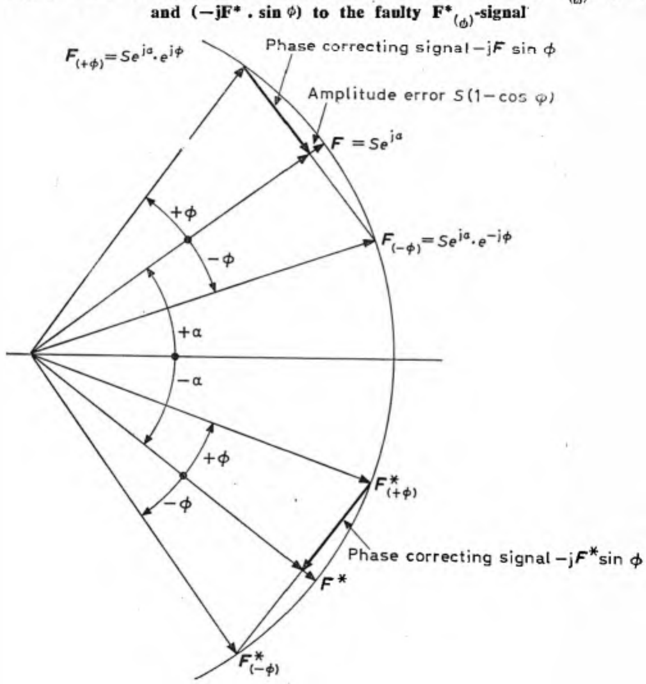

TABLE 1

$\phi_2(°)$	$\Delta S/S \cdot 100\%$	$\phi_{gr}(°)$	k
15	$\pm 0{\cdot}86$	18·2	0·132
30	$\pm 3{\cdot}56$	36·3	0·268
45	$\pm 8{\cdot}23$	54·5	0·414
60	$\pm 15{\cdot}5$	73·0	0·577

Compensation of Amplitude Errors Caused by Phase Correction

To eliminate the remaining amplitude errors another signal may be added, the modulation phasor of which during NTSC-modulated lines is given by:

$$\mathbf{F}_{corr} = \mathbf{F}\,(1 - \cos\phi) = 2\mathbf{F}\sin^2\phi/2 \quad \ldots\ldots\ldots \quad (12)$$

For just one polarity of the error ϕ, say, for ϕ positive, the signal can be approximated by $\mathbf{F} \,.\, k \,.\, \sin\phi$, provided ϕ does not exceed a certain upper limit ϕ_{gr}. The corrected signal is then represented by:

$$\mathbf{F}\,(\cos\phi + k \,.\, \sin\phi)\ (k > 0;\ \phi \geqslant 0) \quad \ldots\ldots\ldots \quad (13)$$

The nominal amplitude is obtained if:

$$\phi_1 = 0 \text{ and } \phi_2 = \arctan k \quad \ldots\ldots\ldots\ldots \quad (14)$$

Thus, a two-point alignment may be achieved for $k > 0$ and $\phi \geqslant 0$. The signal $\mathbf{F} \,.\, k \,.\, \sin\phi$ can be derived from the signal $(-j\mathbf{F} \,.\, \sin\phi)$ which serves for phase correction (equation (10a)) by shifting the phase by 90° and multiplying by k. Fig. 10 shows this approximation for $\phi = 45°$, and Table 1 gives the residual $\Delta S/S$ and ϕ_{gr} for different ϕ_2. As can be seen from the table, an excellent correction is obtainable within the error range $\phi = 0°$ to 35° normally occurring. At $\phi_2 = 30°$, the amplitude error within the range $\phi = 0$ to $\phi_{gr} = 36{\cdot}3°$ does not exceed $\pm 3{\cdot}56$ per cent.

Unfortunately, this compensation method originally found by mathematical considerations works only with

Fig. 9. Vectorscope displays of

(a) undistorted signal
(b) signal containing unwanted phase modulation $\phi_{max} = 36°$
(c) signal same as (b) but with phase error correction applied (remaining amplitude error: $S(1 - \cos\phi)$)
(d) signal with both phase and amplitude correction applied

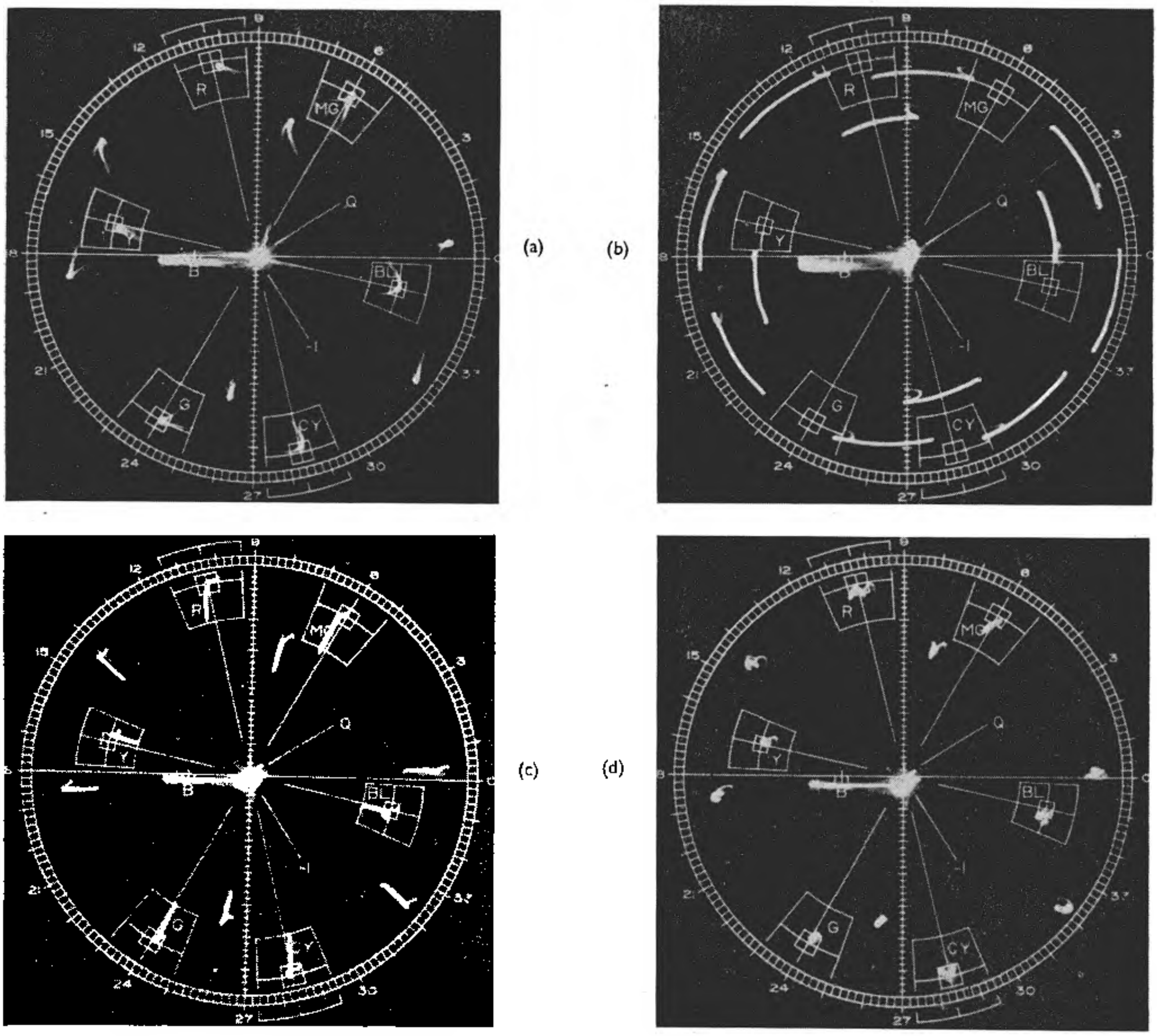

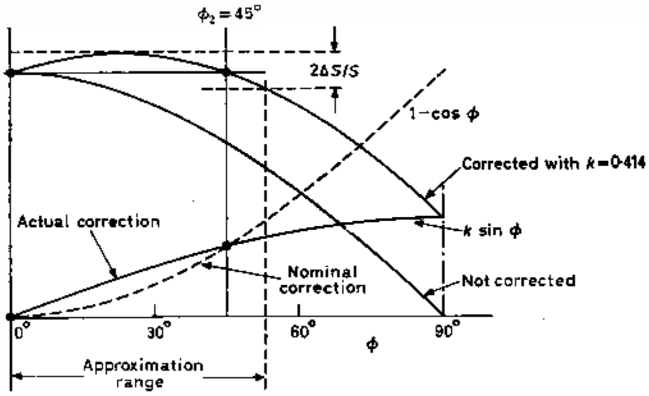

Fig. 10. Approximation of $(1 - \cos\phi)$ by $k \cdot \sin\phi$

positive error angles. This is so because the compensating signal changes its polarity if the angle ϕ becomes negative. Thus, instead of adding the missing portion of the signal, a subtraction would occur which doubles the amplitude error.

Hence, in order to keep the amplitude up to its nominal value even with negative error angles, i.e. for the whole range $(-\phi_{gr}) \leqslant 0 \leqslant (\phi_{gr})$, the change of polarity of the amplitude correcting signal $\mathbf{F} \cdot k \cdot \sin\phi \exp(j\omega_0 t)$ which has been derived from the phase correcting signal $-j\mathbf{F} \cdot \sin\phi \cdot \exp(j\omega_0 t)$, must be cancelled by an additional change of polarity. That is to say, the signal $\mathbf{F} \cdot k \cdot \sin\phi \cdot \exp(j\omega_0 t)$ has to be processed to a signal $\mathbf{F} \cdot k \cdot |\sin\phi| \cdot \exp(j\omega_0 t)$ (see Fig. 11). The principle of a switch capable of inverting the signal is shown in Fig. 12. The switch-over should take place whenever the phasor $\mathbf{F} \cdot \sin\phi$ is displaced 180° from $\mathbf{F}$ of $\mathbf{F}\cos\phi$ (the same applies for $\mathbf{F}^* \cdot \sin\phi$ and $\mathbf{F}^*$). To control the switch-over a reference signal $\mathbf{F} \cdot \cos\phi \cdot \exp(j\omega_0 t)$ or $\mathbf{F}^* \cdot \cos\phi \cdot \exp(j\omega_0 t)$ respectively, is necessary. This reference signal is obtained by addition of the two lines of the right-hand side of Fig. 3:

$$\tfrac{1}{2}(\mathbf{F}_{(\phi)} + \mathbf{F}_{(-\phi)}) = \mathbf{F}\ \frac{e^{j\phi} + e^{-j\phi}}{2} = \mathbf{F}\cos\phi \quad \ldots\ldots \text{(15a)}$$

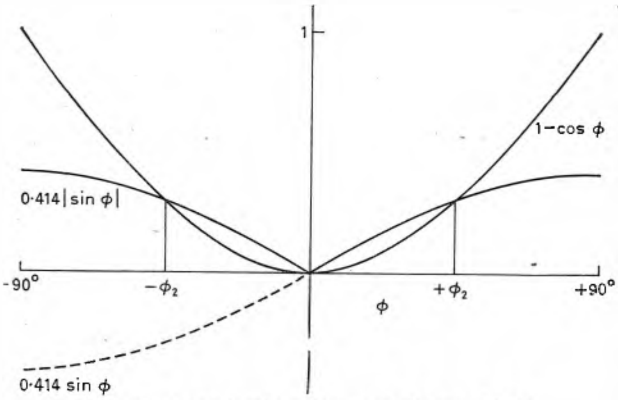

Fig. 11. Approximation of $(1 - \cos\phi)$ by $k \cdot |\sin\phi|$

Fig. 12. Basic circuit of a self-controlled inverting switch to obtain $\mathbf{F} \cdot \sin\phi \exp(j\omega_0 t)$

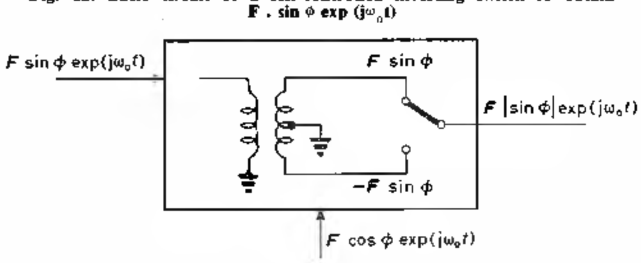

or

$$\tfrac{1}{2}(\mathbf{F}^*_{(\phi)} + \mathbf{F}^*_{(-\phi)}) = \mathbf{F}^*\ \frac{e^{j\phi} + e^{-j\phi}}{2} = \mathbf{F}^*\cos\phi \quad \ldots\ldots \text{(15b)}$$

There are several ways to realize the inverting switch. Quite a simple one has been suggested by G. Mahler. The principle of this solution is illustrated in Fig. 13. The circuit employs diodes controlled by the reference signal $\mathbf{F} \cdot \cos\phi \cdot \exp(j\omega_0 t)$ which was obtained through the addition of equation (15). To begin with, consider the full-line part of the circuit of Fig. 13.

At the secondary terminals of a bifilarly wound balanced transformer, the incoming correction signal is available with both polarities. With the aid of the superimposed reference signal the, say, positive half-cycles of the incoming correction signal are switched through to the resistor R_1 from either the positive or the negative terminal. The signal appearing across R_1, however, contains the

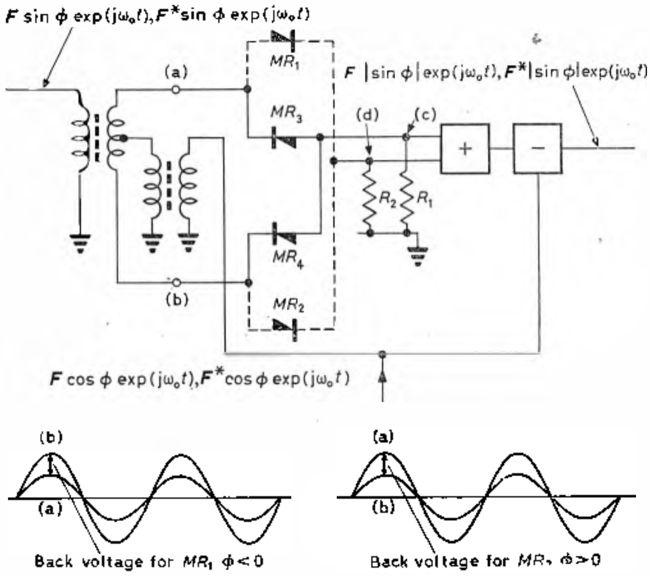

Fig. 13. Practical circuit arrangement of a self-controlled inverting switch

superimposed half-cycles of the reference signal. Whenever ϕ crosses the zero-axis, the polarity of the signal portion switched through to R_1 is changed. This is due to the sum $(\mathbf{F} \cdot \cos\phi + \mathbf{F} \cdot \sin\phi)$ appearing at the point (*a*) and the difference $(\mathbf{F} \cdot \cos\phi - \mathbf{F} \cdot \sin\phi)$ appearing at (*b*), so that in the case $\phi > 0$ the voltage at (*a*) will exceed that at (*b*). The reverse condition applies for $\phi < 0$. Of the two diodes, the one lying across the higher voltage will conduct and thus connect the corresponding transformer terminal to R_1. The part of the circuit considered so far only supplies the positive half-cycles of the correction signal. To provide for the negative half-cycles to be switched through as well, another pair of diodes connected in reverse is required (dotted lines in Fig. 13). The negative half-cycles of the wanted polarity then appear across resistor R_2. The simple addition of both signal parts yields the correction signal of proper phase, still containing, however, a portion of the reference carrier. In a subtracting stage the latter is cancelled, which procedure leaves

$$\mathbf{F} \cdot \sin\phi \quad \text{if } \phi > 0 \text{ and}$$
$$-\mathbf{F} \cdot \sin\phi \quad \text{if } \phi < 0$$

that is to say

$$\mathbf{F} \cdot |\sin\phi| \text{ if } \phi \lesseqgtr 0.$$

Fig. 14 gives further details of the inverting switch. Through the resistors R_1, R_2, and R_3, the positive and the negative half-cycles of the signal $(\mathbf{F} \cdot \cos\phi + \mathbf{F} \cdot \sin\phi)$

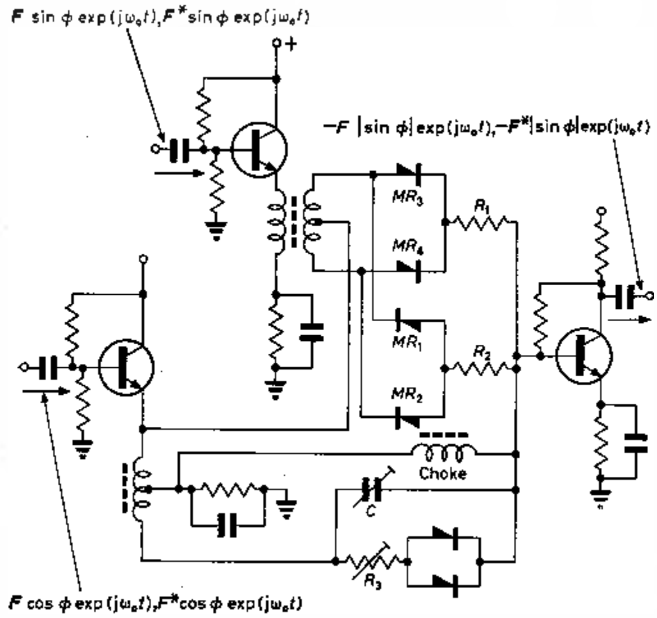

Fig. 14. Actual design of self-controlled inverting switch of Figs. 12 and 13

exp (j$\omega_0 t$) as well as the reference signal (for the cancellation) $-$F cos ϕ . exp (j$\omega_0 t$) are fed to the low input-resistance of a special adding circuit[7]. The variable resistor R_3 together with the trimmer capacitor C_1 serves for zero-adjustment of the reference signal.

To keep the zero-adjustment (to be carried out at $\phi = 0$) independent of the signal level, it is advantageous to connect in series to R_3 a non-linear resistor which simulates the non-linearity of the diodes. Two diodes of the same type as MR_1-MR_4, connected in reverse and in parallel, may well serve for the purpose.

During normal operation, the zero-adjustment will then not be found to be dependent on the signal level. Yet a certain degree of dependency on the signal level proves to be useful since low-level signals are slightly diminished in comparison to high level signals (Fig. 15). The result is a better approximation of the correcting signal to the necessary function (1 $-$ cos ϕ) than would be k . |sin ϕ|.

Alignment of the Error Corrector

The procedures to align the equipment are quite simple. To begin with, the phase correction circuit will be adjusted. If the modifier is working satisfactorily, that is to say, if its modulator is so well balanced that the non-modified carrier signal does not appear at the output, the adjustment can successfully be carried out. By trimming the

Fig. 15. Output against input measurements of inverting switch of Fig. 14, with different signal-input levels applied

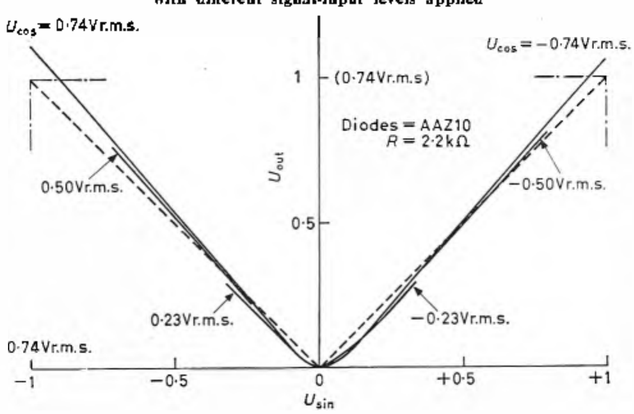

phase of the frequency-doubled reference carrier, which is supplied by the crystal controlled subcarrier regenerator, the delayed and modified colour signal and the direct signal are correctly phased. Simultaneously adjusting the amplitude, the subtraction output is zeroed, with an undistorted signal at the input. The delay occurring in the correction channel which is mostly due to the band-pass filter is matched by a delay line τ_{BP} (see Fig. 16) in the direct video path. A vernier adjustment of the delay, similar to the one used in PAL$_{DL}$ decoders, allows an exact setting of the necessary 90° phase shift between the two carrier signals (see Fig. 7).

To adjust the amplitude of the correcting signal to its nominal value the encoder is switched to NTSC operation and modulated by a signal V only, U being switched off. If amplitude and phase are correctly adjusted the carrier signal at the common output must be zero. This alignment procedure uses the correcting signal itself to cancel the incoming signal, a most precise criterion for a correct setting. With that the phase correcting circuit is properly adjusted.

The additional amplitude correcting circuit requires an adjustment similar to the procedures in the subtraction

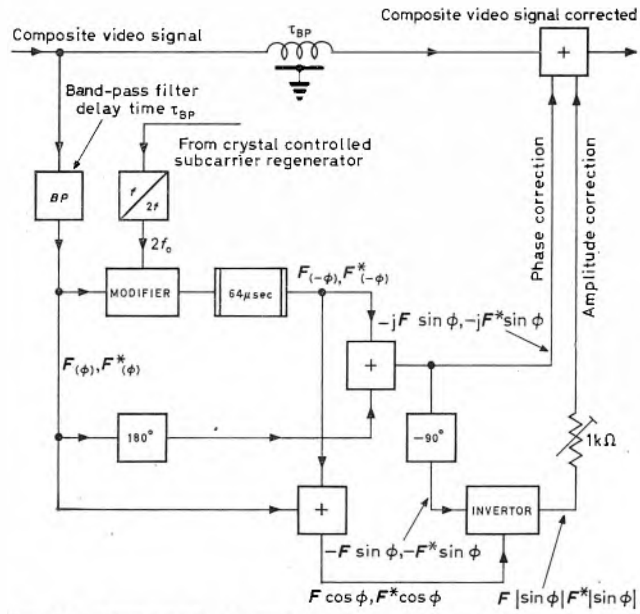

Fig. 16. Arrangement of error corrector containing both phase and amplitude correction

channel of the phase correcting circuit. After that the inverting switch is zero-adjusted. By means of a phase modulating device (as used for producing the diagram of Fig. 9(b)) a constant phase displacement of, say, $\phi = 30°$ is introduced to obtain the desired two-point adjustment. Properly setting the variable resistor k, any amplitude modulation visible on the vectorscope screen is eliminated (Fig. 9(d)).

REFERENCES

1. BRUCH, W. Neue Methoden der Referenzträgersynchronisierung im PAL-Farbfernsehempfänger. *Telefunken Ztg.* *37*, 100 (1964).
2. SCHÖNFELDER, H. Probleme der Phasensynchronisierung im Farbfernsehstudio. *Rundfunktechnische Mitt.* *9*, 33 (1965).
3. BRUCH, W. Transcoder PAL-NTSC—Die Umwandlung eines PAL-Signales in ein NTSC-Signal und die Umkehrung NTSC in PAL. *Telefunken Ztg.* *37*, 115 (1964).
4. BRUCH, W., KÜHLING, J. Automatische Entzerrung von linearen Uebertragungsfehlern der Farbträgeramplitude (Ausgleichsverstärker). *Telefunken Ztg.* *38*, 78 (1965).
5. BRUCH, W. Das PAL-Farbfernsehsystem—Prinzipielle Grundlagen der Modulation und Demodulation. *Nachrichtentech. Z.* *17*, 109 (1964).
6. LOUGHLIN, B. D. Processing of the NTSC Color Signal for One-Gun Sequential Color Display. *Proc. Inst. Radio Engrs.* *42*, 308 (1954).
7. BRUCH, W., KÜHN, K., SCHIRMER, R. Ein transistorisierter Farbfernseh-Coder, umschaltbar für das NTSC- und PAL-Farbfernsehsystem. *Telefunken Ztg.* *38*, 47 (1965).

The Achievement of High Overall Rejection in Difference Amplifiers

By S. Salmons*, B.Sc., M.Sc., A.R.C.S., D.I.C.

The performance of a balanced difference amplifier is impaired by deviations from symmetry, in particular those arising from discrepancies between the characteristics of a pair of valves. A first stage is described in which this difficulty is overcome without using special quality valves or selected components. Rejection factors in excess of 300 000 are obtained by means of a simple compensating adjustment. Furthermore, this adjustment can be used to offset the effects of lack of symmetry elsewhere in the amplifier, with a corresponding improvement in overall rejection properties.

(Voir page 272 pour le résumé en français: Zusammenfassung in deutscher Sprache auf Seite 279)

A MEASUREMENT problem frequently encountered is that of detecting small differences in potential in the presence of comparatively large interfering voltages. Often much of this interference is in-phase, that is, it changes the actual potential level at the points of measurement but not the potential difference between them. The most convenient way of eliminating such interference is therefore to connect the points to a difference amplifier, an instrument which, ideally, responds only to anti-phase signals, that is, differences in potential between its input terminals.

In practice, the output of such an amplifier will be influenced to some extent by the in-phase voltage at the input, the importance of this effect being assessed by the rejection factor for the instrument. The rejection factor, H, can be defined as the ratio between an in-phase voltage and an anti-phase voltage which, applied to the input, produce the same anti-phase voltage at the output. As well as contributing a spurious anti-phase component to the output voltage, an in-phase voltage at the input will give rise to an in-phase voltage at the output. This effect is assessed by means of a second parameter, the discrimination ratio, defined by:

$$F = \frac{\text{Gain to anti-phase signals.}}{\text{Gain to in-phase signals.}}$$

A discrimination ratio much greater than unity is desirable, since a stage which provides less amplification for in-phase signals than for anti-phase signals places less exacting requirements on the rejection of subsequent stages. Indeed, it can be shown that the design of a difference amplifier providing a high degree of rejection of in-phase interference essentially reduces to the design of a first amplifying stage having a high rejection factor and a high discrimination ratio. (Parnum[1]; Klein[2]; Klein and Zaalberg van Zelst[3]).

While fully transistorized difference amplifiers are now becoming commercially available, the bulk of the amplifiers in current use employ valves, at least in the first stage. In many cases rejection factors in excess of 10 000 cannot be maintained without frequent attention to balancing adjustments. The common use of matched pairs makes replacement tedious or expensive. Furthermore, even when the first stage is optimally adjusted, the rejection factor of the complete amplifier is often impaired by lack of symmetry in the input networks, interstage couplings, and gain control.

In this article a first difference amplifying stage is described for which rejection factors in excess of 300 000 have been achieved without the use of special quality valves or selection of components. The stage is provided with a simple compensating adjustment which, it is suggested, could be used to offset the effects of small departures from symmetry elsewhere in the amplifier, with a corresponding improvement in overall rejection.

* *University of Birmingham.*

Circuits Without Balancing Adjustments

Early approaches to the design of difference amplifiers resulted in the development of both single-sided circuits (Schmitt[4]; Tönnies[5]) and double-sided circuits (Matthews[6]; Offner[7]). The double-sided amplifier, in particular that based on the simple 'long-tailed pair' circuit (Fig. 1), has become the more widely used, chiefly because it provides rejection factors which are limited only by the effect of asymmetries in the circuit. In order to assess the rejection properties of the circuit of Fig. 1, an unfavourable case is considered in which the relative differences $\Delta\mu/\mu$, $\Delta g_m/g_m$, $\Delta R_L/R_L$, between the amplification factors, transconductances, and anode loads, respectively, of the two sides have the same sign and assume the maximum values consistent with the normal tolerances of valves and resistors. Under these conditions the rejection factor is a minimum, and its value is given to a close approximation by:

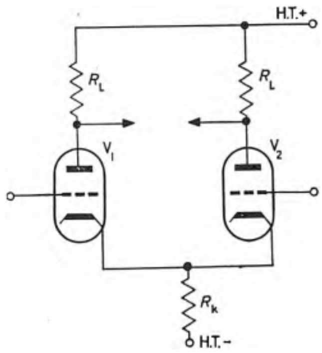

Fig. 1. Long-tailed pair circuit

$$H_{min} = \frac{2\left[2\dfrac{(\mu+1)}{\mu} + \dfrac{R_L + r_a}{\mu R_k}\right]}{1/\mu\,(\Delta\mu/\mu)_{max}\,[2+(R_L/R_k)] + 1/g_m R_k\,[(\Delta g_m/g_m)_{max} + (\Delta R_L/R_L)_{max}]}$$

With the approximations, valid in nearly every case, that $\mu \gg 1$, and $R_k \gg R_L + r_a$, and with the assumptions $(\Delta g_m/g_m)_{max} = (\Delta R_L/R_L)_{max} = \delta$, say, this expression simplifies to:

$$H_{min} = \frac{2}{1/\mu(\Delta\mu/\mu)_{max} + \delta/g_m R_k} \quad \ldots\ldots\ldots\ldots (1)$$

Thus, in designing for high rejection factors the values of μ and R_k should be made high in order to minimize the terms in the denominator of the above expression. Since

$$F = 1 + \frac{2(\mu+1)\,R_k}{R_L + r_a}$$

it can be seen that this procedure simultaneously secures high discrimination (Klein[2]; Klein and Zaalberg van Zelst[3,8]).

These conclusions may be interpreted as follows. To minimize the response of the circuit of Fig. 1 to in-phase voltage variations at the input it must be arranged for the voltage at the common cathode to follow closely that at the two grids. In part this can be achieved by using a high value of cathode resistance, R_k, to develop the requisite changes in common cathode voltage with a minimum of signal current flow. The residual discrepancy between the voltages at the cathode and grid of each valve is due to the effect of anode-to-cathode voltage on the anode current. For optimum performance this effect should be comparatively small, i.e., the ratio

$$-\left(\frac{\text{influence of cathode voltage on anode current}}{\text{influence of grid voltage on anode current}}\right)$$

should be close to unity. For a triode this ratio is equal to $(\mu + 1)/\mu$ and is therefore closer to unity the higher the value of μ.

If R_k is a resistor, its magnitude is limited by the inconveniently large negative voltage supply needed to maintain adequate anode current. Since it is a high incremental resistance that is required, a 'constant current' device such as that in Fig. 2 may be employed. The effective cathode line impedance is the anode impedance of the device; this may be made even higher by using a pentode, two-triode cascode, or three-triode cascode in place of the triode of Fig. 2. In this way the second term in the denominator of the expression for H_{min} can be made very small.

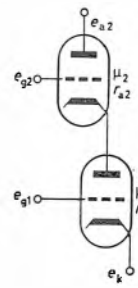

Fig. 2. (Left) Triode as common cathode line impedance

Fig. 3 (Right) Two-triode cascode

To reduce the first term, the triodes of the original circuit may be replaced by other amplifying devices such as pentodes or cascodes. For these devices a quantity μ_c analogous to μ can be defined by equating the ratio

$$-\left(\frac{\text{influence of cathode voltage on anode current}}{\text{influence of grid voltage on anode current}}\right)$$

to $(\mu_c+1)/\mu_c$. It should be noted that μ_c defined in this way is not necessarily the same as the effective amplification factor of the device defined from the point of view of voltage amplification. In particular the value of μ_c for a pentode or cascode depends on the extent to which potential variations at the common cathode are transferred to the screen or 'upper' control grid.

For example, if the two-triode cascode of Fig. 3 is used as a straightforward voltage amplifying device with the 'lower' cathode and 'upper' grid voltages stabilized, the effective amplification factor is given by:

$$\mu_{eff} = (\mu_2 + 1)\,\mu_1$$

However, if there is a signal e_k at the lower cathode, and a fraction k of this signal is transferred to the upper grid, so that $e_{g2} = ke_k$, then:

$$\mu_c = \frac{(\mu_2 + 1)\,\mu_1}{(1-k)\mu_2 + 1}$$

$$= \frac{\mu_{eff}}{(1-k)\,\mu_2 + 1}$$

Thus $\mu_c = \mu_{eff}$ only when $k = 1$ (perfect decoupling); for all other values of k, $\mu_c < \mu_{eff}$, and in particular for $k = 0$, $\mu_c = \mu_1$.

From the point of view of rejection, therefore, the straightforward substitution of pentodes or cascodes for triodes in a long-tailed pair circuit is justified only if it is arranged for the voltage at each screen or upper control grid to follow as closely as possible that at the common cathode. The decoupling arrangement used should be such that its introduction into the circuit does not seriously impair the high common cathode impedance.

The Proposed System of Compensation

The anode impedance of a cathode-loaded pentode or two-triode cascode is so high that when such a device is used in place of R_k the total cathode line impedance will probably be limited by other factors, such as cathode to heater conductance and alternating current paths introduced by the decoupling circuit. The second term in the denominator of the expression

$$H_{min} = \frac{2}{1/\mu_c\,(\Delta\mu_c/\mu_c)_{max} + (\delta/g_m R_k)} \quad \ldots\ldots\ldots \text{(1a)}$$

is then so small that it is not really practicable to reduce the first term to the same order of magnitude merely by increasing μ_c. Such an approach would require each of the

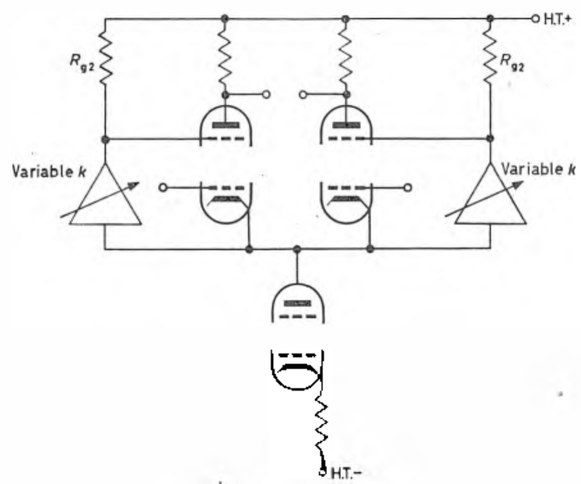

Fig. 4. Principle of proposed compensating system

triodes of the simple long-tailed pair circuit to be replaced by a cascode arrangement of more than three triodes with the associated decoupling arrangements and increased positive supply voltage. In practice, therefore, it is the first term which limits the value of H_{min} attainable. It is possible to reduce this term by using selected or special quality valves to restrict $(\Delta\mu_c/\mu_c)_{max}$ but ideally one would like to eliminate it altogether.

This can in fact be achieved by making use of the dependence of μ_c on the decoupling constant k. The principle of the compensating system is illustrated in Fig. 4. The two sides of the circuit are decoupled separately by means of variable gain amplifiers. The value of μ_c for each side can therefore be varied independently; in particular, any discrepancy between these values can be corrected. The decoupling amplifiers are designed to provide gains close to unity, the setting for which μ_c is highest; the dominant $1/\mu_c\,(\Delta\mu_c/\mu_c)_{max}$ term of equation (1a) can then be reduced to the required level by means of a compensating adjustment of only moderate precision.

It should be noted that the adjustment of k does not change the anti-phase gain of the complete amplifier, since the common cathode potential is virtually unaffected by anti-phase signals. The decoupling amplifiers are of high input impedance so that their presence does not appreciably reduce the total cathode line impedance. In a d.c. amplifier, the compensating adjustment may be associated with a change in static conditions; however, this change is easily corrected by means of an anode-balancing potentiometer.

This system makes it possible to achieve rejection factors even greater than it may at first appear. Since the balancing adjustment permits μ_c to be varied in sign as well as in magnitude, the first term in the denominator of equation (1a) can be made to annul the second term, resulting in a rejection factor which is limited only by the precision of the adjustment. (It is assumed that the effects of balanced modulation may be neglected. In practice this means that each valve must operate over a linear portion of its characteristic if large in-phase voltages are to be tolerated at the input. This requirement is less exacting the higher the discrimination ratio.)

The circuit of Fig. 5 (Salmons[9]) illustrates how the proposed system of compensation could be incorporated into a d.c. first amplifying stage. High values of μ_c and $R_{k(eff)}$ are achieved by the use of two-triode cascodes. Each side is decoupled by a cathode-follower arrangement whose gain can be varied by means of a variable resistance in the anode or the cathode line. As a refinement, variable resistors can be used in both anode and cathode lines, as shown, to provide coarse and fine control, respectively. For convenience, the control of μ_c is arranged to be differential, i.e., such that a decrease in the μ_c of one half of the circuit is associated with a simultaneous increase in the μ_c of the other half. This is achieved by combining the variable resistances in the manner indicated. The compensating adjustment does affect static conditions in the circuit, and normal operating conditions must be restored using the anode-balancing potentiometer provided.

For a.c. applications, the voltage stabilizers of Fig. 5 may be replaced by suitably chosen capacitors. Static conditions in the circuit are then independent of the compensating adjustment.

To set up the amplifier the input terminals are joined and a suitable signal (for example a 4V peak-to-peak sine-wave) is applied. The μ_c-control and anode-balancing potentiometer are then adjusted together (first the coarse and then the fine controls) until the anti-phase signal appearing at the output terminals is a minimum.

This particular circuit was built solely for the purpose of proving the compensating system and measurements were therefore confined to determinations of anti-phase gain, rejection factor, and discrimination ratio at several levels of in-phase input voltage.

Results were as follows. The gain of the circuit to anti-phase signals was 150. For sinusoidal in-phase input signals of frequency 30c/s and magnitude 4V peak-to-peak the discrimination ratio was approximately 10 000 and the rejection factor was in excess of 300 000. Increasing the frequency of the 4V in-phase signal to 1 000c/s had no perceptible effect on rejection. Increasing the size of the in-phase signal to 10V reduced the rejection factor by 50 per cent as a result of balanced modulation. These in-phase voltages were used in order to facilitate measurement, and for smaller in-phase voltages the rejection factor should be considerably in excess of the above figure.

In a series of determinations, the valves of the difference amplifier were interchanged and also exchanged with randomly chosen valves of the same specification. In all cases, appropriate adjustment of the μ_c-control and anode-balancing potentiometer restored the high rejection properties of the original circuit.

Discussion

Returning to the expression for H_{min} (equation (1a)), it has been noted that the first term in the denominator can be varied not only in magnitude but also in sign. Provided that the term $\delta/g_m R_E$ is relatively small, such a variation will be accompanied by a corresponding variation in the magnitude and sign of H_{min}. (A change in the sign of H_{min} merely implies a change in the sense of the anti-phase output voltage). This suggests that the balancing adjustment in the first stage can be used to offset the effects of small departures from symmetry elsewhere.

Consider, for example, the effect of a small disparity

Fig. 5. Circuit of high rejection difference amplifier *(All resistors ± 10%)*

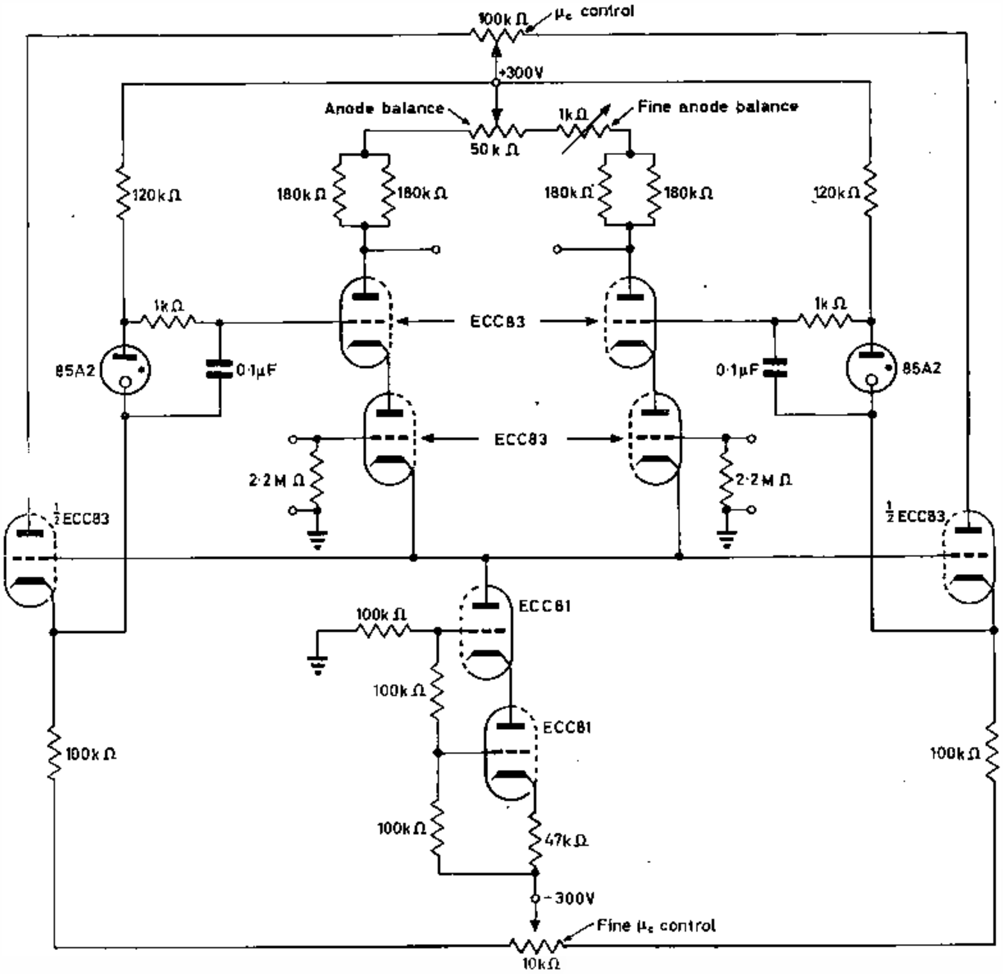

ΔR_s between the internal resistances of the voltage sources. This can be described in terms of a rejection factor H, given by:

$$H = 2R_i/\Delta R_s$$

where R_i represents the input resistance of the amplifier (Klein and Zaalberg van Zelst[10]). The following expression can then be derived for the overall rejection factor, H_{tot}, of the system:

$$1/H_{tot} = \Delta R_s/2R_i + (1/H_{min})$$

By suitable adjustment the second term in the above expression can be made to offset or even annul the first term, thus effecting a considerable improvement in the overall rejection factor. Contributions arising from lack of symmetry in gain controls and interstage couplings are similarly cancelled. (Clearly, however, contributions such as those from RC couplings can be fully compensated only at one frequency.)

It may be that the level of rejection available at optimum adjustment is unnecessarily high for many applications. The significant feature of the system is the ability to maintain adequate rejection without constant readjustment.

Acknowledgments

The author wishes to thank Dr. B.McA. Sayers of the Department of Electrical Engineering, Imperial College, London, for providing laboratory facilities and for his helpful observations on the manuscript. Thanks are also due to Dr. I. C. Whitfield of the Neurocommunications Research Unit, University of Birmingham, for valuable discussion. The work was supported by a grant from the Department of Scientific and Industrial Research, and the manuscript was prepared during the tenure of a Fellowship from the Department of Health, Education, and Welfare, U.S. Public Health Service (HD-00450).

REFERENCES

1. Parnum, D. H. Transmission Factor of Differential Amplifiers. *Wireless Engnr. 27*, 125 (1950).
2. Klein, G. Rejection Factor of Difference Amplifiers. *Philips Res. Rep. 10*, 241 (1955).
3. Klein, G., Zaalberg Van Zelst, J. J. General Considerations on Difference Amplifiers. *Philips Tech. Rev. 22*, 345 (1961).
4. Schmitt, O. H. A Simple Differential Amplifier. *Rev. Sci. Inst. 8*, 126 (1937).
5. Tönnies, J. F. Differential Amplifier. *Rev. Sci. Inst. 9*, 95 (1938).
6. Matthews, B. H. C. A Special Purpose Amplifier. *J. Physiol, 81*, 28P (1934).
7. Offner, F. Push-Pull Resistance-Coupled Amplifiers. *Rev. Sci. Inst. 8*, 20 (1937).
8. Klein, G., Zaalberg Van Zelst, J. J. Circuits for Difference Amplifiers—I. *Philips Tech. Rev. 23*, 142 (1962).
9. Salmons, S. Difference Amplifiers—with an Introduction to Electrophysiological Applications. D.I.C. thesis, Imperial College, London. (1964).
10. Klein, G., Zaalberg Van Zelst, J. J. Circuits for Difference Amplifiers—II. *Philips Tech. Rev. 23*, 173 (1962).

New Colour Television Equipment

A 3-Plumbicon Colour Television Camera System has been developed by Philips Research Laboratories and is now available from Peto-Scott Ltd of Weybridge, Surrey.

The Plumbicon is distinguished by a high signal-to-noise ratio and great stability, while at the same time being free from dark current and lag phenomena. The light sensitive features of the camera enable it to operate at much lower light levels than had previously been possible in colour television.

The colour-splitting device between lens and the three Plumbicons consists of a very compact three element light analysis system. As the three elements are cemented together the dichroic layers are perfectly sealed off against dust and atmospheric influences. The relay optics and other auxiliary lens, used in previous systems, are now avoided, resulting in a considerable improvement in picture contrast and sharpness.

Except for the pre-amplifier input stages, all circuits in the camera chain are fully transistorized, resulting in high reliability, low power consumption and compact design. The input stage of each camera pre-amplifier consists of a cascode circuit with two Nuvistors providing a good signal-to-noise ratio. Almost all the circuits use printed wiring on plug-in circuit boards. This has allowed the system to be broken down into a number of small easily removable units.

Also developed by the Philips Research Laboratories is the new colour 'Eidophor' projector which permits the projection of colour television programmes on to screens as large as 40ft by 30ft.

Like the earlier monochrome Eidophor, it uses the 'control layer' system of television projection and can receive its signal from various sources—a live television programme, colour video tape, film or slides.

The key to the 'control layer' system is the thin film of oil which is constantly revolving on a concave mirror. Both the light from the high powered Xenon lamp and the input electronic impulses converge on the mirror.

The light from the Xenon lamp reaches the mirror by way of a series of reflecting bars. If the system has no 'input' of electronic signals the light will retrace its path from the mirror to the Xenon lamp and the screen will remain black. When a signal source is connected with the Eidophor the input arrives through an electron gun, which 'shoots' the electronic television picture on to the control layer of the mirror.

This signal creates an etching in the otherwise smooth surface of the oil on the mirror. Light from the light source then passes through the etched areas on the control layer and are deflected from their normal course. The light now goes back from the mirror through the etched control layer, through the reflecting bars system, through an optical system and on to the screen.

As with most modern forms of colour television three separate optical systems are required—one for each of the primary colours, red, green and blue. The built-in control system synchronizes the output from the three optical systems to form one colour picture on the screen.

It is also possible to apply the three colour signals to the amplifier in such a way that a black-and-white picture is obtained, or a picture in only one of the primary colours.

The three-plumbicon colour television camera

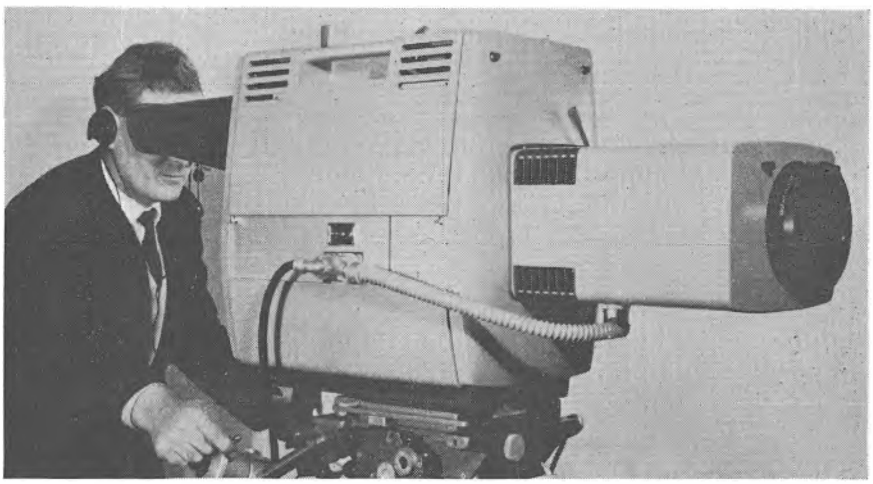

The Design of Input Circuits for Low Noise Transistor I.F. Amplifiers

By R. H. Frater*, B.Sc., B.E.

A design procedure is given for an input network for a transistor amplifier which simultaneously satisfies the requirements of maximum bandwidth, optimum source impedance for low noise, and phase and amplitude responses which track closely for a number of amplifiers. The procedure copes with wide variations in the transistor input impedance. Results are given for a circuit to couple a 408Mc/s mixer to the input of an 11Mc/s transistor amplifier. The method includes a design procedure for double tuned circuits of any bandwidth, where the poles of the transfer function have equal real parts.

(Voir page 273 pour le résumé en français: Zusammenfassung in deutscher Sprache auf Seite 280)

THE variation in parameters from one transistor to another is a constant problem to the circuit designer. As an example of input impedance variations, Fig. 1 shows the results of measurements of the input resistance and capacitance of a group of transistors of the one type (AFZ12). In many situations, where response reproducibility is required, impedance variations can be dealt with by 'swamping' with a suitable parallel resistance and capacitance. In the design of input circuits, however, where noise figure is usually of great importance, the loss introduced by parallel resistance cannot be tolerated, and an alternative design procedure which allows for the variations must be adopted.

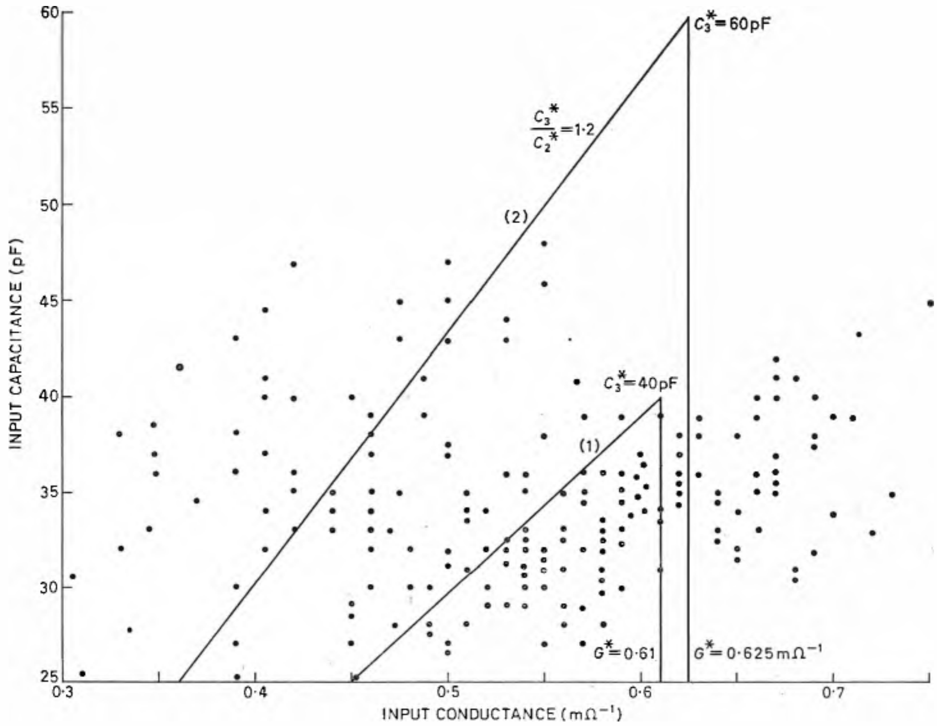

Fig. 1. The input conductances and capacitances for a group of AFZ12 transistors
The triangles enclose transistors that could be used in two possible circuit designs

In Fig. 2 the input of the transistor is represented by an impedance $Z_i(s)$. This is driven from a coupling network, represented by a complex Thevenin source impedance $Z_t(s)$ and a generator $e_t(s)$. For this circuit the voltage $e_o(s)$ developed across $Z_i(s)$ is given by:

$$e_o(s) = \frac{Z_i(s)}{Z_i(s) + Z_t(s)}\, e_t(s)$$
$$= \frac{1}{[Z_t(s)/Z_i(s)] + 1}\, e_t(s) \quad \text{.......... (1)}$$

In order to preserve the response for the different $Z_i(s)$ of a number of transistors, it is necessary that either $Z_t(s)/Z_i(s)$ be maintained constant or that $Z_t(j\omega)/Z_i(j\omega)$ be always real. If it is real, then $e_o(s)$ may vary in amplitude for different values of $Z_i(s)$ although the response shape determined by the denominator will be retained. If $Z_t(s)$ in Fig. 2 is followed by a transformer whose turns ratio is adjusted, together with other parameters, to maintain $Z_t(s)/Z_i(s)$ constant, then the gain will vary due to the change in effective input voltage.

In the circuit proposed, variations in the real part of the input impedance of the transistor are catered for by a change in the effective transformation ratio of the coupling circuit while, to allow for capacitive variations, capacitance is added to the input of the transistor. To perform these two functions, and therefore set the ratio $Z_t(s)/Z_i(s)$, it is necessary to adjust the capacitors C_1, C_2 and C_3 in the circuit of Fig. 3. It will be shown that, within certain restrictions, these values can be varied to allow a large proportion of a group of transistors to be used. The source resistance seen by the transistor is now proportional to its own input resistance, so that the normalized gain variations due to input resistance changes (with changing temperature, for example) may be expected to be similar with transistors of different input resistance.

For a transistor input stage there is an optimum source impedance for minimum noise. Measurements indicate that this optimum, for a particular transistor type, is directly proportional to its input resistance. The circuit described complies with this requirement.

* *University of Sydney.*

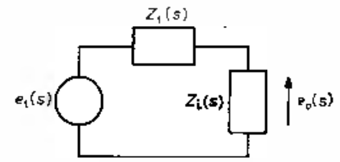

Fig. 2. A transistor, represented by the transform impedance $Z_i(s)$ is driven from a source impedance $Z_t(s)$

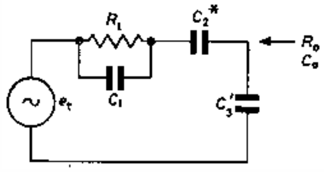

Fig. 5. The source resistance and capacitance seen by a transistor with $G = G^*$ are R_o and C_o. *C_o includes the input capacitance of the transistor*

In the second part of the article, a procedure for the design of double tuned circuits is developed, with the restriction that the poles of the transfer function have equal real parts. This is applied to the design of a double tuned circuit to couple a mixer to a transistor giving maximum input circuit bandwidth. The procedure is more generally applicable to the design of double-tuned interstage coupling networks.

As a design example a circuit to couple a 408Mc/s mixer to an 11Mc/s transistor input stage is described.

The Transistor Matching Circuit

In this section the relationships between the various components in the network of Fig. 3 are investigated with the restriction that the denominator of the transfer function of the circuit be constant. This implies that the amplitude response will remain the same, even though the gain may vary.

The transfer function of the network of Fig. 3 is given by:

$$\frac{e_0(s)}{e_t(s)} = \frac{RC_2S}{[Z_t(s)\,R(C_1C_2+C_2C_3+C_3C_1)]S^2 + [Z_t(s)\,(C_1+C_2) + R(C_2+C_3)]\,S+1} \quad \dots\dots\dots\dots (2)$$

It is possible to choose the value of each capacitance for different values of R so as to preserve the denominator.

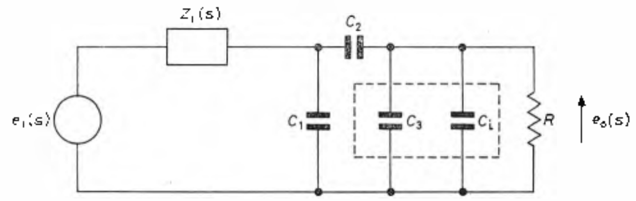

Fig. 3. A capacitive π circuit is used to couple the source to the transistor, now represented by its input resistance and capacitance R and C

Fig. 4. Normalized plots of C_1, C_2 and C_3 against G. *C_1 and C_2 are normalized to C_2^*, C_3 is normalized to C_3^**

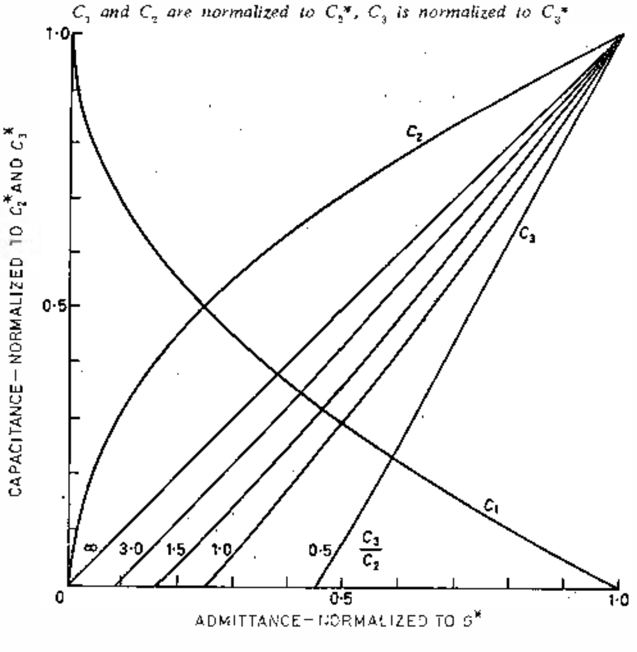

The gain of the circuit, which depends on the product RC_2, will vary. The following relationships may be derived from the requirement that the coefficients of S^2 and S remain constant (see Appendix A):

$$C_1 + C_2 = K_1 \quad \dots\dots\dots\dots (3)$$

$$R(C_2 + C_3) = K_2 \quad \dots\dots\dots\dots (4)$$

$$RC_2^2 = K_3 \quad \dots\dots\dots\dots (5)$$

where K_1, K_2 and K_3 are constants. In practice, R will be the input resistance of the transistor and C_3 will be partly made up by the input capacitance of the transistor and partly by additional capacitance. It may be seen from equations (3) to (5) that as the value of R is reduced, C_2 increases until $C_1 = 0$, This condition gives R^*, the minimum value of R for the circuit. In Fig. 4 normalized curves of the various capacitances are plotted against normalized conductance. The conductance is normalized to $G^*(1/R^*)$, the maximum conductance to be used. C_1 and C_2 are normalized to C_2^*. Curves of C_3 for various values of the ratio C_3/C_2 are plotted, normalized in each case to C_3^*. C_2^* and C_3^* are the values of C_2 and C_3 when $G = G^*$ and $C_1 = 0$. If G^* and C_3^* are selected as the input conductance and capacitance of one of the transistors in Fig. 1, then a series of curves for different values of the ratio C_3/C_2 may be drawn. In Fig. 1 curve (1) is drawn for $C_3/C_2 = 1$. For a different value of C_3/C_2, transistors whose input conductance is less than G^* and whose input capacitance falls below the curve may be brought on to the curve with added capacitance. These transistors will then give the same transfer function in the circuit described. The value of C_3/C_2 chosen determines, in conjunction with the coupling network used, the source impedance seen by the transistor. In practice, it is convenient to choose a value of C_3 at G^* greater than the input capacitance of any of the transistors, in order to include more transistors below the curve. Curve 2 in Fig. 1 is an example of this, with $G^* = 0{\cdot}625\text{m}\Omega^{-1}$ and $C_3^* = 60\text{pF}$. The values of C_1 and C_2 are then obtained from Fig. 4. The use of these curves is discussed in more detail in the design example.

Output Impedance

When the circuit is driven from a source impedance Z_t with an equivalent parallel resistance and capacitance R_t and C_t (see Fig. 5), the resulting equivalent parallel resistance and capacitance R_o and C_o are given by:

$$R_o = R_t\left(\frac{C_t + C_2}{C_2}\right)^2 + \frac{1}{\omega^2R_tC_2^2} \quad \dots\dots\dots\dots (6)$$

$$C_o = C_3 + C_2\,\frac{[1 + \omega^2R_t^2C_t\,(C_t + C_2)]}{\omega^2R_t^2\,(C_t + C_2)^2 + 1} \quad \dots\dots\dots (7)$$

C_3 and C_o both include the transistor input capacitance. Note that C_t may be negative.

The Double-Tuned Input Circuit

In the design procedure to follow, a set of inductance parameters are derived for a transformer to couple from a known source impedance (a parallel resistance and capacitance, a typical output circuit for a crystal mixer) to a transistor. The source impedance is specified by the parameters R_s C_s and $\tau_s = R_sC_s$, while the transistor impedance is specified by R_e C_e and $\tau_e = R_eC_e$. R_e and C_e are the equivalent parallel resistance and capacitance of the π coupling circuit for the case when $R = R^*$, $C_1 = 0$, $C_2 = C_2^*$ and $C_3 = C_3^*$. The circuit is given in Fig. 6.

The inductance parameters used are the measured primary and secondary 'short-circuit' and 'open-circuit' inductances. Thus:

$$L_{p1} = L_a + L_b \quad \ldots\ldots\ldots\ldots\ldots\ldots \quad (8)$$

$$L_{s1} = L_b + L_c \quad \ldots\ldots\ldots\ldots\ldots\ldots \quad (9)$$

$$L_{p2} = \frac{\Sigma L_aL_b}{L_b + L_c} \quad \ldots\ldots\ldots\ldots\ldots \quad (10)$$

$$L_{s2} = \frac{\Sigma L_aL_b}{L_a + L_b} \quad \ldots\ldots\ldots\ldots\ldots \quad (11)$$

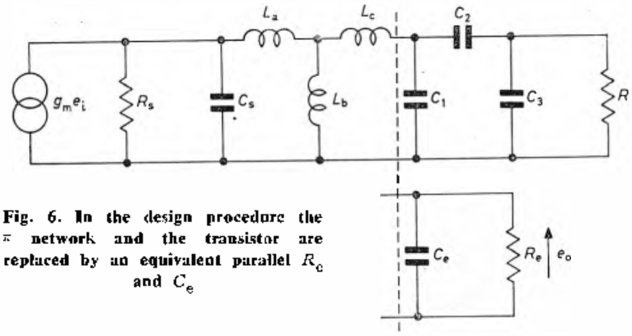

Fig. 6. In the design procedure the π network and the transistor are replaced by an equivalent parallel R_e and C_e

The subscripts p and s refer to primary and secondary while 1 and 2 refer to measurements with the output open-circuited or short-circuited respectively. L_a, L_b and L_c are as shown in Fig. 6.

It is assumed in the procedure that even for large fractional bandwidths a symmetrical amplitude response will result if the poles have equal real parts. The resulting error is calculated in Appendix D.

In the design procedure the centre frequency $j\omega_o$ and the angle α subtended by the poles (see Fig. 7) are selected. The radius a (normalized to the centre frequency ω_o) of the circuit on which the poles lie and a parameter γ relating τ_s and τ_e are calculated. The inductances L_{p1}, L_{s1} and L_{p2} are given in terms of a, α, γ and ω_o. Their derivation is indicated in Appendix B.

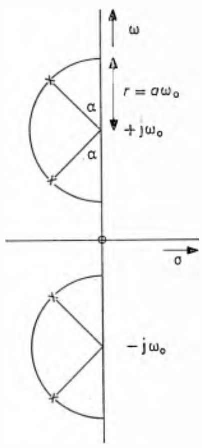

Fig. 7. The parameters used to specify the locations

Design Equations

For the circuit of Fig. 6:

$$R_e = R^* \left(\frac{C_2^* + C_3^*}{C_2^*}\right)^2 + \frac{1}{\omega_o^2R^*C_2^{*2}} \quad \ldots\ldots\ldots\ldots \quad (12)$$

$$C_e = \frac{C_2^*C_3^*}{C_2^*+C_3^*} \cdot \frac{1 + \dfrac{1}{\omega_o^2R^{*2}C_2^*(C_2^* + C_3^*)}}{1 + \dfrac{1}{\omega_o^2R^{*2}(C_2^* + C_3^*)^2}} \quad \ldots \quad (13)$$

To a close approximation, the transfer function obtained using R_e and C_e will differ from the overall function only in amplitude. This is discussed in Appendix C.

$$a = r/\omega_o = \frac{1}{4\omega_o \sin\alpha}[1/\tau_e + 1/\tau_s] \quad \ldots\ldots \quad (14)$$

$$\gamma = 1/(4r\sin\alpha)\,\tau_e = \frac{\tau_s}{\tau_e + \tau_s} \quad \ldots\ldots\ldots\ldots \quad (15)$$

$$L_{p1} = \frac{4aR_s\sin\alpha}{\omega_o(a^4 + 1 - 2a^2\cos 2\alpha)} \times \left[\frac{16a^2\gamma^2(1-\gamma)\sin^2\alpha + (a^2+1) - \gamma(4a^2+2-2a^2\cos 2\alpha)}{(1-2\gamma)/(1-\gamma)}\right] \quad \ldots\ldots\ldots\ldots \quad (16)$$

$$L_{s1} = \frac{4aR_e\sin\alpha}{\omega_o(a^4 + 1 - 2a^2\cos 2\alpha)} \times \left[\frac{16a^2\gamma(1-\gamma)^2\sin^2\alpha + (a^2+1) - (1-\gamma)(4a^2+2-2a^2\cos 2\alpha)}{(2\gamma-1)/\gamma}\right] \quad \ldots\ldots\ldots\ldots \quad (17)$$

$$L_{p2} = \frac{(4aR_s\sin\alpha)\,\gamma(1-\gamma)}{\omega_o} \times \left[\frac{16a^2\gamma(1-\gamma)^2\sin^2\alpha + (a^2+1) - (1-\gamma)(4a^2+2-2a^2\cos 2\alpha)}{(2\gamma-1)/\gamma}\right] \quad \ldots\ldots\ldots\ldots \quad (18)$$

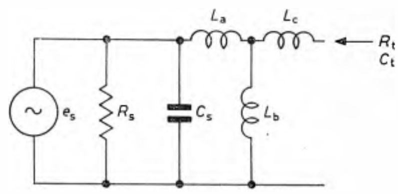

Fig. 8. The resistance and capacitance R_t and C_t seen looking into the transformer with the secondary open-circuited

One or other of these equations break down in the cases where $\gamma = 0$, $\gamma = 0{\cdot}5$, $\gamma = 1{\cdot}0$ and supplementary equations must be used. In these equations it is assumed that $C_s = C_e$ so that the calculated values will require scaling if they differ.

When $\gamma = 0$ $(R_e = \infty)$

$$L_{p1} = \frac{4a(a^2+1)R_s\sin\alpha}{\omega_o(a^4 + 1 - 2a^2\cos 2\alpha)} \quad \ldots\ldots\ldots\ldots \quad (19)$$

$$L_{s1} = \frac{4a(3a^2+1-2a^2\cos 2\alpha)R_s\sin\alpha}{\omega_o(a^4 + 1 - 2a^2\cos 2\alpha)} \quad \ldots\ldots \quad (20)$$

$$L_{p2} = \frac{4aR_s\sin\alpha}{\omega_o(3a^2+1-2a^2\cos 2\alpha)} \quad \ldots\ldots\ldots\ldots \quad (21)$$

When $\gamma = 0{\cdot}5$ $(R_e = R_s)$

$$L_{p1} = \frac{2a(a^2+1)R_s\sin\alpha}{\omega_o(a^4 + 1 - 2a^2\cos 2\alpha)} \quad \ldots\ldots\ldots\ldots \quad (22)$$

$$L_{s1} = \frac{2a(a^2+1)R_e\sin\alpha}{\omega_o(a^4 + 1 - 2a^2\cos 2\alpha)} \quad \ldots\ldots\ldots\ldots \quad (23)$$

$$L_{p2} = \frac{2aR_s\sin\alpha}{\omega_o(a^2+1)} \quad \ldots\ldots\ldots\ldots\ldots\ldots\ldots\ldots \quad (24)$$

When $\gamma = 1{\cdot}0$ $(R_s = \infty)$

$$L_{p1} = \frac{4a(3a^2+1-2a^2\cos 2\alpha)R_e\sin\alpha}{\omega_o(a^4 + 1 - 2a^2\cos 2\alpha)} \quad \ldots\ldots \quad (25)$$

$$L_{s1} = \frac{4a(a^2+1)R_e\sin\alpha}{\omega_o(a^4 + 1 - 2a^2\cos 2\alpha)} \quad \ldots\ldots\ldots\ldots \quad (26)$$

$$L_{p2} = \frac{4aR_e\sin\alpha}{\omega_o(a^2+1)} \quad \ldots\ldots\ldots\ldots\ldots\ldots\ldots\ldots \quad (27)$$

The equivalent parallel resistance and capacitance seen by the matching circuit (see Fig. 8) are given by:

$$R_t = \frac{L_{s1}}{L_{p1} - L_{p2}}\left[(1 - L_{p2}C_s\omega^2)^2 + \frac{\omega^2L_{p2}^2}{R_s^2}\right]R_s \quad \ldots. \quad (28)$$

$$C_t = -\frac{(1-L_{p1}C_s\omega^2)(1-L_{p2}C_s\omega^2)^2 + \omega^2(L_{p1}L_{p2}/R_s^2)}{\omega^2L_{s1}[(1-L_{p2}C_s\omega^2)^2 + \omega^2(L_{p2}^2/R_s^2)]} \quad \ldots \quad (29)$$

When $\gamma = 0$, $\gamma = 0{\cdot}5$ or $\gamma = 1{\cdot}0$, simplified expressions may be used to calculate R_t directly for the case where $\omega = \omega_o$, $C_s = C_e$.

$$\gamma = 0 \quad R_t = \frac{(9a^2 + 16\sin^2\alpha)}{2(a^2 + 2 + \cos 2\alpha)} R_s \quad \ldots\ldots\ldots\ldots (30)$$

$$= \frac{9a^2 + 8}{2(a^2 + 2)} R_s \quad (\alpha = 45°) \ldots (31)$$

$$\gamma = 0{\cdot}5 \quad R_t = \left[\frac{a^2 + 4\sin^2\alpha}{4\cos^2\alpha}\right] R_s \quad \ldots\ldots\ldots\ldots (32)$$

$$= \frac{a^2 + 2}{2} R_s \quad (\alpha = 45°) \ldots (33)$$

$$\gamma \rightarrow 1{\cdot}0 \quad R_t \rightarrow \frac{a^2}{2(a^2 + 2 + \cos 2\alpha)} R_s \quad \ldots\ldots\ldots\ldots (34)$$

$$= \frac{a^2}{2(a^2 + 2)} R_s \quad (\alpha = 45°) \ldots (35)$$

These equations are useful to predict the impedance transformation across a given input transformer.

ESTIMATING THE SOURCE RESISTANCES R_t AND R_o

Before proceeding with a complete calculation it is useful to obtain an estimate of R_t. This assists in the selection of C_3^* and C_3^*/C_2^*.

For the specific case where $\alpha = 45°$ an expression to directly calculate the product R_tC_e/R_sC_s can be derived from equations (16) to (18) and equation (28).

$$\left(\frac{R_tC_e}{R_sC_s}\right)_{\alpha=45°} = \frac{a^2(4\gamma^2 - 6\gamma + 3)^2 + 8(1-\gamma)^2}{16a^2\gamma^4 - 32a^2\gamma^3 + (28a^2+8)\gamma^2 - (12a^2+8)\gamma + (2a^2+4)} \quad \ldots\ldots\ldots\ldots (36)$$

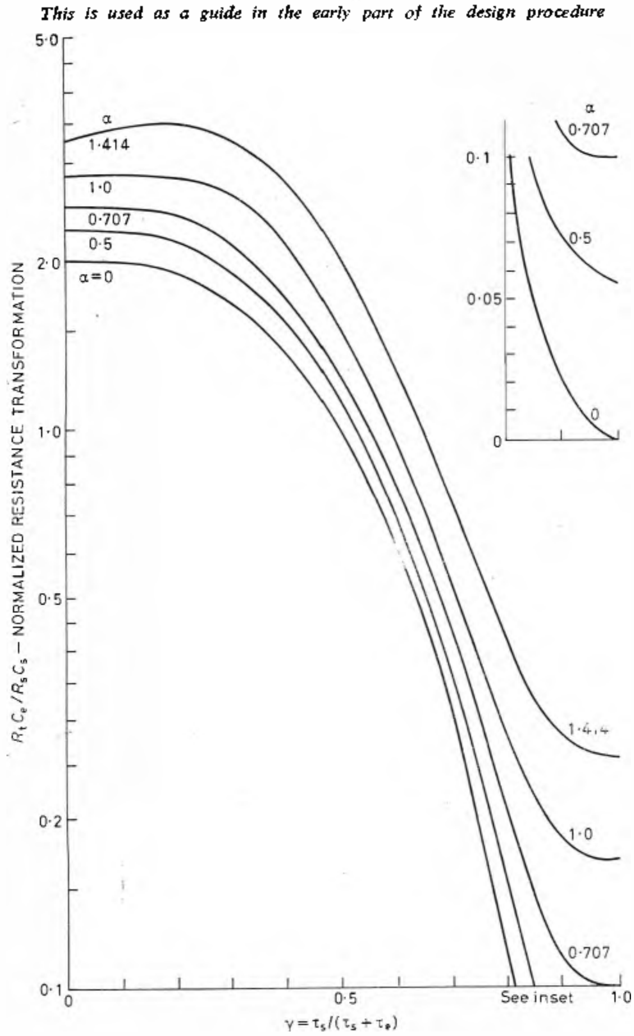

Fig. 9. The normalized resistance transformation across the transformer against γ for the case when $\alpha = 45°$

This is used as a guide in the early part of the design procedure

In Fig. 9 R_tC_e/R_sC_s is plotted against γ for various values of a.

The dependence of R_t on α is indicated by the equations for R_t when $\gamma = 0$, $\gamma = 0{\cdot}5$ and $\gamma = 1{\cdot}0$

i.e. $$R_t = f(a, \alpha) R_s \quad \ldots\ldots\ldots\ldots (37)$$

Now:

$$R_t \simeq \left(\frac{R_tC_e}{R_sC_s}\right)_{\alpha=45°} \times \frac{f(a, \alpha)}{f(a, 45°)} \times (C_s/C_e) \,.\, R_s \quad \ldots\ldots\ldots\ldots (38)$$

As $f(a, \alpha)$ has only been calculated for $\gamma = 0$, $\gamma = 0{\cdot}5$ and $\gamma = 1{\cdot}0$, the expression for γ closest to the actual value is used. Alternatively, an interpolated value may be used.

To obtain an estimate of R_o equation (6) is used. C_t is not yet known, but when $\omega = \omega_o$ $C_t \simeq -C_e$. This value is used.

The subsequent calculation may yield a value of R_o very different from the predicted value, as C_t and $(-C_e)$ may not be equal, as was assumed. In repeating the calculation with new values of C_3^* and C_3^*/C_2^* the ratio $(C_t/-C_e)_1$ actually obtained in the first calculation may be used to predict a more accurate value for C_t in the second

i.e. $$C_{t2} = (C_t/-C_e)_1 C_{e2}$$

INSERTION LOSS

The loss of the transformer may be represented by an equivalent resistance R_d across the secondary.

If Q_p = unloaded primary Q

Q_s = unloaded secondary Q

The equivalent primary loss resistance across the secondary

$$= Q_p\omega L_{p1}R_t/R_s \quad \ldots\ldots\ldots\ldots (39)$$

The equivalent secondary loss resistance

$$= Q_s\omega L_{s1} \quad \ldots\ldots\ldots\ldots (40)$$

$$R_d = \frac{Q_pQ_sL_{p1}L_{s1}\omega^2R_t/R_s}{Q_p\omega L_{p1}R_t/R_s + Q\omega L_{s1}} \quad \ldots\ldots\ldots\ldots (41)$$

The ratio of the power dissipated in R_d to the power dissipated in R_e in parallel with R_t gives the insertion loss of the transformer.

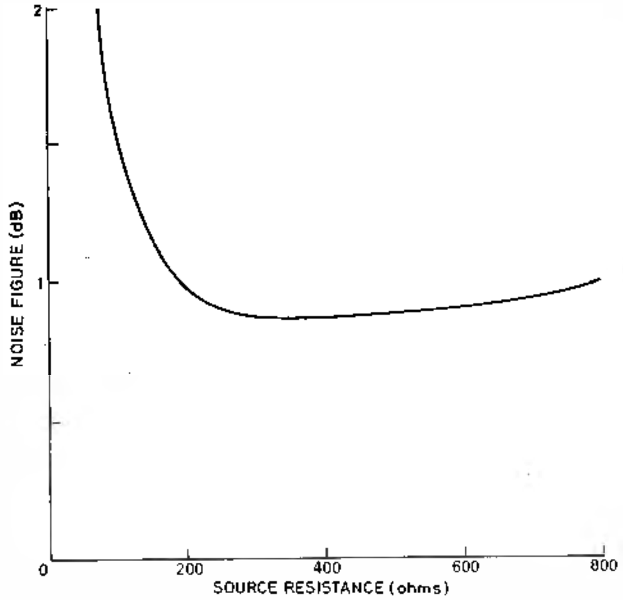

Fig. 10. The average behaviour of six AFZ12 transistors with $G = 0{\cdot}625\,\mathrm{m}\Omega^{-1}$

$$\text{Power Loss} = \frac{R_t R_e}{R_t + R_e} \cdot (1/R_d) \quad \ldots\ldots\ldots \quad (42)$$

Design Example

As an example of the design procedure, a circuit to couple a 400Mc/s to 11Mc/s mixer to a transistor amplifier is considered. The output impedance of the mixer used is 600Ω in parallel with 40pF. The input conductances and capacitances of the transistor to be used are shown in Fig. 1. These transistors had measured noise figures (using a Hewlett Packard noise figure meter) of less than 1dB at a current of 1mA with a source resistance of 400Ω. The transistor input capacitance was not tuned out for this measurement. The optimum source impedance for these transistors was roughly proportional to the particular input resistance, being between 300Ω and 500Ω where the transistor input resistance was 1 600Ω ($G = 0{\cdot}625\text{m}\Omega^{-1}$) (see Fig. 10). In this particular case optimum noise performance is required over a 2Mc/s band centred on 11Mc/s. The source resistance over this band should then be between 300Ω and 500Ω.

Referring to Fig. 1 a value for G^* of $0{\cdot}625\text{m}\Omega^{-1}$ is selected. C_3^* is set at 60pF and a curve is drawn for C_3 with $C_3^*/C_2^* = 1{\cdot}2$. All transistors enclosed by the triangle may now be used.

Now $C_3^* = 60\text{pF}$

$C_2^* = 50\text{pF}$

$R^* = 1/G^* = 1\,600\Omega$

From equations (12) and (13)

$R_e = 7796\Omega$

$C_e = 27{\cdot}4\text{pF}$

$\tau_e = 0{\cdot}214\mu\text{sec}$

$R_s = 600\Omega$

$C_s = 40\text{pF}$

$\tau_s = 0{\cdot}024\mu\text{sec}$

If the input circuit is designed to have a slight dip in the response, it is only necessary to specify the 3dB points and the peak/valley ratio for alignment. This is considerably easier than aligning to 1dB and 3dB points as is necessary for other responses.

If $\alpha = 40°$ the peak/valley ratio is 0·15dB. The actual peak/valley ratio, after correcting for the response of the poles with negative imaginary part (see Fig. 17) is 0·1dB.

From equations (14) and (15):

$a = 0{\cdot}261$

$\gamma = 0{\cdot}101$

Fig. 11. The source resistance seen by a transistor with $G = 0{\cdot}625\text{m}\Omega^{-1}$ against frequency.

The narrower bandwidth of the measured curve is discussed in the design example

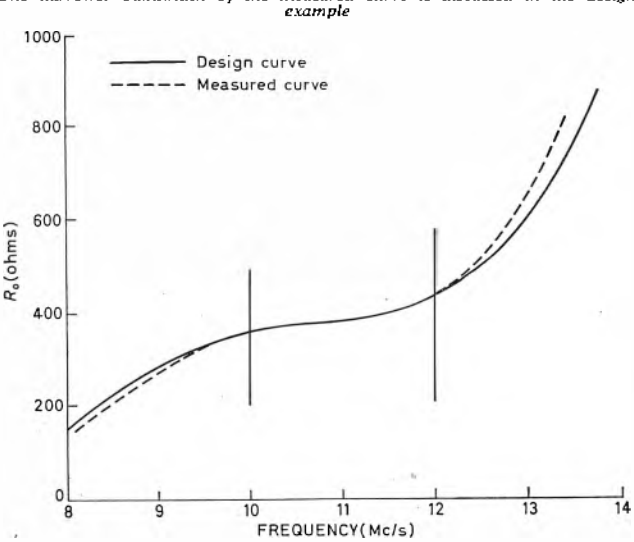

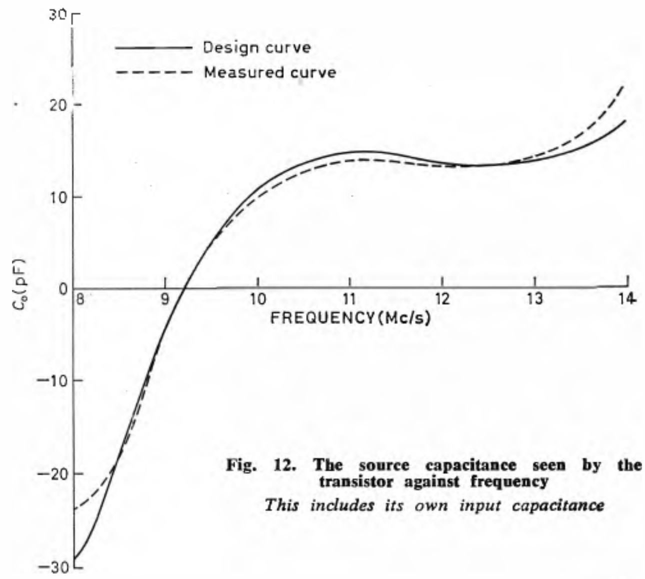

Fig. 12. The source capacitance seen by the transistor against frequency

This includes its own input capacitance

SOURCE IMPEDANCE CHECK

From Fig. 9 $\quad R_t C_e / R_s C_s = 2{\cdot}05$

When $\gamma = 0$ from equation (30)

$f(a, 45°) = 2{\cdot}08$

$f(a, 40°) = 1{\cdot}59$

From equation (38):

$R_t = 1\,370\Omega$

From equation (6), assuming $C_t = -C_e$

$R_o = 279 + 61\Omega$

$= 340\Omega$

This is an acceptable value for R_o. The L parameters are now calculated.

Equations (16), (17) and (18) give:

$L_{p1} = 5{\cdot}65\mu\text{H}$

$L_{p2} = 4{\cdot}46\mu\text{H}$

$L_{s1} = 9{\cdot}16\mu\text{H}$

From these values when $\omega = \omega_o$ equations (28) and (29) give:

$R_t = 1\,330\Omega$

$C_t = -25{\cdot}75\text{pF}$

and equations (6) and (7) give:

$R_o = 374{\cdot}5\Omega$

$C_o = 14{\cdot}1\text{pF}$

In Figs. 11 and 12, R_o and C_o are plotted against ω.

In Fig. 13, C_1, C_2 and C_3 are plotted against G for the case, where:

$G^* = 0{\cdot}625\text{m}\Omega^{-1}$

$C^*_3 = 60\text{pF}$

$C_3^*/C_2^* = 1{\cdot}2$

The appropriate C values for transistors within the large triangle in Fig. 1 are read from these curves. The values for C_1, C_2 and C_3 were set to within 1pF of the nominal.

THE COUPLING COIL

Having obtained the values for the inductances, it is necessary to construct a circuit having these values and as low a loss as possible. At 11Mc/s, Q's of 300 are readily obtained using toroidal type cores of a suitable ferrite material. In this instance a small balun core was used (Ducon type F4035 Q2 material). The primary and secondary windings were wound partly together on the centre section where very high coupling is obtained and then continued individually on the two outer sections (see Fig. 14). For the common portion of the winding the two wires are twisted tightly together. Some adjustment may be obtained by changing the disposition of the turns around the outer sections. The cores were initially selected to 2 per cent for inductance with a one turn loop around the centre section, and then the end giving the highest inductance with one turn selected. This ensured good uniformity in the wound coils.

The construction of the coils in this case does not allow the exact design values to be obtained for the inductances. With the restriction that the inductance values are limited by having to add or subtract whole turns from the windings, the coil is arranged to have the nearest practicable values below the design values. This necessitates an increase in C_s and C_e with a consequent reduction in r. However, if γ is maintained constant at the design value, the correct impedance is still obtained at the centre frequency. In this case an increase of 7 per cent was required in both C_s and C_e. The extra secondary capacitance is connected directly from the output of the coil to ground, i.e., across C_1. It is important to note that this is not inconsistent with the design procedure.

In alignment, the primary and secondary capacitance was varied by a maximum of ± 1pF and the windings adjusted to give the correct peak/valley ratio and the correct centre frequency. The resulting bandwidths were within 2 per cent of the mean. For a group of 20 transistors, the amplitude response obtained was within $\pm 0{\cdot}05$dB of the mean, while the absolute phase was within $\pm 1°$ of the mean over the centre 2Mc/s. This includes variations in the transistor.

INSERTION LOSS

From equation (41):

$$R_d = 102\text{k}\Omega$$

From equation (42):

$$\text{power loss} = 0{\cdot}0111$$

This corresponds to 0·05dB.

APPENDIX

(A) DERIVATION OF EQUATIONS 3 TO 5

Rewriting equation (2):

$$e_o(s) = \frac{RC_2S\ e_i(s)}{Z_t(s)\ R(C_1C_2+C_2C_3+C_3C_1)S^2 + [Z_t(s)\ (C_1+C_2)+R(C_2+C_3)]S+1} \quad \ldots\ldots\ldots\ldots (A1)$$

The amplitude and phase response represented by this function may be preserved for varying values of the components provided that the coefficients of S^2 and S in the denominator remain unchanged. The magnitude of the function, which is determined by the product RC_2, may vary. To preserve the denominator, the following relationships must hold:

$$Z_t(s)\ R(C_1C_2+C_2C_3+C_3C_1) = M_1 \quad \ldots\ldots\ldots\ldots (A2)$$

$$Z_t(s)\ (C_1+C_2)+R(C_2+C_3) = M_2 \quad \ldots\ldots\ldots\ldots (A3)$$

Since $Z_t(s)$ need not be real, it is further required that:

$$Z_t(s)\ (C_1 + C_2) = M_3 \quad \ldots\ldots\ldots\ldots (A4)$$

$$R\ (C_2 + C_3) = M_4 \quad \ldots\ldots\ldots\ldots (A5)$$

where $M_{1,2,3,4}$ are constants.

In order to present the result in the most convenient form, it is necessary to find an expression relating R and one of the capacitors.

Rearranging equations (A2), (A4) and (A5)

$$R(C_1C_2+C_2C_3+C_3C_1) = M_1/Z_t(s) \quad \ldots\ldots\ldots (A6)$$

$$(C_1+C_2) = M_3/Z_t(s) = K_1 \quad \ldots\ldots\ldots (A7)$$

$$R(C_2+C_3) = M_4 = K_2 \quad \ldots\ldots\ldots\ldots (A8)$$

Substituting (A7) and (A8) into (A6):

$$C_1C_2 + (C_1+C_2)\left((K_2/R) - C_2\right) = \frac{M_1}{RZ_t(s)}$$

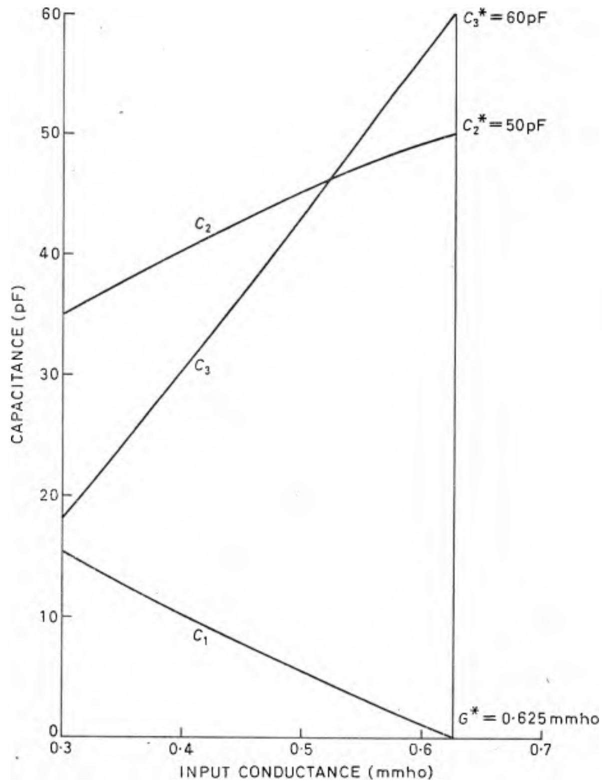

Fig. 13. C_1, C_2 and C_3 plotted against G for the conditions in the design example

$$C_1C_2 - C_1C_2 + C_1(K_2/R) - C_2^2 + (C_2K_2/R) = \frac{M_1}{RZ_t(s)}$$

$$RC_2^2 = K_2K_1 - \frac{M_1}{Z_t(s)} \quad = K_3 \quad \ldots . (A9)$$

Equations (A7), (A8) and (A9) are the required equations (3), (4) and (5).

(B) DERIVATION OF THE TRANSFORMER DESIGN EQUATIONS

For the circuit shown in Fig. 6 the output voltage $e_o(s)$ is given by:

$$e_o(s) = \frac{g_m L_2 S\ e_i(s)}{L_{s1}L_{p2}C_sC_eS^4 + L_{s1}L_{p2}\left(C_s/R_e + C_e/R_s\right)S^3 + \left[\dfrac{L_{s1}L_{p2}}{R_sR_e} + L_{p2}C_s + L_{s1}C_e\right]S^2 + \left[L_{p1}/R_s + L_{s1}/R_e\right]S + 1} \quad \ldots\ldots\ldots\ldots\ldots\ldots (B1)$$

Fig. 14. The type of ferrite core and winding technique used for the input transformer

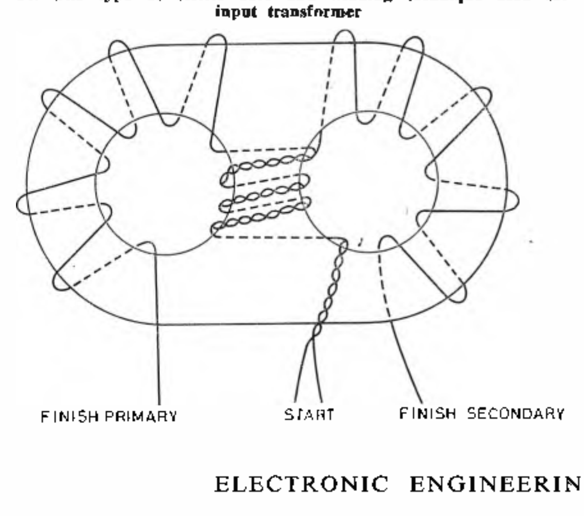

In order to design a coil of maximum bandwidth, the coefficients of the S terms in equation (B1) are equated with those arising through computation of the transfer function represented by the pole positions shown in Fig. 7. The centre frequency ω_0 and the angle α are known. The poles lie on a circle of radius a with its centre at ω_0. a, L_{p1}, L_{s1} and L_{p2} are found by equating coefficients. The transfer function represented by the pole positions in Fig. 7 is given by $f(s)$.

$$f(s) = \cfrac{\cfrac{s}{(r^2+\omega_0^2)^2 - 4r^2\omega_0^2\cos^2\alpha}}{\cfrac{1}{(r^2+\omega_0^2)^2 - 4r^2\omega_0^2\cos^2\alpha} S^4 + \cfrac{4a\sin\alpha}{(r^2+\omega_0^2)^2 - 4r^2\omega_0^2\cos^2\alpha} S^3 + \cfrac{2(a^2+\omega_0^2)+4a^2\sin^2\alpha}{(r^2+\omega_0^2)^2 - 4r^2\omega_0^2\cos^2\alpha} S^2 + \cfrac{4a(a^2+\omega_0^2)\sin\alpha}{(r^2+\omega_0^2)^2 - 4r^2\omega_0^2\cos^2\alpha} S + 1} \quad \ldots\ldots \text{(B2)}$$

Equating coefficients with equation (B1):

$$L_{s1}L_{p2}C_sC_e = \frac{1}{(r^2+\omega_0^2)^2 - 4r^2\omega_0^2\cos^2\alpha} = A \quad \ldots\ldots\ldots \text{(B3)}$$

$$L_{s1}L_{p2}(C_s/R_e + C_e/R_s) = A\,(4r\sin\alpha) = B \quad \ldots\ldots\ldots\ldots \text{(B4)}$$

$$\frac{L_{s1}L_{p2}}{R_sR_e} + L_{p1}C_s + L_{s1}C_e = A\,(2(r^2+\omega_0^2)+4r^2\sin^2\alpha) = D \quad \ldots\ldots\ldots\ldots \text{(B5)}$$

$$L_{p1}/R_s + L_{s1}/R_e = A\,(4r(r^2+\omega_0^2)\sin\alpha) = E \quad \ldots \text{(B6)}$$

From equations (B3) to (B6). Putting $\tau_e = R_eC_e$ and $\tau_s = R_sC_s$:

$$r = (1/4\sin\alpha)(1/\tau_e + 1/\tau_s) \quad \ldots\ldots\ldots\ldots \text{(B7)}$$

$$L_{p1} = R_s\left\{\frac{(A/\tau_s\tau_e) + E\tau_e - D}{\tau_e - \tau_s}\right\} \quad \ldots\ldots\ldots\ldots\ldots\ldots \text{(B8)}$$

$$L_{s1} = R_e\left\{\frac{(A/\tau_s\tau_e) + E\tau_s - D}{\tau_s - \tau_e}\right\} \quad \ldots\ldots\ldots\ldots\ldots\ldots \text{(B9)}$$

$$L_{p2} = \frac{A}{C_sC_eL_{s1}} \quad \ldots\ldots\ldots\ldots\ldots\ldots\ldots \text{(B10)}$$

γ and a are now defined.

$$\gamma = \frac{1}{4r\tau_e\sin\alpha} = \frac{\tau_s}{\tau_s + \tau_e} \quad \ldots\ldots\ldots\ldots\ldots\ldots\ldots\ldots \text{(B11)}$$

$$a = r/\omega_0 \quad \ldots\ldots\ldots\ldots\ldots \text{(B12)}$$

where ω_0 is the centre frequency.

Equations (14) to (18) are obtained by substituting equations (B11) and (B12) into (B7) to (B10).

To derive equations (19) to (21) it is necessary to find

$$\lim_{\tau_e\to\infty} L_{p1},\ L_{p2} \text{ and } L_{s1}$$

In addition, to simplify results, $C_s = C_e$.

Thus $L_{p1} = R_sE$

$$\begin{aligned} L_{s1} &= R_e((E\tau_s/\tau_e) - D) \\ &= (R_e/R_eC_e)(R_sC_sE - D) \\ &= R_sE - (D/C_e) \end{aligned}$$

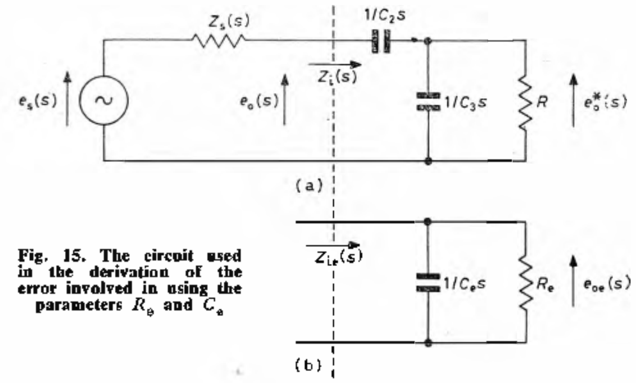

Fig. 15. The circuit used in the derivation of the error involved in using the parameters R_e and C_e

The results follow using equation (B10), (B11) and (B12). Equations (25) to (27) are derived similarly.

Equations (22) to (24) result from calculation of the

$$\lim_{\tau_s\to\tau_e} L_{p1},\ L_{p2},\ L_{s1}$$

From equation (B6) it may be deduced that:

$$L_{p1}/R_s = L_{s1}/R_e = E/2$$

Hence equations (22) to (24).

Substitution of the L parameters for the cases where $\gamma = 0$, $\gamma = 0{\cdot}5$, $\gamma = 1{\cdot}0$ in equation (28) yields equations (30) to (35). These equations are only applicable for $\omega = \omega_0$. When $\alpha = 45°$ equations (16) to (18) are simplified. The resulting expressions are substituted in equation (28) to give equation (36) which is used for calculating the impedance transformation across the transformer.

(c) The Approximation Due to R_e and C_e

It is convenient, in the design of a coupling circuit, to replace the transistor matching circuit with an equivalent parallel resistance and capacitance. It is intended in this section to show that to a good approximation, the transfer function so obtained differs only in gain from the overall transfer function to the input of the transistor.

In Fig. 15(a) the complete circuit is shown. In Fig. 15(b) the transistor matching circuit is replaced by an equivalent parallel R_e and C_e. The prior circuit in each case is represented by a generator $e_s(s)$ and a source impedance $Z_s(s)$. In the circuit design the transfer function $f_e(s) = e_{oe}(s)/e_s(s)$ is used. When the actual circuit is substituted, the transfer function $f'(s) = e_o'(s)/e_s(s)$ results.

$$f(s) = e_o(s)/e_s(s) = \frac{Z_i(s)}{Z_s(s) + Z_i(s)} \quad \ldots\ldots\ldots\ldots\ldots \text{(C1)}$$

$$f_e(s) = e_{oe}(s)/e_s(s) = \frac{Z_{ie}(s)}{Z_s(s) + Z_{ie}(s)} \quad \ldots\ldots\ldots\ldots \text{(C2)}$$

The transfer function required is:

$$f'(s) = e_o's/e_s(s) \quad \ldots\ldots\ldots\ldots\ldots \quad \text{(C3)}$$

From equations (C1) and (C2)

$$f(s) = f_e(s)\,\left(Z_i(s)/Z_{ie}(s)\right) \cdot \frac{1}{f_e(s)\left[\dfrac{Z_i(s) - Z_{ie}(s)}{Z_{ie}(s)}\right] + 1} \quad \ldots\ldots\ldots \quad \text{(C4)}$$

Now $f'(s) = f(s)\,\left(e_o'(s)/e_o(s)\right)$ $\ldots\ldots\ldots\ldots\ldots$ (C5)

$$\text{Also } e_o'(s)/e_o(s) = \frac{R}{RC_3S + 1} \cdot \frac{(RC_3S + 1)\,C_2S}{R(C_2 + C_3)\,S + 1} \quad \ldots\ldots\ldots\ldots \quad \text{(C6)}$$

$$Z_i(s) = \frac{R(C_2 + C_3)\,S + 1}{(RC_3S + 1)\,C_2S} \quad \ldots\ldots\ldots\ldots \quad \text{(C7)}$$

$$Z_{ie}(s) = \frac{R_e}{R_eC_eS + 1} \quad \ldots\ldots\ldots\ldots \quad \text{(C8)}$$

Substituting equations (C4), (C6), (C7) and (C8) into (C5)

$$f'(s) = f_e(s) \,.\, (R/R_e) \,.\, \frac{R_eC_eS+1}{RC_3S+1} \left[\frac{1}{f_e(s)\left(\dfrac{Z_i(s) - Z_{ie}(s)}{Z_{ie}(s)}\right) + 1}\right] \quad \ldots\ldots\ldots\ldots \quad \text{(C9)}$$

If $f_e(s)\left[\dfrac{Z_i(s) - Z_{ie}(s)}{Z_{ie}(s)}\right] \ll 1$

$$f'(s) = f_e(s) \,.\, (R/R_e) \,.\, \frac{R_eC_eS+1}{RC_3S+1}\left[1 - f_e(s)\frac{Z_i(s) - Z_{ie}(s)}{Z_{ie}(s)}\right] \quad \ldots\ldots\ldots \quad \text{(C10)}$$

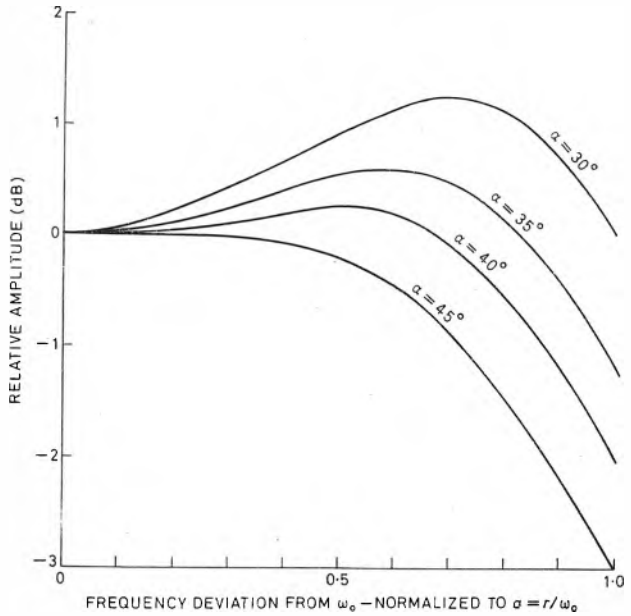

Fig. 17. The response due to poles with positive imaginary part for various values of α

$$f'(j\omega) = f_e(j\omega)\, R/R_e \left[\frac{1+j\omega R_eC_e}{1+j\omega RC_e}\right] \cdot \left[1 - f_e(j\omega)\left(\frac{Z_i(j\omega) - Z_{ie}(j\omega)}{Z_{ie}(j\omega)}\right)\right] \quad \ldots\ldots\ldots \quad \text{(C11)}$$

In the design example the error due to the bracketed terms is less than 0·2dB in the passband of the circuit. It is necessary to check these terms in each case, particularly where $f_e(j\omega)$ may have a magnitude considerably greater than unity. When these terms are close to unity, then:

$$f'(j\omega) \simeq f_e(j\omega) \,.\, (R/R_e) \quad \ldots\ldots\ldots \quad \text{(C12)}$$

(D) The Narrow Band Approximation

The design procedure assumed that the contribution of the zero at the origin and the poles with negative imaginary part need not be considered. It may be shown that the response due to these is given by:

$$|A(j\omega)| = \frac{A\omega}{\sqrt{\left[a^4 + (1+\omega)^4 - 2a^2(1+\omega)^2 \cos 2\alpha\right]}}$$

where A is a constant and the expression is normalized to the centre frequency. This expression is plotted in Fig. 16 for the case where $\alpha = 45°$ and $a = 0·5$ (this gives a fractional bandwidth of unity). Fig. 17 shows the response due to the poles with positive imaginary part for various α. It may be seen that for $\alpha = 45°$ and $a = 0·5$ the error (from Fig. 16) will be 1dB at the nominal lower 3dB point and 0·4dB at the upper 3dB point. The errors at the nominal 1dB points are 0·4dB and 0·2dB respectively.

The modified α required for a flat response may be readily predicted, while the slope is such that it may be corrected in final alignment.

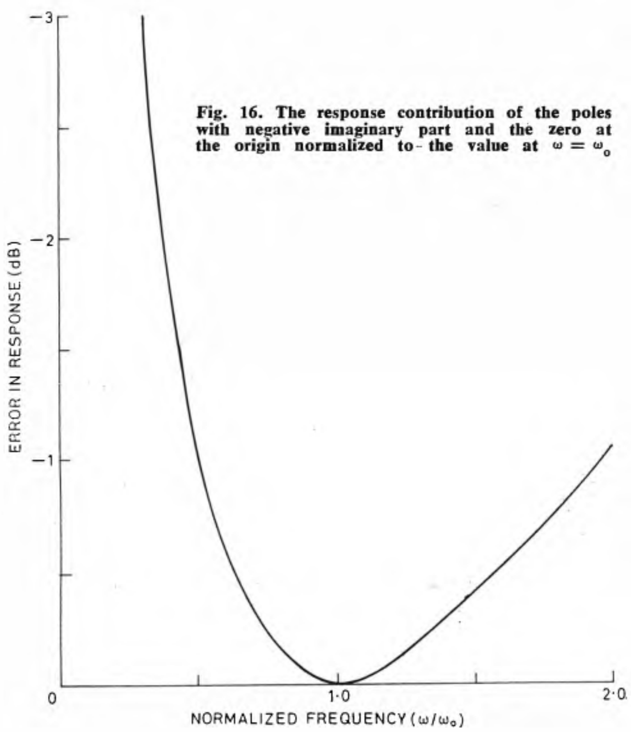

Fig. 16. The response contribution of the poles with negative imaginary part and the zero at the origin normalized to the value at $\omega = \omega_o$

Acknowledgment

The author wishes to thank Professor R. E. Aitchison, C. T. Murray and I. S. Docherty for their discussions on this work and suggestions in the presentation of the article.

The work was carried out by the author on a Nuffield Fellowship. Acknowledgment of financial assistance is made also to the U.S. National Science Foundation.

Critical Inductance for Half-Controlled Thyristor Rectifiers

(Part 1)

By J. L. Storr-Best*, B.Sc.(Eng.), A.M.I.E.E.

This article analyses the critical inductance requirements of choke-input filters for single and three-phase 'half-controlled' thyristor rectifiers, in which only half the elements are thyristors, the remainder being straightforward diodes. A comparison of important points of difference is made between these results and the more well-known ones for full-controlled rectifiers. A table of values of the ratio of peak thyristor current to d.c. output current is given for various firing angles when the inductance is critical. Curves are also given relating peak and mean currents in the by-pass diode to the d.c. output current at various firing angles.

(Voir page 273 pour le résumé en français: Zusammenfassung in deutscher Sprache auf Seite 280)

THE critical inductance of a choke-input filter is an important parameter in ensuring proper operation of a rectifier within its peak current rating and in achieving a good natural regulation for the system. Most textbooks which deal with power supplies[1] give a formula for critical inductance to be applied in cases of ordinary uncontrolled rectification, i.e., diode rectification; inductance is given in terms of supply frequency and load resistance. (A value of $\omega L/R$ is given for each commonly used rectifier circuit, e.g. single-phase bridge, three-phase bridge, etc.) When controlled rectifiers, such as thyratrons and ignitrons and other grid-controlled tubes, first came into use, it was not always realized that the critical inductance-to-load ratio was larger at the reduced conduction angles that were being used. In 1939, however, W. P. Overbeck wrote a paper[2] in which he evaluated critical inductance-to-load ratios for all firing angles of controlled rectifiers and for various numbers of supply phases. His graphs are now accepted as standard and have been reproduced in text-books[3]. The cases which he evaluated dealt only with what may be called 'full-controlled' rectifiers, in which every rectifying element in the full circuit was controlled. The majority of semiconductor controlled rectifiers in common use today, however, are 'half-controlled' in the sense that only half the elements are thyristors, the others being ordinary diodes. The purpose of this article is to demonstrate the rather different critical inductance characteristics obtained in the case of single- and three-phase half-controlled thyristors circuits.

Full-Controlled Single-Phase Bridge Rectifier

Before examining the half-controlled cases, the classic full-controlled circuit, its characteristics and the critical inductance-to-load ratio for any conduction angle will be considered.

Fig. 1 shows the circuit of a full-controlled single-phase bridge rectifier with choke-input filter and shows the rectifier output voltage waveforms at various values of the firing angle, α. The mean d.c. output is at a level such that it divides the a.c. waveform into equal areas, as shown by the shaded portions of the diagrams. This illustration assumes of course that there is a relatively negligible voltage drop in the rectifiers and the choke and that the ripple is perfectly smoothed by the LC filter.

When the firing angle is delayed, for example by 45° as shown in Fig. 1, the rectifier output voltage becomes negative at the end of each half-cycle; this is because there is still current flowing into the choke at zero voltage (inductive current lagging behind driving voltage) and

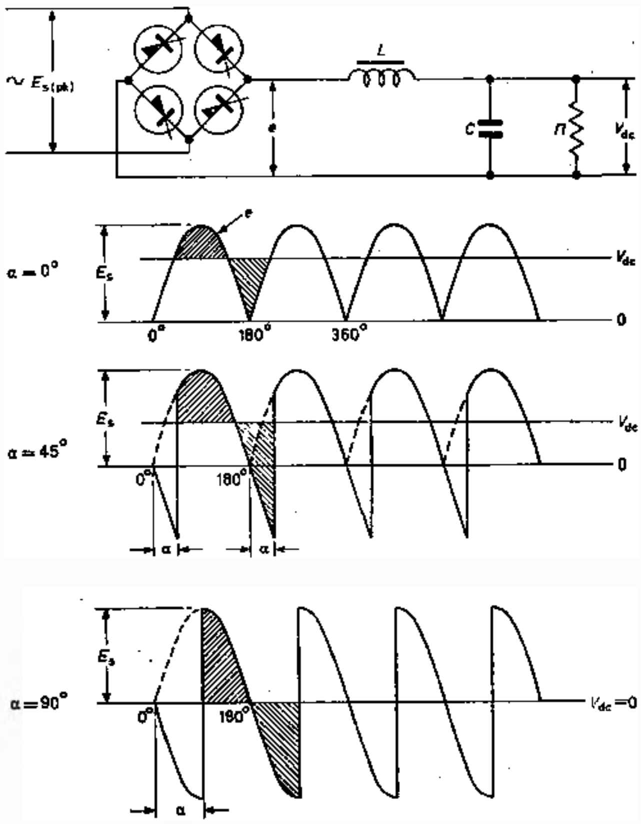

Fig. 1. Full controlled single-phase bridge rectifier

Circuit diagram and voltage waveforms for various triggering angles

therefore the thyristors which were conducting during the previous half-cycle are still forced to conduct. Assuming that the choke inductance is made large enough to maintain current flow until the delayed thyristors are triggered on, then the waveform is as shown in Fig. 1 for $\alpha = 45°$; the triggering of the new thyristors connects the supply in opposite phase to the existing rectifier output and the sharp change of output voltage from a negative value to an equal positive value reverse-biases the previously conducting thyristors and turns them off. At $\alpha = 90°$, V_{dc}

* *Standard Telephones and Cables Limited.*

must be zero to divide the waveform into equal areas; hence full control of output voltage, from a maximum value (which is almost equal to that of a diode bridge) down to zero, is obtained with a firing angle range of 0° to 90°.

The shape of the current waveform may be deduced by noting that twice in each half-cycle $e = V_{dc}$, this equality occurring where the rectifier output voltage waveform and the d.c. voltage line intersect. These intersections correspond to the points at which the voltage across the choke passes through zero; since $V = L(di/dt)$ for a pure inductance, it follows that at these intersections $di/dt = 0$, and that these points therefore correspond to current maximum and minimum.

Fig. 2 is a magnified picture of two half-cycles of the voltage waveform corresponding to $\alpha = 45°$; the choke current waveform has been sketched in to show the coincidence of maximum and minimum with voltage waveform intersections. If the choke inductance had been at the critical value for this condition, the current would just have reached zero at its minimum point; variations in inductance above this value merely alter the amplitude of the current excursion about the mean value I_{dc} but do not alter the shape of the current waveform nor the phase angles at which maximum and minimum occur.

The equation for i can be derived by integrating the choke voltage because it is known that:

$$v_{CH} = L\,(di/dt)$$

where v_{CH} is the instantaneous value of the voltage across the choke.

Hence:

$$i = 1/\omega L \int_{\alpha}^{\omega t} v_{CH}\,.\,d\omega t + \text{an integration constant.}$$

Now v_{CH} is the difference between the instantaneous value of the rectifier output and the mean d.c. output, and may therefore be written:

$$v_{CH} = E_S \sin \omega t - V_{dc}$$

And V_{dc} may be shown to be:

$$V_{dc} = (2/\pi)\,E_s \cos \alpha$$

The integration constant may be evaluated for the case of critical inductance, L_c, by setting $i = 0$ at $\omega t = \alpha$.

The resulting expression for the instantaneous value of the current i at any point in the cycle (i.e. at any value of ωt) becomes:

$$i = E_s/\omega L_c \left[\{1 - (2/\pi)(\omega t - \alpha)\} \cos \alpha - \cos \omega t\right]$$

The mean current, I_{dc}, can now be obtained by integrating in turn this expression for i over the complete half-cycle, i.e. from $\omega t = \alpha$ to $\pi + \alpha$.

So

$$I_{dc} \times \pi = \int_{\alpha}^{\pi+\alpha} i\,.\,d\omega t$$

which gives:

$$I_{dc} = E_s/\omega L_c\,.\,\frac{2 \sin \alpha}{\pi}$$

Now since:

$$V_{dc} = (2/\pi)\,E_s\,.\cos \alpha$$

and

$$R = V_{dc}/I_{dc}$$

then

$$R = \omega L_c \cot \alpha$$

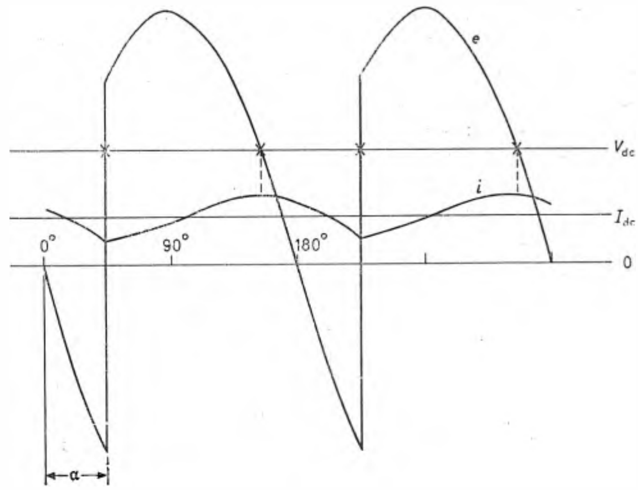

Fig. 2. Illustrating coincidence of current maxima and minima with d.c. and a.c. voltage intersections (x) (Full-controlled single-phase bridge rectifier)

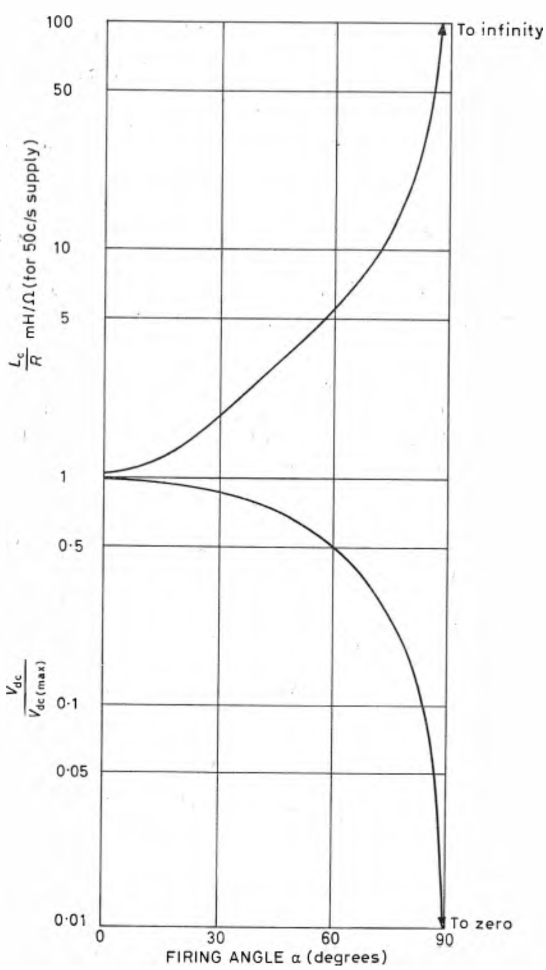

Fig. 3. Critical inductance and output voltage against firing angle for full-controlled single-phase bridge rectifier

or:

$$\omega L_c/R = \tan \alpha \quad \ldots\ldots\ldots\ldots\ldots\ldots \quad (1)$$

This expression is true for all except small angles of α. Referring to Fig. 2 it will be seen that the current minimum occurs where $\omega t = \alpha$ since at this point the rising edge of the triggered waveform intersects the V_{dc}

line. However, at angles of α of approximately 32·5° and below, the rising edge terminates before reaching the V_{dc} line and the intersection subsequently occurs on the sine-wave portion of the waveform at some angle, ϕ, greater than α. Fortunately it is easy to calculate ϕ for any angle below 32·5° since the following equation defines the intersection:

$$E_s \sin \omega t = V_{dc} \text{ (at } \omega t = \phi)$$

Hence:

$$E_S \sin \phi = (2/\pi)\, E_S \cos \alpha$$

So:

$$\phi = \sin^{-1}((2/\pi) \,.\, \cos \alpha)$$

The resulting expression for $\omega L_c/R$ for values of α between 0° and 32·5° is a bit more complex than the equation (1) above, and works out to:

$$\frac{\omega L_c}{R} = \frac{\pi}{2 \cos \alpha}\left[\cos \phi + (2/\pi) \sin \alpha - (2/\pi) \cos \alpha \left((\pi/2) + \alpha - \phi\right)\right] \quad \ldots\ldots\ldots\ldots\ldots\ldots (2)$$

(It can be seen by inspection that this reduces to $\omega L_c/R = \tan \alpha$ when $\alpha = \phi$ as for angles of α greater than 32·5°.)

Equations (1) and (2) are the basis of W. P. Overbeck's curve (Fig. 5, $n = 2$, in his article[2]) which is reproduced here in Fig. 3; for convenience L_c/R has been plotted (instead of $\omega L_c/R$) against α, having normalized to a 50c/s supply.

Fig. 3 illustrates how the mean voltage output drops with increasing α and how the L_c/R ratio starts from a finite value at $\alpha = 0$ (equal to the textbook value for diode rectifiers of course) and rises rapidly as α increases, tending towards infinity as α approaches 90°.

One practical way of looking at the criterion for L_c is to observe that, when the inductance is just critical, the peak a.c. swing must just equal the mean d.c. value in order that the instantaneous value may just fall to zero at some point in the half-cycle. Referring back to the waveforms of Fig. 1 it is not now difficult to see why the critical inductance is infinite at $\alpha = 90°$. At this value of α it will be seen that, although the mean d.c. output voltage of the rectifier is zero, there is a very substantial a.c. input voltage to the filter. To reduce the a.c. current produced by this finite a.c. voltage down to the infinitely small level necessary to match the zero d.c. current must obviously require infinite inductance. By looking at the half-controlled rectifier cases in this way, a practical understanding will be obtained of why the critical inductance never goes to infinity in this manner.

Half-Controlled Single-Phase Bridge Rectifier

Fig. 4 shows the circuits of some commonly used half-controlled single-phase rectifiers. In the bridge circuits note that two of the diodes are controlled (thyristors) and the other two are uncontrolled (diodes). Referring to Fig. 4(a) it will also be seen that it has been necessary to add an extra 'bypass'* diode at the output of the bridge; this is necessary in the case of inductive loads to prevent the possibility of uncontrolled current flow through the thyristors. This could otherwise occur at the end of each half-cycle when inductively-maintained current would flow in a closed loop through a thyristor and its adjacent diode, e.g. MR_1-SCR_1 in Fig. 4(a). MR_3 acts to bypass this diode-thyristor circuit; it clamps the output voltage to zero and turns off the previously conducting thyristor.

Figs. 4(a), (b) and (c) show possible variations in the positions taken by the thyristors, a particular configuration being chosen to suit the preferred requirement in any given application. For example, (a) has the advantage of offering common thyristor cathodes so that only a three-terminal gate triggering source is necessary: (b) offers common thyristor anodes, and, since the anode is generally the stud of stud-ended thyristors, this arrangement allows a common heat sink to be used; (c) provides a series diode path from negative to positive d.c. rails without the necessity of adding a further by-pass diode.

Fig. 4(d), the push-pull circuit, is included to complete the family of single-phase full-wave controlled rectifier circuits, although it will be clear that this is a full-controlled rectifier in its own right unlike the bridges which have been shown; it may be used satisfactorily with or without the bypass diode, the advantage offered by adding the diode being a lower value of critical inductance at all firing angles. When used with the bypass diode the choke inductance, and current and voltage waveforms, are

Fig. 4. Half-controlled single-phase bridge and push-pull rectifiers

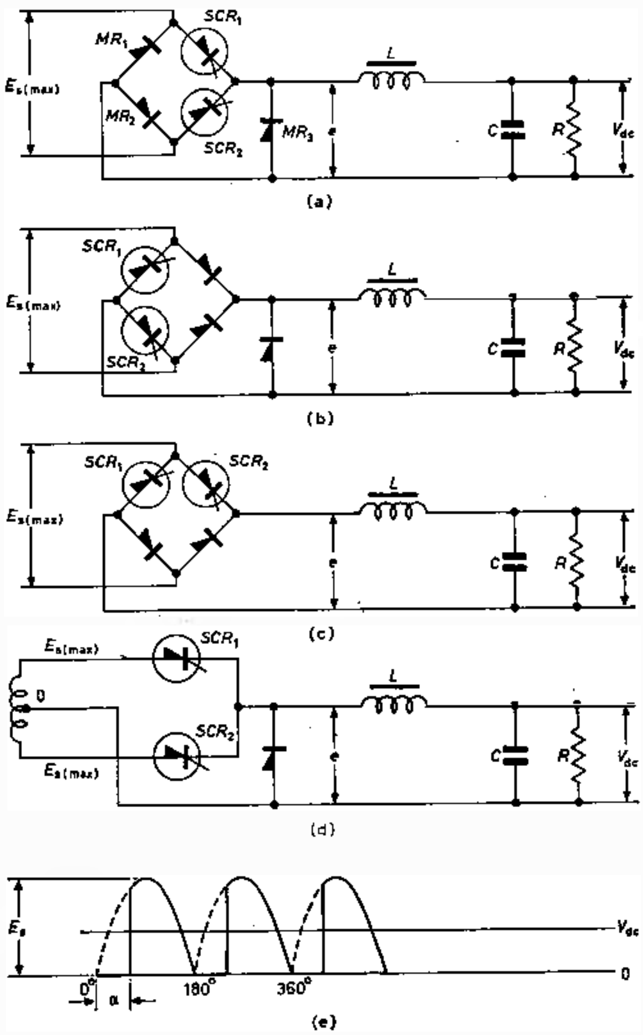

* Sometimes called 'commutating', 'free-wheel' or 'flywheel' diode.

identical to those of the three bridges and therefore no separate analysis is needed.

The voltage waveform, Fig. 4(e), applies to all the circuits shown in this figure. Note the zero-clamped voltage between phase angles of 0° to α and the consequent fact that all these circuits require a range of phase control between angles of 0° and 180° instead of only 90° as for full-controlled rectifiers.

An important point of difference with these circuits compared to the full-controlled one previously discussed is that, at zero output, there is neither d.c. output voltage nor a.c. Therefore a.c. ripple current is automatically attenuated as well as d.c. when α is retarded, which as observed did not happen in the full-controlled bridge. The significance of this is that the critical inductance does not soar to infinity as the output approaches zero; by observing the ratio of a.c. to d.c. as α approaches 180° it is found that, as so often happens, nought divided by nought turns out to be finite and hence the critical inductance is finite right down to zero output.

An expression for $\omega L_c/R$ can be worked out by a similar method to that shown previously for the full-controlled circuit. However, the integration is a little more complicated owing to the discontinuity in the waveform caused by the zero clamping. The equation for the mean d.c. output voltage remains a simple function of α at all angles, but the equation of the instantaneous rectifier output voltage, e, is different above and below any chosen value of α. ($e = 0$ up to the firing point and $e = E_s \sin \omega t$ above the firing point.) As before, there are two sets of results according to whether α is low enough to bring the d.c./a.c. voltage waveform intersection on to the sinusoidal part of the waveform, or is high enough to make the intersection occur on the rising edge of the triggered waveform. The results are as follows:

For values of α between 0° and 35·5°

$$\left(\phi = \sin^{-1}\frac{1+\cos\alpha}{\pi}\right)$$

$$i = E_s/\omega L_c\left[\cos\phi - \cos\omega t + \left(\frac{1+\cos\alpha}{\pi}\right)(\phi - \omega t)\right]$$

from $\omega t = \alpha$ to π

$$i = E_s/\omega L_c\left[1 + \cos\phi + \left(\frac{1+\cos\alpha}{\pi}\right)(\phi - \omega t)\right]$$

from $\omega t = \pi$ to $\pi + \alpha$

$$I_{dc} = E_s/\omega L_c\left[\cos\phi + \frac{\alpha+\sin\alpha}{\pi} + \left(\frac{1+\cos\alpha}{\pi}\right)(\phi - \alpha - (\pi/2))\right]$$

$$\omega L_c/R = \phi - \alpha - (\pi/2) + \frac{\alpha + \sin\alpha + \pi\cos\phi}{1+\cos\alpha}$$

For values of α between 35·5° and 180° ($\phi = \alpha$)

$$i = E_s/\omega L_c\left[\cos\alpha - \cos\omega t + \left(\frac{1+\cos\alpha}{\pi}\right)(\alpha - \omega t)\right]$$

from $\omega t = \alpha$ to π

$$i = E_s/\omega L_c\left[(1+\cos\alpha)\left(1 + \frac{\alpha - \omega t}{\pi}\right)\right]$$

from $\omega t = \pi$ to $\pi + \alpha$

$$I_{dc} = E_s/\omega L_c\left[\frac{\alpha + \sin\alpha}{\pi} - \frac{1-\cos\alpha}{2}\right]$$

$$\omega L_c/R = -(\pi/2) + \frac{\alpha + \sin\alpha + \pi\cos\alpha}{1+\cos\alpha}$$

The expressions for $\omega L_c/R$ are plotted as the continuous full line curve of Fig. 5, which is normalized for 50c/s. The dotted line shows the full-controlled curve for comparison. To facilitate the comparison the abscissa is taken as 'percentage of maximum d.c. output voltage' rather than 'firing angle α' as in Fig. 3; this is a more convenient common scale owing to the difference in range of α needed for the two cases. It will be noted that at any chosen percentage output setting the inductance required in the half-controlled case is lower than that in the full-controlled case; furthermore, at zero output the inductance-to-load ratio is finite in the half-controlled case whereas it is infinite in the full-controlled case.

Fig. 5. Comparison of critical inductance requirements for half and full-controlled single-phase bridge rectifiers

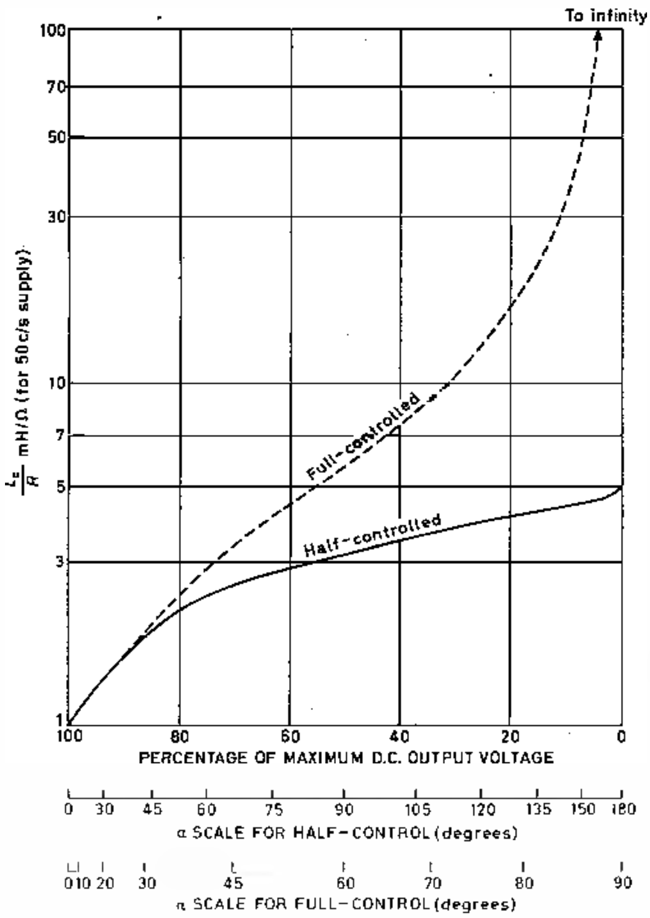

REFERENCES

1. TERMAN, F. E. Radio Engineering, p. 561 (McGraw-Hill Book Company Inc. 1947).
2. OVERBECK, W. P. Critical Inductance and Control Rectifiers. *Proc. Inst. Radio Engrs.* p. 655 (Oct. 1939).
3. SEELY, S. Electron-Tube Circuits, p. 304 (McGraw-Hill Book Company Inc. 1950).

(To be continued)

An Off-line Punched Card to Punched Tape Convertor

By D. W. W. Rogers*, A.M.I.E.R.E.

This article deals with the design of a punched-card to punched paper tape convertor. A commercial punched card reader capable of reading at 22 cards a minute, transfers the information stored on twelve holes of the punched card, via suitable logical networks, to buffer storage. A Teletape 110 high speed tape punch then transfers the information stored in the buffer to eight hole punched paper tape. A 64 character plugboard prior to the buffer storage enables information to be re-arranged, deleted and inserted on to the tape, thus providing inherent flexibility. A high order of reliability is achieved by the use of direct coupled resistance logic, simple circuits and economy of components. Self checks are provided to detect errors in the punched card, and a KDF9 even order parity check is built into the logical networks. Semiconductors are used throughout.

(Voir page 273 pour le résumé en français: Zusammenfassung in deutscher Sprache auf Seite 280)

A REQUIREMENT arose for an off-line punched card to paper-tape convertor in order to translate various codes on a punched card to that of the KDF9 paper tape.

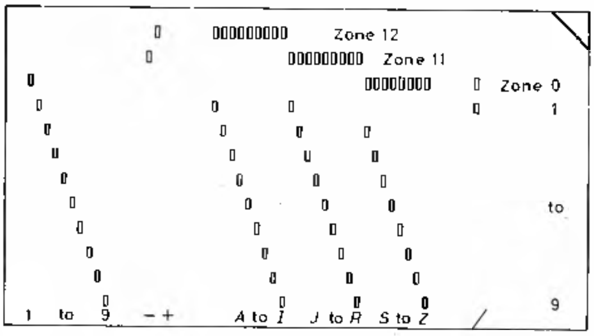

Fig. 1. Punched card

Specimens of a card and tape respectively are shown in Figs. 1 and 2.

The input and output equipment of commercial card handling channels are usually limited to their own unique commercial codes. For example the cards, although generally having the same external dimensions, may differ in various aspects which include rectangular or circular holes, different codes and various forms of printed timing marks which indicate by optical means the precise hole location.

A simplified diagram of the convertor is shown in Fig. 3, from which it may be seen that two proprietary pieces of equipment are required. These are the card reader and the tape punch. The choice concerning the particular type of punch rests on two facts. In the first place it is advantageous to use the same type in the convertor as employed in the particular KDF9 computer in order to provide a spare punch for both the computer itself and the convertor. Secondly, as a comparatively slow punching speed is compatible with the convertor, the type 110 Teletape punch has been chosen, and its specification (Fig. 4) is sufficient to formulate a design for the convertor.

The maximum punching speed of the type 110 Teletape punch is limited to 110 characters/sec. This latter speed sets, in turn, an equivalent limit to the number of cards read per minute. For example—110 characters/second = 6600 characters/min, so that an equivalent 'end on' card reading speed corresponds to $6600/(80\times2) = 41$ cards/min, if an arbitrary space equivalent to one card is allowed between cards. Clearly the tape punch must be faster than the reader to avoid missing characters.

At first it may appear that with suitable modification to

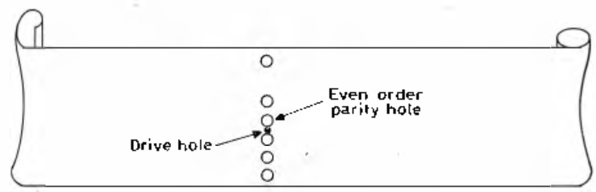

Fig. 2. KDF9 tape

Fig. 3. (a) Simplified diagram of convertor
(b) Circuit diagram of bistable store
(c) Arrangement of buffer store

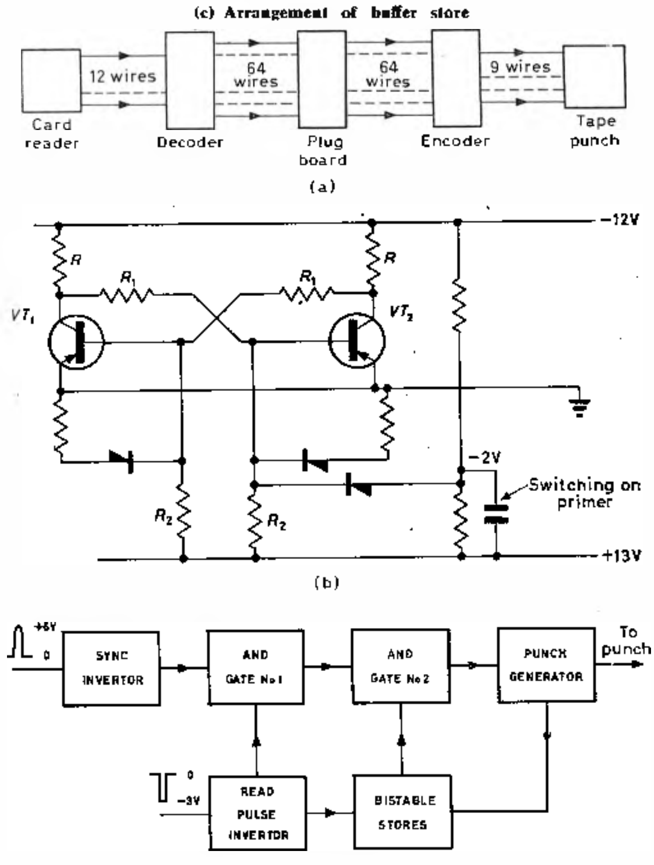

* *Oldham Technical College, Lancashire.*
The author holds the Diploma of Graduate Studies of the University of Birmingham.

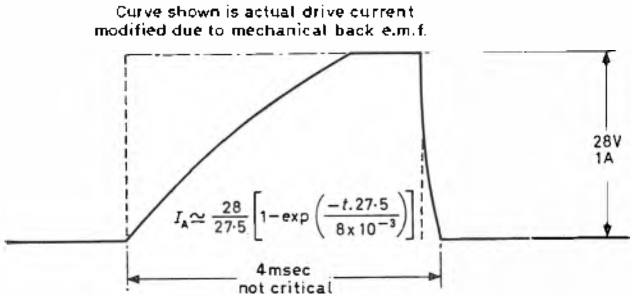

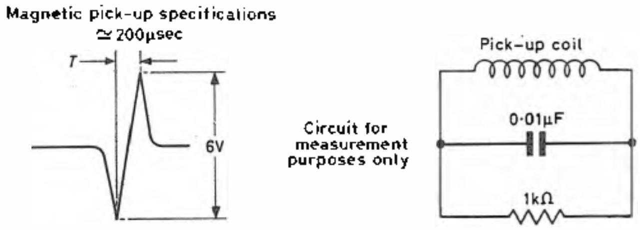

STANDARD SPEEDS

(1) 110 operations (or characters) per (1 100 words per minute).
(2) 63·3 operations (or characters) per (633 words per minute).

MAGNET SPECIFICATIONS

	Transistor Operation	Valve Operation
Attract Time (msec)	2	2
Release Time (msec)	2	2
Magnet Coil Resistance (Ω)	2·9	74-82
Magnet Coil Inductance (mH)	8	100
External Current Limiting Resistance (Ω)	25	686-694
Code and Feed Pulse Requirements		
Current (A) (I)	1	0·150
Voltage (d.c.)	28	115
Length (msec)	4 ± 10%	4 ± 10%

Fig. 4. Teletype 110 card punch specifications

easily capable of dealing with 300 cards/min, there is still ample margin for future improvements if and when the need arises. As the requirement is for a special purpose one-off low-speed convertor, the major aspect of design is centred on reliability and simplicity. The 'end on' card convertor is therefore a natural choice and eliminates the need for large buffer stores and counters, which would be necessary for a 'broadside on' reader.

The particular card reader to be used reads twelve holes at a time by means of twelve brushes which make contact through the holes with an electrically conductive plate, which in addition to being a conductor, partially supports a tray in which the cards are read. A typical card reading cycle is of the order of 40 holes per second with 0·75sec between cards, operated by means of dogtooth escapement mechanisms, which may be arrested. Similarly the card selector mechanism can be arrested during a cycle except for the case when a card is reading the 80th hole. It is not possible to arrest the card, once it is in motion in a high speed reader.

General Description of the Convertor

Where possible direct resistance coupling is employed in order that the logic will function at zero frequency. In this way any particular card character may be simulated indefinitely and fault-finding is simplified. For the same reason passive diode gating is preferred in view of its simplicity and effective clamping properties. The AND-OR gates of the decoder-encoder are driven initially from low impedance sources, namely 300Ω about earth potential, to provide adequate protection from spurious impulses, and to minimize the pyramid ratio. The 64 hole plug-board located at the interfaces of the decoder and encoder is therefore also in shunt with this low impedance source,

Fig. 5. Tape and Card Coding

	TAPE HOLES	CARD HOLES		TAPE HOLES	CARD HOLES
0	0 0 0 0 1 1 0 0	0	T	0 0 1 0 1 1 1 0	3
1	1 0 0 0 0 1 0 0	1	U	1 0 1 0 0 1 1 0	4
2	0 1 0 0 0 1 0 0	2	V	0 1 1 0 0 1 1 0	5
3	1 1 0 0 1 1 0 0	3	W	1 1 1 0 1 1 1 0	6
4	0 0 1 0 0 1 0 0	4	X	0 0 0 1 1 1 1 0	7
5	1 0 1 0 1 1 0 0	5	Y	1 0 0 1 0 1 1 0	8
6	0 1 1 0 1 1 0 0	6	Z	0 1 0 1 0 1 1 0	9
7	1 1 1 0 0 1 0 0	7	+	1 0 1 1 0 1 0 0	12
8	0 0 0 1 0 1 0 0	8	−	0 1 1 1 0 1 0 0	11
9	1 0 0 1 1 1 0 0	9	NO HOLES	0 0 1 0 1 0 0 0	NO HOLES
A	1 0 0 0 0 0 1 0	1 12	/	1 1 1 1 0 0 0 0	0 1
B	0 1 0 0 0 0 1 0	2 12		0 0 1 1 1 1 0 0	;
C	1 1 0 0 1 0 1 0	3 12		1 1 1 1 1 1 0 0	.
D	0 0 1 0 0 0 1 0	4 12		1 1 0 1 0 1 0 0	SUBSCRIPT
E	1 0 1 0 1 0 1 0	5 12		0 1 0 1 1 1 0 0	÷
F	0 1 1 0 1 0 1 0	6 12		1 0 1 1 1 1 1 0	→
G	1 1 1 0 0 0 1 0	7 12		0 1 0 0 1 0 0 0	NEW LINE
H	0 0 0 1 0 0 1 0	8 12		0 1 1 0 0 0 0 0	SHIFT
I	1 0 0 1 1 0 1 0	9 12		1 1 1 0 1 0 0 0	NORMAL
J	0 1 0 1 1 0 1 0	1 11		0 0 0 0 1 0 0 1	SPACE
K	1 1 0 1 0 0 1 0	2 11		0 1 1 1 1 1 1 0	ESCAPE
L	0 0 1 1 1 0 1 0	3 11		1 1 1 1 1 1 1 1	DELETE
M	1 0 1 1 0 0 1 0	4 11		0 1 0 1 0 1 0 1	ERROR AND STOP
N	0 1 1 1 0 0 1 0	5 11			
O	1 1 1 1 1 0 1 0	6 11			
P	0 0 0 0 0 1 1 0	7 11			
Q	1 0 0 0 1 1 1 0	8 11			
R	0 1 0 0 1 1 1 0	9 11		TOTAL OF 52 CHARACTERS	
S	1 1 0 0 0 1 1 0	2			

the motorized driving mechanism, that a faster card reader could be adequately slowed down. This scheme is unsuitable, however, as only the speed of the card selection may be reduced. The 'end on' platform traversal speed is generally unaltered and although an appropriate store could make such a system feasible, the additional equipment and complication is undesirable. Fortunately there is a commercial end-on card reader with a speed of 22 cards/min. The maximum number of cards that may be read in a year with this speed is about three and a half million, assuming a forty hour, five day week. This reading speed therefore is entirely adequate to meet most requirements, and as the circuit to be described is and the capacitive loading of the plugboard is minimized at zero logic level. The convertor logic may be divided into two sections:

(1) The input interface.

(2) The output interface.

THE INPUT INTERFACE

It is necessary to have some mechanism whereby the read pulse from the card reader may accurately be strobed, in order that the data on the card may be correctly interpreted and fed in an accurate sequence of pulses to the AND-OR gate matrices as the card is fed longitudinally under the array of brushes. This mechanism is complicated by the fact that the motion of the card during reading is non-uniform with respect to time. In addition it is necessary to distinguish between two cases when the brushes make contact. In the first case when the reading tray is vacant, and secondly when the tray is occupied and the brushes are located in the holes of the card. Similarly it is necessary to have some means whereby the reader can identify the leading and trailing edges of the card when the brushes will not be in contact and also the small piece of card between any two holes. The timing of the strobe pulses may be generated in a variety of ways, of which the following method used in commercial card readers has the distinct advantage of being directly related to the cards' motion. After the commencement of a card cycle, and a card has been selected from the stacking containers, it will come to rest in the card tray. The card tray locates the card in a predetermined position ready for reading, and by means of a floating cam, dog and escape mechanism, the tray will move, holding the card a distance corresponding to one hole at a time over the 12 brushes. The dog and escape mechanism closes simultaneously a switch, and in this way provides a timing pulse for the strobe at each of the 80 holes in the card. As the strobe timing pulses are initiated only by the stepwise movement of the tray, the AND-OR logical network will register 'no holes' if the tray is vacant. However, by means of suitable logic, controlled by a brush on the card tray which is only closed when the tray is occupied by a card, the 'no holes' character shown in Fig. 5 is inhibited, and therefore the tape is neither punched nor stepped forward. A similar closed brush located on the card tray energizes the dog and escape mechanism. When the tray is occupied and the 'SKIP' switch is 'ON', a 'no holes' signal from the card will punch the appropriate KDF 9 coding shown in Fig. 5, and step the tape forward for the next character. However, if a 'no holes' signal occurs when the 'SKIP' switch is at 'OFF' position, the 'no holes' signal permanently inhibits the punch synchronization pulse and resets the read cycle switch. In this case the card tray completes the 80 holes reading cycle, but does not commence the next read cycle until the 'READ' switch is depressed again. The strobing pulse shown in the timing diagram of Fig. 6 is necessary for the following reasons:

(a) In order to prevent transients and contact chatter from the brushes causing faulty reading of the holes.

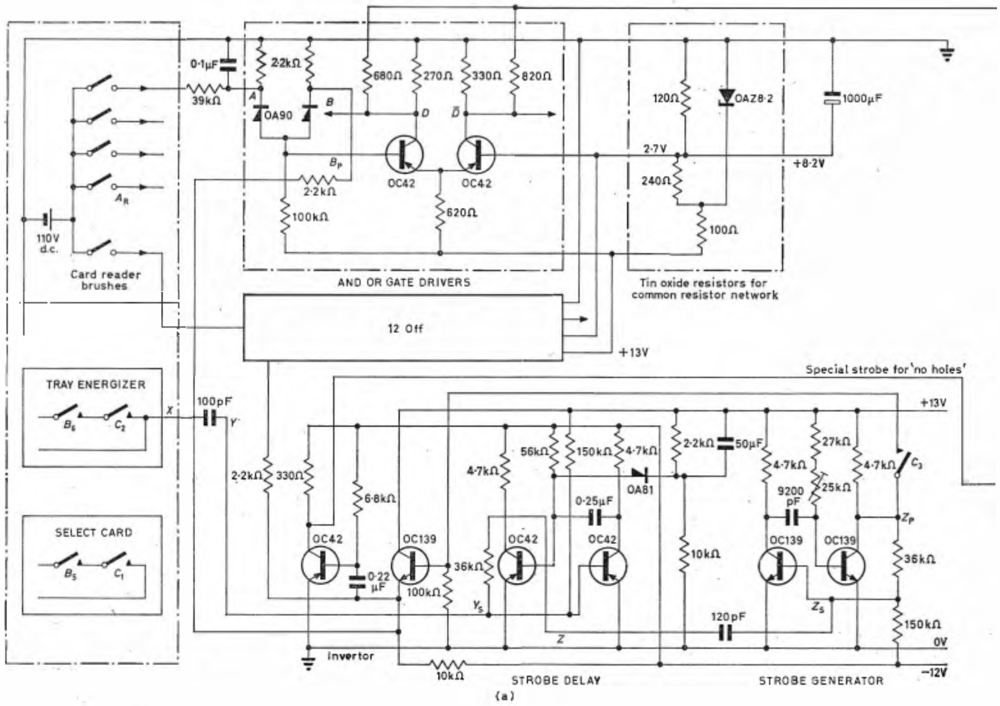

Fig. 6(a) (above and right). Detailed circuit of the convertor

Fig. 6 (b) (below). Timing diagram

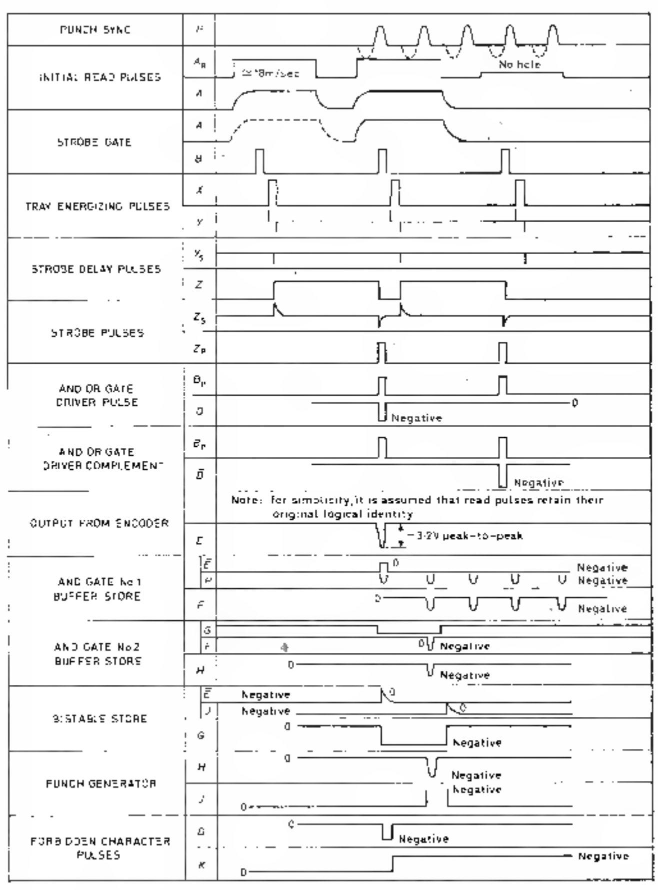

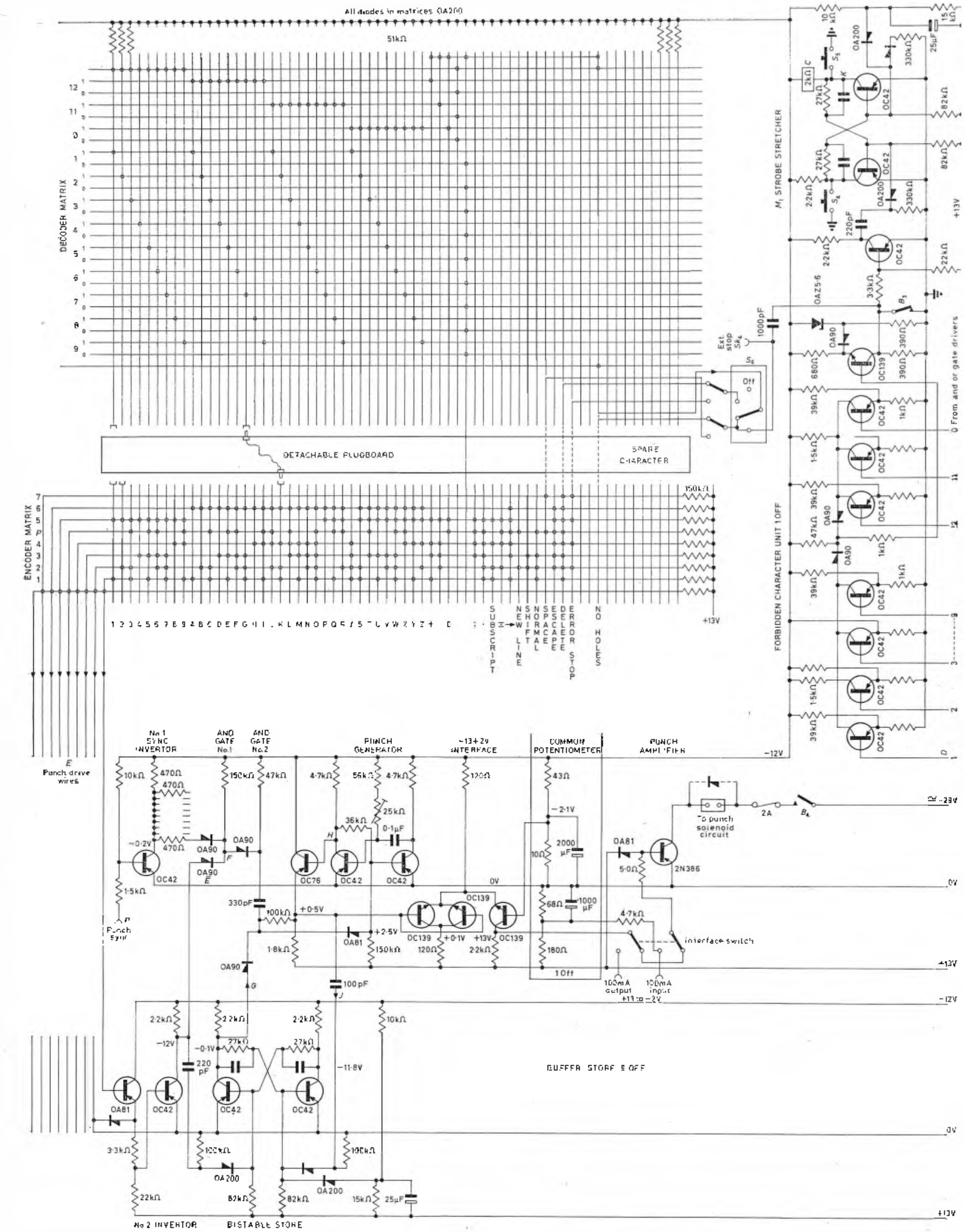

(b) Clearly within practical limits the short width of the strobe pulse minimizes the initial error of alignment of the twelve punched holes in the card due to the actual perforating tool, providing the error is less than half the width of one hole. (Such a large error is very improbable).

(c) Given approximately the same central location, it is possible to read cards having circular or rectangular holes.

A simple *RC* integrating network, shown in Fig. 3(a), with a time-constant of 4msec serves to ensure that the actual read pulse is partially smoothed before strobing. The strobe pulse, delayed by the strobe delay unit, and the 12 read pulses are fed via the driver and gates to the AND-OR gate drivers, shown in Fig. 3(b), the latter circuits supplying the AND-OR gate matrices with a parallel 12 hole negative logic corresponding to each column of the card.

The Output Interface

The Teletape 110 tape punch provides a 6V synchronizing pulse, see Fig. 4, which occurs approximately every 9msec. This pulse indicates the time at which the punch unit is ready to receive; the timing of the pulse is adjustable for varying conditions of operation. As the punching speed is faster than the hole reading speed of the card reader, and in any case the hole pulses will occur irregularly, it is necessary to have a one bit memory, which holds the read pulse until a punch synchronizing pulse occurs. This latter pulse in the store and the punch synchronizing pulse then operate an AND gate which triggers in turn a 4msec pulse from the punch generator, which is of the correct duration to operate the tape punch unit. A main shaft in the tape punch unit transfers motion from the solenoids, energized by the punch amplifiers, to the tape feeding and perforating mechanism. Under the control of the code solenoids, the perforating mechanism punches code holes in the tape by means of pins in a punch block. A pin not under the control of a solenoid is driven through the tape to punch a feed hole with every code combination. Each time a code combination is perforated the feed mechanism, under the control of a feed solenoid, advances the tape by means of a ratchet and feed wheel arrangement. The trailing edge of the 4msec pulse from the punch generator resets the bistable store.

In order to make the punch unit of the convertor interchangeable with that of the main computer, a -13 to $+2$V interface is provided. This facility is built into the convertor by means of a long-tailed npn pair, which can deliver 100mA peak-to-peak at the appropriate d.c. level to the 2N386 power amplifiers, which will in turn feed 28V peak-to-peak at 1A to the punch solenoids, and tape feed mechanism.

Three power supplies are required. Two stabilized d.c. supplies providing -13V and $+12$V 2A lines with respect to earth and an unstabilized supply of 28V at 4A. The two stabilized supplies are provided with an interlocking system which ensures that the two supplies are either on together or both off. Further, the 1A solenoid driver amplifiers cannot be energized until the two stabilized supplies are switched on. This safety precaution ensures that the base supply to the 2N386 drivers is established and safeguards the punch solenoid circuits when switching on the convertor.

Logical Networks

The main logical network, shown in detail in Fig. 6(a), is concerned with translating 12 bits at a time from the card into the alphabet, the numbers 0 to 9, and the characters /, +, −. These 39 cyphers together with the corresponding code of the KDF 9 tape are tabulated in Fig. 5.

In each column are twelve punching positions, one each for the digits 0 to 9, and one each for the zones 0, 11 and 12. When the '0' is punched alone in a column it represents the digit zero. Digits are recorded by punching a single hole in the corresponding digit (or zero) position of the desired column. A letter is recorded as a combination of one zone and one digit punch in the desired column.

For example, A is recorded by holes in the 12, (X) zone and the digit 1 positions, N by 11 (Y) zone and the digit 5 positions, and Z by a 0 (zero) zone and the digit 9 positions.

The 'no holes' and 'forbidden character logic' is operative only after certain operations involved in switching on are completed. Such precautionary measures are necessary to avoid faulty operation due to switching transients. Accordingly the system logic will be described in a chronological order from the time of switching on. Such a timing sequence is most easily built into the convertor by means of interlocking relays. As all of these relays will only be concerned with an occasional switching during the switching-on period, a possible decrease in reliability due to the extra components should be amply offset by the improved operational facilities. The partial fault-finding provided by the automatic indicator lamps is essential for maximum availability.

Description of Circuit Action

The control sequence is described in relation to Fig. 7.

(1) The spring return switch S_1 labelled 'operate' on the control panel is depressed to ON; indicator lamps Lp_1, Lp_3 and Lp_7 being illuminated if the -12 and $+13$V stabilized power supplies, the -28V power supply, and the card reader are energized with 230V a.c.

(2) The internal double pole d.c. isolating switch S_2 is normally left in the ON position, so that the indicator lamps Lp_2 across the stabilized outputs will both be illuminated, if the supplies are available.

(3) If both of the d.c. stabilized supplies are available together, within a predetermined small interval of time, the differential relay A, will not trip the main a.c. cut-out contacts A_1. If these conditions are satisfied, relay B will be energized by the full 25V, closing contacts B_1, B_2, B_4, B_5, B_6 and opening contacts B_3. Thus the -28V supply is available after approximately 4msec; the forbidden character unit, and the tape punch are now in the 'ready to read' condition. The card reader is also primed for 'read'. The indicator lamp Lp_4 illuminates if the -28V supply is available.

(4) When the double-pole marginal test switch S_3 switches the -12V supply to -11V, the differential relay A is automatically compensated in order to keep the differential current well below the threshold a.c. cut-off level.

(5) Assuming that the indicator lamps, Lp_1, Lp_2, Lp_3, Lp_4, Lp_5 and Lp_7 are now all illuminated, the logical networks are now operative, including the forbidden character unit, which was held off by contact B_3 initially to avoid an inadvertent 'error pulse' triggering relay C. The 200μsec synchronizing pulse is now available, but the tape punch will not perforate the tape, or step-forward 'one hole' until the card reader spring return switch S_5 is depressed, when the bistable stores subsequently receive logical information after a card has been selected and placed into the card tray.

(6) After the spring return switch S_5 has been depressed, the card cycle will commence due to the closing of contacts C_1, C_2 and C_3. At this time assuming that the forbidden character unit has not detected an 'error', the card after selection will come to rest in the reading tray. The card at this time has closed a pair of brush contacts, which complete the circuit of the dog-tooth, escapement solenoid. The card tray will then be stepped forward one hole across the reading platform. Simultaneously the strobe delay unit will be triggered, the subsequent delay being sufficient to place the strobe pulse in the centre of the first hole in the card.

(7) Assume now that the card is traversing the card reading platform, and the forbidden character unit detects an error. The bistable multivibrator M_1 is triggered, opening contacts C_1, C_2, C_3 and C_4. The dog-tooth and escapement energizer, the select card mechanism and the strobe pulse are all arrested, and the 'read' lamp Lp_6 is switched off. The tape punch will print either an 'error' or 'delete' cypher according to the operator's requirements.

(8) When the card reader encounters a 'no hole' column, the convertor will obey one of the following instructions determined by the position of the 'skip' control.

(a) The tape punch perforates the cypher 'no holes' or 'space,' both the card selector mechanism and the tray energizer being arrested. This action is accomplished by closing S_6 before reading is commenced, i.e. the 'skip' control is turned to 'no holes —stop.'

(b) The tape punch perforates the cypher for the 'no holes' or 'space,' but the card reader tray will travel forward at high speed, due to the prewired instructions of its own plug board and 'emitter.' In this case the strobe trigger is inhibited by the card reader's own logic. The 'skip' control is turned to 'skip one hole,' which opens S_6. The card reader will commence reading again at a character predetermined by its own plug board.

The 'no holes' operation is fundamental to the operation of the convertor, and a detailed explanation of this function and the 'release' mechanism will now be given. Assume that a set of strobed read pulses register 'zero' for 'no holes', (note that the strobe at this time is generated from the last hole) when the 'no holes' AND gate will load the store. The dog tooth escapement energizer moves the tray forward so that the next column of the card is over the 'read' brushes. If the no-holes-

Fig. 7. Detailed diagram of convertor

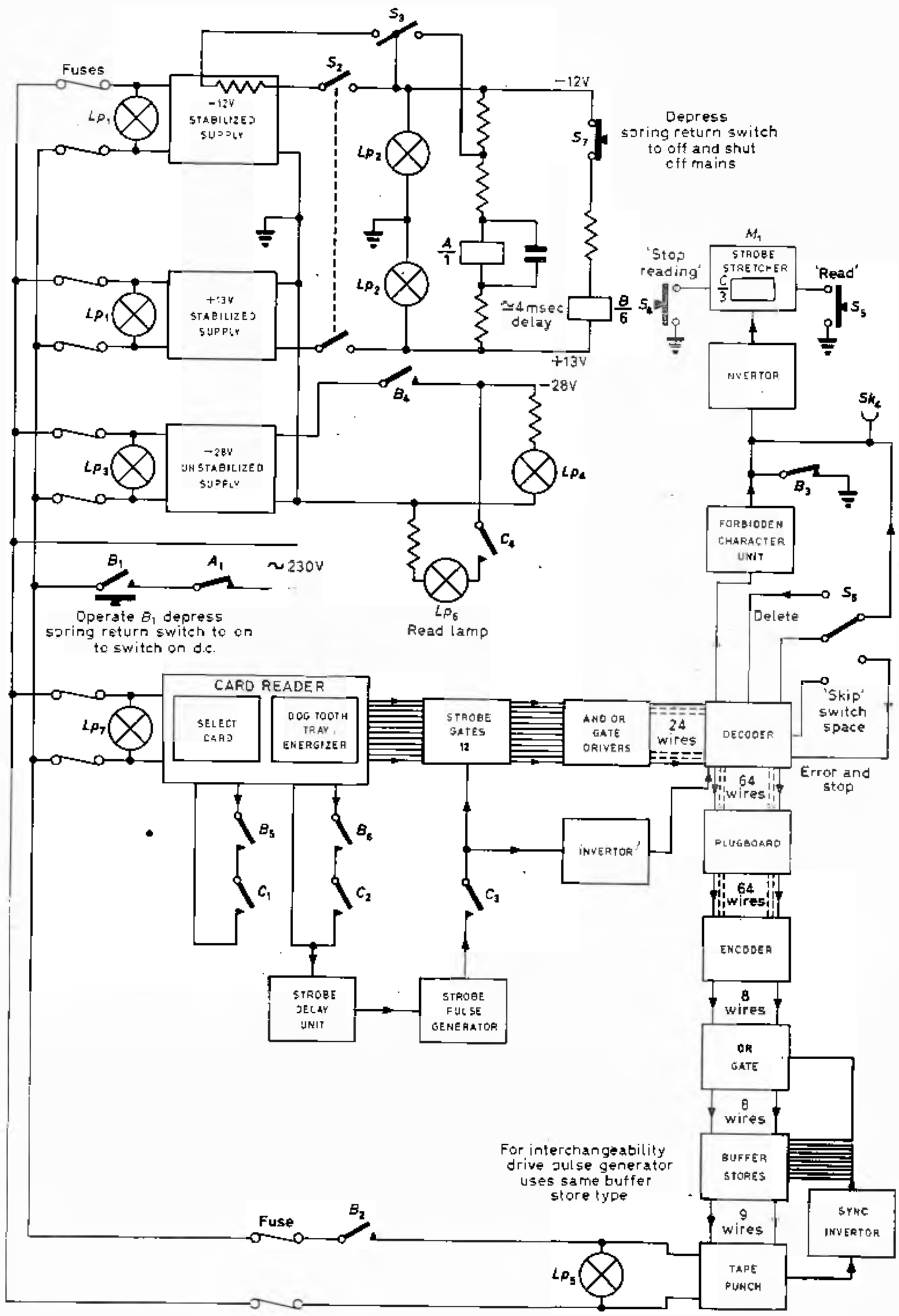

'stop' position on the 'skip' control is engaged, then contact C_3 has disconnected the output of the strobe generator and also the 'no holes' AND gate of the decoder. By this means the tape punch will perforate the 'no holes' cypher once and then stop. Both the card cycle and the tray energizer are now immobile. The operator after removing the card, will depress the spring return switch labelled 'release' on the control panel, thereby closing S_5. The card reader will now be ready to receive the next card. Alternatively, after depressing the 'release' switch S_5, the card already in the tray will automatically step forward one column, leaving the 'no holes' column behind. and recommence reading. This action should be initiated by means of the 'no-holes-stop' position on the 'skip' control. Of course the same procedure would take place for a forbidden character error.

A switching input socket SK_1 is provided to trigger the pulse stretcher M_1, and arrest the card reader by means of an external source.

Decoder Matrix Logic and Minimization

The logical networks for the 39 characters could rapidly be deduced by a cut and try method. However, the following method employing the principle of factorization is simpler and more informative. It depends on the properties of a cannonic symmetrical Boolean term defined by Shannon.

Let A = zone 12

B = zone 11

C = zone 0

D = 1 to 9

then the Boolean function for the 39 characters is:

$$F_B = \underset{12}{A\bar{B}\bar{C}\bar{D}} + \underset{\text{or } 11}{B\bar{A}\bar{C}\bar{D}} + \underset{\text{or } 0}{C\bar{A}\bar{B}\bar{D}} + \underset{\text{or } A \text{ to } I}{A\bar{B}\bar{C}D} + \underset{\text{or } J \text{ to } R \text{ or} /,}{\bar{A}B\bar{C}D} +$$

$$\underset{S \text{ to } Z}{\bar{A}\bar{B}CD} + \underset{\text{or } 1 \text{ to } 9}{\bar{A}\bar{B}\bar{C}D}$$

collecting terms:

$$F_B = [A\bar{B}\bar{C} + \bar{A}B\bar{C} + \bar{A}\bar{B}C][D + \bar{D}] + \bar{A}\bar{B}\bar{C}D$$

$$= (A + B + C)[\bar{A}\bar{C} + \bar{A}\bar{B} + \bar{B}\bar{C}] + \bar{A}\bar{B}\bar{C}D$$

Clearly the factor $\bar{A}\bar{C} + \bar{A}\bar{B} + \bar{B}\bar{C}$ is a cyclic common term and may be omitted as the remaining terms are still unique with respect to $\bar{A}\bar{B}\bar{C}D$

$$\therefore\ F_B = (A+B+C)D + (A+B+C)\bar{D} + D[\bar{A}\bar{B}\bar{C}]$$

ALPHABET, or 12 or 11 or '0' or Number 1 to 9

$\therefore$ Number of diodes $= 6\times9+3\times2+9 + 9\times2\times3 =$ 90 diodes + 3 extra for 'no holes' as D saves 9 diodes

$\therefore$ diodes saved $= 268 - 93 = 175$ at least.

The decoder matrix is shown in detail in Fig. 6(a).

The 'no holes' AND gate in the decoder includes an AND gate for the strobe alone, in order to distinguish a 'no hole' and the pieces of card adjacent to it. Accordingly, the 'no holes' cypher will only be punched when a card column is unperforated. This action is shown in the timing diagram Fig. 6(b). Three additional diodes are required for this purpose.

Encoder Matrix Logic

The encoder is basically composed of 52 sets of OR gates which translate the literal cyphers into the KDF9 code.

The number of perforated holes for each character in the paper tape must be even.

This even order parity code is built into the encoder as shown in Fig. 6(a). By this means the extra equipment in terms of binary counters and stores normally required to provide parity is avoided. However, although parity introduced in this way, breaks up the symmetry by which an effective minimization, and hence an economy in diodes may be achieved, this is a minor consideration as the cost of the diodes in the encoder is small. Of far greater importance is the fact that the simple direct coupling shown in Fig. 6(a) is more reliable and conducive to easy fault finding.

Forbidden Character Check

The forbidden character unit is shown in detail in Fig. 6(a). If more than two zones occur simultaneously (12, 11 and 0) or more than two numbers occur simultaneously (1 to 9), a negative going pulse of 3·4V magnitude appears at the collector of the OC139 detector stage.

The design employs the emitter-follower property, in order that a given base voltage will produce a very precise proportioned voltage in the collector circuits of the OC42's. The OC42's are normally held off, by 0·3V bias, due to the 0·3mA emitter forcing current. The object of this small bias is to off-set the −0·3V worse case 'zero'.

By means of this analogue method, the OC139 output stage is still maintained in an off position when one OC42 stage of the forbidden character unit switches on. However, the voltage drop in the common 1·5kΩ collector resistor, is approximately twice as large when two OC42 stages switch on. In this case the voltage drop is sufficiently large to switch the OC139 detector stage hard on. The 1 to 9 and the 0, 11, 12 zones analogue sections are separated from each other by means of a simple OR gate.

By means of the OC139, the effective biasing arrangements using the Zener diode OAZ5·6 and the point contact diode OA90, two advantages are obtained. Firstly the pyramid ratio is held constant, and secondly the complete forbidden character unit is sensitive to the variations in only the −12V supply, assuming that the −0·3V 'zero' bias level is not greatly exceeded. The voltage levels corresponding to the detector stage being 'on' and 'off' are shown in Fig. 6(a).

Bistable Multivibrator

The multivibrator is triggered capacitively, and series diodes are arranged to disconnect, after passing the desired impulse. The silicon diode OA200 gives a twofold advantage in this application. Firstly the exceedingly high reverse resistance, and secondly the forward bias of −0·1V between the base and emitter of an 'on' transistor shown in Fig. 3(b) is insufficient to bring the 100kΩ earth return resistor fully into play. The differentiating capacitors were optimized for minimum capacitance under marginal conditions in order to obtain reliable triggering and minimum reaction between the multivibrator and adjacent circuits.

Calculations of R_1 and R_2

As $R_1 \gg R_L$, then $I_{sat} = 12/2{\cdot}2 \,.\, 10^3 = 5{\cdot}45$mA and $\alpha_{min}' = 40$, $\therefore$ 0·25mA base current is adequate to give saturation. Assume from OC42 curves that $V_{c(sat)} = -0{\cdot}14$V, $V_b = -0{\cdot}2$V, and $I_{co} = -1{\cdot}5\mu$A max., VT_1 is in saturation, then:

$$12 - 0{\cdot}14 = 2{\cdot}2\,(10)^3\,[1{\cdot}5 \,.\, 10^{-6}] + [R_1 + 2{\cdot}2 \,.\, 10^3]\,[0{\cdot}25 \,.\, 10^{-3} + (13{\cdot}2/R_2)] \quad \ldots\ldots\ldots \quad (1)$$

Further assuming a safe base cut-off voltage of +3V, then:

$$\frac{13-3}{R_2} = 1{\cdot}5\,(10)^{-6} + (3{\cdot}14/R_1) \quad \ldots\ldots \quad (2)$$

Solving equations (1) and (2):

$$0{\cdot}25\,.\,10^{-3}R_1^2 - 7{\cdot}16R_1 + 9{\cdot}14\,.\,10^3 = 0$$

giving values for R_1 and R_2 of 27·3kΩ and 86kΩ respectively. Accordingly the preferred values of 27kΩ and 82kΩ were chosen for R_1 and R_2 respectively. Tolerances of ±5 per cent are adequate in view of the generous initial assumptions made in respect of $I_{b(sat)}$ and the safe base cut-off voltage.

PUNCH GENERATOR

The design of the monostable multivibrator is similar to that above for the resistive coupling R_1 and R_2.

$$V_{cc} - V_{bs} = -R_L I_{co} + (R_1 + R_L)\, I_{bs} + \frac{V_{bb} + V_{bs}}{R_2} \quad \ldots\ldots \quad (1)$$

and:

$$\frac{V_{bb} - V_{bo}}{R_2} + I_{co} = \frac{V_{bo} + V_{cs}}{R_1} \ldots\ldots\ldots \quad (2)$$

$R_L = 4{\cdot}7$kΩ, I_{bs} say 0·2mA, i.e., $1{\cdot}5\,.\,I_{b(sat)}$ and $V_{bo} = -2{\cdot}5$V then $11{\cdot}86 = -4{\cdot}7\,.\,10^3\,.\,1{\cdot}5\,.\,10^{-6} + (R_1 + 4{\cdot}7\,.\,10^3)$

$$(0{\cdot}2\,.\,10^{-3} + (13{\cdot}2/R_2) \ldots\ldots\ldots \quad (3)$$

and:

$$\frac{13-2{\cdot}5}{R_2} - 15\,.\,10^{-6} = (2{\cdot}64/R_1) \quad \ldots\ldots\ldots \quad (4)$$

Finally from equations (3) and (4):

$$0{\cdot}2\,.\,10^{-3}R_1^2 - 7{\cdot}6\,R_1 + 15{\cdot}6\,.\,10^3 = 0$$

hence R_1 and R_2 are 35·8kΩ and 140kΩ respectively. Accordingly the preferred values chosen were 36kΩ and 150kΩ for R_1 and R_2 respectively.

The capacitive coupling is designed as follows:

$$R = \frac{12 - 0{\cdot}2}{0{\cdot}2\,.\,10^{-3}} = 59\text{k}\Omega \quad \text{preferred value} = 56\text{k}\Omega$$

The effective time-constant $\tau = CR \ln$

$$\left[1 + \frac{V_{cc} - V_{cs} - V_{bs}}{V_{cc} - I_{co}R}\right]$$

for reasonably low speeds I_{co} at 35°C may be neglected

$$\therefore \tau = CR \ln \frac{(2V_{cc} - V_{cs} - V_{bs})}{V_{cc}}$$

Now it is necessary to catch the positive swing at +10V in order to avoid exceeding the OC42 reverse bias of −12V then:

$$\tau = CR \ln \frac{(1{\cdot}835\,.\,12 - 0{\cdot}34)}{12} = CR \ln 1{\cdot}81$$

$\therefore\ \tau = 0{\cdot}59\,CR$ instead of the usual 0·69 and for a design centre of 4msec, $C = 0{\cdot}12\mu$F.

The value of R is preset using an additional variable resistor of 25kΩ to give a 4msec pulse with a capacitor of 0·1μF.

−13V TO +2V OUTPUT INTERFACE

The OC139 long-tailed pair caters for the requirement of a −13V to +2V interface, which operates by means of the switch shown in Fig. 6(a). The OC139's should be mounted in transistor clips which provide an adequate heat sink.

PUNCH AMPLIFIER

The 2N386 transistors in the punch amplifier switch between cut-off and saturation with a possible maximum m.s.r. of 0·4. Consequently an aluminium heat sink of dimensions 3in × 3in × 1/16in for each 2N386 is entirely adequate. As the maximum current feed is 1A, a 2A series fuse safeguards the punch solenoid circuits.

Conclusions

A detailed design has been given of an off-line punched card to paper tape convertor, in which reliability has been achieved by simple diode logic and end-on operation.

Acknowledgment

The author wishes to thank Professor D. G. Tucker for providing the research facilities and Mr. J. C. Cluley of the Electrical Engineering Department of the University of Birmingham for invaluable suggestions.

REFERENCES

1. BLOCH, E., PAULSEN, R. C. Magnetic Core Logic in a High-Speed Card-to-Tape Convertor. *I.R.E. Trans. Electronic Comput.* *EC-8*, 113 (1959).
2. PRESSMAN, A. I. Design of Transistorised Circuits for Digital Computers. (Chapman and Hall Ltd).
3. NEETESON, P. A. Junction Transistors in Pulse Circuits. (Philips Technical Library).
4. CHU, Y. Digital Computer Design Fundamentals. (McGraw-Hill).
5. MALEY, G., EARLE, J. The Logic Design of Transistor Digital Computers. (Prentice-Hall).
6. CLULEY, J. C. A Comparison of Duplicate and Triplicate Schemes for Binary Logical Networks. Department of Electrical Engineering, University of Birmingham.
7. CLULEY, J. C. Low Level Redundancy as a Means of Improving Digital Computer Reliability. Department of Electrical Engineering, University of Birmingham.
8. SHWOP, J. E., SULLIVAN, H. J. Semi-Conductor Reliability. (Chapman and Hall Ltd).
9. Component Fault Data from Electronic Data Processing Equipment. A.T.E. Co. Ltd, Electronics Division, Cheapside, Liverpool.
10. Mullard Semi-Conductor Reliability. 1963 (T.P. 767).

Laser Holograms

A new method of three dimensional photography known as 'holography' has recently been developed by which the object to be photographed is illuminated by a laser beam.

This type of photography which can be carried out without the use of conventional lenses was originally proposed in 1948 by Dr. D. Gabor* of Imperial College London.

At that time it was not possible to develop the technique because of the lack of a light source of sufficient coherence and intensity, but this difficulty has now been overcome by the introduction of the laser.

To obtain a three dimensional photograph or 'hologram', the laser, the object to be studied and the photographic plate are so arranged that part of the laser beam falls on the object and is reflected back to the plate, while another part of the beam passes directly to the plate, the laser beams being diffracted into two plane waves by a separator.

A network of irregularly distributed interference micro-fringes is set up and can be recorded on the plate thus producing a hologram.

If the developed plate or hologram is now illuminated in a similar manner by a laser beam and viewed from the front, the original three dimensional object is shown in relief.

Scientifica Ltd of Acton, London has developed a gas-laser suitable for general studies of holography. Holograms have also been demonstrated recently by the Compagnie Generale de Telegraphie sans Fils (C.S.F.) at their Courbeville Laboratories in France.

One of the applications of holography is a method of precise measurements in engineering and a study is now being carried by the National Physical Laboratory in conjunction with Atomic Weapons Research Establishment.

Their work has shown that holography can be used to carry out interferometric measurements on rough surfaces of ordinary 'engineering' shapes. Hitherto these measurements, which record small changes caused by mechanical strain or thermal expansion, have only been possible where the surface is highly polished and of a simple shape, such as flat or spherical.

* GABOR, D. *Nature*, *161*, 777 (1948).
GABOR, D. *Proc. Royal Soc. A*, *197*, 454 (1949).

Composite Characteristics of Series-Connected Tunnel Diodes

By J. B. Earnshaw* and Z. C. Tan*

Two methods for deriving the composite characteristics of chains of series-connected tunnel diodes are described. A critical discussion of these characteristics with some comments on circuits using tunnel diode chains follows the description.

(Voir page 273 pour le résumé en français: Zusammenfassung in deutscher Sprache auf Seite 280)

THE static composite characteristic of a number of tunnel diodes connected in series (Fig. 1) depends significantly upon the relative d.c. parameters of the individual tunnel diodes. Composite characteristics have previously been described[1,2,3,4,5] but some of these descriptions appear to have been based on a rather naive approach. An attempt at a more rigorous discussion of the composite characteristics of series-connected tunnel diode chains followed by some comments on circuits using these chains are presented herein.

Graphical Methods for Deriving the Static Characteristic Curves of Tunnel Diode Chains

The typical static characteristic of a single tunnel diode showing the principal d.c. parameters appears in Fig. 2.

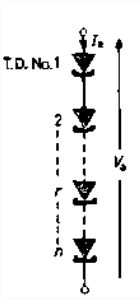

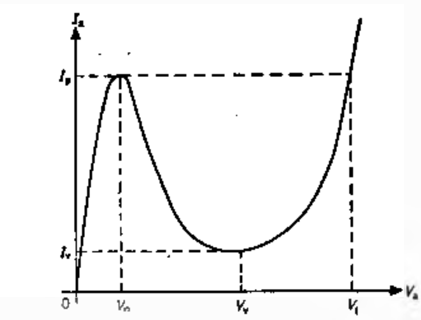

Fig. 1 (left). A chain of series-connected tunnel diodes

Fig. 2 (right). Typical static characteristic of a tunnel diode

I_p = peak current, I_v = valley current, V_p = peak voltage, V_v = valley voltage, V_f = forward voltage

Starting with the static characteristic of each tunnel diode in the chain, it is possible to determine graphically the static composite characteristic of the whole chain. There are two methods for plotting this composite characteristic depending upon whether the approach is made from a current or voltage point of view. To illustrate both methods a chain of two similar† tunnel diodes whose peak and valley currents satisfy the condition‡ ($I_{p1}<I_{p2}$; $I_{v1}<I_{v2}$) is considered.

From the current point of view, the current flowing through the chain is common to both the tunnel diodes. Therefore, for any current $I = I_n$ flowing through the chain, the voltage $V = V_n$ across the chain is the sum of the voltages across the individual tunnel diodes (see Fig. 3(a)). To illustrate the first method Fig. 3(b) shows how 8 arbitrarily chosen points ($n = a, b \ldots h$) on the composite characteristic are determined. For example, point a corresponds to current I_a flowing through the chain, and V_a, the voltage across the chain, is $V_{a1} + V_{a2}$. This method can be extended to plot the composite characteristic for a chain of any number of tunnel diodes.

From a voltage point of view[6] one of the tunnel diodes is considered to be the load of the other. For any voltage V across the chain, tunnel diode No. 1 can be considered to be the load of tunnel diode No. 2. A non-linear load line corresponding to tunnel diode No. 1 can be drawn over the characteristic of tunnel diode No. 2. The load line is formed by taking the mirror image about the current axis of the characteristic of tunnel diode No. 1 and displacing it along the voltage axis by an amount V. The

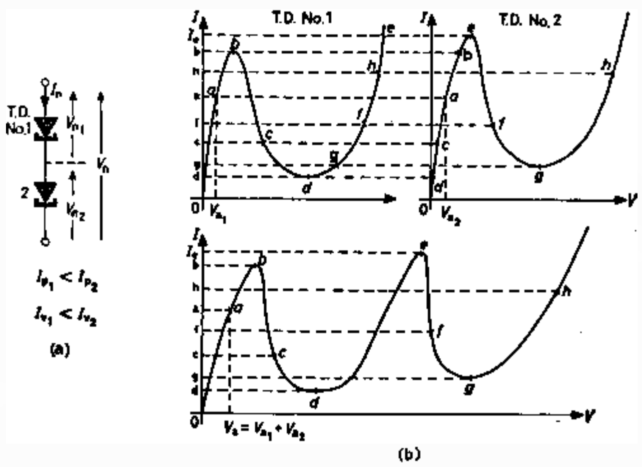

Fig. 3. Current approach method for plotting the composite characteristic of a tunnel diode chain

Fig. 4. 'Load-line' method for plotting the composite characteristic of a tunnel diode chain

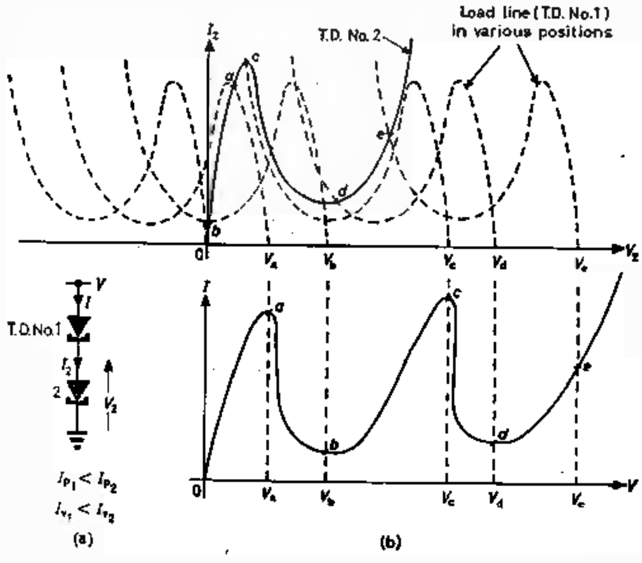

* *University of Auckland, New Zealand.*

† *The V_1 values are not significantly different.*

‡ *This condition will be considered at greater length later.*

current I flowing through the chain corresponding to the voltage V across the chain can then be readily obtained from the intersection of the load line with the characteristic of tunnel diode No. 2. Fig. 4(b) demonstrates the method by indicating six positions of the load line for six arbitrarily selected values $V = 0$, V_a, . . . V_e across the chain. This alternative method can also be extended to plot the composite characteristic for a chain of any number of tunnel diodes, but in this case it is necessary to plot a completely new composite characteristic each time another tunnel diode is added to the chain, e.g., for a chain of three tunnel diodes, the composite characteristic for two of them is first obtained, and then considering the third tunnel diode as the load of the other two, the load line corresponding to the third tunnel diode is moved over this composite characteristic to obtain the composite characteristic for the whole chain.

Of the above two methods, the latter although more tedious turns out to be superior. In particular, for chains of tunnel diodes whose peak and valley currents do not satisfy the condition set out in the simple case just con-

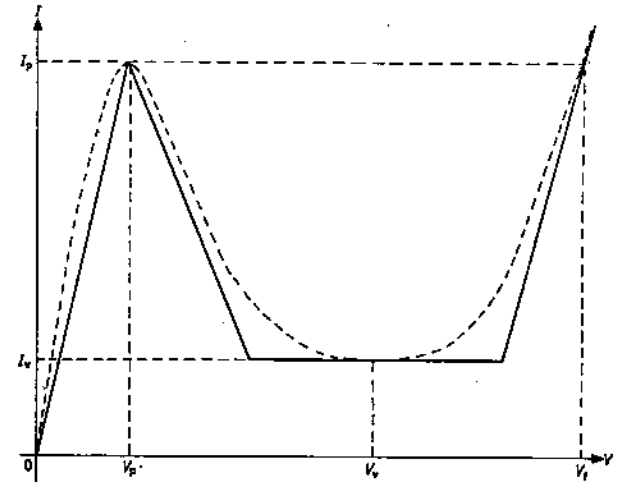

Fig. 5. A four-section linear approximation of the characteristic curve of a tunnel diode

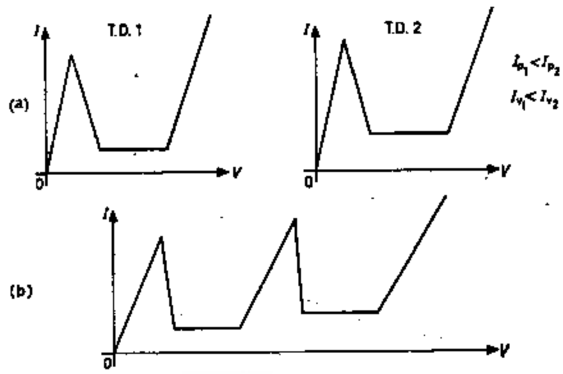

Fig. 6. Theoretical composite characteristic for a chain of two tunnel diodes in the regular case
(*a*) *Individual characteristics*
(*b*) *Composite characteristic*

Fig. 7. Experimental composite characteristic (Regular case)
(*a*) *Individual characteristics*
(*b*) *Composite characteristic*

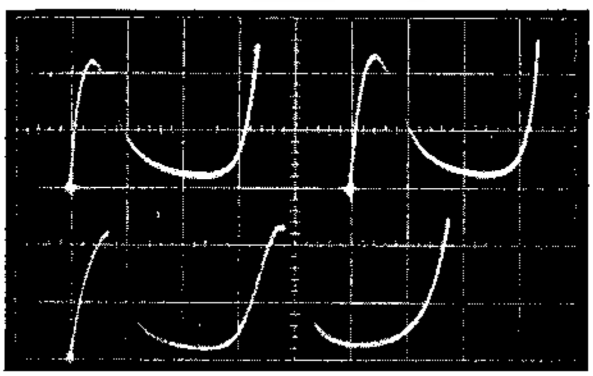

(a)

(b)

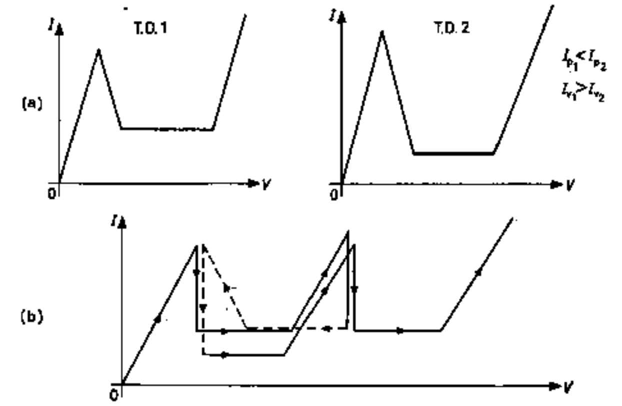

Fig. 8. Theoretical composite characteristic for a chain of two tunnel diodes in the irregular case
(*a*) *Individual characteristics*
(*b*) *Composite characteristic*

(a)

(b)

(c)

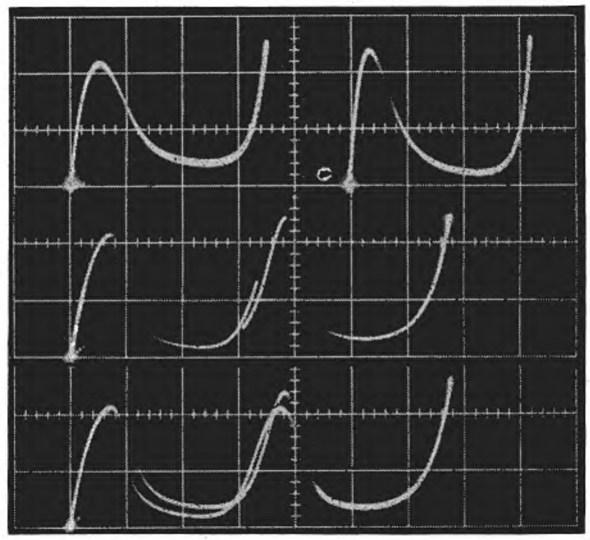

Fig. 9. Experimental composite characteristic (Irregular case)
(*a*) *Individual characteristics*
(*b*) *Composite characteristic (with ordinary curve tracer)*
(*c*) *Composite characteristic (with low impedance curve tracer)*

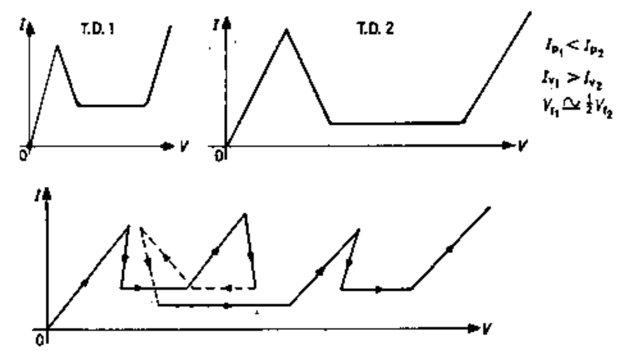

Fig. 10. Theoretical composite characteristic for a chain of two tunnel diodes in the irregular case (*with V_f condition*)

sidered, there exist convolutions in the composite characteristics resulting in the presence of additional peaks not normally observed when the composite characteristics are obtained by means of curve tracers. It is in the derivation of these rather complex composite characteristics that this 'load-line' method is used to advantage.

Types of Composite Characteristics

It has already been mentioned that composite characteristics of tunnel diode chains depend upon conditions satisfied by the peak and valley currents of the tunnel diodes. It will assist in later discussion if the composite characteristics are classified according to the fulfilment of these conditions.

With reference to Fig. 1, let I_{pr}, I_{vr} and V_{fr} be respectively the peak current, valley current and forward voltage of tunnel diode *r* in the chain. The composite characteristics are grouped into three distinct classes as follows:

Regular Case

V_f values are similar.

$I_{p1} < I_{p2} < \ldots < I_{pr} < \ldots < I_{pn}$

$I_{v1} < I_{v2} < \ldots < I_{vr} < \ldots < I_{vn}$

Irregular Case

V_f values are similar.

$I_{p1} < I_{p2} < \ldots < I_{pr} < \ldots < I_{pn}$

$I_{v1} > I_{v2} > \ldots > I_{vr} > \ldots > I_{vn}$

Irregular Case (with V_f condition)

$V_{f1} \leqslant \frac{1}{2}V_{f2} \leqslant \ldots \leqslant \frac{1}{2}V_{fr} \leqslant \ldots \leqslant \frac{1}{2}V_{fn}$

$I_{p1} < I_{p2} < \ldots < I_{pr} < \ldots < I_{pn}$

$I_{v1} > I_{v2} > \ldots > I_{vr} > \ldots > I_{vn}$

Theoretical and Experimental Composite Characteristics

The graphical derivation of the composite characteristic of a chain by means of the 'load-line' method is tedious. To remove some of the drudgery the characteristic curves of the individual tunnel diodes are represented by four-section linear approximations (see Fig. 5).

Considering first the case of a two tunnel diode chain, the composite characteristic for the regular case (see Figs. 6 and 7) is straightforward and does not warrant further discussion. For the irregular case, however, (see Figs. 8,

Fig. 11. Composite characteristics for a chain of three tunnel diodes with similar values of V_f and $I_{p1} < I_{p2} < I_{p3}$

(a) Theoretical *(b) Experimental*

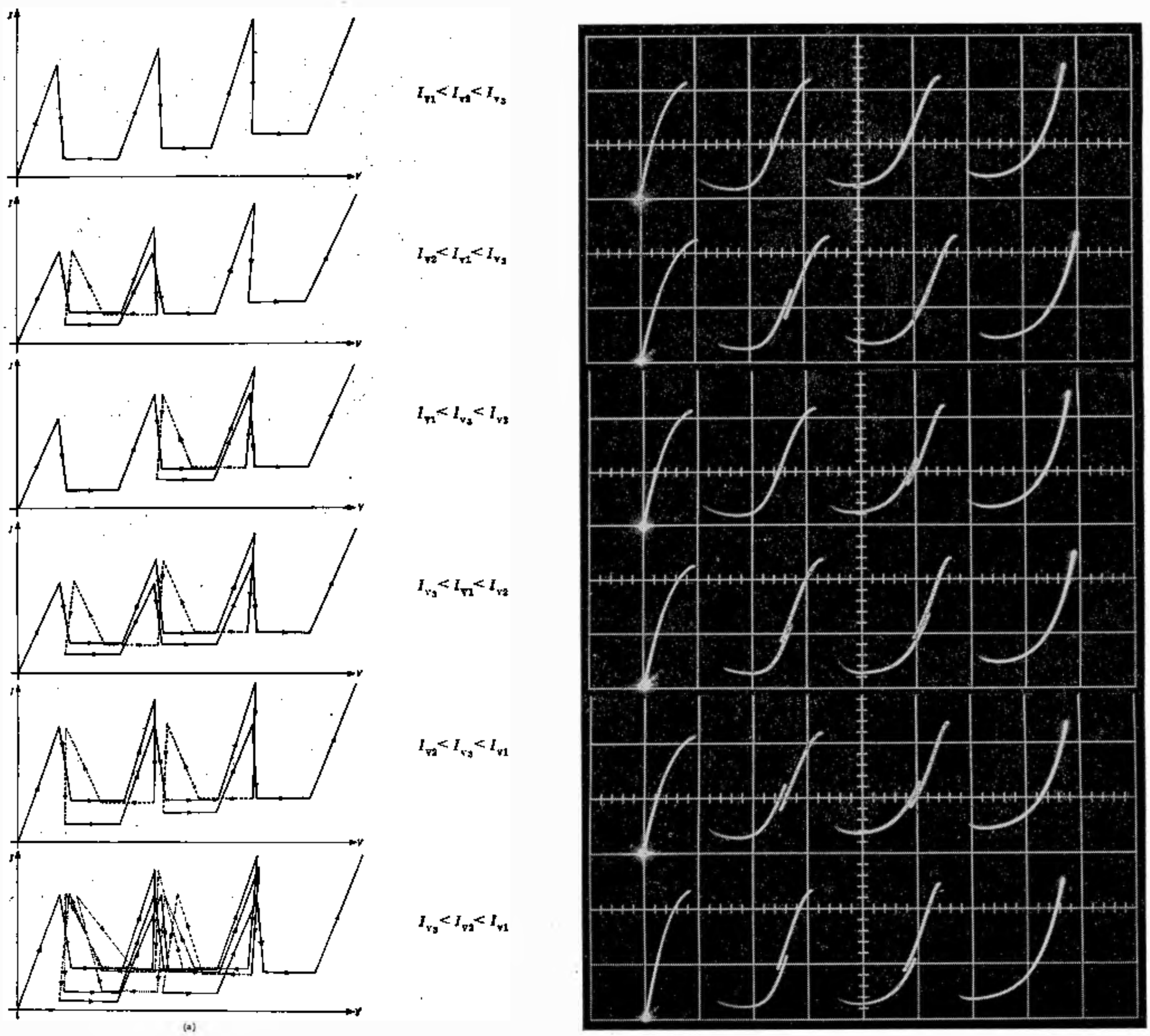

9(a) and 9(b)) the existence of a convolution in the theoretical composite characteristic and its apparent absence in the experimental curve obtained from a curve tracer, requires some explanation.

To display a characteristic curve, a curve tracer in general relies upon stable intersections of its source impedance load line with the characteristic curve. This load line, usually linear, is moved forwards and then backwards across the voltage axis by the voltage source* of the curve tracer, and in so doing displays part of the characteristic curve during its forward motion and part during its backward motion. It is clear then that it is not always possible, especially in cases where the curves have convolutions, to display the complete curve and what is displayed will, to a large extent, depend upon the impedance of the load line. By comparing Figs. 9(b) and (c) it can be seen that when the source impedance of the curve tracer is reduced† a greater portion of the convoluted characteristic is displayed.

Having treated the regular and irregular cases for chains of two tunnel diodes with similar values of V_f, the irregular case where conditions are imposed upon the V_f values still remains to be considered. A significant difference between the regular and irregular cases where the V_f values are similar is that the composite characteristic of the irregular case possesses an additional peak (see Fig. 8(b)). This peak, the result of a convolution in the composite characteristic, is not in a suitable position in relation to the other peaks for it to be of any practical use. However, if a suitable condition[7] is imposed upon the V_f values it is possible to reposition all the peaks so that they are regularly spaced on the current-voltage diagram (see Fig. 10), and can all be utilized[9,10].

For a chain of three tunnel diodes, the situation is rather more complex. Instead of the single irregular case as with two tunnel diodes, there are now five irregular cases distinguished by five possible different I_r conditions (see Fig. 11(a)). Because of reasons already discussed, the experimental composite characteristics (Fig. 11(b)) show neither convolutions nor additional peaks. Nevertheless, these convolutions and additional peaks do exist as indicated by the discontinuous overlapping sections.

In general for a chain of n similar tunnel diodes there are $n!-1$ irregular cases and only 1 regular case. The possible number of peaks varies from n for the regular case to 2^n-1 for the extreme irregular case. Irrespective of the degree of irregularity, curve tracers will display only n peaks separated by n valleys and these peaks will appear in ascending order of magnitude corresponding to increasing values of n. Similarly the valleys separating the peaks will also appear in ascending order of magnitude. However, only in the regular case will the valley between peaks r and $r+1$ correspond to I_{vr}.

* *To display only the forward characteristic a rectified sinusoidal voltage is usually used.*

† *There are problems of instability associated with stray inductances[8] to overcome.*

Circuits Employing Tunnel Diode Chains

Many circuits employing tunnel diode chains have been described[1,5,6,10,11-12]. Some of these descriptions have been based on a somewhat superficial understanding of the composite characteristics. The composite characteristics discussed above are static characteristics. During switching of the tunnel diodes these characteristics are no longer valid and it may be preferable to use dynamic characteristics. Alternatively, a mathematical analysis which does not explicitly use the dynamic characteristics may be employed. It is intended to discuss some of these points at greater length in conjunction with a tunnel diode scaler to be described elsewhere.

REFERENCES

1. Spiegel, P. High Speed Scalers Using Tunnel Diodes. *Rev. Sci. Instrum.* *31*, 754 (1960).
2. Gentile, S. P. Basic Theory and Application of Tunnel Diodes, p. 156 (Van Nostrand, New York, 1962).
3. G.E. Tunnel Diode Manual, p. 47, 1961 edition.
4. Chow, W. F. Principles of Tunnel Diode Circuits, p. 316 (John Wiley & Sons, New York, 1964).
5. Swamy, M. N. S. A High Speed Tunnel Diode Scaler. *Electronic Engng.* *37*, 225 (1965).
6. Tan, Z. C. A Study of Some of the Switching Characteristics of Tunnel Diodes and their Application in the Design of a High Speed Scaler. M.Sc. Thesis, University of Auckland (December 1964).
7. Rabinovici, B., Klapper, J. Designing Tunnel-Diode Circuits Using Composite Characteristics. *Electronics*, *33*, 46 (February 1962).
8. Dill, H. G., MacPherson, N. R. Tracing Tunnel Diode Curves. *Electronics*. *33*, 62 (5 August 1960).
9. Rabinovici, B. Tunnel Diode Decade Counter. *Rev. Sci. Instrum.* *33*, 1391 (1961).
10. Salama, C. A. T. The Static and Dynamic Characteristics of Series-Connected Tunnel Diodes and their Application in Digital Circuits. M.A.Sc. Thesis, University of British Columbia (December 1962).
11. Aleksander, I., Scarr, R. W. A. Tunnel Devices as Switching Elements. *J. Brit. Instn. Radio Engrs.* *23*, 177 (1962).
12. Foote, R. S., Johnson, D. High Speed Decade Pulse Counting. *Rev. Sci. Instrum.* *35*, 1126 (1964).

'Integrated Screen' Transistors

Neutralizing circuits in television i.f. amplifiers are now made unnecessary by a completely new type of high-gain npn silicon planar transistor announced by Mullard Ltd.

In these devices an integrated screen formed by an additional layer diffused into the collector surface under the base contact bonding area reduces, by a factor of four, the high feedback capacitance inherent in planar construction.

The new integrated screen TVistors*, types BF167 and BF173, are part of a comprehensive new range of seven low-cost silicon planar devices announced by Mullard for television, radio and audio applications.

Because of their very low feedback capacitance—only 150mpF for the BF167 and 230mpF for the BF173—and high forward transfer admittance, the integrated screen devices have a figure of merit which is four times greater than that of a conventional planar transistor. This enables the designer to produce simple i.f. amplifiers with consistent performance and adequate gain to meet the most demanding specification. The elimination of neutralizing simplifies i.f. transformer design and construction and, coupled with the competitive price of the transistors enables setmakers to produce cheaper i.f. amplifiers with improved performance.

The integrated screen is a thin layer of p-type material diffused into the collector surface under the base contact bonding area. The junction between the n-type collector and the p-type screen acts, in effect, as a reverse biased diode.

Without the screen the base-collector bonding area capacitance would be in the region of 500mpF to which must be added the junction capacitance of the actual transistor. In a typical BF167 with integrated screen, the total feedback capacitance is only 150mpF—less than a quarter of that of the unscreened device.

Due to the presence of the screen, the base contact area capacitance is transformed into additional capacitance at the input and ouput of the transistor. In i.f. amplifiers these capacitances do not cause any problems because they form part of the tuning capacitances of the band-pass filters.

The transistors are designed for grounded emitter operation and lead-out configuration from the TO-18 encapsulation is arranged to give minimum capacitance for use in this circuit arrangement.

The BF167 is intended for use as a television i.f. amplifier with forward gain control. Its characteristics provide consistent control of up to 60dB over the required current range. The i.f. gain-control characteristic is controlled in order to maintain consistency in the transfer of a.g.c. from the i.f. amplifier to the tuner.

The BF173 has a high dissipation (200mW at 45°C), a low bottoming voltage and maintains its gain over a wide range of current levels.

* *TVistors are Mullard transistors designed for use in television receivers.*

A Precision Diode Gate for Analogue Computers

By F. Fallside*, Ph.D. and N. Thedchanamoorthy*, B.Sc.

Semiconductor diode gates are widely used for integrator mode control in analogue computers operating at moderate or high repetition rates. Their sensitivity to variation in h.t. voltages however makes them less suitable for very slow computing and relays are often preferred. A new type of gate arrangement is described which is highly insensitive to h.t. voltage variations. In addition a simple but accurate analysis is made of the transfer function of gate controlled integrators which shows a good agreement with experiment.

(Voir page 273 pour le résumé en français: Zusammenfassung in deutscher Sprache auf Seite 280)

THE two most commonly used types of integrator with diode gates for mode selection[1] are shown in Figs. 1 and 2. Type 1 is used less frequently than type 2 since it requires a gate for each signal input and has a lower input impedance but it is inherently less sensitive to variations in the h.t. voltages E_1 and $-E_2$. It is shown in the present article that it can be made practically insensitive to these variations. The resulting gate thereby combines the low drift behaviour of relay gates and the high switching rate property of diode gates and can be used for very slow computing as well as high repetition rate computing.

The operation of the gates is well known. For example when MR_5 is held at $+P$ and MR_6 at $-P$ the diodes in bridge B_1 conduct and $V_3 = V_s$ to within a small error, whereas when MR_5 is switched to $-N$ and MR_6 to $+N$ diodes MR_5 and MR_6 conduct, the bridge B_1 is non-conducting and V_3 is isolated from V_s.

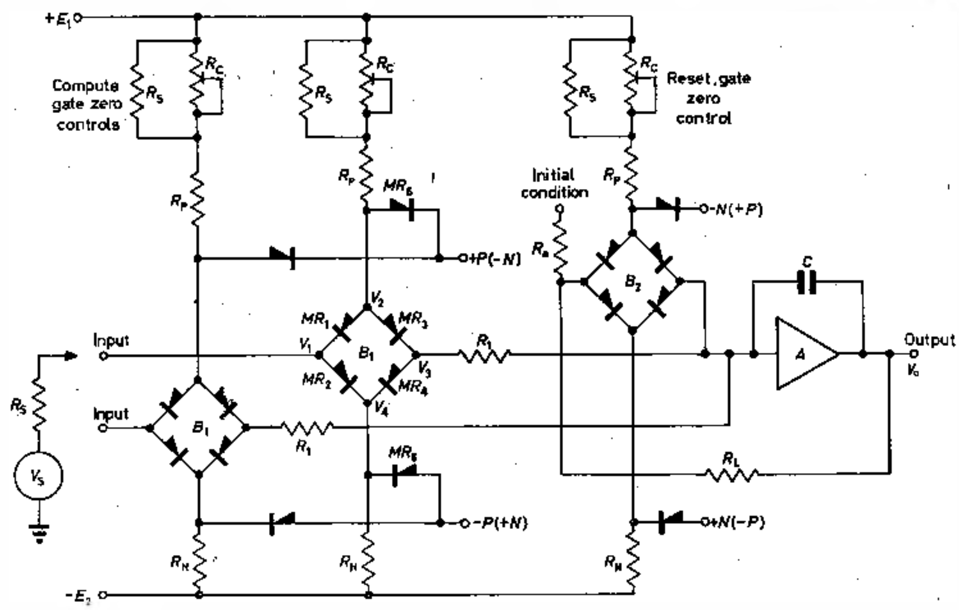

Fig. 1. Type 1 integrator

An accurate analysis is made of the type 1 integrator first and then an improvement of the basic circuit is given. Finally a comparison is made between the two types of integrators.

Type 1 Integrator

TRANSFER FUNCTION

The analysis is for a type 1 integrator as shown in Fig. 1 in its 'compute' mode, with the bridges B_1 conducting and B_2 non-conducting. Using conventional assumptions and considering one input only, see Appendix 1, the transfer function of the bridge B_1 is found to be

$$V_3/V_s = \frac{1}{1 + (r/R_N) + (r/R_1) + \dfrac{r^2}{2R_N R_1}} \quad \ldots\ldots\ldots (1)$$

where r is the incremental resistance of the bridge diodes MR_1 to MR_4.

Since $V_o = -V_3/(DCR_1)$, the overall transfer function of the integrator is

$$V_o/V_s = -\frac{1}{DCR_1}\left[\frac{1}{1 + (r/R_N) + (r/R_1) + \dfrac{r^2}{2R_N R_1}}\right] \quad \ldots\ldots\ldots (2)$$

Now the integrator time-constant with no gate is $T = CR_1$ and so one effect of the gate is to introduce a scale factor error which, on neglecting second order terms since $r \ll R_N, R_1$, is given by

$$\triangle T/T = \frac{V_s - V_3}{V_s} = (r/R_N) \times \left[1 + (R_N/R_1) + (r/R_N) \times (R_N/2R_1)\right] \ldots\ldots (3)$$

This expression can be evaluated for a given circuit when the incremental resistance, r, is known. The diodes MR_1 to MR_4 are matched at the standing value of bridge current and so their values of r may be assumed equal. Previous workers[2] have assumed a constant value for this, here a more accurate analysis is used.

Assuming that in the forward conduction region the diode current i_f and voltage v_f are related by

$$i_f = A\exp(\alpha v_f)$$

then $r = dv_f/di_f = 1/(\alpha i_f)$.

Now in the circuit of Fig. 1 the current in each diode,

* *University of Cambridge.*

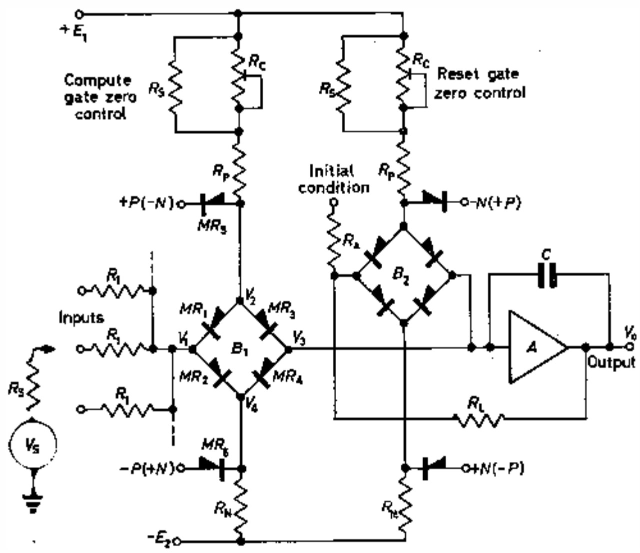

Fig. 2. Type 2 integrator

MR_1 to MR_4, during conduction is given approximately by

$$i_f = E/(2R_N),$$

assuming the h.t. supplies are equal $E_1 = E_2 = E$. Accordingly $r/R_N = 2/(\alpha E) = k/E$ say, and equation (3) can now be written

$$\Delta T/T = (k/E)\,[1 + (R_N/R_1) + (k/E) \times (R_N/2R_1)]$$

For a typical silicon planar diode (1N914), $A \simeq 2{\cdot}5 \times 10^{-8}$A and $\alpha \simeq 40$ and so to a first approximation

$$\Delta T/T = (k/E)\,(1 + R_N/R_1) \quad \ldots\ldots\ldots\ (4)$$

The scale factor error can thus be reduced, and kept constant, by using large h.t. voltages $\pm E$ and a small value of R_N; R_1 being determined solely by computer requirements. However, to avoid an excessive current drain on the h.t. source (E/R_N when the bridge is conducting) and on the gate pulse source ($(E + N)/R_N$ when the bridge is non-conducting) the value of R_N must be kept reasonably high.

Results from a typical gate are shown in Table 1. This gate employs 1N914 diodes and $E = 22$V, $R_1 = 100$kΩ, $C = 10\mu$F. A compromise value of $R_N = 10$kΩ is used and under these conditions $r \simeq 50\Omega$.

Substituting values into equation (4), the time-constant error is found to be $\Delta T/T \simeq 0{\cdot}55$ per cent. This is seen to agree well with the experimental results for input signals V_s over the range ± 15V. Outside this range, as is seen in the next section, the gate is beginning to depart from its idealized behaviour.

Using the simpler assumption[2] that $v_f = i_f\, R_f$, R_f is found to be approximately 600Ω and the predicted error is 7 per cent.

As has been mentioned the scale factor error can be reduced by increase of E. In cases where this is not practicable the error can be compensated for by reducing R_1 to a new value R_2 given by

$$R_2 = \frac{R_1}{1 + (r/R_N) + (r/R_2) + \dfrac{r^2}{2R_N R_2}} \quad \ldots\ldots\ldots\ (5)$$

$$\simeq R_1\,(1 - (r/R_N) - (r/R_2)) \quad \ldots\ldots\ldots\ (5a)$$

$$\simeq R_1\,(1 - (r/R_N) - (r/R_1)) \quad \ldots\ldots\ldots\ (5b)$$

Limitations on Gate Voltages

The operating range of the circuit is limited by the requirement that the bridge must remain conducting over the range of the input signal V_s. It is shown in Appendix 2 that conduction ceases when E is less than a minimum value E_{min} given by

$$E = E_{min} = V_s(1 + (R_N/R_1)) + v_o \quad \ldots\ldots\ (6)$$

or, for a given E, when

$$V_s = V_{s(max)} = \frac{E - v_o}{1 + R_N/R_1} \quad \ldots\ldots\ldots\ldots\ldots\ (7)$$

For the circuit previously considered, where $v_o \simeq 0{\cdot}4$V, the value of $V_{s(max)}$ predicted by equation (7) is 19·6V which agrees closely with the operating range shown in Table 1.

The corresponding expression arrived at by previous workers[2] is

$$V_{s(max)} = \frac{E}{2 + R_N/R_1}$$

For the same circuit this gives an over-conservative maximum input signal of 10·5V.

The other voltage restrictions on the gate circuit concern the control voltages P and N. Their requirements are (a) when the bridge is conducting

$$P \geqslant P_{min} = V_{s(max)} + v_o \quad \ldots\ldots\ldots\ (8)$$

and (b) when the bridge is non-conducting

$$N \geqslant N_{min} = 2\,v_o \quad \ldots\ldots\ldots\ldots\ (9)$$

Input Resistance

As shown in Appendix 1 the exact expression for the input resistance of the integrator during conduction is

$$R_g = \frac{R_N R_1 + r\,(R_N + R_1 + r/2)}{R_N + 2\,R_1 + r} \quad \ldots\ldots\ldots\ (10)$$

This may be reduced to simpler forms depending on the relative magnitudes of R_N and R_1. The three cases are, neglecting second order terms,

(a) $R_N \ll R_1$,

$$R_g \simeq (R_N/2)\,(1 - (R_N/2R_1)) \quad \ldots\ldots\ldots\ (10a)$$

(b) $R_N \simeq R_1$,

$$R_g \simeq R_N/3 \simeq R_1/3, \quad \ldots\ldots\ldots\ (10b)$$

(c) $R_N \gg R_1$

$$R_g \simeq R_1\,(1 - (2R_1/R_N)) \quad \ldots\ldots\ldots\ (10c)$$

For the circuit previously considered the input resistance, as given by equation (10a) is 4·75kΩ.

Compensated Type 1 Integrator

So far it has been assumed that the h.t. supplies E_1 and

TABLE 1

INPUT VOLTAGE V_s	OUTPUT FROM GATE V_3	PERCENTAGE ERROR $\frac{V_s - V_3}{V_s} \times 100 = \frac{\Delta T}{T} \times 100$
20·00	19·53	2·35
19·50	19·28	1·13
15·00	14·9	0·64
10·00	9·94	0·60
5·00	4·975	0·50
1·00	0·995	0·50
0	0	0
−1·00	−0·995	0·50
−5·00	−4·97	0·60
−10·00	−9·94	0·60
−15·00	−14·89	0·73
−19·50	−19·24	1·33
−20·00	−19·53	2·35

$-E_2$ are constant. However, even with highly stable supplies $\Delta E = E_1 - E_2$ can be of the order of 10mV and will vary during a computation. (Symmetrical gate supplies $E_1 = E_2$, nominally, are assumed here, asymmetric gates can be compensated by the same method.) If ΔE is taken into account it can be shown by the same method as before that the integrator transfer function is

$$V_o = -\frac{1}{DCR_1}\left[\frac{V_s + \frac{1}{2}\Delta E}{1 + (r/R_N) + (r/R_1) + \dfrac{r^2}{2R_N R_1}}\right] \quad \ldots (11)$$

and using an input resistor R_2 as defined by equation (5) this reduces to

$$V_o = -\frac{1}{DCR_1}(V_s + \tfrac{1}{2}\Delta E) \quad \ldots\ldots\ldots\ldots (12)$$

This refers to an integrator with a single input. For n inputs and gates it becomes

$$V_o = -\frac{1}{DCR_1}\left[\sum_{j=1}^{n} V_{sj} + (n/2)\Delta E\right] \ldots\ldots\ldots (13)$$

Thus the h.t. voltage drift appears as a spurious input signal to each gate of magnitude $\frac{1}{2}\Delta E$. This can lead to considerable computing errors when V_s is small and, particularly, when very slow integration is used. It is one of the main objections to the acceptance of diode gates for slow analogue integration.

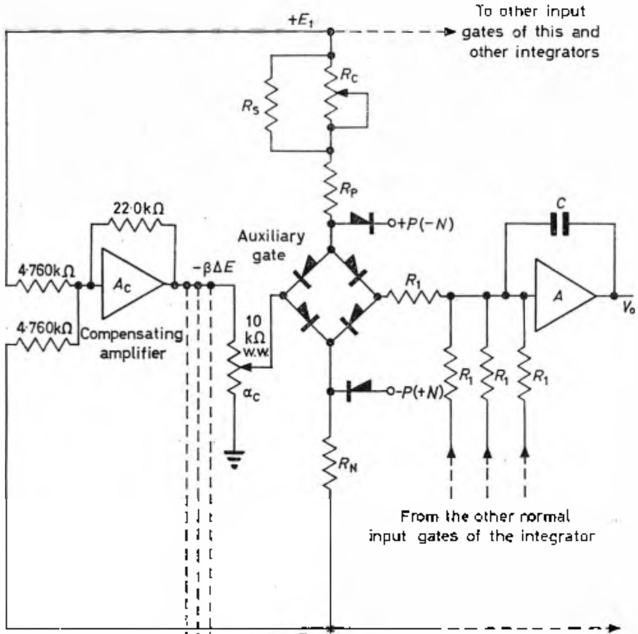

Fig. 3. Compensation against h.t. drift in type 1 integrators

TABLE 2

ΔE (mV)	UNITY TIME-CONSTANT INTEGRATOR DRIFT (mV/sec)			
	(a) Uncompensated gate		(b) Compensated gate	(c) Relay
	Measured	Calculated		
−50	74	75	−0·7	0·5
−10	14	15	−0·4	0·5
0	0	0	−0·33	0·5
10	−15	−15	−0·4	0·5
50	−76	−75	−0·6	0·5

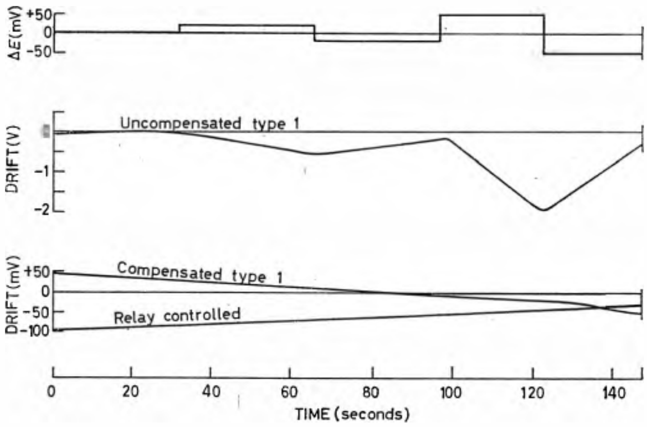

Fig. 4. Drift performance of integrator

In the 'reset' mode ΔE gives rise to a spurious output voltage of magnitude $(R_L/R_N) \cdot \Delta E$, which is negligible. It has no effect in the 'hold' mode since both gates are off. Thus if the effect of ΔE can be nullified during the 'compute' mode the diode gate controlled integrators are acceptable for accurate slow time computation in addition to their customary use for fast repetitive computation.

A successful scheme for implementing this is shown in Fig. 3. An additional, 'auxiliary' gate is added to each integrator and these are all fed by compensating signals from one amplifier. The amplifier, A_c, is a high quality chopper stabilized operational amplifier which generates a voltage, $-\beta\Delta E$, directly proportional to the drift ΔE. Its magnitude is arranged to be about twice $(n/2)\Delta E$.

All the signal gates of any one particular integrator and the auxiliary gate are first set up under the condition $\Delta E = 0$, one at a time, with the other gates disconnected from the virtual earth of the integrator. Then, with all the gates connected, a fraction α_c of the compensating voltage $-\beta\Delta E$ is applied to the auxiliary gate through the potential divider. The control resistance R_c of the auxiliary gate and the setting of the compensating potentiometer α_c are then successively adjusted to produce zero integrator drift when ΔE is given equal positive and negative changes (typically ± 10mV), alternately. Finally, the drift is checked to be zero when $\Delta E = 0$. The integrator requires hardly any subsequent adjustment in spite of changes of ΔE. The output of the same compensating amplifier A_c can be used to compensate any number of integrators within its current capability.

Table 2 shows the drift performance of an integrator with $V_s = 0$, whose mode selection is performed by (a) type 1 diode gates not compensated for ΔE, (b) type 1 diode gates compensated for ΔE, and (c) electromechanical relay. For this integrator $n = 3$ and the theoretical results for the uncompensated gate were calculated from equation (13). The actual drift recordings are shown in Fig. 4.

It can be seen that the performance of the compensated integrator is as good as the relay controlled integrator and considerably better than the uncompensated integrator. (During the course of setting up a number of such integrators it was found that the figures (column (b)) could be improved by as much as a factor of 10. This improvement over relay control is made possible since the compensation acts as an additional and very fine zero control for the integrator amplifier.)

Setting-up Details

The remaining setting-up procedure, which is necessary for the type 1 integrator whether or not compensation is used, is as follows. Referring to Fig. 1, the zero control resistor, R_c, of the compute gate is adjusted to give zero integrator drift with the gate pulses as shown. The gate pulses are then reversed and the zero control R_c of the reset gate is adjusted to give zero d.c. offset at the integrator output. (In each gate the resistor R_p is about 50 to 100Ω less than R_N, and R_s is about 100 to 150Ω, as a result a very fine balance is achieved by R_c and the assumption (b), Appendix 1, holds accurately.)

Type 2 Integrator

The main disadvantages of the type 1 integrator are

(a) A large standing current is required in the bridge since the forward currents in the diodes MR_1 and MR_2 vary considerably with the input signal V_s.

(b) The input impedance is low (less than R_1).

(c) Each input requires a separate gate.

In the type 2 integrator the standing current in the bridge can be quite small since variations in the diode currents i_1 and i_2 are the same order as the signal current i_s. Its input impedance is high, R_1, and only one signal gate is required per integrator, but as will be seen it is extremely sensitive to h.t. voltage drift.

Transfer Function

Using a method similar to that used for the type 1 integrator it can be shown that the integrator output is

$$V_o = -\frac{1}{DCR_1} \times \left[\frac{V_s + \dfrac{\Delta E}{2R_N + r}(2R_1 + (R_1/R_N)r + r + (r^2/2R_N))}{1 + (r/R_N) + (r/R_1) + \dfrac{r^2}{2R_N R_1}}\right] \quad \ldots\ldots\ldots\ (14)$$

When $\Delta E = 0$ this equation reduces to equation (2) and the time-constant scale factor error can be corrected for as before.

For $\Delta E \neq 0$, on neglecting second order terms, equation (14) becomes

$$V_o = -\frac{1}{DCR_1}(V_s + (R_2/R_N)\Delta E) \quad \ldots\ldots\ (15)$$

which may be compared with equation (12).

Thus the compensating signal required is $-(R_2/R_N)\Delta E$, which is considerably higher than for the type 1 integrator; by a factor of 20 in the design quoted previously. This requires a considerably higher gain from the compensating amplifier A_c with attendant errors due to noise, d.c. offset and drift. Experimental attempts to compensate a type 2 integrator by this method have been a failure, the integrator drifting to saturation within a few seconds.

This is to be expected since disturbances due to ΔE are applied directly at the virtual earth of the integrator. The type 2 integrator is thus inherently unsuited to slow speed computation.

Computing With Gate-Controlled Integrators

Effect of Source Resistance

So far it has been assumed that the signal source resistance R_s is negligible, in comparison with r. When this assumption does not hold the transfer function of the bridge, see Appendix 1, is

$$V_3/V_s = \frac{1}{\left(1 + (r/R_N) + (r/R_1) + \dfrac{r^2}{2R_N R_1} + (2R_s/R_N) + (R_s/R_1) + \dfrac{R_s r}{R_N R_1}\right)} \quad \ldots\ldots\ldots\ldots\ (16)$$

A common cause of source resistance is when the integrator is fed from a coefficient setting potentiometer. In that case R_s is variable and may be comparable with R_N and R_1 and so its effect cannot be compensated for by the method used to compensate r. Considerable errors will be introduced when the coefficient potentiometer is set with the integrator in its reset mode, since the potentiometer loading is incorrect. The following methods can be adopted to overcome this:

(a) A unity gain amplifier can be interposed between the potentiometer and the gate input.

(b) The input resistance of the integrator, R_g, can be evaluated from equation (10) and connected as a load across the potentiometer during setting up and subsequently removed.

(c) The compute gate can be switched on in addition to the reset gate while setting coefficients. This ensures that the potentiometer is loaded correctly and the reset gate, being on, ensures that the integrator does not overload.

Of these (c) has been found the most convenient in practice.

Effect of Gates in Non-conducting State

So far attention has been restricted to conduction of the compute gate. During computation the behaviour of the diode gates in their non-conducting state is also important and account must also be taken of the effect of the reset gate states during the various integrator modes. The most serious of these is found to be the effect of the compute gate in its non-conducting mode. The analysis is analogous to that for the conducting state except that the diodes present an incremental reverse resistance R_b and that the bridge is now taken to h.t. supplies $\pm N$ via resistors R_t. The transfer function for this state is found to be

$$V_o = -\frac{1}{DCR_1}\left[\frac{V_s + \frac{1}{2}\Delta N}{1 + (R_b/R_t) + (R_b/R_1) + \dfrac{R_b^2}{2R_t R_1}}\right] \quad (17)$$

$$\simeq -\frac{1}{DCR_1}\left[\frac{V_s + \frac{1}{2}\Delta N}{\dfrac{R_b^2}{2R_t R_1}}\right]$$

Evaluating this for the integrator design which was discussed earlier,

$$V_o \simeq -\frac{1}{DCR_1}\left[\frac{V_s + \frac{1}{2}\Delta N}{6\cdot 4 \times 10^9}\right]$$

Effectively complete isolation of the integrator from the input signal may thus be assumed.

Conclusions

An integrator arrangement employing a compensated diode gate has been put forward which is extremely insensitive to common mode drift in the gate h.t. supplies, and a simple analysis has been made which gives good agreement with experimental results.

At the cost of slightly greater complexity the gate is capable of mode setting for both high- and low-speed integrators. The type 1 integrator has been used successfully in modelling computations in which one part of the computer operates repetitively and the other operates in real time. It has also been used in track and hold circuits[3] for parameter optimization schemes.

A number of improvements are possible. With higher h.t. voltages E_1 and $-E_2$ a higher value of R_N increases the input resistance of the gate. The use of matched quad-diode bridges (e.g., G.E. 12X235) would be an improvement over the existing bridges which are matched at their standing current values only.

No attempt has been made to analyse the high frequency behaviour of the integrators. They have, however, been used satisfactorily at repetition rates up to 1kc/s. This could be improved by using lower capacitance diodes. Care is required in circuit layout at these frequencies since switching transients are enhanced by stray capacitance. The main limitation is the ability of the operational amplifier to supply the large charging and discharging currents to the integrator capacitor during mode switching[4].

Acknowledgments

One of the authors (N.T.) wishes to thank the Institution of Electrical Engineers for a Research Scholarship held during the period of this work.

Appendix 1

The following assumptions are made in deriving the transfer function of the type 1 integrator shown in Fig. 1.

(a) The virtual earth of a high gain d.c. operational amplifier is at ground potential.

(b) The quantity $\dfrac{E_1}{R_D + \dfrac{R_s R_c}{R_s + R_c}}$ is exactly equal to the quantity E_2/R_N, and for the case of symmetrical h.t. voltages $E_1 = E_2 = E$, and therefore $R_D + \dfrac{R_s R_c}{R_s + R_c} = R_N$ and R_N is used throughout the text to denote both these quantities.

(c) Over the entire operating point, the diode can be treated as a piecewise linear model satisfying

$$v_f = v_o + i_f r$$

where v_f is the forward voltage drop across the diode when it carries a current i_f, v_o is the intercept made on the voltage axis by the tangent line through (v_f, i_f), and r is the slope or dynamic resistance corresponding to this tangent line.

If the more accurate exponential relationship $i_f = A\exp(\alpha v_f)$ (A, α being parameters depending on the type of semiconductor, the temperature, etc.) is used, the solution of the bridge equations becomes extremely tedious. Hence the two segment straight line model is used to derive the transfer function expression, while the value of r at any point is evaluated from the exponential relationship.

Only one signal gate is considered, the case of multiple gates being easily treated by superposition. When the bridge B_1 is conducting, let

i_1 to i_4 be the forward currents in diodes MR_1 to MR_4

i_s = Signal current in the resistor R_1

R_s = Source resistance

V_s = Signal voltage

I_L = Current drain on the signal source

E = Balanced h.t. voltage

V_1 to V_4 = Potentials of the point marked in Fig. 1.

The following equations can be written:

$$E - V_2 = (i_1 + i_2) R_N \quad \text{(A 1)}$$

$$V_3 = i_s R_1 \quad \text{(A 2)}$$

$$E + V_4 = (i_3 + i_4) R_N \quad \text{(A 3)}$$

$$V_s - V_1 = I_L R_s \quad \text{(A 4)}$$

$$i_3 = i_4 + i_s \quad \text{(A 5)}$$

$$I_L = i_2 - i_1 \quad \text{(A 6)}$$

$$V_2 - V_1 = v_o + i_1 r \quad \text{(A 7)}$$

$$V_1 - V_4 = v_o + i_2 r \quad \text{(A 8)}$$

$$V_2 - V_3 = v_o + i_3 r \quad \text{(A 9)}$$

$$V_3 - V_4 = v_o + i_4 r \quad \text{(A10)}$$

On eliminating all the current terms and the voltages V_1, V_2, V_4 and E, the following expression is obtained:

$$V_s = V_3 \left[1 + (r/R_N) + (r/R_1) + \frac{r^2}{2R_N R_1} + (2R_s/R_N) + (R_s/R_1) + \frac{R_s r}{R_N R_1} \right] \ldots \text{(A11)}$$

For the normal case in which the integrator is fed from the output of a negative feedback d.c. operational amplifier, R_s is a fraction of an ohm and hence the above expression can be further simplified to

$$V_s = V_3 \left[1 + (r/R_N) + (r/R_1) + \frac{r^2}{2R_N R_1} \right] \ldots\ldots \text{(A12)}$$

By solving for I_L in terms of V_1 it can be shown that the input resistance of the integrator, $R_g = V_1/I_L$ satisfies the relationship

$$R_g = \frac{R_N R_1 + r(R_N + R_1 + r/2)}{R_N + 2R_1 + r} \ldots\ldots \text{(A13)}$$

Appendix 2

For satisfactory performance of the integrator all four diodes in any one bridge must remain conducting over the entire 'compute' period. To satisfy this it is necessary that the h.t. voltage E must satisfy $E \geqslant E_{min}$, where E_{min} is the minimum voltage necessary to maintain the bridge conducting when the applied signal is V_s. Also

$i_3 \geqslant i_s$

and $i_1 \geqslant 0$.

From the equations of Appendix 1 it can be shown that

$$E = v_o + V_3 + i_3 (R_N + r) + i_1 R_N$$

For the limiting case of $E = E_{min}$, $i_3 = i_s$ and $i_1 = 0$,

$$E_{min} = v_o + V_3 + (V_3/R_1)(R_N + r)$$

$$= v_o + \frac{V_s \left(1 + \dfrac{R_N + r}{R_1}\right)}{1 + (r/R_N) + (r/R_1) + \dfrac{r^2}{2R_N R_1} + (2R_s/R_N) + (R_s/R_1) + \dfrac{R_s r}{R_N R_1}}$$

For the usual case of negligible R_s and $r \ll R_N, R_1$, this can be replaced by the approximate relation

$$E_{min} = V_s (1 + (R_N/R_1)) + v_o \ldots\ldots \text{(A14)}$$

References

1. HUSKEY, H. D., KORN, G. A. Computer Handbook, Ch. 6-28. (McGraw-Hill, 1962).
2. MILLMAN, J., PUCKETT, T. H. Accurate Linear Bidirectional Diode Gates. *Proc. Inst. Radio Engrs.* *43*, 29 (1955).
3. ANDREWS, J. M. The Dynamic Storage Analogue Computer—DYSTAC. *Instrum. Control Syst.* *33*, 1540 (1960).
4. KORN, G. A. Performance of Operational Amplifiers with Electronic Mode Switching. *I.E.E.E. Trans. Electronic Comput.* *EC-12*, 310 (1963).

An Electromechanical Torsional Driver with Electrically Controllable Inertia

By V. Zakian*, Ph.D. and J. G. Thomas†, Ph.D.

An electromechanical torsional driver and accessory electronic apparatus are described. The driver has a range of angular traverse which exceeds 100°, and can develop a maximum torque of 14·1 × 10⁴ dyne cm. The inertia of the moving parts is 7g-cm² and this may effectively be reduced to zero with the use of an electronic feedback circuit.

(Voir page 273 pour le résumé en français: Zusammenfassung in deutscher Sprache auf Seite 280)

IN the course of an investigation into the dynamics of eye rotation[1,2] an electromechanical torsional driver and accessory apparatus were constructed for the purpose of applying vibratory torques of precisely controllable magnitude and frequency, or step torques, to the eyeball of anaesthetized dogs. The apparatus may have wider applications in torsional mechanical studies.

Some of the requirements of the experiments were to vibrate the load at frequencies in the range 0·1 to 100c/s, and at sufficiently high angular excursions to allow for a study of amplitude and velocity non-linearities. These, together with other requirements, gave rise to the following chief specifications: the linear range of angular traverse of the driver should not be less than 100°; the maximum torque developed should not be less than 6×10^4 dyne cm; the inertia of the moving parts of the driver should be less than 8g-cm².

A diagram of the apparatus is shown in Fig. 1. The driver coil is effectively current fed by the output of the direct coupled transistor power amplifier, thereby generating a torque proportional to the sum of the signals at the input of the amplifier. A sensing coil is mounted on the shaft, and its output voltage, proportional to the angular velocity of the shaft, is amplified by a direct coupled voltage amplifier of conventional design. The sinusoidal oscillator and the phase sensitive voltmeter were part of a commercial (Solartron) transfer function analyser; the latter served to measure the phasor (vector) angular velocity of the shaft relative to the oscillator output. A step function generator was sometimes used in place of the oscillator, in which case the voltmeter was replaced by an oscilloscope and a pen recorder. The unit labelled differentiator is composed of operational amplifiers, connected as a differentiator and phase invertors. The unit was used to cancel the effect of the mechanical output impedance of the driver, hence making the torque applied to the load, dependent only on the oscillator signal.

Design and Construction of the Driver

To obtain a high ratio of maximum torque to inertia, the design of the driver was based on the principle of the D'Arsonval moving-coil galvanometer. To provide a strong magnetic field a standard magnetron permanent magnet was used. The soft iron pole pieces were shaped as concentric arcs of circles subtending 120° at the centre of the shaft, thus ensuring a uniform radial field in the air-gap for an arc subtending 100°. The asymmetrical construction of the pole pieces has the following advantages over the conventional construction: only half the necessary effective air-gap is present, thus nearly doubling the magnetic flux if no saturation occurs; the coil can be allowed a much wider range of angular traverse; the necessity for suspending rigidly a cylindrical piece of soft iron between the pole pieces is avoided.

For convenience of assembly the pole pieces were split symmetrically along their lengths.

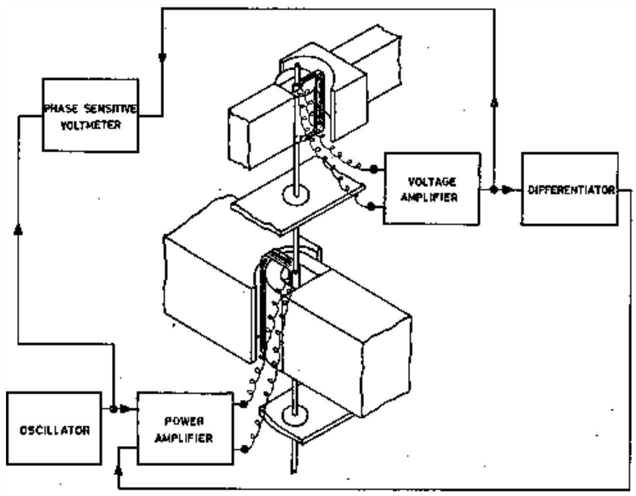

Fig. 1. Torsional driver and accessory apparatus
Signals leading into the power amplifier are summated

The length and breadth of the coil were made 3·5 and 2·5cm respectively. Its d.c. resistance was 0·4Ω and it was made up of 25 turns of copper wire. If needed a 40 per cent increase in maximum torque to inertia ratio would have been possible by using aluminium wire which has a density-resistivity product which is 48 per cent that of copper.

To minimize the inertia, the coil was constructed without a former. The wire used had an enamel coating and cotton insulation, this double insulation was useful in preventing accidental inter-turn short-circuits. The wire was wound on a removable former, the coil was then impregnated with Araldite, which was allowed to harden before removing the former. The coil was cemented to aluminium sleeves which fitted tightly on the shaft, this allowed for coil alignment after assembly.

A non-magnetic stainless steel rod ⅛in in diameter was used for the shaft. This material was chosen for its high rigidity and non-ferromagnetic properties. Due to its nearness to the magnet a ferromagnetic shaft presented difficulties in mounting and also introduced undesirable lateral thrust on the bearings. The shaft was mounted on two low friction ball bearings.

The velocity sensing coil was, except for its smaller dimensions (2 × 1·5cm) and thinner wire, a replica of the driver coil. Its d.c. resistance was 3Ω.

In order to minimize mutual inductance, the two coils

* *Loughborough University of Technology.*
† *University College, Cardiff.*

were oriented with their planes approximately at right-angles to each other.

The driver was always used with its shaft parallel to the gravitational field, thus avoiding the introduction of a counterweight for the coils.

Characteristics of the Driver

To include the effect of leads and ball bearings, the moment of inertia of all the moving parts was measured after assembly and found to be $7 \pm 0{\cdot}5$g cm^2. This was determined by loading the shaft with a light torsional metal spring of known elastic constant and measuring the resonant frequency of the resulting system.

The sensitivity of the driver was calibrated by connecting its shaft to a simple balance, and was found to be $9{\cdot}4 \times 10^4$ dyne cm/A, and constant to within 2 per cent for all angular positions of the coil, in a range of 100°. This meant that a maximum torque of $14{\cdot}1 \times 10^4$ dyne cm was available, when the coil was fed with 1·5A. The sensitivity was found to be not significantly affected by the presence of the sensing coil magnet or by the earth's magnetic field.

The effective impedance of the driver coil, including its back e.m.f. under conditions of no mechanical load, was measured and found to be less than 1Ω at frequencies below 150c/s.

The frequency response of the driver was determined by feeding the driver coil with sinusoidal currents of constant amplitude and measuring the resulting peak output voltage of the sensing coil. The product of this voltage and the frequency was found to be constant, to within 2 per cent, in the range 0·1 to 300c/s, indicating that within this range the dynamics of the driver were due predominantly to its inertia. Below 0·1c/s the frequency response was reduced because of the action of the weak elasticity of the leads and the slight friction of the ball bearings. Above 300c/s the finite rigidity of the portion of the shaft between the coils, formed a resonant system with the inertias of the coils, and gave rise to a resonance peak at 2kc/s in the response curve.

The output voltage of the velocity sensing coil was calibrated by exciting the driver sinusoidally at a known frequency, and measuring the extent of the resulting angular displacements with an optical lever, made by sticking on the shaft a small front silvered concave mirror. The calibration constant was found to be $2{\cdot}8 \times 10^{-3}$V/rad sec^{-1}. The source impedance of the sensing coil was measured to be less than 10Ω below 150c/s. The contribution made by the sensing coil to the total inertia was calculated to be less than 1g cm^2.

The Power Amplifier

The power amplifier, shown in Fig. 2, was direct coupled throughout and its measured characteristics were as follows:

Overall current gain	= 5 400
Input impedance	= 10Ω
Output impedance	= 1 000Ω
Frequency bandwidth	= 0 to 1 000c/s (−3 dB)
Non-linear distortion	= Less than 1 per cent
Drift (after 15min warming up)	= 1mA/min
Maximum output current	= ±1·5A
Stabilized d.c. power supply	= −14V 4A

The output stage (4) of the amplifier is an elaborate emitter coupled pair, fed single ended by the previous stage (3), and feeding the driver coil by push-pull action. In designing the output stage the following requirements had to be satisfied: its output impedance had to be sufficiently high to current feed the 1Ω impedance of the driver coil; no quiescent current had to pass through the coil (this was in order to avoid unnecessary heating and the consequent use of heavier wire); it had to be capable of feeding more than 1A into the coil. With conventional design procedures, in order to satisfy these conditions, collector resistors of more than 100Ω would have had to be used for transistors VT_8 and VT_{12}. This would have entailed the use of an expensive stabilized power supply for the amplifier, capable of delivering about 4A at 200V. To avoid this difficulty npn transistors VT_7 and VT_{11} were used to act as high dynamic resistances for the collectors of VT_8 and VT_{12}. This reduced the necessary voltage from the power supply to 14V.

Fig. 2. Power amplifier

* *VT_7 and VT_{11} are silicon npn transistors with characteristics similar to OC29*

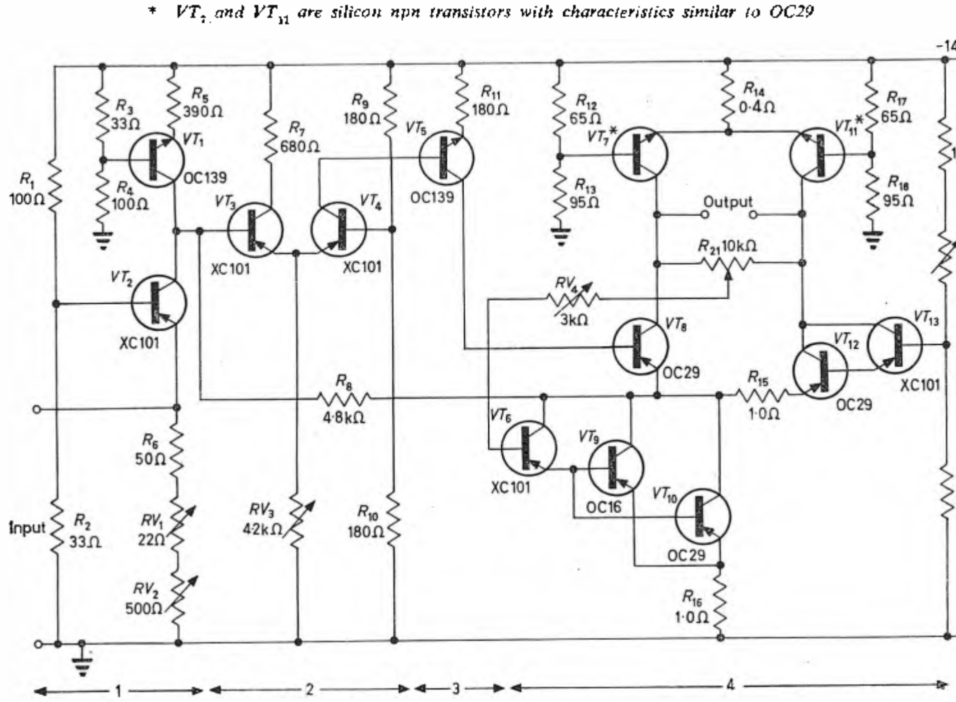

The part of the circuit composed of transistors VT_8 and VT_7 (or VT_{12} and VT_{11}) which may be referred to as the collector-collector configuration, does not appear to have been used before and it is necessary to inquire into the stability of the voltage at the collectors (i.e. at the left-hand output terminal in Fig. 2). If V is the value of the incremental voltage at the collectors, then

$$V = (I_8 - I_7)\, R_{07} R_{08}/(R_{07} + R_{08})$$

where I_8 and R_{08}, and I_7 and R_{07} are the incremental collector currents and the dynamic output resistances of VT_8 and VT_7 respectively. When the amplifier was first constructed it was found that due to the difference in the drifts of I_8 and I_7, and to the relatively high values R_{08} and R_{07}, the drift in V was too large. This drift was reduced to an acceptable level by introducing mean level negative feedback acting via RV_4.

It is worth pointing out that in a previous analysis of the collector-collector configuration[3] it was erroneously concluded that the voltage at the collectors is indeterminate. This conclusion was based on the false assumption that the transistors behave as ideal current sources.

Transistors VT_6, VT_9 and VT_{10} acted as a high dynamic resistance. VT_9 and VT_{10} are connected in parallel to simulate a single transistor of high current rating.

To stabilize and linearize the gain, increase the frequency bandwidth and increase the output impedance of the amplifier, 34dB of current negative feedback was applied from the output stage, via the current divider $R_{15}R_8$, to the input of stage (2). This overall feedback also serves to stabilize the quiescent conditions of the amplifier, including the quiescent base voltages of VT_5 and VT_8, more efficiently than could be obtained with the use of local feedback circuits, and in addition, the use of interstage circuits is avoided. Due to some non-linearity introduced by VT_{12} into the current divider of the feedback path, the effectiveness in reducing distortion is less than is usually expected with 34dB of feedback.

In order to summate signals feeding into the amplifier, a virtual earth condition was obtained at its input by utilizing transistor VT_2 in common base configuration. This yielded a 10Ω input impedance, but if needed, it was possible to reduce this figure even to negative values by making a positive feedback connexion, through a suitable resistor, between the base of VT_2 and the collector of VT_3.

The quiescent output current could be controlled within the range 0 to $\pm 1{\cdot}5$A with RV_1 and RV_2, and a universal meter set on direct current range and connected in series with the driver coil, was used to monitor its value. With this arrangement it was possible to control precisely the static torque generated, and to correct for the accumulated drift current at ten minute intervals.

The variable resistors RV_3, RV_4 and RV_5 were used for the final adjustment of quiescent conditions and were then replaced by fixed resistors.

Cancellation of Driver Inertia

The facility was required to study the dynamic properties of the load attached to the driver in isolation from the dynamics of the moving parts of the driver. With conventional procedures a torque transducer is used to measure the torque applied to the load, and a velocity transducer to measure the resulting angular velocity. The torque transducer may be made by incorporating a relatively stiff piece of torsional piezoelectric or piezoresistive material which would form a part of the shaft between the driver coil and the load. The method used in this study[4] has the merit of not requiring a torque transducer. The method consists in utilizing a positive feedback system to cancel the effect of the driver mechanical output impedance, hence making the torque applied to the load proportional only to the known signal delivered by the electronic oscillator. To cancel inertia, a signal proportional to the angular acceleration is derived and fed back to the input of the power amplifier. With the present apparatus this was obtained considerably more simply by differentiating the signal derived from the velocity sensing coil with an operational amplifier differentiator. Further operational amplifier circuits also provide the facility for cancelling positive or negative amounts of damping, but this was seldom used because the damping introduced by the ball bearings was negligible.

An important application of this apparatus was in the cancellation of the driver and load inertia, thus simplifying the study of the dynamics and the non-linearities of the load.

A rapid calibration procedure was developed to indicate at what value of the loop-gain the driver inertia was completely cancelled. A simple resonant mechanical system, with 0·1 coefficient of damping and precisely known velocity resonant frequency (that is, the frequency at which the magnitude of the velocity is a maximum) was connected as the load to the driver. The oscillator frequency was set as accurately as possible to be equal to the resonant frequency of the load, and that value of the loop-gain was found which gave a maximum in the peak velocity of the forced oscillations of the load. This gain was taken to correspond to the complete cancellation of the driver inertia. The errors in this method of calibration depend almost entirely on the difference between the frequency setting of the oscillator and the resonant frequency of the load, and errors of less than 2 per cent were obtained.

The stability of this system, with positive feedback, was studied in terms of its open-loop frequency response. Disregarding the case of conditional stability, such a system would be unstable only if the response magnitude is equal to or greater than unity, when the response phase is zero or an integral multiple of 360°. A consequence of this is that the system would be unstable if its loop gain is set to overcancel the inertia.

The open-loop frequency response of the system was measured under conditions of no mechanical load. In the range 0·1 to 100c/s the magnitude was found to be constant and the phase lag less than 1°. At 2 100c/s there was a resonance peak in the response magnitude, due to the shaft-coils mechanical resonant system. Above 100c/s the phase lag increased due to the power amplifier, the shaft-coils resonant system, and the differentiator, reaching 360° at 2 400c/s. Due to the resonance peak the ratio of the magnitude of response at 2 400c/s to that at 1c/s was 1·4, and instability occurred for loop gain settings equivalent to more than 70 per cent of inertia cancellation. To permit up to 100 per cent inertia cancellation, the phase lag was reduced by 40° at 2 400c/s, by decreasing the differentiator time-constant from 100 to 20μsec.

A further source of instability was due to the parasitic feedback resulting from the mutual inductance between the coils. This instability was eliminated for values of loop gain equivalent to up to 14g cm² of inertia cancellation, by reducing the area of the sensing coil, by orientating the coils with an angle between them (found empirically to be about 86°) which gave a minimum magnetic coupling, and by inserting a magnetic screen between them.

The differentiator introduced a slight deterioration in signal-to-noise ratio. To maintain a high signal-to-noise ratio the voltage amplifier preceding the differentiator was designed to have low noise, and an out-of-phase to in-phase discrimination ratio of 1 000; d.c. stabilized supplies were used for the high tension voltage and all heater filaments. The amplifier gain was set at 20, and the loop gain for inertia cancellation was controlled with a potentiometer connected after the differentiator. A cathode-follower connected after the potentiometer presented a constant source impedance to the power amplifier.

REFERENCES

1. STONE, S. L., THOMAS, J. G., ZAKIAN, V. Direct Measurement of the Parameters of the Passive Oculorotatory System of the Dog. *J. Physiol.* *172*, 63P (1964).
2. STONE, S. L., THOMAS, J. G., ZAKIAN, V. The Passive Rotatory Characteristics of the Dog's Eye and its Attachments. *J. Physiol. 181*, pp. 337-349 (1965).
3. BERTOYA, H. C. High Resistance Transistor Circuits. *J. Brit. Instn. Radio Engrs. 26*, 13 (1963).
4. MACHIN, K. E. The Electronic Simulation of the Load Applied to an Insect Muscle. *Electronic Engng. 31*, 740 (1959).

SHORT NEWS ITEMS

The Electronics Group of the Association of Special Libraries and Information Bureaux (ASLIB) has published the third issue of the "List of Recently-Coined Terms in Electronics for Librarians and Information Officers in Electrical and Electronic Engineering."

This issue, replacing the issue of June 1963, contains about 90 additional terms.

Copies are available (5s to ASLIB members and 7s 6d to non-members) on application to the Secretary of the ASLIB Electronics Group c/o Plessey Telecommunications Group, Ericsson Telephones Ltd, Beeston, Notts.

The Scientific Instrument Manufacturers' Association has set up a new group—The SIMA Process Control and Allied Instrumentation Group—to represent the special interests of members closely concerned in that field. The Group is to make a particular point of establishing close liaison with the users of its products through the appropriate manufacturing and research organizations. It will also work closely with government departments concerned with automation, education authorities and the British Scientific Instrument Research Association; members of the latter organization are included in the Steering Committee.

The Group has been formed to meet the specialized and growing needs of those concerned in process control and allied instrumentation, which have not hitherto been covered elsewhere, and will also maintain close liaison with the SIMA Machine Tool and Production Equipment Group.

The Sixth International Conference on Microwave and Optical Generation and Amplification sponsored by the Electronics Division of the Institution of Electrical Engineers and the Institution of Electronic and Radio Engineers will be held at Cambridge University on 12 to 16 September this year.

The programme will cover Microwave and Optical Generation by Solid State, Plasmas and other active devices, as well as by the classical forms of Microwave Tubes. In addition, it will include the application of various principles and phenomena relevant to the generation and amplification of coherent electromagnetic waves without strict frequency limitation.

Intending contributors will be required to submit 250-word abstracts of their proposed paper by 1 May.

Further details are obtainable from the Joint Conference Secretariat, I.E.E. Savoy Place, London, W.C.2.

The British Standards Institution has recently published the first of a new series of British Standards dealing with electronic measuring instruments and associated equipment.

This Standard (B.S. 3966) entitled, "Microwave Measuring Instruments" specifies the performance requirements for resonant frequency meters, slotted-section standing-wave meters, attenuators, power meters, impedance bridges, phase changers and terminations. Requirements are specified for instruments of two grades of accuracy, Grade 1 for design applications and high-accuracy laboratory work and Grade 2 for routine laboratory and work-bench measurements where the highest degree of accuracy is not required.

Appendices to the standard give requirements for a reference standard waveguide and short-circuit termination, and details of some typical methods of testing microwave measuring instruments.

Copies of B.S. 3966 may be obtained from the BSI Sales Branch, 2, Park Street, London, W.1. Price 10s. each. (Postage 9d will be charged extra to non-subscribers).

The Electronic Engineering Association has issued Publication 18 entitled, "EEA Guide to the Preparation of Specifications For Fast Stores". This is concerned with the manner of specifying fast random-access storage systems and its purpose is to draw attention to the various factors which should be agreed between supplier and user when a formal specification is prepared.

The Guide is restricted to stores which are conventionally addressed and does not apply to such stores as associative memories.

Fast stores have been taken as meaning stores which involve no mechanical movement; typical examples are core, magnetic film, tunnel diodes, inductive and capacitive fixed stores. The term random-access excludes such systems as delay line stores.

Copies of this Guide are available free of charge from The Electronic Engineering Association, Berkeley Square House, Berkeley Square, London, W.1.

The Department of Electronics at the University of Southampton has received a grant of £30 000 from the University Grants Committee to further the Post-graduate Course in Quantum Electronics which the Department has set up.

This course, which is of twelve months duration, is open to university graduates with degrees in electronics, physics, mathematics or electrical engineering, and consists of lectures, seminars and laboratory work with an individual research project.

A brochure giving full details of the course is available from the Department of Electronics.

A Technical Colloquium on Low Temperature Refrigeration for Microwave Systems, sponsored by the Arthur D. Little Organisation, Berkeley Square House, Berkeley Square, London W.1., is to be held at Frankfurt-am-Main, Germany on 28 and 29 April this year.

The Colloquium will deal with the latest techniques for achieving and maintaining the low temperatures required for the satisfactory operation of low-noise microwave amplification devices such as those used for Mariner Mars IV, Telstar, Early Bird and other satellite systems.

A European Meeting of Statisticians is to be held at the Imperial College of Science and Technology, London on 5 to 10 September this year.

This meeting is being organized by the Royal Statistical Society (Research and Industrial Applications Sections), the Institute of Mathematical Statistics (European Region) and the International Association for Statistics in Physical Sciences, a section of the International Statistical Institute.

Registration forms are obtainable from The Permanent Office, International Statistical Institute, 2, Oostduinlaan, The Hague, Netherlands.

The British Radio Valve Manufacturers' Association (BVA) and the Electronic Valve and Semiconductor Manufacturers' Association (of Great Britain) (VASCA) announce that exports of valves, tubes and semiconductor devices maintained their high level in the final quarter of 1965, showing a further increase on the previous quarter, the combined total being £3 766 612 as against £3 165 115, an increase of 19 per cent. Over the whole year, total exports of valves, tubes and semiconductors reached a record level of £13 320 466, an overall increase of 17 per cent (total exports for 1964 were valued at £11 392 584). Semiconductor exports in 1965 rose by 37 per cent and valves and tubes by 13 per cent. One of the major increases was in the field of "other electron optical devices", including camera tubes, where the percentage increase over 1964 was 42 per cent.

The Guided Weapons Division of British Aircraft Corporation has been selected, in conjunction with Radiation Incorporated of the U.S.A., to supply the magnetic flight test recording system for the Concorde supersonic airliner. This will be the largest-capacity data acquisition and continuous recording system so far designed for this type of application.

The Concorde flight test programme calls for the acquisition and processing, to a high degree of accuracy, of a massive amount of data. This will demand the use of pulse code modulation techniques, as it will be necessary to provide more than 2 500 channels of continuously recorded information to ensure that the exhaustive test programme is completed on schedule.

Collaboration between the two companies on the Concorde flight test recording system wil provide an entry for the U.K. into a vital and rapidly expanding branch of technology. B.A.C. Guided Weapons Division foresees many important applications of p.c.m. technology within the U.K., both in the aerospace and the industrial fields.

The Compania Telefonica Nacional de Espagna (CTNE) is to purchase a satellite communication earth terminal from the International Telephone and Telegraph Corporation for installation near Madrid.

The earth terminal, equipped with an 85ft diameter fully steerable parabolic reflector antenna, will provide tracking for satellites in orbits ranging from 5 000 nautical miles to synchronous orbits 22 300 miles high.

The terminal will be designed for television transmission and reception as well as voice and data traffic. A microwave relay system would carry message traffic from the earth station to Madrid.

Painton & Co. Ltd of Kingsthorpe, Northampton has entered into an exclusive licence agreement with Chauvin Arnoux, Paris covering the manufacture of their entire range of OK Relays in Great Britain. Painton have the exclusive selling and distribution rights for these relays, not only in Great Britain, but in Eire, Australia, New Zealand, Canada and South Africa.

Hawker Siddeley Dynamics has sold for an initial fee of £50 000 their electronic pulse system technique to the Hamilton Standard Division of the United Aircraft Corporation of America.

This system was developed by the Electronic Control Group of Hawker Siddeley Dynamics to overcome the inaccuracies of the conventional systems using transducers to convert a physical parameter into a proportional voltage or current.

In the new system the physical parameters involved are converted into electrical form by a simple pulse generator, which gives a precise pulse repetition rate for any given rotational or linear speed, pressure, temperature or position. This frequency is compared with a highly stable reference frequency, which is equivalent to the old demand setting. The error signal, a precise frequency or pulse repetition rate, is injected into a power switching circuit, the output of which is applied to a corrective action.

The British Post Office, in collaboration with the Companhia Portuguesa Radio Marconi, has invited tenders for making and laying a new submarine telephone cable between the United Kingdom and Portugal. The cable will land in Cornwall not far from the Goonhilly Satellite Station, and in Portugal, at a point to the south of Lisbon.

The new cable will replace the existing telephone and telegraph connexions with Portugal via France and Spain, and will be available for connexion with circuits to Spain, Italy and other Mediterranean countries; it will also connect with a new cable to South Africa which is to be laid from Cape Town to Portugal by the South Atlantic Cable Co.

The new cable, which will have a capacity of 480 4kc/s circuits, is expected to be laid and ready for service by the end of 1968.

International Systems Controls Ltd has changed its title to G.E.C. Computers and Automation Ltd now that it has been completely acquired by the General Electric Company.

G.E.C. Computers and Automation Ltd will continue to sell industrial and process control systems and computer systems for scientific, engineering and educational purposes.

In addition, it will in future be responsible for data links and data handling, remote control and telemetry, and the electronic control equipment which was previously the responsibility of the Industrial Division of G.E.C. (Electronics) Ltd.

Development Laboratories for civil and military purposes are to be established at the G.E.C. Applied Electronics Laboratories at Stanmore, Middlesex.

The Company also intends to promote the programme of Anglo-French cooperation on research and development for computer equipment and techniques resulting from previous agreements between I.S.C. and the Compagnie Européene d'Automatisme Electronique (C.A.E.), the computer subsidiary of C.I.T.E.C. in France.

British Aircraft Corporation announce that its Guided Weapons Division has received a contract valued at £250 000 from Junkers Flugzeug Motorenwerke A.G. of Munich for the design and manufacture of elements of the HEOS (Highly Eccentric Orbit Satellite) scientific satellite.

The HEOS satellite contract is the third to be issued by the European Space Research Organization and has been awarded to Junkers.

HEOS will carry seven experiments from research institutes in Germany, Great Britain, Italy, France and Belgium and will spend a significant time outside the magnetosphere and the shock wave of the earth in its orbit through the solar plasma.

BAC's main contribution to HEOS will be the satellite's attitude-sensing system and associated electronics. The principle of the system is that, as the spinning satellite rotates, attitude sensors monitor the direction of the sun and earth and also the rate of spin. This information is telemetered back to earth and, together with the knowledge of the satellite position obtained by tracking from the earth, enables the satellite attitude to be determined by computation. Two types of sensors will be used, monitoring either infra-red or visible light emissions from the sun and earth.

The British Radio Equipment Manufacturers' Association (BREMA) has issued figures showing that during 1965 the number of television receivers despatched to the trade was 1 681 000 compared with 1 903 000 during 1964 and 1 678 000 during 1963.

Corresponding figures for radio receivers were 1 730 000 compared with 2 139 000 (1964) and 2 616 000 (1963).

The Marconi Company Ltd has received an order valued at over £5M for the supply of a complete communications system and advanced radar data handling and display facilities for the Saudi Arabian defence system.

Marconi, who will be sub-contractors to AEI Electronics, will equip each of the AEI type 40 radar control stations with an automation data handling system based on the Marconi MYRIAD microelectronic computer together with fully transistorized radar and tabular displays.

The communications system will provide digital data, telegraph and voice communication channels between the control stations and the radar and missile sites in the defence system. This will be achieved by a combination of high reliability, long distance tropospheric scatter links with supporting networks of fixed and mobile h.f. stations together with v.h.f. and microwave multichannel radio systems. The Marconi Company has also received an order valued at over £1M from the Kuwait Ministry of Guidance and Information for the supply of three 750kW broadcast transmitters for the Voice of Kuwait. These transmitters are fully transistorized throughout the low power driving circuits. Crystal control is used to give very high stability of the radiated frequency. Vapour cooled tetrode valves are employed in the modulator and high power radio frequency output stages.

The Independent Television Authority during the next three years will build thirteen new transmitting stations to extend and improve its coverage along the western side of the United Kingdom.

In Scotland, three stations will be built along the coast to cover central Ayrshire, Helensburgh and Rothesay.

In Wales, six small stations will be built to bring Independent Television to some of the larger valley communities in central Wales. At present, because of the mountainous nature of the region, television coverage of West and North Wales is virtually limited to the coastal area. The main towns in the areas to be covered by these transmitters are Abergavenny, Bala, Brecon, Ffestingiog, Llandrindod Wells and Llandovery.

In the West of England, a station will be built between Hereford and Gloucester, another near Bath, and one near Barnstaple and Bideford, a further station will be built near Whitehaven, Cumberland.

The Atomic Energy of Canada Limited (AECL) has recently placed an order with the Compagnie Francaise Thomson Houston for a TH N 202 CEA system mass spectrometer. This installation will mark the first time a French mass spectrometer has been exported to America.

This type of mass spectrometer was originally designed by the "Commissariat a l'Energie Atomique" (CEA) and has been developed under licence by Thomson in their Chatou centre. The unit is capable of measurement to better than 1 per cent precision for isotopic analysis of hydrogen and deuterium.

LETTERS TO THE EDITOR

(We do not hold ourselves responsible for the opinions of our correspondents)

A Technique for Decade Counting with Binary Scalers

DEAR SIR,—A number of techniques[1,2,3,4] have been developed for obtaining decade counting from a four-stage binary counter.

This note introduces a new technique for binary to decade conversion. The circuit adjustments are non-critical and give stable operation of the decade counter.

Fig. 1 depicts the full circuit of the decade counter. Starting from the zero state of the counter, binary operation proceeds until the ninth count. At the eighth count the 4^{th} stage is put in the 'one' state, and it activates transistor VT_9 to the conducting state. This transistor in turn loads the 2^{nd} stage so much that it would be incapable of changing its zero state and taking part in the normal binary operation.

At the tenth count, as the 1^{st} stage returns to its zero state, it tends to trigger both stages two and four (the latter by means of the direct coupling between VT_1 and VT_4), the former to the 'one' state and the latter to the zero state. It is the aim to prevent the triggering of the 2^{nd} stage at this instant. As the 4^{th} stage comes to the zero state, it tends to lift the loading of the 2^{nd} stage by making transistor VT_9 non-conducting, apparently enabling the 2^{nd} stage to resume its binary operation and be sensitive to the triggering from the 1^{st} stage at this instant. However, it can be so arranged as described below that at the tenth count the transistor VT_4 of the 2^{nd} stage is not yet ready to function normally, so that the 2^{nd} stage does not get triggered from its zero state. Thus the counter as a whole returns to its zero state at the 10^{th} count; the desired result.

As mentioned above, for the decade counter to operate it is essential that the transistor VT_4 of the second stage is inoperative at the 10^{th} count, when at this instant, it receives a trigger from the 1^{st} stage. For this purpose, the transistor VT_9 must be in saturated state while conducting, so that as VT_8 becomes conducting at the 10^{th} count and tends to make VT_9 non-conducting, it (VT_9) does not become immediately so due to its bottomed state. Alternatively, if VT_9 is not in saturation, VT_4 must be in a deeper saturation state than in normal binary operation so that at this instant when VT_9 just becomes non-conducting, VT_4 requires a larger trigger power for change of state than it gets in normal binary operation.

In actual operation, it was noticed that the circuit of Fig. 1 worked due to saturation of VT_9 while in some other circuits using common emitter with only one supply, VT_4 had gone in its deeper saturation state due to loading of VT_9. It seems that getting into saturation of the loading transistor VT_9 gives a better and more reliable operation.

The decade counter has good speed characteristics. For a binary counter having a speed of 40kc/s, the decade obtained from it did not show any loss of speed while for high speed binary, there was a slight loss of speed for the decade. Still, this decade showed almost identical speed characteristics compared

Fig. 1. The decade counting circuit

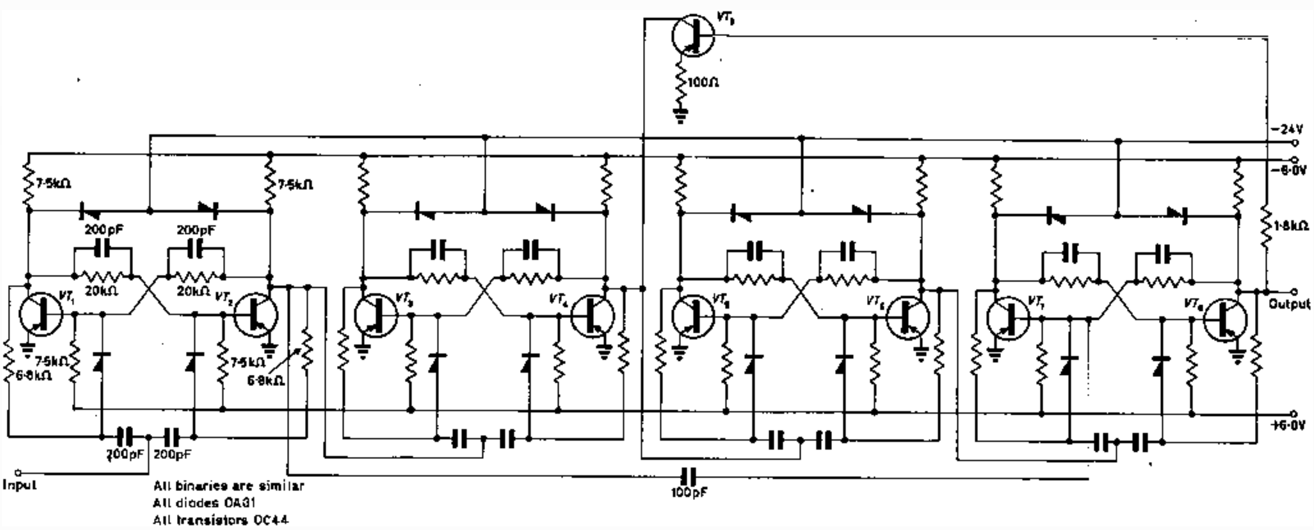

with some of the other binary to decade conversion methods reported in literature.

Yours faithfully,

R. PAVSHAD, S. P. SURI, T. SINGH,
National Physical Laboratory,
India.

REFERENCES

1. POTTER, J. T. A Four Tube Counter. *Electronics*, p. 110 (June 1944).
2. GROSDOFF, I. E. Electronic Counters. *RCA Rev.* 7, 428 (1946).
3. MALHOTRA, P. K., PARSHAD, R. Novel Coincidence Technique for Transistor Decade Counter. *Electronics* (15 Feb., 1963).
4. MALHOTRA, P. K., PARSHAD, R., SINGH, S. K. A Simple Diode Gating Method for Obtaining Decade Scaling from Binary Counters. *J. Instn. Telecomm. Engrs.* *10* (Nov. 1964).

A Random Signal Generator

DEAR SIR,—The article by Mr. Tait and Mr. Skinner in your January issue has prompted me to make some observations concerning random signals in general.

Noise as a test signal has been used for many years, principally for measuring the noise factors of receivers. As is well known, the temperature limited thermionic diode provides a standard source of high frequency noise, while gas tubes are convenient secondary standards of noise at microwave frequencies. But for low frequencies, say below 10kc/s, naturally occurring physical effects are untrustworthy because they are subject to the phenomenon called 'flicker noise'. Flicker noise is in excess of that which is explicable by simple physical laws, and its spectral density usually increases continuously with decrease of frequency. It is exhibited by thermionic and solid-state devices and sets a limit to the sensitivity of amplifiers at low frequencies.

Random test signals for low frequencies must, therefore, be produced artificially. This has usually been done by combining a random high frequency noise source with circuits that perform some kind of logical operation to give a low frequency random source with controlled properties. The Tait-Skinner design is the latest and most elaborate of a line of such circuits, whose genealogy can be traced back to a famous theoretical paper by Rice[1]. Rice's paper included, as light relief from his more weighty conclusions, a description of two types of random telegraph signal. One of these (type A) was exploited as a low frequency noise source by Douce and Shackleton[2], the other (type B) by myself[3] and now by Tait and Skinner.

It is perhaps worth noting that the type B waveform has a well-defined spectral density, though this is not defined in Mr. Tait's article. If a binary stage of output p.d. either $+V$ or $-V$ volts is set randomly every T_c seconds, the spectral density is $G(f)$ volts² per c/s, given by

$$G(f) = 2V^2T_c\left(\frac{\sin \pi fT_c}{\pi fT_c}\right)^2$$

If n independent outputs of this type are summed the spectrum becomes $nG(f)$. Fig. 3(b) in the article has the caption 'normalized amplitude spectral density' and is a plot of $[G(f)/G(0)]^{\frac{1}{2}}$. It can be argued that this is misleading, since it implies that the spectral density of a random waveform may be measured in volts per c/s.

A final comment concerns 'crest factor'. One wonders if this is a very significant feature of a test waveform, because unless the circuit or mechanism under test is aperiodic the crest factor of the response will differ from that of the input. Suppose for example that a random telegraph signal with unity crest factor feeds a low-pass filter whose effective bandwidth B c/s is small compared with $f_c = (1/T_c)$. The r.m.s. value of the output signal is $[2V^2B/f_c]^{\frac{1}{2}}$ and if the filter response to a step is monatonic the peak signal is V, so the crest factor has increased to $(f_c/2B)^{\frac{1}{2}}$. If this last quantity is in the region of 2·5 or more, the signal emerging from the filter is nearly gaussian in distribution.

Yours faithfully,

H. SUTCLIFFE,
Royal College of Advanced Technology,
Salford.

REFERENCES

1. RICE, S. O. Mathematical Analysis of Random Noise. *Bell Syst. Tech. J.* *23*, 282 (1944) and *24*, 46 (1945).
2. DOUCE, J. L., SHACKLETON, J. M. Low frequency random signal generator. *Electronic and Radio Eng.* *35*, 295 (1958).
3. SUTCLIFFE, H. Noise-spectrum measurement at subaudio frequencies. *Proc. Instn. Elect. Engrs.* *112*, 301 (1965).

The Authors' Reply:

DEAR SIR,—We have read Mr. Sutcliffe's comments with appreciation and agree with his general remarks. The following comments on his particular observations are offered.

The suggestion of elaborateness in our design may be warranted, but the pay-off is in the parallel digital output, which, to give an immediate example, allowed the ready production of the very satisfactory distribution curves shown in the article.

We deliberately avoided the use of an expression for spectral density which involves a unit such as volts-squared-seconds. Our view is that discrete frequency or 'line' spectra can be quoted in volts r.m.s. so why not continuous spectra? It can be argued that the 'power spectrum' cannot be known unless both the current and voltage spectra are known!

The last point concerns the variable crest factor facility. Certainly, subsequent (linear) filtering of the output from our instrument will generally cause an increase in crest factor, but the new crest factor is still variable in the same ratio as before. For example, if the rectangular distribution signal is filtered to produce a signal having a crest factor of say, 3, then this can be increased in steps of $\sqrt{2}$ to a maximum value of 30, without change of peak value or spectral shape. We submit that this is of doubtful value only in that it is a new facility in signal generators whose full value is yet to be exploited.

Yours faithfully,

D. A. G. TAIT,
M. J. SKINNER,
The Solartron Electronic Group Ltd.

Invertor Protection Circuit

DEAR SIR,—The elaborate invertor protection circuit of Messrs. Ross and Goodger described in the September 1965 issue could be replaced by the arrangement shown in Fig. 1.

The sensing resistor is bridged by the cathode-gate circuit of a small s.c.r. The relay coil being placed in series with the anode lead to the positive rail. As the minimum triggering voltage of the s.c.r. is 1·5 to 2V the circuit is fairly sensitive. In the above case a 2N3525 fired at a current of 7·5A. The circuit can be reset by opening and reclosing S. The

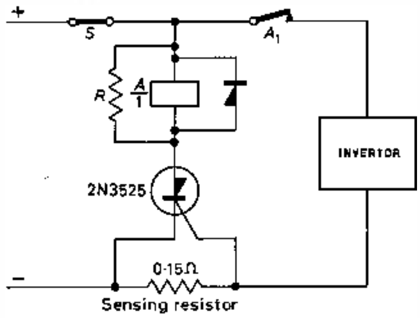

Fig. 1. Simple protection circuit

sensitivity may be adjusted by variation of the sensing resistor or inclusion of a small adjustable resistor in the gate lead.

The inductance of the relay coil may prevent proper s.c.r. firing by restricting start holding current. This is overcome by inclusion of bleed resistor R.

Yours faithfully,

R. F. REDFERN,
Redfern Radio,
New Zealand.

The authors reply:

DEAR SIR,—The protection circuit shown in our s.c.r. invertor described in the September 1965 issue was not designed for this circuit but made up from existing units. It can be simplified in a number of ways, in particular by a single transistor which acts as both switch and relay amplifier.

However the circuit submitted by R. F. Redfern appears to be a particularly suitable one for this type of invertor. Being essentially a locking switch, the s.c.r. used does away with the need for locking contacts on the relay.

Yours faithfully,

D. I. ROSS,
B. E. G. GOODGER,
Victoria University of Wellington,
New Zealand.

NEW BOOKS

Integrated Circuits Design Principles and Fabrication

By Motorola Inc. 385 pp. Crown 4to. McGraw-Hill. 1965. Price 180s.

THIS is the first of two volumes on integrated circuits to be produced by the Semiconductor Products Division of Motorola Inc. It is intended that the second volume will deal with actual design procedures and analysis of circuits, and will supplement Volume I, under review here, which deals broadly with the basic design principles and techniques of integrated circuits.

The Motorola staff have very correctly first defined their terminology, which can be very confusing, even to an expert in the field. A useful chart is given, which follows the definitions recommended by the Electronic Industries Association (U.S.A.)*.

It is fast becoming a tradition that books dealing with any aspect of semiconductor technology (even those on transistor circuit applications) should include a chapter on semiconductor physics. Probably the necessity for this is no longer as important as it was now that there are many standard text books on the subject. The book under review is no exception. It is divided into three parts: Part I (chapters 1-4) is devoted to a very simplified treatment of basic semiconductor physics, followed by chapters on the theory and properties of junctions, on impurity diffusion, and on basic transistor engineering. This last chapter of Part I attempts to relate the electrical characteristics of transistors as circuit elements to the actual physical properties of the different regions, junctions, and electrode structures used in the device. There is some justification for including these chapters on basic principles in Volume I, because the main emphasis is on the semiconductor integrated circuit, which is so closely bound up with device technology as to be inseparable.

Part II (chapters 5-10) deals with the fundamentals of monolithic and hybrid circuit design. This is followed by chapters on methods of preparation and electrical properties of active devices, including transistors, diodes, field effect transistors, tunnel diodes, etc. Passive components for integrated circuits are also dealt with in a separate chapter which includes a description of the junction capacitors and diffused resistors associated with semiconductor integrated circuits. It also deals with thin film components, capacitors, resistors and inductors of the type used in thin film integrated circuits, and indicates how a useful intermarriage of techniques is taking place between the two basic technologies.

The final section of the book (Part III—chapters 11-15) deals with the fabrication of integrated circuits, and describes the main steps and techniques of manufacture, commencing with the growing of single crystal material, right through to encapsulation of completed circuits. No doubt users would have liked to be presented with some indication of failure mechanisms and reliability figures in this section. Some tests are described, but no results given. It is possible that more attention should have been given to the subject of thin film integrated circuits, because the background information and volume of work on thin films is probably as great as in the semiconductor approach to integrated electronics. The references to this section are rather remote, and do not reflect the vast amount of work that is being carried out on thin films.

The book is well produced and on the whole gives adequate coverage of the subjects presented. The diagrams are clear and useful, and there is a good subject index. There are sufficient references for additional details to be obtained. In the reviewer's opinion the book will be useful to both the manufacturer and the user of semiconductor integrated circuits, particularly as previous books dealing with integrated electronics have tended to be a collection of individual papers rather than a coherent treatment of the subject.

G. SIDDALL

* *Published in Microsystems Electronics Bulletin, Vol. I, by the Electronics Industries Association, New York, December 1962. A similar statement also appeared in* ELECTRONIC ENGINEERING, *December 1963, page 816.*

Principles of Television Engineering

By R. C. Whitehead. Vol. 1 178 pp., Vol. 2 270 pp. Demy 8vo. Iliffe Books Ltd. 1965. Price Vol 1 25s., Vol. 2 35s.

THE author sets out to serve the student whose aim is to make a career in virtually any branch of television engineering, and the books are said to be easily followed by those having only an elementary knowledge of physics and mathematics.

As the range of the books is so vast it is to be expected that the treatment of many aspects of television engineering must be somewhat superficial. As one would expect from the author some parts of the transmission side of the industry are well covered, e.g. the scanning process as a means of developing a suitable signal for transmission and reception, the factors which have led to the various standards, interlacing, aspect ratios and front and back porches. Gamma, its measurement and control is also well covered. The generation, amplification, control, distribution and mixing of video signals and synchronizing and blanking pulses, as well as the recording of such signals on film and tape is described in a useful manner.

The chapter on video amplifiers and the appendix on the production of 75Ω sources, d.c. restoration and clamping and d.c., h.t. and e.h.t. stabilizers give basic details of such circuits, again overwhelmingly for those interested in the transmission end of the chain.

Chapter 6 deals with camera tubes, including the vidicon, and covers much of the very practical as well as the theory of the tubes, such as resting them after 200 to 300 hours' use and four hours' minimum use per month to clear up occluded gases.

Chapter 4 on transmitters is, however, very superficial indeed and consists of less than eight pages.

Chapter 5 of Vol. 2 deals briefly with receivers and must be of little use to a student wanting up-to-date knowledge about receiver problems and typical solutions. The service engineer would find even less of help.

In the opinion of the reviewer far too much is attempted in these books and they have therefore become very superficial in many parts. For instance, in the chapter on scanning, a cathode coupled multivibrator is the only oscillator described, while third harmonic tuning, line linearity methods, dual standard switching problems, desaturated line transformers and stabilized circuits are not covered at all.

Not enough care is given to the presentation of material to make it suitable for students just coming into the industry. In Fig. 1.15, for instance, about telerecording, it appears as if film is exposed while the camera shutter is shown closed. In Fig. 6.8, about coupling characteristics of tuned circuits, a rectangular response is shown as being obtained by a "combination of any infinite number of ideal tuned circuits".

In the chapter on receivers there are two plates, one showing various camera tubes and one showing part of the inside of an image orthicon.

Nothing at all in the way of transistor circuits is described, not even in studio and such control equipment.

In view of the increasing importance and use of transistors this is a surprising omission, yet relatively unimportant circuits such as sound and vision interference limiters are included.

It is this odd selection of material and widely differing level of treatment of the selected material which the reviewer finds unacceptable.

C. H. Banthorpe

Analogues for the Solution of Boundary Value Problems

B. A. Volynskii and V. Ye Bukhman. 460 pp. Med. 8vo. Pergamon Press. 1965. Price 90s.

Boundary value problems, requiring solutions to often complex non-linear partial differential equations, present a particular challenge to the applied mathematician or engineer. Such analytic solutions as have been obtained are usually approximate, and while they are of importance for giving insight into the fundamental nature of the problem, the designer or engineer is interested in obtaining numerical solutions over a wide range of the relevant parameters. To such people the use of computer methods is clearly of the greatest importance, and this book describes recent Soviet advances in the use of analogue techniques for the solution of boundary value problems.

Starting with mathematical principles and the classical analytic solutions the reader is led to finite difference approximations to partial differential equations and thence to the setting up of analogue networks. An important aspect is that of taking measurements from the network, and this problem is given due consideration. The final chapters describe actual computers, both universal and special purpose, which are being used in Russian Institutes for the solution of boundary value problems.

Solutions for unlimited domains present particular problems, and the application of the Star Integrating Network in this connexion is of great interest. Also worthy of note is their application to definite integrals and integral equations.

Boundary value problems may be divided into three types viz.: elliptic, hyperbolic, and parabolic. This classification has a significant effect on the techniques to be used for the solution of a particular problem. While examples of each type are considered in the text, it is felt that an adequate discussion of this important distinction is lacking.

A supplementary chapter describing further developments has been added to the English edition. In this chapter emphasis has been given to the use of integral methods for solution. In some circumstances these methods are more powerful than the more conventional difference approach.

This book should be of great value to engineers and designers, and many new and important ideas are described therein.

P. L. Owen

Optical and Electro-Optical Information Processing

By J. T. Tippett et al. 780 pp. Med. 8vo. The M.I.T. Press. 1965. Price 225s.

This book contains the 40 papers presented at the Symposium on Optical and Electro-optical Information Processing Technology held at Boston, Massachusetts, in November 1964, covering optical and electro-optical techniques for storage, logic, display and sensing together with device and circuit research in optical generation, detection, modulation, amplification and control.

Other aspects include optical character reading, information retrieval and digital processing systems.

A Laboratory Manual of Electronics

By K. J. Dean. 143 pp. Demy 8vo. Blackie and Sons Ltd. 1965. Price 12s.

The 66 experiments described in this manual are intended for students of electronics, electrical engineering and applied physics and start with the measurement of the parameters of valves and transistors and cover the various types of amplifiers, oscillators; pulse shaping, counting and logic circuits.

The level of physics and mathematics is that of the advanced level, G.C.E. in these subjects.

Transistors in Logical Circuits

By J. Ph. Korthals Altes. 117 pp. Demy 8vo. Iliffe Books Ltd. 1965. Price 16s.

By way of introduction, a description is given of the fundamentals of Boolean algebra and of binary systems, followed by the industrial applications of switching circuits using semiconductors, comparisons being made with existing relay switching techniques.

Advanced Studies in Electrical Power System Design

By R. A. Hore. 385 pp. Demy 8vo. Chapman and Hall Ltd. 1966. Price 70s.

This book is based on some 15 years of practice, study and research by the author on power systems and deals principally with the electromechanical aspects of system design and problems arising from the use of large quantities of power.

The treatment throughout is practical and illustrative worked examples are included.

Reliability of Electronic Components

By C. E. Jowett. 165 pp. Demy 8vo. Iliffe Books Ltd. 1965. Price 42s.

This book presents the relevant facts concerning the properties and stabilities of various classes of components and materials, together with a summary of information based on testing and evaluation.

The introductory chapter is concerned with the effects of environment and atmosphere, and describes possible hazards and best ways of protection. The remaining chapters deal with the various types of components including r.f. cables, electrical contacts, printed circuits and wiring.

Crystals, Diamonds and Transistors

By L. W. Marrison. 312 pp. Foolscap 8vo. Penguin Books Ltd. 1966. Price 8s. 6d.

This small paperback is intended as an introduction for the layman to the science of crystallography.

Semiconductor Devices

By J. R. Brophy. 130 pp. Demy 8vo. George Allen & Unwin Ltd. 1966. Price 18s.

The operation, structure and characteristic of the more important semiconductor devices are explained in a descriptive and non-mathematical style in this book.

Kempe's Engineers' Year-Book

3 000 pp. Crown 8vo. Morgan Brothers (Publishers) Ltd. 1966. Price £4 15s.

This year-book covers practically every branch of engineering and in this new edition for 1966 is a revised chapter on Nuclear Energy. The chapter on Aircraft Propulsion now includes details on Rocket Engines, Rocket Theory and Fuels.

Colour Television Explained

By W. A. Holm. 130 pp. Pott 4to. Philips Technical Library. 1965. Price 21s.

When the first edition of this book was published in September 1963 the NTSC colour television system was virtually the only system. Since then, the SECAM and PAL systems have entered into the choice for the European colour television system and the second edition of this book now includes a description of the basic principles of these two systems.

Microwave Antenna Theory and Design

Edited by S. Silver. 623 pp. Demy 8vo. Constable. 1965. Price 24s.

This book is an unabridged and unaltered republication of the work first published by McGraw-Hill in 1949 as Volume 12 in the Massachusetts Institute of Technology Radiation Laboratory series.

Propagation of Short Radio Waves

Edited by D. E. Kerr. 728 pp. Demy 8vo. Constable. 1965. Price 24s.

This book is an unabridged and unaltered republication of the work first published by McGraw-Hill in 1951 as Volume 13 in the Massachusetts Institute of Technology Radiation Laboratory series.

Threshold Signals

Edited by J. L. Lawson and G. E. Uhlenbeck. 388 pp. Demy 8vo. Constable. 1965. Price 18s.

This book is an unabridged and unaltered republication of the work first published by McGraw-Hill in 1950 as Volume 24 in the Massachusetts Institute of Technology Radiation Laboratory series.

Digitale Rechenanlagen (Digital Computers)

By A. P. Speiser. 2nd revised edition. 454 pp. Royal 8vo. Springer Verlag, Berlin. 1965. Price DM.69.-

This book deals with the principles, circuits, operation and reliability. After a comprehensive introduction requiring no previous detailed knowledge of the subject, the author proceeds to deal step-by-step with all aspects required for the design of computers. An extensive bibliography gives references for those wishing to go deeper into certain points.

Ein Operatorenkalkül zur Lösung gewöhnlicher und partieller Differenzengleichungssysteme von Funktionen diskreter Veränderlicher und seine Anwendungen (An operational calculus for the solution of ordinary and partial difference equation systems of functions of discrete variables and its application)

By Prof. Dr. P. L. Butzer and Dipl.-Phys. H. Schulte. Research Report No. 1557 of the Land Nordrhein-Westfalen. 53 pp. 3 ill. Royal 8vo. Westdeutscher Verlag, Cologne. 1965. Paperback, DM.49.-

The authors examine the substitution of the z-transformation—which has been successfully applied hitherto—by the operational calculus which has the advantage of direct and simple application without resource to the theory of functions. Calculated examples are intentionally drawn from widely varying fields of application.

NEW EQUIPMENT

A description, compiled from information supplied by the manufacturers, of new components, accessories and test instruments.

(Voir page 267 pour la traduction en français; Deutsche Übersetzung Seite 274)

LOGIC TUTOR

System Computors Ltd, Fossway, Newcastle upon Tyne, 6

(Illustrated below)

A new logic tutor which can be used either as a teaching aid or as a design tool is announced by System Computors Ltd.

For teaching purposes it can be used to demonstrate the elements of combinational logic and the operational principles of digital computers. By using comparatively cheap patch panels one logic tutor can serve any number of students. Logic circuits can be prepared on the panels and checked before being brought to the machine. This offers

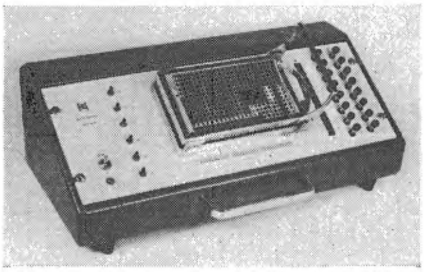

fuller participation by the student and, further, protects the logic elements by allowing errors to be rectified before being put on the machine. Permanent patched panels can be kept as demonstration set pieces.

In its role as a design tool, the logic tutor can aid the design and development of logic control systems. It allows for rapid and easy interconnexion of the elements of a logic control system so that it can be verified without the need to wire up circuits or connect power supplies.

The logic tutor, which weighs only 20 lb, is self-contained and portable. It can be used conveniently on a desk and requires only a 230V mains input.

EE 92 751 *for further details*

MICRO-MINIATURE LAMP

Thorn Special Products Ltd, Great Cambridge Road, Enfield, Middlesex

(Illustrated above right)

Capable of being operated directly from the output of a transistor, the Thorn Mite-T-Lite micro-miniature lamp has a current consumption of only 35mA at 1·5V d.c. making it a suitable com-

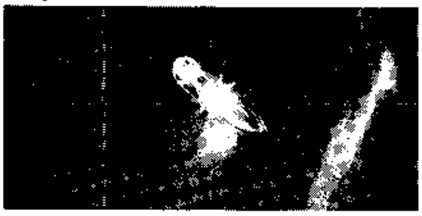

ponent for photo-electric logic systems, compact matrix displays, medical equipment or micro-miniature battery-operated techniques.

When operated at 1·5V the light output is 45 to 55 millilumens and the average lamp life is approximately 500 hours. On operation at 1V the lamp life is extended in excess of 2 500 hours.

The tungsten wire filament, diameter 0·00025in, is wound in a coil of approximately 40 turns and, having a low thermal inertia, its light output will follow voltage impulses of up to 100p/s.

Overall dimensions of the Mite-T-Lite are: diameter 0·055in and length 0·175in.

EE 92 752 *for further details*

BROADBAND SAMPLING VOLTMETER

Hewlett-Packard, Dallas Road, Bedford

(Illustrated below)

Using a sampling principle, Hewlett-Packard's model 3406A reads a.c. voltages from 10kc/s to 1Gc/s, resolves differences as small as 50μV, and has a low input capacitance. In use it requires no tuning. The meter has full-scale ranges from 1mV to 3V.

To improve its usefulness in measuring voltages at hard-to-reach points in r.f. circuits, it has a push-button con-

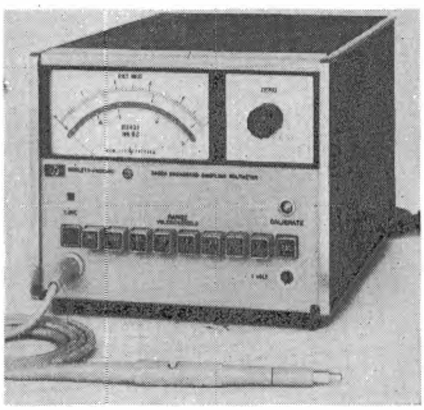

veniently located in its probe. So long as the button is pressed, the meter will retain its reading.

In its lower frequency range (10kc/s to 100Mc/s) the accuracy is ±3 per cent. At higher frequencies (100Mc/s to 800Mc/s) it is ±5 per cent. At the upper extreme (800Mc/s to 1Gc/s) it is ±8 per cent. Useful sensitivity is provided from 1kc/s to 2Gc/s.

The new instrument operates by internally generating an audio-rate sample that is statistically identical with the unknown r.f. signal. The sample is then measured. Because the sampling rate is constantly varying, it will not accidentally coincide with the unknown to produce an erroneous sample.

The meter operates conventionally, reading absolute average calibrated in r.m.s. However, its audio output is available on a back outlet. Since this output presents a statistical image of the unknown, its true r.m.s. value may be measured on a low-frequency true r.m.s. meter; a proportional-to-peak measurement may be made with a low-frequency meter of that type also. There is, in addition, a d.c. recorder output.

While the meter's input feeds directly to the sampler, ample protection is provided against overload. Recovery is quick, and no damage is done, by 1 000-to-1 overload of the 1mV range.

Facilities to calibrate the meter are built-in. A 1V standard is presented on the front panel. To reset zero, the probe may simply be inserted in the calibrate socket, which is shorted whenever the calibrate push-button is disengaged.

EE 92 753 *for further details*

F.M. TEST SET

Distributed by: Livingston Laboratories Ltd, Greycaines Estate, Bushey Mill Lane, North Watford, Hertfordshire

(Illustrated on page 261)

Livingston Laboratories Ltd has been appointed sole U.K. representatives for the range of telecommunication test equipment manufactured by Amalgamated Wireless (Australasia) Ltd of Sydney.

Included in the range of instruments to be marketed in this country are a number of portable modular solid state test sets covering the frequency range 10c/s to 520Mc/s.

Among them is the battery-operated A.W.A. test set type A410, a compact,

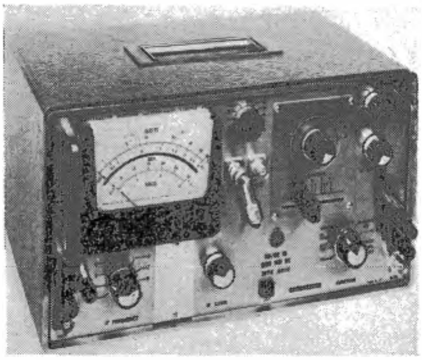

solid state instrument designed for field service and maintenance of f.m. two-way radio equipment.

Consisting of a f.m. v.h.f./u.h.f. signal generator, crystal i.f. calibrator, f.m. deviation meter, a.f. and r.f. power meter, it can be used for both receiver and transmitter measurement in the frequency range 30Mc/s to 520Mc/s.

EE 92 754 *for further details*

PHOTO-DETECTORS

Mullard Ltd, Mullard House, Torrington Place, London, W.C.1

Two new fast-response photo-detectors sensitive to pulsed or modulated radiation in the 2μm to 25μm waveband are announced by Mullard Ltd. Of copper-doped germanium, they are the first of their kind to be manufactured in the U.K. and will be of particular interest to physicists and spectroscopists. Their introduction extends the spectral coverage already provided by the company's lead sulphide and indium antimonide detectors.

The new detectors, type RPY37 and RPY40, are cooled to 4·2°K in cryostats filled with liquid helium. Once filled they require no further attention for at least seven hours. Compared with the thermal detectors they offer an improved sensitivity and a faster response time—the intrinsic response time of the sensitive element in both of the new devices is less than 1μsec.

The rapid response of both detectors is valuable in the study of transient phenomena. The RPY37, which has a sensitive area of 6mm by 1mm, provides the spectroscopist with a means of obtaining high resolution at wavelengths up to 25μm. The larger sensitive area of the RPY40 makes this device suitable for the examination of transient phenomena such as pulsed or modulated emission from long wavelength gas and solid state lasers. In this work there may be only a few milliseconds in which a particular effect can be observed, for example, while a large pulsed magnetic field is applied to the specimen under test.

Other applications for these detectors will be the examination of radiation phenomena encountered in shock tube studies, plasma studies and solid state research.

The detectors are in stainless steel construction.

EE 92 755 *for further details*

D.C. POWER SUPPLY

Gresham Lion Electronics Ltd, Twickenham Road, Hanworth, Middlesex

(Illustrated below)

A further addition to its range of power supplies has been announced by Gresham Lion Electronics Ltd. The GLE 60 general purpose workshop power supply converts a 225V 50c/s single phase input to 28V d.c. at 60A (max.).

The new power supply can be used in all climates and is particularly suited to arduous tropical and desert conditions. It was originally designed for driving radio equipment, but the production version can meet various electronic power supply requirements.

The GLE 60, which was developed as a private venture by Gresham Lion Electronics Ltd, has been selected for service with the British Army and meets Ministry of Defence requirements for Ground Equipment DEF 133. It has been allocated NATO Stock Number 5820-99-104-7480. It operates at temperatures from −25°C to +50°C in humidities of between 0 and 90 per cent.

Output variation is held to 1V for a

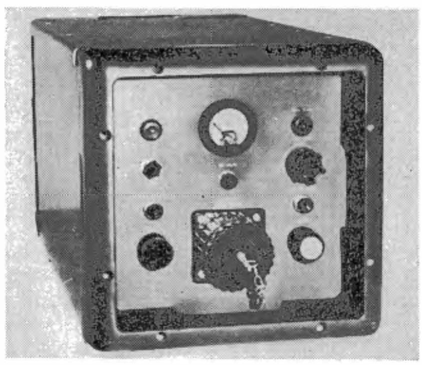

variation of ±15V and a load variation of 60A. Ripple is less than 1·4V r.m.s. under all conditions of load and input voltage. Overloads of 15A at maximum load can be accepted for 100μsec after a 30A step load change.

The unit, which weighs 140 lb, is housed in an aluminium container and air cooled by a blower motor. A special support can be supplied for vehicle mounting. Light electronic circuits are on printed circuit boards with test points for simple servicing. The GLE 60 can be supplied on a special quick-release mounting tray.

Full fuse protection, automatic overload cut-out and thermostatic warning devices are incorporated in the equipment. The equipment is also available for civilian use.

EE 92 756 *for further details*

A.C. CALIBRATION EQUIPMENT

Dynamco Instruments Ltd, Salisbury Grove, Mytchett, Aldershot, Hampshire

Dynamco Instruments Ltd (incorporating Digital Measurements Ltd) announce two new instruments which, when used with standard test equipment, enable the 0·01 per cent calibration of a.c. instruments over the range 30c/s to 100kc/s.

The D3101 a.c. calibration unit contains a thermocouple transfer standard with backing-off supply and a three-decade a.c. divider having a diversion accuracy of 1 part in 10^5. The divider is used for checking linearity and setting attenuators, the thermocouple with back-off is used to check frequency response, and the transfer standard is used for absolute calibration against a d.c. standard.

The D3100 sine wave generator produces a sine wave with a total harmonic distortion of less than 0·005 per cent (essential for high accuracy calibration), an amplitude stability of 0·005 per cent short-term and has a frequency range of 10c/s to 100kc/s. The output is 5V r.m.s. from 600Ω via a 0 to 80dB attenuator.

Other equipments required are: a stable d.c. power supply, such as the Dynamco D3000, a sensitive galvanometer, and a 100V or 1000V amplifier for calibration at higher voltage levels.

EE 92 757 *for further details*

CASSETTE-LOADED TAPE READER

G.E.C. (Electronics) Ltd, East Lane, Wembley, Middlesex

(Illustrated below)

A cassette-loaded photo-electric tape reader designed particularly for programming computers in the field has been developed by G.E.C. (Electronics) Ltd. This compact equipment reads standard 5 hole punched tape at 200 characters/sec with rewind at the same speed. It can also be supplied to read 8 hole tape. It will stop within one character on demand and automatic stop is provided at the end of rewind.

A feature of the equipment providing a number of advantages for service use in the field is that the 600ft reels of standard tape accepted by the reader are loaded into cassettes. This greatly increases the ease and speed of loading under operational conditions and affords extra protection to the tapes. It also permits rapid reprogramming, as other cassettes containing alternative programmes can be quickly loaded on the spot.

The equipment is constructed in three units: the tape deck; the power unit; and the electronics pack. The power unit and the electronics are all solid state.

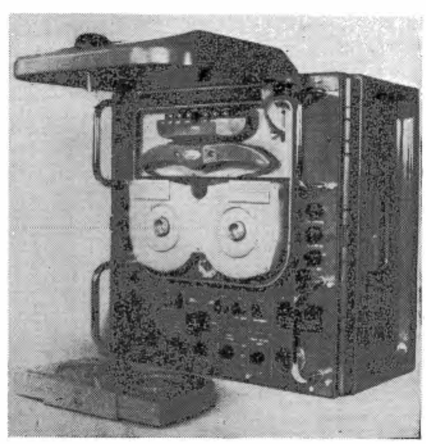

The tape deck, which includes all the tape handling mechanism can be used with any other equipment requiring tape reading facilities. The complete assembly when fitted into a standard R.A.E. instrument case measures only 17½in wide × 12in high × 9in deep approximately.

Normally power supply for the equipment is 200V 400c/s three-phase. It can also operate from 28V d.c., and can be adapted to run off 230V 50c/s. The reader can be used in either a horizontal or a vertical position in the temperature range −40°C to +55°C. It is suitable for use aboard aircraft, is completely weatherproof and has been fully tested against vibration and shock.

EE 92 758 *for further details*

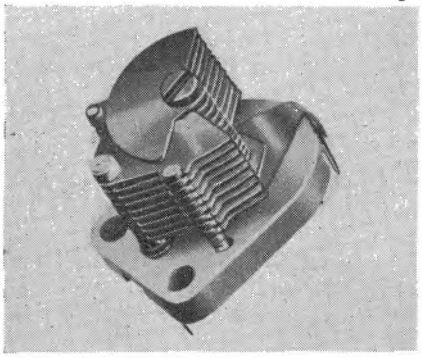

VARIABLE CAPACITORS

Wingrove & Rogers Ltd, Domville Road, Liverpool, 13

(Illustrated above)

Type C.31-51/6 is an air dielectric trimmer mounted on a ceramic base. Designed specifically for mounting on 0·1in module printed wiring boards the dimension between stator and rotor contacts is 0·9in.

A new method of construction and support of the stator assembly together with a special rotor contact gives this component high mechanical and electrical stability. The requirements of DEF.5141 are adequately met.

The minimum capacitance is 4pF and the capacitance swing up to 67·5pF. The base area is 0·65in by 0·925in overall.

EE 92 759 *for further details*

POWER SWITCHING TRANSISTOR

The Marconi Co. Ltd, Chelmsford, Essex

A new transistor, one of the types that has made the Marconi MYRIAD computer possible, has just been placed on the general market by the Microelectronics Division of The Marconi Co. Ltd.

The performance of this transistor, in terms of switching speed and power handling capacity, is believed to be higher than for any other similar device currently available.

Designed as a high power driving transistor for very fast ferrite core stores with cycling times of as little as 1·2μsec, this device also has wide applications in data processing systems, where a large number of logic elements have to be driven simultaneously.

The transistor, type 203-03, is now in quantity production for MYRIAD and for the recently announced English Electric-Leo-Marconi, System 4 computer range. It is available off the shelf in evaluation quantities, and can be provided on short delivery for large orders.

This new transistor is an npn silicon planar transistor mounted in a standard (3 lead) TO-5 encapsulation. The combination of high breakdown voltage and current handling capacity with low saturation voltage and fast switching times are believed to be unique.

In a typical circuit, the total time taken to switch on is 14nsec, and the total time taken to switch off is 90nsec. The collector-emitter saturation voltage is of the order of 0·3V and maximum collector-base leakage is 0·1μA. Minimum collector-base and collector-emitter breakdown voltages are both 45V with a minimum emitter-base breakdown of 4·0V.

EE 92 760 *for further details*

WAVEGUIDE SWITCHES

Decca Radar Ltd, Decca House, Albert Embankment, London, S.E.1

(Illustrated below)

The Instrument Division of Decca Radar Ltd has recently introduced a new automatic waveguide switch, which incorporates a new type of demountable actuator mechanism.

Hitherto, servicing could only be carried out by removing the complete switch from the waveguide system. In the new range, the actuator operating mechanism can be removed or replaced in a few minutes without removing the waveguide switch section from the system.

Another new feature is that the switch can be operated manually while the actuator mechanism is being serviced.

At present, a standard mechanism is available for use with all Decca dual channel switches in waveguide sizes 14, 15, 18, 20 and 22, and is fully interchangeable between sizes. Demountable mechanisms are under development for use with the larger waveguide sizes, and for three-channel switches.

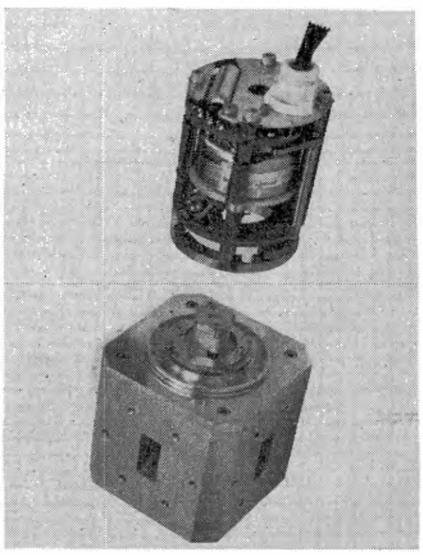

Switches already in use can be modified to take the new mechanism and Decca offers the new actuator for sale as a separate item, with the backing of a modification service.

The illustration shows a switch for size 14 waveguide with the demountable actuator mechanism removed.

EE 92 761 *for further details*

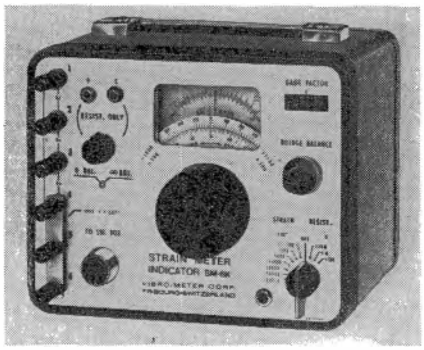

STATIC STRAIN INDICATOR

Vibro-Meter Corporation, Fribourg, Switzerland. British Office: Haletop Civic Centre, Wythenshawe, Manchester, 22

(Illustrated above)

This is a fully transistorized portable read-out instrument for the measurement of static strain by means of strain gauges in half- or full-bridge circuit. The manual compensation method is employed and the meter is calibrated from 5 to 150 000 microstrain. The accuracy is better than 0·5 per cent and the gauge factor is continuously adjustable from 1·8 to 2·2. The carrier frequency is 165c/s.

A built-in ohmmeter is provided for the measurement of the resistance of the strain gauges and the insulation resistance between the gauge and the test surface (ranges: 2Ω to 200MΩ).

The instrument can be operated from batteries or the mains.

EE 92 762 *for further details*

S.W.R. METER

Hewlett-Packard, Dallas Road, Bedford

(Illustrated on page 263)

The new Hewlett-Packard model 415E s.w.r. meter can be used in r.f. and microwave measurement systems, not only to measure standing wave ratio, but also to measure attenuation, gain, or any other parameter determined by the difference between two signal levels. Like other meters of its type, model 415E is a tuned amplifier-voltmeter calibrated in decibels and s.w.r. for use with square-law detectors. Its low noise-figure of less than 4dB enables accurate measurements to be made at low signal levels.

A high precision attenuator is incorporated in the instrument and an expand-offset feature allows any 2dB

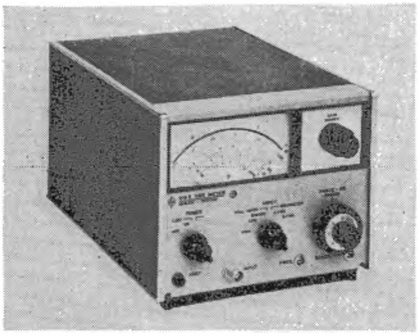

portion of the instrument's 70dB range to be expanded to full scale for maximum resolution, at a specified linearity of ±0·02dB.

Model 415E operates with either crystal or bolometer detectors, with capability to operate from both low (100Ω) and high (5kΩ) source impedance crystals. It provides precise bias currents of 4·5 or 8·7mA, as selected on the front panel, to activate all standard bolometers. Bias is peak-limited for bolometer protection.

The instrument has both recorder and amplifier outputs, which are isolated. Fully transistorized, it weighs less than 8 lb and consumes only about 2W. For portability or isolation from ground loop effects an internally-mounted rechargeable battery pack is available as an option.

EE 92 763 *for further details*

INTEGRATOR AMPLIFIERS

Distributed by: General Test Instruments Ltd, Station Point, Wokingham, Berkshire

(Illustrated below)

The new Burr-Brown models 1663 and 1666 sample and hold/switched integrator amplifiers serve a dual function. When used as sample and hold units, the 1663 has a 10μsec acquisition time, and a 10msec nominal hold time for 0·1 per cent full scale accuracy. The 1666, being a long hold unit, has a 100μsec acquisition time and a hold time of 1sec for 0·1 per cent accuracy. When used as integrators, the 1663 will integrate at a rate of 10^4 or 10^3 V/V sec and the 1666 will integrate at the rate of 10^2 and 10 V/V sec.

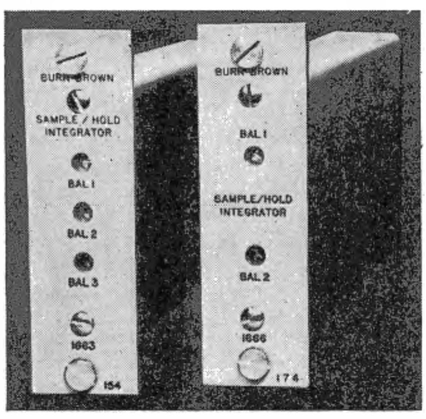

Up to 16 of these units can be mounted in a 3½in × 19in rack.

EE 92 764 *for further details*

ULTRASONIC TESTER FOR ECHO-ENCEPHALOGRAPHY

Ultrasonoscope Co. (London) Ltd, Sudbourne Road, London, S.W.2

(Illustrated below)

The Ultrasonoscope mark 3CM is an ultrasonic diagnostic instrument developed specially for echo-encephalography.

The instrument permits observation of any displacement of the mid-line echo from the brain and this may be used in the diagnosis of intercranial lesions.

The normal position of the mid-line is found by placing two probes on opposite sides of the head and a high frequency sound pulse is transmitted from one to the other.

One of the probes is then used as a transmitter-receiver. The echo from a symmetrical mid-line structure will be at

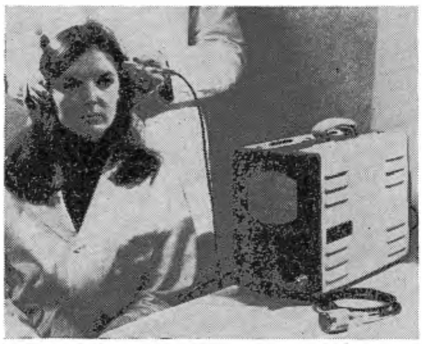

the same screen position as the direct transmission signal since the pulse takes the same time to go out to and back from the mid-line as it did to travel across the skull.

Any shift of the mid-line is clearly shown on the 13cm diameter cathode-ray tube. The extremely short pulse probes give excellent resolution and the display is very easy to interpret. 1½Mc/s probes are used for adults and 2½Mc/s for children.

EE 92 765 *for further details*

ANALOGUE COMPUTER

A. M. Lock & Co. Ltd, Prudential Buildings, Oldham, Lancashire

(Illustrated above right)

The 'Teachaid' is a low cost transistorized analogue computer primarily developed for individual student use. The front panel clearly displays the four operational amplifiers in graphic style. Computation can be single-shot, or repetitive for display on an oscilloscope. Solution repetition is 25 times per second, the compute period is approximately 35msec and the reset time is 5msec. A 10V pulse is provided for synchronising the oscilloscope time-base. Facilities are provided for problem scaling and adjustment to loop gain. The 'Teachaid' is capable of solving up to a third order differential equation by plugging in a resistor or capacitor in the feedback path

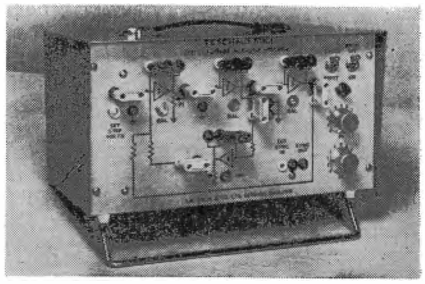

of the operation amplifiers. It is possible to solve much higher order differential equations by means of the transfer function approach and the use of simulation techniques. In this approach a complex network is plugged into the operational amplifier feedback path instead of merely *R* or *C*.

By means of the sync-in and sync-out terminals, up to three 'Teachaids' can be linked together. They are completely safe to use because the maximum voltage on the front panel is 12V.

The 'Teachaid' is supplied complete with carrying handle, fold away stand, lugs for power cable stowage and a selection of plugs with components for plugging into the feedback paths.

EE 92 766 *for further details*

PHASE METER

Dawe Instruments Ltd, Western Avenue, Acton, London, W.3

(Illustrated below)

A new transistorized phase meter is available from Dawe Instruments Ltd. Designated the type 632 it allows comparisons to be made between symmetrical input signals over a wide frequency range (50c/s to 100kc/s). Input attenuators permit a high ratio of signal levels (10mV to 10V, i.e. 60dB), both of which can be measured by a panel voltmeter. Accurate balancing of the input levels is unnecessary, and there are no frequency-sensitive controls. The phase meter scale is expanded to give f.s.d. for each quadrant range, thus improving resolution.

The instrument comprises a reference and a signal channel, each with a fully compensated attenuator (30mV to 10V f.s.d. in six steps). The panel voltmeter

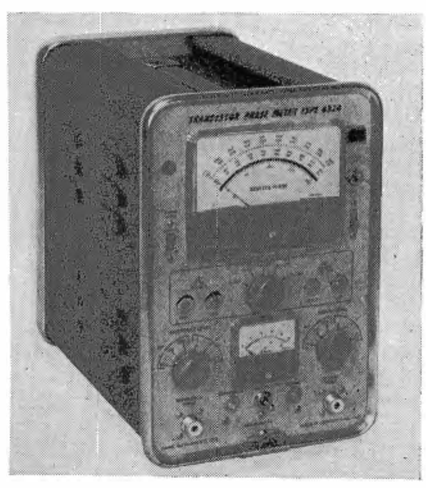

may be switched to either channel, both of which incorporate limiting amplifiers and feed the bistable circuits of an output unit. The output unit is triggered at the zero voltage excursions of the amplifier signals, and feeds to the phase meter a pulsed output signal with a mark-to-space ratio proportional to the phase difference between the two input signals. Direct readings of phase difference are given on four quadrant ranges (0°-90°, 90°-180°, 180°-270°, and 270°-360°), and two auxiliary ranges of 0°-360° and 180°-0°-180°.

The input impedance of each channel is 1MΩ in parallel with approximately 40pF. Accuracy of phase measurement is ±1·5° from 50c/s to 25kc/s, and ±5° from 25kc/s to 100kc/s. Accuracy of voltage measurement is ±5 per cent of f.s.d. Silicon epitaxial planar transistors are used throughout the amplifiers to ensure temperature stability.

EE 92 767 *for further details*

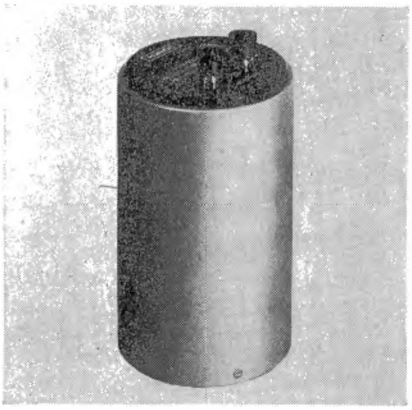

TEMPERATURE CONTROLLED STANDARD CELL

Muirhead & Co. Ltd, Beckenham, Kent

(Illustrated above)

To satisfy the need for a highly accurate and stable source of e.m.f. for reference purposes, Muirhead & Co. Ltd has introduced a standard cell housed in a small temperature controlled unit. The unit is capable of achieving a stability of one part in a million. Weighing only 25 oz, 6½in long and 3¼in diameter, it can be incorporated into recording and measuring apparatus or it can be housed as a free-standing bench instrument. It is sufficiently robust to be transported by any normal means without affecting its high stability characteristics.

EE 92 768 *for further details*

DIGITAL CLOCK

Racal Instruments Ltd, Western Road, Bracknell, Berkshire

(Illustrated above right)

Racal Instruments Ltd is producing a versatile, fully transistorized digital clock system type SA.7100. Designed as a 24h 'time-of-day' indicator, or for use in industrial process control and data logging applications, the SA.7100 provides a digital indication of time in hours, minutes and seconds, on a six-digit

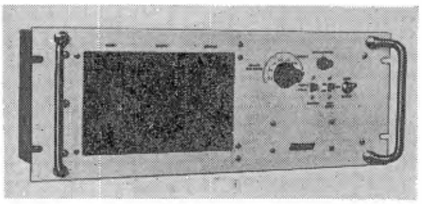

columnar or in-line display and includes facilities for the operation of a digital recorder.

Several versions are available—the type SA.7100A has an accuracy determined by the 50c/s mains supply, while in the SA.7100C the accuracy is referenced to a precision quartz crystal oscillator to afford a system accuracy of better than 2 parts in 10^9 per day. An external standard may be used for greater accuracy applications.

The digital clock is available for standard 19in rack mounting, and for operation in ambient temperatures from 0°C to 45°C. Facilities are included to enable the display to be synchronized in steps of 0·01, 0·1 and 1sec. Power supply requirements are 115 to 230, 50c/s or 115V 400c/s, or external batteries.

EE 92 769 *for further details*

MILLIVOLTMETER

Marconi Instruments Ltd, St. Albans, Hertfordshire

(Illustrated below)

This fully transistorized instrument (type TF 2603) is designed for direct measurements from 300μV to 3V, through the frequency range 50kc/s to 1 500Mc/s.

The ½in diameter measuring probe contains a pair of fast germanium diodes in a full-wave circuit; the response is close to true r.m.s. with inputs of less than 30mV, and peak-to-peak in the 0·5 to 3V regions. This full-wave arrangement minimizes errors when measuring signal voltages whose waveform is complex. A heater is incorporated in the probe to reduce the effects of variation in the ambient temperature.

The easy-to-read meter scales are 5in long, and calibrated in the r.m.s. value of a sine wave. The use of semiconductor devices instead of thermionic valves not only ensures reliability and freedom from microphony, but allows battery operation of the instrument as an alternative to the normal mains supply.

A 100 : 1 multiplier, type TM 7947, is supplied with the instrument. This device permits voltage measurements from 30mV to 300V in the frequency

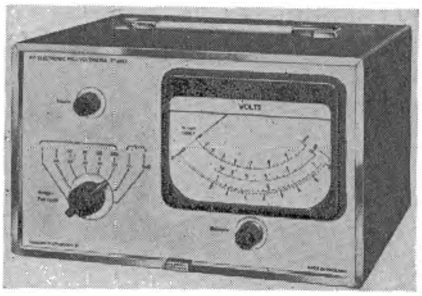

range 500kc/s to 500Mc/s; its input impedance is considerably higher than a thermionic diode valve-voltmeter can offer over the same voltage and frequency range. Optional accessories include a coaxial T-connector for voltage measurements on 50Ω coaxial systems.

EE 92 770 *for further details*

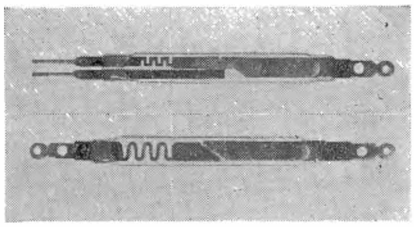

SEALED CONTACT RELAYS

Telefonbau und Normalzeit GmbH, 6 Frankfurt/Main 7, Mainzer Landstrasse, Germany

(Illustrated above)

TN sealed contact relays possess all the advantages of reed relays plus 50 per cent saving in space.

The patent flat contacts which are sealed in a flat glass envelope containing an inert gas have built in flexibility and a contact face design which results in a sliding action with rapid make and break. These relays are particularly suitable for use in electronic circuits and printed circuits where a highly reliable, low cost and simple relay action is required. Performance features include: low contact resistance; high insulation resistance; low capacitance; low switching time; immunity from atmospheric conditions and long life.

EE 92 771 *for further details*

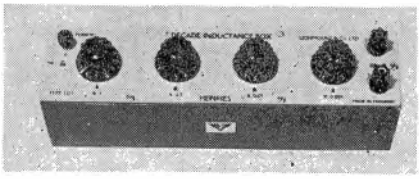

DECADE INDUCTANCE BOX

Lionmount & Co. Ltd, Bellevue Road, New Southgate, London, N.11

(Illustrated above)

The inductance box type LD1 is a four-decade unit with a maximum inductance of 11·11H adjustable in 1mH steps. The accuracy at 1 000c/s is 2 per cent but the usable frequency range for the best values of Q lies in the band of 3kc/s to 300kc/s.

Each decade is comprised of one ferrite pot core tapped at 10 points, and with this arrangement long-term stability of 0·2 per cent can be expected, with Q values between 50 and 200 attainable.

As with all inductors having a magnetic core, the applied voltage depends largely on the frequency for any given winding, and in these units the voltage should be restricted to a few hundred millivolts to avoid saturation of the core.

The residual inductance is 1·6μH, and further information will be issued on incremental inductance, and variation of Q and inductance with frequency.

Ceramic wafer switches are used, and the mahogany box is lined for screening purposes.

EE 92 772 *for further details*

MODULAR RACK

Vero Electronics Ltd, South Mill Road, Regent's Park, Southampton

(Illustrated below)

The most recent introduction by Vero Electronics Ltd is a 7in extra volume modular rack in which fullest use is made of the complete height of the unit, it being possible to accommodate Vero-boards of 6in by 8in or 6in by 11in. The modular rack unit will fit standard racks of 19in width, and accommodate module depths of either 11in or 14in. Module panel widths of 1in, 2in, 4in and 8in can be used.

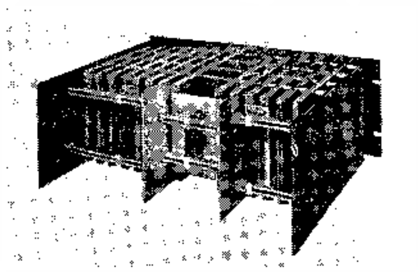

EE 92 773 *for further details*

ETCHING MACHINE

Lee-Smith Photomechanics Ltd, Lyon Way, Hatfield Road, St. Albans, Hertfordshire

(Illustrated above right)

A new, larger version of the Rota-Etch precision etching machine has been introduced by Lee-Smith Photomechanics Ltd. Developed from the 9in machine, the latest Rota-Etch is equipped with a circular work-table on which components having a maximum diagonal dimension of 18in can be mounted.

Rota-Etch machines are designed specifically for the precision etching of standard, subminiature and micro-printed-circuit boards and the production of evaporation masks and similar items by chemical milling.

Workpieces to be etched are fitted to the circular work-table mounted on the hinged lid of the machine's tank. During etching the table rotates at a constant 10rev/min and the etchant is sprayed up on to the workpiece by three revolving corrugated plastic diffuser drums. In this manner all parts of the workpiece are uniformly saturated with the etchant solution.

Intensity of etching can be altered by changing the speed of rotation of the diffuser drums. These can be set to revolve at any speed between 0 and 2 000rev/min.

To achieve consistent results it is imperative that the temperature of the etchant be maintained at a uniform level. Silica heater elements together with water cooling tubes are fitted in the etchant tank for this purpose. The

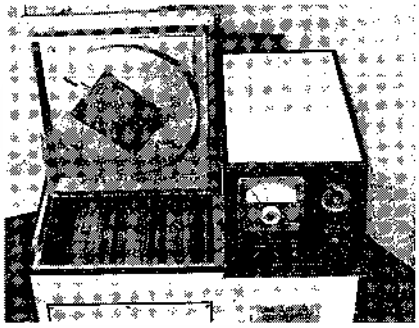

etchant solution is continuously recirculated and can be maintained at any preset temperature within the range of 50°F to 130°F.

Processing times are pre-set on a timer and the machine is automatically switched off at the end of the selected period.

As a safety precaution a switch cuts off the electrical power supply to the machine when the lid of the tank is raised.

EE 92 774 *for further details*

COMPONENT LINEARITY TESTER

Distributed by: Livingston Laboratories Ltd, Greycaines Estate, Bushey Mill Lane, North Watford, Hertfordshire

(Illustrated below)

It has been shown that a relationship exists between the reliability of capacitors and resistors and their linearity. Radiometer of Copenhagen has now introduced an instrument which applies this technique to indicate the reliability of components.

Known as the model CLT 1 component linearity tester, the instrument available in the U.K. from Livingston Laboratories Ltd, measures third harmonic voltages generated through component non-linearity, and is capable of checking up to 20 components a second with impedances of 1Ω to 100MΩ.

An internal oscillator supplies a very pure 10kc/s fundamental frequency at up to 560V amplitude with its third harmonic suppressed to 180dB. The third harmonic of 30kc/s, generated as a result of the non-linearity of the component under test, is indicated on a meter

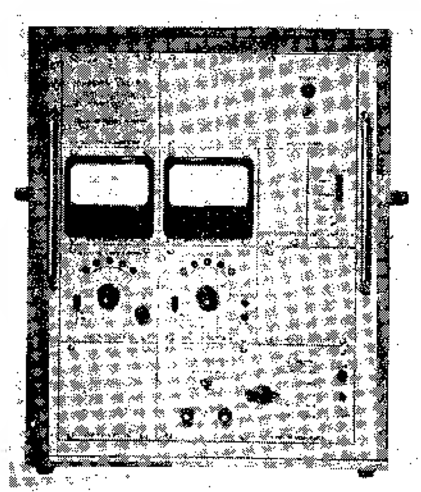

which can detect signal levels as low as −160dB.

Either linear or logarithmic meter response may be selected, with a 60dB range for quick production evaluation.

EE 92 775 *for further details*

SOLAR ENERGY CELLS

The Plessey Co. Ltd, Dielectric and Magnetic Division, Towcester, Northamptonshire

(Illustrated below)

A range of integrated arrays of silicon photovoltaic cells designed to form ground level solar energy convertor power supplies has been introduced by the Dielectric and Magnetic Division, Plessey Components Group.

The arrays provide a long-life, high reliability power supply requiring a minimum of servicing attention, which is particularly suitable for installations

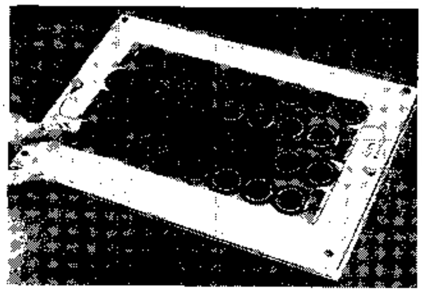

where access is difficult. Extensive surveys have been completed of the average yearly insolation (incident solar energy) available throughout the world, and field trials have provided data on arrays suitable for a wide range of power supply requirements.

To maintain constant power output the arrays are designed to maintain the charge of nickel-cadmium storage batteries. A voltage regulator prevents the battery from reaching its dissociation potential, reducing electrolyte losses and consequent servicing requirements to an absolute minimum. Single array panels approximately 1ft² in area now available are capable of maintaining a battery supply of up to 50mA at 12V indefinitely at favourable locations, and attention is likely to be required only once in four or five years, even in hot climates.

Higher currents and voltages are accommodated by suitable interconnexion of a number of array panels.

Corrosion is prevented by embedding the cells in epoxy resin under a glass panel, which is highly resistant to abrasion by wind-blown sand. This design gives almost unlimited array life, and ensures that the power supply can be expected to be substantially more reliable and longer lived than the equipment which it supplies.

Applications include communication, meteorological and navigational equipment on remote sites. Theoretically, any power requirement can be met, but practical considerations make the arrays most suitable for levels up to 10W continuous.

EE 92 776 *for further details*

Meetings THIS Month

THE INSTITUTION OF ELECTRICAL ENGINEERS

All meetings will be held at Savoy Place, commencing at 5.30 p.m., unless otherwise stated.

Ordinary Meetings

Date: 28 April.
Lecture: Scientific Research in Space.
By: H. Massey.

Control and Automation

Date: 1 April.
Discussion: Sequence Control of Plant Operations.
Opened by: M. F. Binney, K. H. Higgens, T. K. M Korytke and D. A. G. McInnes.
Date: 5 April.
Lecture: Mechanical Analogue/Digital Convertors.
By: B. Adams and W. Bamford.
(Joint meeting with the Automatic Control Group of the Institution of Mechanical Engineers.)
Date: 5 April.
Lecture: Teaching by Television.
By: B. R. Webster.
Date: 15 April.
Lecture: Equilibrium Coding for Pulse Code Modulation.
By: A. H. Reeves.
Date: 20 April.
Lecture: The West London Area Traffic Control Experiment.
By: B. M. Cobbe.
Date: 26 April.
Discussion: Problems in the Design and Installation of Surge-Proof Transistorized Control Equipment.
Opened by: R. F. Eade, D. Harrison and B. E. Noltingk.

Electronics

Date: 4 April.
Lecture: Measurements on Semiconducting Material.
By: G. A. Allen.
Date: 14 April.
Discussion: Non-Optical Transmissions.
Date: 18 April.
Discussion: Computer Bulk Storage.
Opened by: D. T. Gwillim, B. Birch and G. Pirkhoffer.
(Joint meeting with I.E.R.E. Computer Group.)
Date: 19 April.
Lecture: A High Input Impedance Clip-on A.C. Voltmeter.
By: G. F. Turnbull.
Date: 19 April.
Lecture: Automatic Corona Loss Measuring Equipment.
By: E. Rawlinson, P. H. King and P. K. Richardson.
Date: 20 April. Time: 6 p.m.
Lecture: Automatic Landing.
By: B. D. Armstrong.
Date: 29 April.
Lecture: Distribution of Mechanical Forces in Magnetized Material.
By: G. W. Carter.
Discussion: A Note on the Distribution of Mechanical Forces in Magnetized Material.
By: C. J. Carpenter.
Lecture: Evaluation of Magnetized Energy Density in Magnetized Matter.
By: B. D. Popovic.

Power

Date: 1 April.
Discussion: Problems of Short Term Loading of Semiconductor Devices.
Opened by: S. A. Stevens.
Date: 18 April.
Lecture: Electricity for Grain Drying.
By: E. C. Claydon.
Date: 19 April.
Lecture: Automatic Corona Loss Measuring Equipment.
By: E. Rawlinson, P. H. King and P. K. Richardson.
Date: 22 April. Time: 10 a.m.
Colloquium: Electrical Services in System Building.
(All wishing to attend must apply to the Secretary for a ticket. No fee for I.E.E. members; non members £1 1s.)
Date: 25 April.
Discussion: Breakdown of Large Air-gaps and Effect of Voltage Wave Shape.
Opened by: F. D. A. Boylett and D. F. Oakeshott.

INSTITUTION OF ELECTRONIC AND RADIO ENGINEERS

Joint I.E.E.-I.E.R.E. Computer Group

Held at: Institution of Electrical Engineers, Savoy Place, London W.C.2.
Date: 18 April. Time: 5.30 p.m.
Discussion: Computer Bulk Storage.

Electro-Acoustics Group

Held at: I.E.R.E. Lecture Room, 9 Bedford Square, London W.C.1.
Date: 20 April. Time: 6 p.m.
Lecture: Low Distortion Transistor Audio Amplifiers—Some Important Design Characteristics.
By: P. J. Baxandall.
Held at: London School of Hygiene and Tropical Medicine, Keppel Street, Gower Street, London W.C.1.
Date: 27 April. Time: 6 p.m.
Papers on: The U.K.3 Satellite—Data Handling and Telemetry Equipment.
By: W. M. Lovell.
Paper on: The Satellite and its Ground Checkout Equipment.
By: F. P. Campbell.

Joint I.E.R.E.-I.E.E. Medical Electronics Group

Held at: I.E.R.E. Lecture Room, 9 Bedford Square, London W.C.1.
Date: 27 April. Time: 6 p.m.
Discussion: Physiological and Psychological Hazards of High Intensity Sound and Light.
Opened by: B. Shackel.

East Anglian Section

Held at: Barstable Grammar and Technical School, Basildon, Essex.
Date: 19 April. Time: 6.30 p.m.
Lecture: Digital Magnetic Recording.
By: J. H. Streeter.

West Midland Section

Held at: Department of Electronic and Electrical Engineering, University of Birmingham.
Date: 19 April. Time: 9.30 p.m.
Symposium: Communication in Industry.
(Joint meeting with the Institution of Electrical Engineers. Registration necessary; further details from Mr. E. L. Gardiner, 223 Tettenhall Road, Wolverhampton, Staffs.)

Yorkshire Section

Held at: Department of Electrical Engineering, Leeds University.
Date: 7 April. Time: 7 p.m.
Lecture: D.C. Stabilized Power Supplies.
By: T. F. Cryer.

North Eastern Section

Held at: Institute of Mining and Mechanical Engineers, Neville Hall, Westgate Road, Newcastle.
Date: 13 April. Time: 6 p.m.
Lecture: Instrumental Colour Matching.
By: J. Hambleton.

Thames Valley Section

Held at: Clarendon Laboratory, Park Road, Oxford.
Date: 19 April. Time: 7.30 p.m.
Lecture: Hybrid Analogue/Digital Computers.
By: C. H. Vincent.

THE INSTITUTION OF POST OFFICE ELECTRICAL ENGINEERS

Held at: Conference Room, Fleet Building, 70 Farringdon Street, E.C.4.
Date: 5 April. Time: 5 p.m.
Lecture: Exchange Contract Delays.
By: H. J. Thurlow.

THE TELEVISION SOCIETY

Meetings are held in the Conference Suite, I.T.A., 70 Brompton Road, London S.W.3, and commence at 7 p.m.
Date: 21 April.
Lecture: The Fleming Memorial Lecture—The Implications for Television of Modern Thinking on the Visual Process.
By: W. D. Wright.
(Admission to this meeting is by ticket only.)
Date: 29 April.
Annual General Meeting.

Publications Received

PRINCIPLES OF ELECTROSTATICS is the title of the first book in a new series of 'minibooks' announced by The Mullard Educational Service.

Based on the successful series of filmstrips and slides produced by the Service, the new books are expected to become popular with both student and teacher.

'Principles of Electrostatics' is a 32-page book with an A5 international size format (15cm by 21cm). Its thirteen sections each cover a particular aspect of electrostatics. Typical headings are: insulators and conductors; the electrification theory; the gold-leaf electroscope; capacitance and capacitors; electrostatic machines; electrostatic instruments.

Illustrations are black and white representations of the full colour artwork originally used in the filmstrip of the same name. Thus as well as being a useful work of reference in its own right, the Mullard 'minibook' can also be used as illustrated lecture notes for teachers using the filmstrip and as handout material for classes seeing the strip.

'Principles of Electrostatics' is available from The Mullard Educational Service, Mullard Ltd, Mullard House, Torrington Place, London, W.C.1, price 2s. 6d. (including postage), cash with order. For bulk orders a discount is offered.

MULTI-LINGUAL GLOSSARY OF INDUSTRIAL DIAMOND TERMS lists 912 technical terms in English, German, French, Dutch, Italian, Spanish, Swedish and Japanese, and has a separate index in each language. Although compiled specifically for the diamond industry, many of the terms are common to other technologies. This glossary is available as a cost of £1 from the Industrial Diamond Information Bureau, Arundel House, 36-43 Kirby Street, London, E.C.1.

RUMANIAN INDUSTRY—ELECTRICITY is one in a special series giving data on major Rumanian industries. It is anticipated that the introduction which contains general data on Rumania will be common to all the booklets, while the succeeding parts will deal with a specific industry.

Copies of this booklet are available from Joseph Crosfield & Sons Ltd, Warrington, Lancashire.

HOW TO ORGANIZE QR CAMPAIGNS is a booklet which has been specially written for firms which may be thinking of staging quality and reliability campaigns, whether as a step towards improving QR control systems or as a means of reviving interest in these activities. It has been produced in conjunction with the National Quality and Reliability Year by the British Productivity Council in association with the National Council for Quality and Reliability.

Copies of the booklet are available, price 10s. 6d. post paid, from the British Productivity Council, Vintry House, Queen Street Place, London, E.C.4.

BNC CONNECTORS are described in a new series of leaflets which give
(1) An outline drawing and a photograph of each item.
(2) Dimensions in inches and millimetres.
(3) Inner conductor and cable entry dimensions.
(4) NATO Stock Nos., U.S. Military Nos., and Patterns 15 and 16 Style References.
(5) Panel piercing, front and rear mountings.
(6) Assembly instructions.
(7) Full details of the cables that can be accommodated.

Copies of these leaflets are available on request from Greenpar Engineering Ltd, Station Works, Harlow, Essex.

NOUVELLES Réalisations

Traduction des pages 260 à 265

Une description basée sur des renseignements fournis par les fabricants de nouveaux organes, accessoires et instruments d'essai

INSTRUCTEUR LOGIQUE

System Computers Ltd, Fossway, Newcastle upon Tyne, 6

(*Illustration à la page 260*)

Un nouvel instructeur logique, pouvant être utilisé soit comme appareil de démonstration soit comme outil de dessin, a été mis au point par la société Systems Computers Ltd.

Pour les besoins de l'enseignement pratique, il peut être utilisé pour démontrer les éléments de la logique par combinaisons ainsi que les principes opérationnels des calculatrices numériques. En utilisant des panneaux relativement peu coûteux, un instructeur logique peut servir à n'importe quel nombre d'étudiants. Les circuits logiques peuvent être préparés sur les panneaux et vérifiés avant d'être apportés à la machine. Ce procédé assure une plus large participation des étudiants et, de plus, protège les éléments logiques en permettant de corriger les erreurs avant d'introduire les données dans la machine. Des panneaux permanents peuvent être conservés pour les démonstrations.

En tant qu'outil de dessin, l'instructeur logique peut faciliter la conception et la réalisation de systèmes de contrôle logique. Il permet d'interconnecter rapidement et facilement les éléments d'un système de contrôle logique, de manière à pouvoir le vérifier sans bobiner les circuits ou connecter les alimentations.

L'instructeur logique, qui ne pèse que 9 kg, est autonome et portatif. Il peut être utilisé de manière pratique sur un pupitre et n'exige qu'une entrée de courant secteur de 230 V.

EE 92 751 *pour plus amples renseignements*

LAMPE MICROMINIATURE

Thorn Special Products Ltd, Great Cambridge Road, Enfield, Middlesex

(*Illustration à la page 260*)

La lampe microminiature Thorn Mite-T-Lite fonctionne directement sur la tension de sortie d'un transistor. Sa consommation de courant n'est que de 35 mA à 1,5 V c.c. et elle est donc un composant particulièrement indiqué pour les systèmes logiques photoélectriques, l'affichage de matrices compactes, le matériel médical et les appareils microminiature fonctionnant sur batterie.

Lorsqu'elle fonctionne à 1,5 V, la sortie de lumière est de 45-55 millilumens et la durée de vie moyenne d'une lampe est d'environ 500 heures. Lorsqu'elle n'est utilisée qu'à 1 V, sa durée de vie peut dépasser 2500 heures.

Le filament en tungstène dont le diamètre est de 0,00025 pouce est enroulé sur une bobine d'environ 40 tours; en raison de sa faible inertie thermique, sa sortie de lumière peut suivre des impulsions de tension allant jusqu'à 100 p/sec.

Les dimensions hors-tout de la lampe microminiature Mite-T-Lite sont: diamètre 0,055 pouce et longueur 0,175 pouce.

EE 92 752 *pour plus amples renseignements*

VOLTMÈTRE D'ÉCHANTILLONNAGE À LARGE BANDE

Hewlett-Packard, Dallas Road, Bedford

(*Illustration à la page 260*)

Le voltmètre Hewlett-Packard modèle 3406A, basé sur le principe de l'échantillonnage, lit des tensions alternatives de 10 kHz à 1 GHz, résoud des différences d'un minimum de 50 μV et a une faible capacité d'entrée. Il ne nécessite aucun accord en cours d'usage. Ses gammes vont de 1 mV à 3 V.

Pour améliorer sont utilité dans la mesure des tensions à des points de circuit HF difficiles à atteindre, il a été muni d'un bouton-poussoir ingénieusement logé dans sa sonde. Tant que l'on presse le bouton, le voltmètre continue de fournir des indications.

Dans sa gamme inférieure de fréquence (10 kHz à 100 MHz), la précision est de ±3%. Aux fréquences plus élevées (100 à 800 MHz), elle est de ±5%. Aux extrêmes élevés (800 MHz à 1 GHz), elle est de ±8%. Une sensibilité effective est assurée de 1 kHz à 2 GHz.

Le nouvel instrument fournit intérieurement un échantillon de basse fréquence statistiquement identique au signal inconnu de HF. L'échantillon est ensuite mesuré. En raison de la variation constante de la vitesse d'échantillonnage, cet échantillon ne coïncidera pas accidentellement avec le signal inconnu pour produire un échantillon erroné.

Le voltmètre fonctionne de façon classique, donnant une indication de la moyenne absolue étalonnée en valeur efficace. Toutefois, sa sortie basse fréquence est fournie sur une ouverture à l'arrière. Etant donné que cette sortie présente une image statistique du signal inconnu, sa valeur efficace réelle peut être mesurée sur un instrument de valeur efficace réelle à basse fréquence; une mesure proportionnelle à la crête peut être effectuée également avec un instrument de mesure à basse fréquence de ce type. L'instrument comprend, en outre, une sortie d'enregistreur de courant continu.

Pendant que l'entrée du voltmètre alimente directement l'échantillonneur, une protection adéquate est assurée contre les surcharges. Le rétablissement est rapide et nul dommage n'est occasionné par une surcharge de 1 000-à-1 de la gamme de 1 mV.

L'étalonnage du voltmètre se fait par dispositif incorporé. Le panneau frontal comprend un étalon de 1 V. Pour le réenclenchement à 0, la sonde peut être insérée simplement dans la douille d'étalonnage qui est mise en court-circuit lorsque le bouton-poussoir d'étalonnage est relâché.

EE 92 753 *pour plus amples renseignements*

APPAREIL DE CONTRÔLE À MODULATION DE FRÉQUENCE

Distributeurs: Livingston Laboratories Ltd, Greycaines Estate, Bushey Mill Lane, North Watford, Hertfordshire

(*Illustration à la page 261*)

La société Livingston Laboratories Ltd a été nommée agent exclusif pour le Royaume-Uni pour la gamme d'appareils de contrôle de télécommunication fabriqués par la société Amalgamated Wireless (Australasia) Ltd, Sydney.

La gamme d'instruments devant être commercialisés en Grande-Bretagne comprend divers appareils de contrôle modulaires portatifs, constitués de corps solides et couvrant la gamme de fréquence de 10 Hz à 520 MHz.

Signalons, entre autres, l'appareil de contrôle A.W.A., type A410, fonctionnant sur batterie. Il s'agit d'un instrument compact et constitué de corps solides, prévu pour l'utilisation sur le terrain et l'entretien de matériel radiophonique à deux directions et à modulation de fréquence.

Cet appareil, qui se compose d'un générateur de signaux VHF/UHF à modulation de fréquence, d'un calibreur MF à cristal, d'un instrument de mesure de déviation à modulation de fréquence et d'un instrument de mesure de la puissance HF, peut être utilisé tant pour la mesure d'émission que pour la mesure de réception dans la gamme de fréquence de 30 MHz à 520 MHz.

EE 92 754 *pour plus amples renseignements*

DÉTECTEURS PHOTOÉLECTRIQUES

Mullard Ltd, Mullard House, Torrington Place, London, W.C.1

La société Mullard Ltd vient d'annoncer la création de deux nouveaux détecteurs photoélectriques à réponse rapide et sensibles aux radiations modulées ou par impulsions dans la bande d'ondes de 2 à 25 µm. Ces détecteurs en germanium enduit de cuivre sont les premiers du genre à être fabriqués au Royaume-Uni et ils seront donc d'un intérêt particulier pour les physiciens et les spectroscopistes, leur introduction étant la plage spectrale déjà assurée par les détecteurs à antimoniure d'indium et au sulfure de plomb de la société Mullard Ltd.

Les nouveaux détecteurs, type RPY37 et RPY40, sont refroidis à 4,2° K dans des cryostats remplis d'hélium liquide. Une fois remplis, les détecteurs ne nécessitent plus aucune attention pendant au moins sept heures. Par rapport au détecteurs thermiques, ils offrent une sensibilité plus élevée et un temps de réponse plus rapide: le temps de réponse intrinsèque de l'élément sensible dans les deux nouveaux détecteurs est inférieur à 1 µsec.

La réponse rapide des deux détecteurs est des plus utiles pour l'étude des phénomènes transitoires. Le RPY37, dont la surface sensible est de 6 mm × 1 mm, fournit aux spectroscopistes le moyen d'obtenir une résolution élevée à des longueurs d'ondes maxima de 25 µm. La plus grande surface sensible du RPY40 le rend propre pour l'examen des phénomènes transitoires tels que les émissions modulées ou par impulsions de lasers gazeux et constitués de corps solides à grandes longueurs d'onde. Dans ces travaux, on ne dispose parfois que de quelques millisecondes pour observer un effet particulier, par exemple, pendant qu'un grand champ magnétique à impulsions est appliqué au spécimen soumis à l'essai.

D'autres applications pour ces détecteurs comprennent l'examen des phénomènes de radiation observés dans l'étude des tubes de choc et du plasma et dans la recherche sur les corps solides.

Les nouveaux détecteurs sont en acier inoxydable.

EE 92 755 *pour plus amples renseignements*

BLOC D'ALIMENTATION EN TENSION CONTINUE

Gresham Lion Electronics Ltd, Twickenham Road, Hanworth, Middlesex

(*Illustration à la page 261*)

La société Gresham Lion Electronics Ltd vient d'ajouter un nouveau modèle à sa série de blocs d'alimentation. Le bloc d'alimentation d'atelier universel, GLE 60, convertit un courant d'entrée monophasé de 225 V, 50 Hz, en une tension continue de 28 V à 60 A (max.).

Le nouveau bloc d'alimentation peut être utilisé sous toutes les latitudes et il est tout particulièrement utile dans les climats désertiques et tropicaux. Il a été originellement conçu pour alimenter le matériel radioélectrique mais le modèle de série peut répondre à diverses applications d'alimentation électronique.

Le GLE 60, qui a été mis au point indépendamment par la Gresham Lion Electronics Ltd, a été choisi par l'armée britannique et répond aux conditions du ministère de la défense pour l'équipement de sol DEF 133. Il a reçu le numéro de stock de l'OTAN 5820-99-104-7480. Il fonctionne à des températures de −25°C à +50°C dans une humidité de 0 à 90%.

La variation de sortie est maintenue à 1 V pour une variation de ±15 V et une variation de charge de 60 A. L'ondulation est inférieure à 1,4 V efficace dans toutes les conditions de charge et de tension d'entrée. Des surcharges de 15 A à une charge maxima peuvent être reçues pendant 100 µsec après un changement de charge de 30 A.

Le bloc, qui pèse 63,5 kg, est logé dans un coffret en aluminium et il est refroidi par air au moyen d'un souffleur. Un support spécial peut être fourni pour le montage sur véhicule. Les circuits électroniques légers sont sur plaquette de circuit imprimé avec point de contrôle pour l'entretien simple. Le GLE 60 peut être fourni sur un plateau de montage spécial.

La protection des fusibles, la coupure automatique des surcharges et l'alarme thermostatique sont assurés par des dispositifs incorporés à l'appareil. Il peut être utilisé également pour des applications non-militaires.

EE 92 756 *pour plus amples renseignements*

EQUIPMENT D'ÉTALONNAGE À TENSION ALTERNATIVE

Dynamco Instruments Ltd, Salisbury Grove, Mytchett, Aldershot, Hampshire

La société Dynamco Instruments Ltd (incorporant la Digital Measurements Ltd) vient d'annoncer la création de deux nouveaux instruments qui, lorsqu'ils sont utilisés avec des contrôleurs classiques, permettent d'effectuer l'étalonnage à 0,01% d'instruments à tension alternative dans la gamme de 30 Hz à 100 kHz.

L'appareil d'étalonnage à tension continue D3101 comporte un étalon de transfert à thermocouple avec alimentation contre-balancée et un diviseur à tension alternative à trois décades ayant une précision de division de une partie dans 10^5. Le diviseur est utilisé pour contrôler la linéarité et régler les atténuateurs, le thermocouple contrebalancé est utilisé pour vérifier la réponse de fréquence et l'étalon de transfert est utilisé pour l'étalonnage absolu par rapport à un étalon à tension continue.

Le générateur d'ondes sinusoïdales D3100 produit une onde sinusoïdale avec une distorsion harmonique totale inférieure à 0,005% (essentielle pour l'étalonnage de haute précision). Sa stabilité d'amplitude est de 0,005% à court terme et sa gamme de fréquence s'étend de 10 Mz à 100 Hz. La sortie est de 5 V efficaces à partir de 600 Ω à travers un atténuateur de 0 à 80 dB.

D'autres équipements nécessaires sont: un bloc d'alimentation stable en continu, tel que le Dynamco D3000, un galvanomètre sensible et un amplificateur de 100 V ou 1000 V pour l'étalonnage aux niveaux de tension plus élevés.

EE 92 757 *pour plus amples renseignements*

LECTEUR DE BANDES À CASSETTE

G.E.C. (Electronics) Ltd, East Lane, Wembley, Middlesex

(*Illustration à la page 261*)

La société G.E.C. Electronics Ltd. a réalisé un lecteur de bandes photoélectrique à cassette, spécialement conçu pour les calculatrices de programmation sur le terrain. Cet appareil compact peut lire des bandes perforées standard de 5 trous à la vitesse de 200 caractères par seconde avec rebobinage à la même vitesse. Il peut être également prévu pour la lecture de bandes à 8 trous. Il peut s'arrêter à un caractère près sur commande et un arrêt automatique est prévu à la fin du rebobinage.

Une des caractéristiques de l'enregistreur qui assure un certain nombre d'avantages pour l'utilisation sur le terrain est le fait que les rouleaux de 183 m de bande standard reçus par le lecteur sont logés dans des cassettes. Cela accroît considérablement la facilité et la vitesse de charge dans les conditions opérationnelles et fournit une protection supplémentaire aux bandes. On peut en outre effectuer une reprogrammation rapide car d'autres cassettes contenant des programmes différents peuvent être chargées rapidement sur le champ.

L'équipement se compose de trois éléments: le pont de la bande, le bloc d'alimentation et le bloc électronique. Le bloc d'alimentation et l'électronique sont entièrement constitués de corps solides. Le pont de la bande qui comprend tous les mécanismes d'avance de la bande peut être utilisé avec n'importe quel autre équipement exigeant des facilités de lecture de bande. L'assemblage complet, lorsqu'il est monté dans un coffret d'instrument standard, ne mesure que 44,45 cm de large × 30,48 cm de hauteur × 22,86 cm de profondeur.

L'équipement est normalement alimenté en tension triphasée de 200 V, 400 Hz. Il peut être utilisé également sur tension continue de 28 V et il peut être adapté pour l'utilisation sur tension de 230 V, 50 Hz. Le lecteur peut être utilisé soit dans la position horizontale soit dans la position verticale dans une gamme de température de −40° C à +55° C. Il peut être utilisé dans les avions. Enfin, il est entièrement à l'épreuve des intempéries et il a été pleinement contrôlé pour résister aux vibrations et aux chocs.

EE 92 758 *pour plus amples renseignements*

CONDENSATEURS VARIABLES

Wingrove & Rogers Ltd, Domville Road, Liverpool, 13

(Illustration à la page 262)

Le condensateur type C.31-51/6 est un trimmer diélectrique à air monté sur une base en céramique. Conçu spécifiquement pour le montage sur plaquette de circuit imprimé du module de 0,25 cm, la distance entre les contacts de stator et de rotor est de 2,25 cm.

La nouvelle méthode de construction et de support de l'assemblage du stator, ainsi que le contact spécial du rotor, donne à ce composant une stabilité mécanique et électrique élevée. Les conditions de la spécification DEF.5141 sont donc pleinement remplies.

La capacité minima est de 4 pF et l'excursion de capacité s'étend jusqu'à 67,5 pF. Les dimensions de la base sont de 0.65 pouce × 0,925 pouce.

EE 92 759 *pour plus amples renseignements*

TRANSISTOR DE COMMUTATION DE PUISSANCE

The Marconi Co. Ltd, Chelmsford, Essex

Un nouveau transistor, du type ayant permi de réaliser la calculatrice Marconi Myriad, vient d'être mis sur le marché par la Division de Microélectronique de la société The Marconi Co. Ltd.

La performance de ce transistor, en ce qui concerne la vitesse de commutation et la puissance, serait supérieure à celle de n'importe quel autre dispositif similaire pouvant être obtenu actuellement.

Conçu comme transistor d'entraînement de haute puissance pour mémoires à noyau de ferrite à action très rapide avec des temps de cyclage minima de 1,2 μsec, ce dispositif trouve également des applications étendues dans les systèmes de traitement de données où un grand nombre d'éléments logiques doit être entraîné simultanément.

Le transistor type 203-03 est maintenant produit en série pour la calculatrice Myriad ainsi que pour la calculatrice système 4 dont English Electric-Leo-Marconi viennent d'annoncer la création. Il peut être livré en petites quantités sur demande et en plus grandes quantités pour des commandes à bref délai.

Le nouveau transistor est un dispositif planaire au silicium npn monté dans une capsule standard T0-5 à trois conducteurs. La combinaison de tension de rupture élevée, de capacité de réception de courant à une faible tension de saturation et de temps de commutation rapide serait unique en son genre.

Dans un circuit type, le temps total mis pour allumer serait de 14 nsec et le temps total mis pour rompre le contact est de 90 nsec. La tension de saturation à l'émetteur-collecteur est de l'ordre de 0.3 V et le courant de fuite maximum à la base-collecteur est de 0.1 μA. Les tensions de rupture minima à l'émetteur-collecteur et à la base-collecteur sont toutes deux de 45 V avec une rupture minima à la base émetteur de 4,0 V.

EE 92 760 *pour plus amples renseignements*

COMMUTATEURS DE GUIDES D'ONDES

Decca Radar Ltd, Decca House, Albert Embankment, London, S.E.1

(Illustration à la page 262)

La division des instruments de la société Decca Radar Ltd a récemment mis au point un nouveau commutateur automatique de guides d'ondes qui comprend un nouveau type de mécanisme de commande démontable.

Jusqu'ici, l'entretien ne pouvait être effectué qu'en retirant l'ensemble du commutateur du système de guides d'ondes. Dans le nouvel équipement, le mécanisme de commande peut être retiré ou replacé en quelques minutes sans qu'il soit nécessaire de retirer le commutateur de guides d'ondes du système.

L'équipement se caractérise également par le fait que le commutateur peut être actionné à la main durant l'entretien du mécanisme de commande.

Le mécanisme normal est actuellement prévu pour l'emploi avec tous les commutateurs Decca à double canal des formats 14, 15, 18, 20 et 22, et il est pleinement interchangeable entre les différents formats. Des mécanismes démontables sont en cours de mise au point et pourront être utilisés avec de plus grands guides d'ondes ainsi qu'avec les commutateurs à trois canaux.

Les commutateurs déjà en service peuvent être modifiés pour recevoir le nouveau mécanisme et la société Decca offre le nouveau mécanisme de commande sous forme d'élément à part. Elle offre également l'appoint d'un service de transformation.

Notre gravure montre un commutateur pour guides d'ondes du modèle 14 dont le mécanisme de commande démontable a été retiré.

EE 92 761 *pour plus amples renseignements*

JAUGES DE CONTRAINTE STATIQUE

Vibro-Meter Corporation, Fribourg, Suisse. Agents en Angleterre: Haletop Civic Centre, Wythenshawe, Manchester, 22

(Illustration à la page 262)

Il s'agit ici d'un instrument entièrement transistorisé et portatif pour mesurer la contrainte statique au moyen d'extensomètres dans des circuits en pont ou en demi-pont. L'appareil est à compensation manuelle et l'instrument de mesure est étalonné de 5 à 150 000 microcontraintes. La précision est supérieure à 0,5% et le facteur de jauge est à réglage continu de 1,8 à 2,2. La fréquence porteuse est de 165 Hz.

Un ohmmètre incorporé est prévu pour la mesure de la résistance des extensomètres et la résistance à l'isolement entre la jauge et la surface de contrôle (gammes: 2 Ω à 200 Ω).

L'instrument peut être utilisé sur batterie ou sur courant secteur.

EE 92 762 *pour plus amples renseignements*

INSTRUMENT DE MESURE DU TAUX D'ONDES STATIONNAIRES

Hewlett-Packard, Dallas Road, Bedford

(Illustration à la page 263)

Le nouvel instrument de mesure du taux d'ondes stationnaires, Hewlett-Packard, modèle 415E, peut être utilisé dans les systèmes de mesure H.F. et microondes, pour mesurer non seulement le taux d'ondes stationnaires mais également l'atténuation, le gain ou tout autre paramètre déterminé par la différence entre deux niveaux de signaux. Comme les autres instruments de mesure de ce type, le modèle 415E est un amplificateur-voltmètre accordé et étalonné en décibels et en taux d'ondes stationnaires pour l'emploi avec des détecteurs quadratiques. Son faible indice de bruit, inférieur à 4 dB, permet d'effectuer des mesures précises à de faibles niveaux de bruit.

L'instrument comprend un atténuateur de haute précision ainsi qu'un dispositif extenseur-décaleur qui permet d'étendre n'importe quelle partie de 2 dB de la gamme de 70 dB de l'instrument à l'échelle totale pour obtenir une résolution maxima à une linéarité spécifiée de ±0,02 dB.

Le modèle 415E fonctionne soit avec détecteurs à cristal soit avec détecteurs à bolomètre; il peut en outre être utilisé soit avec des cristaux à faible impédance de source (100 Ω) soit avec des cristaux à impédance de source élevée (5 kΩ). Il fournit des courants de polarisation précis de 4,5 ou 8,7 mA, pouvant être choisis sur le panneau frontal pour activer tous les types de bolomètres standard. La polarisation est à limite de crête pour la protection du bolomètre.

L'instrument comprend des sorties isolées d'enregistrement et d'amplification. C'est un appareil transistorisé pesant moins de 4 kg et sa consommation n'est que d'environ 2 W. Une batterie rechargeable et montée à l'intérieur peut être fournie comme accessoire facultatif pour assurer la portabilité de l'instrument ou l'isoler contre les effets du circuit de terre.

EE 92 763 *pour plus amples renseignements*

AMPLIFICATEURS INTÉGRATEURS

Distributeurs: General Test Instruments Ltd, Station Point, Wokingham, Berkshire

(Illustration à la page 263)

Les nouveaux amplificateurs intégrateurs à commutation Burr-Brown, modèles 1663 et 1666, répondent à une double fonction. Lorsque le modèle 1663 est utilisé comme échantillonneur, il a un temps d'acquisition de 10 μsec et un temps de tenue nominale de 10msec pour une précision sur la totalité de l'échelle de 0,1%. Le modèle 1666, qui est un appareil de longue tenue, a une durée d'acquisition de 100 μsec et une durée de tenue de 1 sec pour une précision de 0,1%. Lorsque ces appareils sont utilisés comme intégateurs, le 1663 peut intégrer à la vitesse de 10^4 ou de 10^3 V/Vsec et le 1666 peut intégrer à la vitesse de 10^2 et 10 V/Vsec.

On peut monter jusqu'à 16 de ces éléments sur un châssis de 48,2 cm × 8,25 cm.

EE 92 764 *pour plus amples renseignements*

CÔNTROLEUR À ULTRASONS POUR L'ENCÉPHALOGRAPHIE ACOUSTIQUE

Ultrasonoscope Co. (London) Ltd, Sudbourne Road, London, S.W.2

(Illustration à la page 263)

L'Ultrasonoscope Mark 3CM est un instrument de diagnostic à ultrasons, spécialement conçu pour l'encéphalographie acoustique.

L'instrument permet d'observer tout déplacement de l'écho de la ligne médiane du cerveau et cette observation peut être utilisée pour le diagnostic des lésions intercrâniennes.

La position normale de la ligne médiane est obtenue en plaçant deux sondes aux côtés opposés de la tête et en émettant une impulsion sonore à haute fréquence d'un côté à l'autre.

L'une des sondes est alors utilisée comme émetteur-récepteur. L'écho d'une structure de ligne médiane symétrique se trouvera à la même position d'écran que le signal d'émission directe, vu que l'impulsion met autant de temps pour sortir de la ligne médiane et y revenir que pour traverser le crâne.

Tout déplacement de la ligne médiane est clairement indiqué sur le tube cathodique d'un diamètre de 13 cm. Les sondes à impulsions extrêmement courtes donnent une excellente résolution et l'image est très facile à interpréter. Des sondes de 1,25 MHz sont utilisées pour les adultes et des sondes de 2,5 MHz pour les enfants.

EE 92 765 *pour plus amples renseignements*

CALCULATRICE ANALOGIQUE

A. M. Lock & Co. Ltd, Prudential Buildings, Oldham, Lancashire

(Illustration à la page 263)

Le "Teachaid" est une calculatrice analogique transistorisée à bas prix principalement conçue pour l'usage individuel des étudiants. Le panneau frontal affiche clairement les quatre amplificateurs opérationnels sous forme graphique. Le calcul s'effectue d'un seul coup ou à répétition pour l'affichage sur un oscilloscope. La répétition de la solution s'effectue 25 fois par seconde, la période de calcul étant d'environ 35 msec et la durée de réenclenchement étant de 5 msec. Une impulsion de 10 V est prévue pour la synchronisation de la base de temps de l'oscilloscope.

Des dispositifs sont prévus pour l'intégration des problèmes et l'ajustement au gain de circuit. Le "Teachaid" peut résoudre une équation différentielle du troisème ordre lorsqu'on branche une résistance ou un condensateur dans le parcours de réaction des amplificateurs opérationnels. On peut résoudre des équations différentielles d'un ordre beaucoup plus élevé au moyen de la fonction de transfert et par l'emploi des méthodes de simulation. Dans ce dernier processus, un réseau complexe est branché sur le parcours de réaction de l'amplificateur opérationnel, plutôt que de brancher simplement la résistance ou le condensateur.

Au moyen des bornes de synchronisation d'entrée et de sortie, on peut accoupler jusqu'à trois "Teachaids". Il sont d'un emploi entièrement sûr car la tension maxima sur le panneau trontal est de 12 V.

Le "Teachaid" est fourni complet avec poignée de transport, support pliable, des cosses pour l'entassement du câble de puissance et un choix de fiches et de composants pour la connexion au parcours de réaction.

EE 92 766 *pour plus amples renseignements*

PHASEMÈTRE

Dawe Instruments Ltd, Western Avenue, Acton, London, W.3

(Illustration à la page 263)

La société Dame Instruments Ltd a réalisé un nouveau phasemètre transistorisé, à savoir le type 632. Cet instrument permet d'effectuer des comparaisons entre des signaux d'entrée symétriques dans une gamme de fréquence étendue (de 50 Hz à 100 kHz). Les atténuateurs d'entrée permettent d'obtenir un rapport élevé de niveaux de signaux (10 mV à 10 V, c'est à dire 60 dB), tous deux pouvant être mesurés par un voltmètre de panneau. L'équilibrage précis des niveaux d'entrée n'est pas nécessaire et l'appareil ne comprend pas de commandes sensibles aux fréquences. L'échelle du phasemètre peut être étendue pour indiquer la déviation sur la totalité de l'échelle pour chaque gamme de quadrant, améliorant ainsi la résolution.

L'instrument comprend un canal de référence et un canal de signaux, tous deux munis d'un atténuateur entièrement compensé (30 mA à 10 V déviation sur la totalité de l'échelle en six degrés). Le voltmètre du panneau peut être commuté sur n'importe lequel des deux canaux, qui comportent tous deux des amplificateurs limiteurs et qui alimentent les circuits bistables d'un élément de sortie. L'élément de sortie est déclenché aux excursions de tension nulle des signaux d'amplification et il injecte ainsi au phasemètre un signal de sortie à impulsion dont le rapport marque/espace est proportionnel à la différence de phase entre les deux signaux d'entrée. Des lectures directes des différences de phase sont données sur quatre gammes de quadrant (0°-90°, 90°-180°, 180°-270° et 270° et 270°-360°), et sur deux gammes auxiliaires de 0°-360° et 180°-0°-180°.

L'impédance d'entrée de chacun des canaux est de 1 MΩ en parallèle avec environ 40 pF. La précision de la mesure de phase est de ±1,5° de 50 Hz à 25 kHz et de ±5° de 25 kHz à 100 kHz. La précision de la mesure de tension est de ±5 pour cent de la déviation sur la totalité de l'échelle. Des transistors planaires épitaxiaux au silicium sont utilisés dans les amplificateurs pour assurer la stabilité de température.

EE 92 767 *pour plus amples renseignements*

CELLULE STANDARD À TEMPÉRATURE CONTRÔLÉE

Muirhead & Co. Ltd, Beckenham, Kent

(Illustration à la page 264)

Pour satisfaire à la demande d'une source stable et de grande précision de f.é.m. pour les opérations de référence, la société Muirhead & Co. Ltd a réalisé une cellule standard logée dans un petit élément à température contrôlée. Cet appareil peut réaliser une stabilité d'une partie dans un million. Ne pesant que 700 g et mesurant 16,51 cm de long × 8,89 cm de diamètre, il peut être incorporé à un appareil de mesure et d'enregistrement ou monté comme instrument de banc d'essai indépendant. Il est suffisamment robuste pour pouvoir être transporté par n'importe quel moyen normal sans que ses caractéristiques élevées de stabilité en soient affectées.

EE 92 768 *pour plus amples renseignements*

HORLOGE NUMÉRIQUE

Racal Instruments Ltd, Western Road, Bracknell, Berkshire

(Illustration à la page 264)

La société Racal Instruments Ltd a créé un système d'horloge numérique type SA.7100, entièrement transistorisé et d'une grande souplesse d'emploi. Prévue comme indicateur de temps de 24 heures ou comme instrument de contrôle de processus industriels et de concentration de données, l'horloge numérique SA.7100 fournit une indication numérique du temps en heures, minutes et secondes sur un tableau à colonnes ou en lignes à six chiffres et comprend des dispositifs pour actionner un enregistreur numérique.

Il existe différents modèles: le type SA.7100A dont la précision est déterminée par l'alimentation secteur de 50 Hz, le type SA.7100C, dont la précision est établie par référence à un oscillateur à cristal de quartz de précision, pour fournir une précision de système supérieure à deux parties dans 10^9 par jour. Un étalon extérieur peut être utilisé pour les applications de plus grande précision.

L'horloge numérique est prévue pour montage sur châssis standard de 47,5 cm ainsi que pour le fonctionnement dans des températures ambiantes de 0°C à 45°C. L'instrument permet également la synchronisation de l'affichage par plots de 0,01 01 et 1 sec. La consommation électrique est de 115 à 230 V, 50 Hz, ou 115 V, 400 Hz ou par batterie extérieure.

EE 92 769 *pour plus amples renseignements*

MILLIVOLTMÈTRE

Marconi Instruments Ltd, St. Albans, Hertfordshire

(Illustration à la page 264)

Cet instrument "tout transistors" (type TF 2603) a été étudié pour la mesure directe de 300 μV à 3 V à travers la gamme de fréquences de 50 kHz à 1500 MHz.

La sonde de mesure d'un diamètre de 1,25 cm contient une diode au germanium rapide dans un circuit à ondes complètes; la réponse est proche de la valeur efficace réelle avec des entrées inférieures à 30 mV, et de crête dans les regions de 0,5 à 3 V. Ce dispositif à ondes totales minimise les erreurs lorsqu'on mesure des tensions de signaux dont la forme d'onde est complexe. La sonde comporte un dispositif de chauffage pour réduire les effets des variations de température ambiante.

Le échelles de 12,5cm de long du voltmètre sont d'une lecture facile et étalonnée dans la valeur efficace d'une onde sinusoïdale. L'emploi de semi-conducteurs au lieu de tubes thermioniques assure non seulement la fiabilité de l'instrument et l'absence de toute microphonie, mais permet également le fonctionnement sur batterie comme variante à l'alimentation secteur normale.

Un multiplicateur 100:1, type TM 7947, est fourni avec l'instrument. Ce dispositif permet d'effecteur la mesure de tension de 30 mV à 300 V dans la gamme de fréquence de 500 kHz à 500 MHz; son impédance d'entrée est considérablement supérieure à celle que peut offrir un voltmètre à tube thermionique dans la même gamme de tension et de fréquence. Les accessoires facultatifs comprennent un connecteur T coaxial pour la mesure de tension sur les systèmes coaxiaux de 50 Ω.

EE 92 770 *pour plus amples renseignements*

RELAIS À CONTACT SCELLÉ

Telefonbau und Normalzeit GmbH, 6 Frankfurt/Main 7, Mainzer Landstrasse, Allemagne

(Illustration à la page 264)

Les relais à contact scellé TN possèdent les avantages des relais à lame vibrante plus une économie d'espace de 50%.

Les contacts plats brevetés qui sont scellés dans une enveloppe plate de verre contenant un gaz inerte ont une flexibilité inhérente et une face de contact qui assure une action glissante avec fermeture et ouverture rapide. Ces relais sont particulièrement indiqués pour l'emploi dans les circuits électroniques et les circuits imprimés qui exigent une action de relais simple, à bas prix et de haute fiabilité. Les principales caractéristiques de ces relais sont: une résistance de contact réduite; une résistance élevée à l'isolement, une faible capacité; un temps de commutation réduit; l'immunité contre les conditions atmosphériques et une longue durée de vie.

EE 92 771 *pour plus amples renseignements*

BOÎTE D'INDUCTION À DÉCADE

Lionmount & Co. Ltd, Bellevue Road, New Southgate, London, N.11

(Illustration à la page 264)

La boîte d'induction type LDI est un élément à quatre décades et à inductance maxima de 11,11 H réglable en plots de 1 mH. La précision à 1000 Hz est de 2%, mais la gamme de fréquences utilisable pour les meilleures valeurs de Q se trouve dans la bande de 3 kHz à 300 kHz.

Chaque décade se compose d'un noyau à ferrite portant 10 prises et grâce à ce dispositif une stabilité à long terme de 0,2% peut être obtenue avec des valeurs de Q entre 50 et 200.

Comme dans tous les inducteurs à noyau magnétique, la tension appliquée dépend dans une grande mesure de la fréquence de n'importe quel bobinage donné, et dans ces éléments la tension doit être limitée à quelques centaines de millivolts pour éviter la saturation du noyau.

L'inductance résiduelle est de 1,6 μH, et des informations supplémentaires seront données sur l'induction différentielle et les variations d'induction et de Q en fonction de la fréquence.

Des commutateurs à galette de céramique sont utilisés et le coffret en acajou est doublé pour l'effet d'écran.

EE 92 772 *pour plus amples renseignements*

BAIE MODULAIRE

Vero Electronics Ltd, South Mill Road, Regent's Park, Southampton

(Illustration à la page 265)

La toute dernière création de la société Vero Electronics Ltd est une baie modulaire d'un volume supplémentaire de 17,5 cm, dans laquelle l'usage maximum est fait de la hauteur complète de l'élément. On peut ainsi y introduire des "Veroboards" de 152,4 mm × 203,8 mm ou de 152,4 mm × 279,4 mm. La baie modulaire peut recevoir des châssis standard d'une largeur de 483 mm et des profondeurs de module de 279,4 ou 355 mm. Des largeurs de panneaux modulaires de 25,4 50,8 101,6 et 203,8 mm peuvent être utilisées.

EE 92 773 *pour plus amples renseignements*

MACHINE À GRAVER

Lee-Smith Photomechanics Ltd, Lyon Way, Hatfield Road, St. Albans, Hertfordshire

(Illustration à la page 265)

Une nouvelle et plus grande version de la machine à graver de précision Rota-Etch a été mise au point par la société Lee-Smith Photomecanics Ltd. Découlant de la machine à 22,5 cm, la Rota-Etch du dernier modèle est munie d'une table de travail circulaire sur laquelle on peut monter des composants d'une dimension diagonale maxima de 45 cm.

Les machines Rota-Etch sont spécifiquement conçues pour la gravure de précision de plaquettes de circuit imprimé standard, submiature et micro-miniature et la production de masques d'évaporation et d'articles analogues par le fraisage chimique.

Les pièces devant être gravées sont fixées à la table de travail circulaire montée sur le couvercle à charnières du réservoir de la machine. Durant la gravure, la table tourne à une vitesse constante de 10 tours/minute et la pièce est arosée d'eau forte par trois tambours tournants de diffusion en matière plastique ondulée Toutes les parties de la pièce sont ainsi uniformément saturées par la solution d'eau forte.

L'intensité de la gravure peut être modifiée en changeant la vitesse de rotation des tambours diffuseurs. Cette vitesse peut être réglée à n'importe quel degré de rotation entre zéro et 200 tours/minute.

Pour obtenir des résultats uniformément bons, il est essentiel de maintenir la température de l'eau forte à un même niveau. Des éléments de chauffage au silice ainsi que des tubes de refroidissement d'eau sont montés dans le réservoir à cet effet. La solution d'eau forte est remise en circulation de mainière continue et peut être maintenue à n'importe quelle température préréglée dans la gamme de 50°F à 130°F.

Les temps de traitement sont préréglés sur une minuterie et la machine est automatiquement débranchée à la fin de chaque période choisie.

Comme précaution de sécurité, un commutateur coupe l'alimentation en courant électrique lorsque le couvercle du réservoir est soulevé.

EE 92 774 *pour plus amples renseignements*

CONTRÔLEUR DE LINÉARITÉ DE COMPOSANTS

Distributeurs: Livingston Laboratories Ltd, Greycaines Estate, Bushey Mill Lane, North Watford, Hertfordshire

(Illustration à la page 265)

Il a été démontré qu'il existe un rapport entre la fiabilité des condensateurs et des résisteurs et leur linéarité. La société Radiometer de Copenhague vient d'introduire un instrument qui applique cette méthode pour l'indication de la fiabilité de composants.

Le contrôleur de linéarité de composants, modèle CLT 1, est fourni dans le Royaume-Uni par la société Livingston Laboratories Ltd. Il mesure les tensions de troisième harmonique produites par l'absence de linéarité de composants et il peut contrôler jusqu'à 20 composants par seconde avec des impédances de 1 Ω 100 MΩ.

Un oscillateur interne fournit une fréquence fondamentale très pure de 10 kHz à une amplitude allant jusqu'à 560 V, sa troisième harmonique étant supprimée à 180 dB.

La troisième harmonique de 30 kHz, produite par suite de l'absence de linéarité du composant soumis à l'essai, est indiquée sur un instrument de mesure qui peut détector des niveaux de signaux minima de −160 dB.

On peut choisir soit la réponse linéaire soit la réponse logarithmique avec une gamme de 60 dB pour l'évaluation rapide de production.

EE 92 775 *pour plus amples renseignements*

CELLULES À ÉNERGIE SOLAIRE

The Plessey Co. Ltd, Dielectric and Magnetic Division, Towcester, Northamptonshire

(Illustration à la page 265)

La Division de Composants Diélectriques et Magnétiques du groupe des composants Plessey a réalisé une gamme de réseaux intégrés de cellules photovoltaïques au silicium, conçue pour former des alimentations de conversion d'énergie solaire au sol.

Ces cellules fournissent une alimentation de longue durée et de grande fiabilité n'exigeant qu'un minimum d'entretien, ce qui convient particulièrement aux installations dont l'accès est difficile. Des études poussées on été effectuées quant à l'ensoleillement moyen (énergie solaire incidente) dans le monde, et des essais sur le terrain ont fourni des données sur des cellules convenant pour une gamme étendue de besoins d'alimentation.

Pour maintenir une sortie de puissance continue, les cellules ont été étudiées pour assurer la charge de batterie d'enmagasinement au nickel-cadmium. Un régulateur de tension empêche la batterie d'atteindre son potentiel de dissociation, réduisant ainsi les pertes électrolytiques et la nécessité d'entretien qui s'ensuit à un minimum absolu. Des panneaux de réseaux de cellules d'une surface d'environ 0,092 m² sont maintenant livrables; ils sont capables de maintenir indéfiniment l'alimentation d'une batterie jusqu'à 50 mA à 12 V à des emplacements favorables et ils ne nécessitent un entretien qu'une fois tous les quatre ou cinq ans, même dans les climats chauds.

Des courants et des tensions plus élevés peuvent être reçus par l'interconnexion appropriée d'un certain nombre de panneaux de réseaux.

On empêche la corrosion en noyant les cellules dans la résine d'époxyde sous un panneau de verre, ce dernier résistant à l'abrasion dûe au sable soufflé par le vent. Ce mode de réalisation assure une durée de vie presque illimitée et l'alimentation devient substantiellement plus sûre et de plus longue durée que l'équipement qu'elle alimente.

Les applications comprennent les communications, le matériel météorologique et de navigation aux emplacements éloignés. Théoriquement, on peut répondre à tout besoin de puissance mais des considérations pratiques rendent les réseaux de cellules plus appropriés aux niveaux de tension continue allant jusqu'à 10 V.

EE 92 776 *pour plus amples renseignements*

Résumés des Principaux Articles

La correction de l'erreur de phase d'une émission de télévision en couleurs PAL par W. Bruch

Résumé de l'article aux pages 212 à 217

Cet article décrit une nouvelle méthode pour corriger les erreurs dans un signal de télévision en couleurs PAL. Un phaseur à couleurs correctrices est ajouté à l'image en couleurs composées et compense la modulation de phase indésirable. Cette tension de compensation provient de la différence entre les deux signaux de couleurs, dont l'un est obtenu par le canal direct et l'autre par un modificateur de couleurs combiné à un dispositif de retard. Une correction d'amplitude supplémentaire supprime l'erreur de cosinus qui en résulte. La forme de compensation choisie n'affecte pas le signal de luminance.

Le rejet global élevé dans les amplificateurs de différence par S. Salmons

Résumé de l'article aux pages 218 à 221

Le comportement d'un amplificateur de différence équilibrée est affecté par les déviations de symétrie, en particulier celles dues à des disparités dans les caractéristiques d'une paire de tubes. L'auteur décrit le premier stade par lequel on surmonte cette difficulté sans utiliser des tubes de qualité spéciale ou des composants choisis. On obtient des facteurs de rejet dépassant 300.000 au moyen d'un simple réglage de compensation. De plus, ce réglage peut être effectué pour compenser les effets du manque de symétrie dans d'autres parties de l'amplificateur. On obtient ainsi une amélioration correspondante dans les propriétés de rejet global.

L'étude précise des circuits d'entrée pour amplificateurs M.F. à transistors à faible bruit par R. H. Frater

Résumé de l'article aux pages 222 à 229

L'auteur traite de la conception d'un réseau d'entrée pour un amplificateur à transistors qui répond aux conditions suivantes: largeur de bande maxima, impédance de source optimum pour un bruit réduit, réponse de phase et d'amplitude pour un certain nombre d'amplificateurs. La conception de ce réseau d'entrée tient compte de variations étendues dans l'impédance d'entrée du transistor. L'auteur indique les résultats obtenus pour un circuit accouplant un mélangeur de 408MHz à l'entrée d'un amplificateur à transistors de 11MHz. Cette méthode prévoit également des circuits accordés doubles de n'importe quelle largeur de bande dont les pôles de la fonction de transfert ont des parties réelles égales.

Inductance critique des redresseurs à thyristors "mi-contrôlés" par J. L. Storr-Best

Résumé de l'article aux pages 230 à 233

Cet article analyse les conditions d'inductance critique des filtres à impédances pour redresseurs à thyristors monophasés et triphasés "mi-contrôlés" dont la moitié seule des éléments est constituée de thyristors, l'autre moitié étant composée de diodes ordinaires. L'auteur compare les principales différences entre les résultats obtenus avec ces redresseurs et les résultats plus connus, obtenus avec des redresseurs entièrement contrôlés. Il donne un tableau des valeurs de courant de pointe des thyristors par rapport au courant continu de sortie, ce tableau s'appliquant aux divers angles d'amorçage lorsque l'inductance est critique. Des courbes sont également données des courants moyens et de pointe allant de la diode de découplage jusqu'au courant continu de sortie à divers angles d'amorçage.

Un convertisseur à opération indirecte de cartes perforées en bandes perforées par D. W. W. Rogers

Résumé de l'article aux pages 234 à 241

Cet article traite de la réalisation d'un convertisseur de cartes perforées en bandes perforées. Un lecteur de cartes perforées de type commercial capable de lire à la vitesse de 22 cartes par minute transmet, au moyen de circuits logiques appropriés, l'information emmagasinée dans douze trous de la carte perforée à un enregistrement intermédiaire. Une perforatrice de bande à action rapide, modèle Teletype 110, transmet ensuite l'information emmagasinée dans le dispositif intermédiaire à une bande de papier perforé à huit trous. Grâce à une plaquette à fiches à 64 caractères, placée devant le dispositif intermédiaire, cette information peut être soumise à une nouvelle disposition, effacée, puis introduite dans la bande. Un degré élevé de fiabilité peut être atteint par l'emploi d'un circuit logique de résistance à couplage direct, de circuits simples et de composants essentiels. L'auto-vérification est prévue pour détecter les erreurs éventuelles dans la carte perforée et un dispositif de vérification de parité d'ordre KDF9 est incorporé au réseaux logiques. Le convertisseur est entièrement muni de semi-conducteurs.

Les caractéristiques composées des diodes-tunnel montées en série par J. B. Earnshaw et Z. C. Tan

Résumé de l'article aux pages 242 à 245

Cet article traite de deux méthodes permettant de déterminer les caractéristiques composées des diodes-tunnel montées en série. Ces caractéristiques sont en suite analysées de manière détaillée et sous un angle critique. L'article conclue par une étude de quelques circuits comportant des chaînes de diodes-tunnel.

Un circuit de précision à déclenchement périodique à diode pour calculatrice analogique
par F. Fallside et N. Thedchanamoorthy

Résumé de l'article aux pages 246 à 250

Les circuits à diode semiconductrice sont utilisés dans une grande mesure pour le contrôle du mode intégrateur dans les calculatrices analogiques fonctionnant à des fréquences de répétition moyennes ou élevées. Toutefois, leur sensibilité aux variations de haute tension les rendent peu appropriées pour le calcul très lent et les relais leurs sont préférés. Le nouveau modèle de dispositif à déclenchement périodique décrit dans cet article est presque entièrement insensible aux variations de haute tension. De plus, une analyse simple mais précise de la fonction de transfert des intégrateurs commandés par circuits à déclenchement périodique s'accorde parfaitement avec les résultats pratiques obtenus.

Un élément électromécanique de commande de torsion à inertie contrôlable électriquement
par J. G. Thomas et V. Zakian

Résumé de l'article aux pages 251 à 253

Cet article décrit un élément électromécanique de commande de torsion et l'appareillage électronique auxiliaire. L'élément de commande a une portée de parcours angulaire dépassant 100° et il peut développer un couple maximum de 14,1 × 10^4 dynes-cm. L'inertie des parties mobiles est de 7g-cm^2 et cette inertie peut être réduite à zéro par l'emploi d'un circuit à réaction électronique.

NEUE AUSRÜSTUNGEN

Übersetzung der Seiten 260 bis 265

Beschreibung neuer Bauelemente, Zubehörteile und Prüfgeräte auf Grund der von Herstellern gemachten Angaben.

Logik-Lehrgerät

Systems Computers Ltd, Fossway, Newcastle upon Tyne, 6

(*Abbildung Seite 260*)

Systems Computers Ltd kündigt ein neues Logik-Lehrgerät an, das entweder als Lehrmittel oder Entwurfshilfe Anwendung finden kann.

Im Unterricht kann es die Elemente der Verknüpfungslogik und die Arbeitsweise von Digitalrechnern veranschaulichen. Verwendung verhältnismässig billiger Steckfelder gestattet, dass mehrere Studenten ein "Logic Tutor"-Gerät benutzen. Logische Schaltungen werden auf den Steckfeldern vorbereitet, dann kontrolliert, bevor sie am Logic Tutor zum Einsatz kommen. Dadurch wird bessere Beteiligung seitens der Studenten erreicht, und ausserdem werden die logischen Elemente vor Beschädigung geschützt, da Fehler berichtigt werden, ehe sie das Gerät erreichen. Zur Darstellung bestimmter Probleme kann man verdrahtete Schaltfelder benutzen.

Als Entwurfshilfe kann der "Logic Tutor" für die Entwicklung logischer Steuersysteme eingesetzt werden. Er gestattet schnelle und bequeme Verknüpfung der Elemente eines logischen Steuersystems, so dass es ohne Verdrahtung und Anschluss an Stromversorgungen überprüft werden kann.

Der Logic Tutor wiegt nur 9 kg, ist in sich geschlossen und tragbar; er kann bequem auf dem Tisch stehend benutzt werden und erfordert lediglich Anschluss an das 230-V-Netz.

EE 92 751 *für weitere Einzelheiten*

Mikrominiaturlampe

Thorn Special Products Ltd, Great Cambridge Road, Enfield, Middlesex

(*Abbildung Seite 260*)

Die Thorn-Mikrominiaturlampe "Mite-T-Lite" kann direkt über den Ausgang eines Transistors angesteuert werden und hat einen Stromverbrauch von nur 35 mA bei 1,5 V–. Sie eignet sich daher für Anwendung in fotoelektrischen Logiksystemen, komplexen Matrixdarstellungen, medizinischen Ausrüstungen oder der batteriebetriebenen Mikrominiaturtechnik.

Bei Betrieb mit 1,5 V ist die Lichtausbeute 45 ... 55 Millilumen und die durchschnittliche Lebensdauer der Lampe etwa 500 Stunden. Bei Betrieb mit 1 V wird die Lebensdauer auf über 2500 Stunden verlängert.

Der 0,0063 mm starke Wolframleuchtfaden wird als 40gängiger Wendel hergestellt. Dank seiner niedrigen thermischen Trägheit kann die Lichtausbeute Spannungsimpulsen bis zu 100 Hz folgen.

Aussenabmessungen der Mite-T-Lite sind 1,4 mm Durchmesser und 4,5 mm Länge.

EE 92 752 *für weitere Einzelheiten*

Breitband-Samplingvoltmeter

Hewlett-Packard, Dallas Road, Bedford

(*Abbildung Seite 260*)

Das nach dem Sampling-Prinzip arbeitende Hewlett-Packard Modell 3406A zeigt Wechselspannungen von 10 kHz... 1 GHz an, löst Differenzen von nur 50 μV auf und hat eine niedrige Eingangskapazität. In Betrieb ist keine Abstimmung erforderlich. Die Vollausschlagbereiche des Instrumentes liegen zwischen 1 mV und 3 V.

Die Nützlichkeit beim Messen von Spannungen an schwer zugänglichen Stellen in HF-Schaltungen wird durch eine bequem im Tastkopf angeordnete Drucktaste erhöht. Die Anzeige bleibt so lange bestehen wie die Taste gedrückt wird.

Die Messunsicherheit ist im niedrigsten Frequenzbereich (10 kHz...100 MHz) ± 3 Prozent, im höheren Bereich (100...800 MHz) ± 5 Prozent und im höchsten Bereich (800 MHz...1 GHz) ± 8 Prozent. Das Gerät hat eine brauchbare Empfindlichkeit von 1 kHz... 2 GHz.

Das neue Gerät erzeugt intern eine Stichprobe mit Tonfrequenzrate, die statistisch mit dem unbekannten HF-Signal identisch ist. Die Stichprobe wird dann gemessen. Da die Samplingrate laufenden Änderungen unterliegt, kann sie nicht zufällig mit dem unbekannten Signal zusammenfallen und eine fehlerhafte Stichprobe erzeugen.

Das Messgerät arbeitet in herkömmlicher Weise, zeigt absolute Mittelwerte an und ist in Effektivwerten geeicht. Den Tonfrequenzausgang kann man jedoch auf der Rückseite entnehmen. Da dieser Ausgang ein statistisches Bild des unbekannten Signals darstellt, kann der echte Effektivwert mittels eines niederfrequenten Messinstrumentes für echte Effektivwerte gemessen werden. Mit einem niederfrequenten Messgerät dieser Art lässt sich auch eine "Proportional-zum-Spitzenwert"-Messung durchführen. Es gibt auch einen Anschluss für ein Gleichspannungsregistriergerät.

Der Eingang des Gerätes speist direkt in den Abtaster, der gut gegen Überlastung geschützt ist. Selbst bei einer 1000:1 Überlastung des 1-mV-Bereiches erfolgt die Erholung schnell, und es wird kein Schaden verursacht.

Das Gerät hat eine eingebaute Eichvorrichtung. Ein 1-V-Normal wird auf der Frontplatte dargestellt. Für Rückstellung auf Null wird der Tastkopf in die Eichbuchse eingeführt, die dann kurzgeschlossen wird, sowie die Eichtaste freigegeben wird.

EE 92 753 *für weitere Einzelheiten*

FM-Testgerät

Vertrieb: Livingston Laboratories Ltd, Greycaines Estate, Bushey Mill Lane, North Watford, Hertfordshire

(*Abbildung Seite 261*)

Amalgamated Wireless (Australasia) Ltd in Sidney hat Livingston Laboratories Ltd als alleinige Vertreter für den Vertrieb ihrer Prüfgeräte für die Fernmeldetechnik in Grossbritannien bestellt.

Zu den Geräten, die in England auf

den Markt kommen, gehört eine Reihe tragbarer Festkörper-Testgeräte in Modultechnik, die die Frequenzen von 10 Hz bis 520 MHz überstreichen.

Darunter befindet sich das A. W. A.-Testgerät A410, ein kompaktes Festkörper-Testgerät, das für den Aussendienst und die Wartung von FM-Gegenverkehr-Sprechfunkausrüstungen entwickelt wurde.

Die Ausrüstung besteht aus einem FM-Messender für UKW und UHF, Quarz-ZF-Eichgerät, FM-Hubmesser, sowie Leistungsmesser für Ton- und Hochfrequenz; sie kann für Messungen an Sender und Empfänger im Frequenzbereich 30...520 MHz eingesetzt werden.

EE 92 754 *für weitere Einzelheiten*

Fotodetektoren

Mullard Ltd, Mullard House, Torrington Place, London, W.C.1

Zwei neue, schnellansprechende Fotodetektoren der Mullard Ltd sind im Wellenband 2...25 μm für impulsförmige oder modulierte Strahlungen empfindlich. Sie bestehen aus kupferdotiertem Germanium, sind die ersten ihrer Art, die in England hergestellt werden, und interessieren hauptsächlich Physiker und Spektroskopiker. Diese Modelle erweitern den von den Bleisulfid- und Indiumantimonid-Detektoren der Firma überstrichenen Spektralbereich.

Die neuen Detektoren RPY37 und RPY40 werden in mit flüssigem Helium gefüllten Kryostaten auf 4,2° K gekühlt. Nach dem Füllen erfordern sie für mindestens sieben Stunden keine Wartung. Im Vergleich mit thermischen Detektoren bieten sie höhere Empfindlichkeit und schnellere Ansprechzeit: die Eigenansprechzeit der empfindlichen Elemente liegt in beiden neuen Detektoren unter 1 μs.

Das schnelle Ansprechen beider Detektoren ist besonders wertvoll für Untersuchungen von Einschwingvorgängen. Der RPY37 mit seiner empfindlichen Fläche von 6 × 1 mm gibt dem Spektroskopiker ein Mittel zur Erzielung hoher Auflösung bei Wellenlängen bis zu 25 μm. Wegen der grossen empfindlichen Fläche eignet sich der RPY40 vor allem zur Untersuchung von Einschwingvorgängen, wie sie z.B. bei impulsförmigen oder modulierten Emissionen von Gas- oder Festkörperlasern für hohe Wellenlängen auftreten. Während dieser Untersuchungen ist der gewünschte Effekt oft nur für wenige Millisekunden zu beobachten, z.B. wenn der Prüfling einem starken impulsförmigen Magnetfeld ausgesetzt wird.

Andere Anwendungsmöglichkeiten bestehen für diese Detektoren in Untersuchungen der bei Stossrohrversuchen auftretenden Strahlungsvorgänge, Plasmauntersuchungen und Festkörperforschung.

Die Detektoren werden aus rostfreiem Stahl konstruiert.

EE 92 755 *für weitere Einzelheiten*

Gleichspannungs-Speisegeräte

Gresham Lion Electronics Ltd, Twickenham Road, Hanworth, Middlesex

(Abbildung Seite 261)

Eine Ergänzung ihres Speisegerätprogramms wurde von Gresham Lion Electronics Ltd bekanntgegeben. Das Universal-Werkstattspeisegerät GLE60 setzt eine einphasige Eingangsspannung von 225 V 50 Hz in 28 V— bei maximal 60 A um.

Das neue Speisegerät kann in allen Klimas eingesetzt werden und ist besonders für schwierige Bedingungen in Tropen und Wüsten geeignet. Die Originalausführung wurde für das Treiben von Funkausrüstungen entwickelt; das Serienmodell genügt aber den verschiedensten Ansprüchen für elektronische Speisegeräte.

Das auf Privatinitiative von Gresham Lion Electronics Ltd entwickelte Modell GLE60 wurde jedoch für Ausrüstungen der britischen Armee bestellt, genügt dem Pflichtenblatt DEF113 des Verteidigungsministeriums für Bodenausrüstungen und hat die NATO-Katalognummer 5820-99-104-7480. Es kann bei Temperaturen von −25° C bis zu +50° C und Feuchtigkeiten von 0 bis 90 Prozent betrieben werden.

Bei Schwankungen von ±15 V und Lastschwankungen von 60 A treten nur Ausgangsspannungsänderungen von 1 V auf. Die Restwelligkeit ist niedriger als 1,4 V_{eff} für alle Belastungen und Eingangsspannungsbedingungen. Bei Höchstbelastung können Überlastungen von 15 A für 100 μA nach einer schrittweisen 30-A-Laständerung vertragen werden.

Das Gerät wiegt 63,5 kg, ist in ein Aluminiumgehäuse eingebaut und wird durch einen Gebläsemotor gekühlt. Für Fahrzeugmontage sind Sonderbeschläge lieferbar. Die elektronischen Schaltungen sind als Druckplatten mit Messpunkten zur Vereinfachung des Service ausgeführt. Das GLE60 ist auf einem Spezialeinsatz mit Schnellverschluss zu haben.

Das Gerät ist mit Schmelzsicherungen, Schütz und eingebauten thermostatischen Alarmeinrichtungen gesichert und auch für Zivilanwendung lieferbar.

EE 92 756 *für weitere Einzelheiten*

Wechselstrom-Eichgeräte

Dynamco Instruments Ltd, Salisbury Grove, Mytchett, Aldershot, Hampshire

Dynamco Instruments Ltd, in die Digital Measurements Ltd aufgegangen ist, kündigt zwei neue Geräte an, die bei Einsatz mit Standard Testausrüstung Wechselstrominstrumente im Bereich 30 Hz...100 kHz mit 0,01 Prozent Genauigkeit eichen können.

Das Wechselstrom-Eichgerät D3101 enthält ein Thermoelement-Übertragungsnormal mit Kompensationsstromversorgung und einem Dreidekaden-Wechselspannungsteiler mit 1 × 10^5 Teilgenauigkeit. Der Teiler findet zur Prüfung der Linearität und Einstellung des Abschwächers Verwendung, das Thermoelement mit Kompensator für den Frequenzgangtest und das Übertragungsnormal für die absolute Eichung gegen ein Gleichspannungsnormal.

Der Sinuswellengenerator D3100 erzeugt eine Wellenform mit weniger als 0,005 Prozent Gesamtklirrfaktor (für Präzisionseichung notwendig), einer kurzfristigen Amplitudenkonstanz von 0,005 Prozent und einem Frequenzbereich von 10 Hz...100 kHz. Die Ausgangsspannung ist 5 V_{eff} von 600 Ω über einen 0...80-dB-Abschwächer.

Für Einsatz sind folgende weitere Geräte erforderlich: eine Konstant-Gleichspannungsversorgung wie z.B. die Dynamco D3000, ein empfindliches Galvanometer und ein 100-V- oder 1 000-V-Verstärker für Eichung bei höheren Spannungspegeln.

EE 92 757 *für weitere Einzelheiten*

Kassetten-Streifenleser

G.E.C. (Electronics) Ltd, East Lane, Wembley, Middlesex

(Abbildung Seite 261)

G.E.C. (Electronics) Ltd hat zum Programmieren von Rechnern beim Kunden einen fotoelektrischen Kassetten-Lochstreifenleser entwickelt. Standard-Fünfkanal-Lochstreifen werden in diesem Gerät, das mit derselben Geschwindigkeit zurückspult, mit 200 Zeichen pro Sekunde gelesen. Es ist auch für Achtkanal-Lochstreifen lieferbar. Auf Verlangen stoppt es innerhalb eines Zeichens und automatisch am Ende des Rücklaufs.

Eine Geräteeinrichtung, die im Aussendiensteinsatz Vorteile mit sich bringt, ist das Einlegen von ca. 183 m des für den Leser geeigneten Lochstreifens auf Spulen in Kassetten. Dadurch kann das Laden unter Betriebsbedingungen wesentlich schneller und einfacher ausgeführt und die Lochstreifen besser geschützt werden. Mittels anderer Kassetten mit alternativen Programmen kann man schnellstens an Ort und Stelle umprogrammieren.

Das Gerät besteht aus drei Baugruppen: dem Laufwerk, dem Netzgerät und der Elektronik. Netzgerät und Elektronikteil sind durchweg in Festkörpertechnik konstruiert. Das Laufwerk, das auch die Streifenabtaster enthält, lässt sich mit jeder anderen Ausrüstung einsetzen, die Lochstreifenleser erfordert. Die komplette Ausrüstung ist in ein Standard-R.A.E.-Gehäuse von etwa 445 mm Breite, 305 mm Höhe und 229 mm Tiefe eingebaut.

Das Netzgerät wird üblicherweise für 200 V, 400 Hz geliefert. Es kann auch mit 28 V— betrieben oder für 230 V, 50 Hz geändert werden. Der Leser kann sowohl in horizontaler wie vertikaler Lage im Temperaturbereich −40° ... +55°C betrieben werden. Er ist für Einbau als Bordgerät eines Flugzeugs geeignet, völlig wetterfest und hat Schwingungs- und Stossproben bestanden.

EE 92 758 *für weitere Einzelheiten*

Abgleichkondensatoren

Wingrove & Rogers Ltd, Domville Road, Liverpool, 13

(*Abbildung Seite 262*)

Typ C.31-51/5 ist ein Trimmer mit Luftdielektrikum auf einer keramischen Grundplatte für Montage auf gedruckte Schaltungen mit 2,54 mm Raster. Der Abstand zwischen den Stator- und Rotorkontakten ist 22,9 mm.

Eine neue Bauart und Stütze für das Statorpaket sowie ein Spezialkontakt für den Rotor geben diesem Bauelement hohe elektrische und mechanische Stabilität. Den Anforderungen der Vorschrift DEF.5141 wird ausreichend genügt.

Die Mindestkapazität ist 4 pF und die Kapazitätsänderung bis zu 67,5 pF. Die Aussenabmessungen der Grundplatte sind 16,5 × 23,5 mm.

EE 92 759 *für weitere Einzelheiten*

Leistungsschalttransistoren

The Marconi Co. Ltd, Chelmsford, Essex

Der Geschäftsbereich Mikroelektronik der Marconi Co Ltd hat gerade einen neuen Transistor auf den Markt gebracht, und zwar einen der Typen, die den Marconi-Digitalrechner MYRIAD möglich machten.

Die Leistung dieses Transistors hinsichtlich Schaltgeschwindigkeit und Belastbarkeit scheint höher zu sein, als die irgendwelcher ähnlicher, derzeitig lieferbarer Elemente.

Dieser Halbleiter wurde als Hochleistungs-Treibertransistor für sehr schnelle Ferritkernspeicher mit einer Zykluszeit von nur 1,2 μs entwickelt und hat breitere Anwendungsmöglichkeiten in Datenverarbeitungssystemen, in denen eine grosse Anzahl logischer Elemente gleichzeitig getrieben werden muss.

Der Transistor Typ 203-03 ist nunmehr in Serienfertigung für den MYRIAD und das vor kurzem angekündigte System 4 der English Electric-Leo-Marconi Co. Er ist in kleinen Quantitäten für Bewertung ab Lager, für grössere Aufträge kurzfristig lieferbar.

Der neue Transistor ist ein npn-Silizium-Planartransistor in einem Standardgehäuse TO-5 mit drei Anschlüssen. Die Kombination der hohen Durchbruchsspannung und Strombelastbarkeit mit niedriger Sättigungsspannung und schnellen Schaltzeiten ist, wie man glaubt, einzigartig.

In einer typischen Schaltung ist die Schaltzeit 14 ns und die Gesamtzeit für Abschalten 90 ns. Die Kollektor-Emitter-Sättigungs-Spannung ist in der Grössenordnung von 0,3 V und der höchste Kollektor-Basis-Reststrom 0,1 μA. Die niedrigste Kollektor-Basis- und Kollektor-Emitter-Durchbruchsspannung sind beide 45 V mit einer Emitter-Basis-Mindestdurchbruchsspannung von 4,0 V.

EE 92 760 *für weitere Einzelheiten*

Hohlleiterschalter

Decca Radar Ltd, Decca House, Albert Embankment, London, S.E.1

(*Abbildung Seite 262*)

Der Geschäftsbereich Instrumente der Decca Radar Ltd hat vor kurzem einen neuen automatischen Hohlleiterschalter mit demontierbarem Betätigungsmechanismus eingeführt.

Für Service war es bisher notwendig, den kompletten Schalter aus dem Hohlleitersystem auszubauen. In dem neuen Baumuster kann der Betätigungsmechanismus in wenigen Minuten demontiert und ausgewechselt werden, ohne den Hohlleiterschalter-Abschnitt aus dem System auszubauen.

Ein weiteres Konstruktionsmerkmal erlaubt manuelle Betätigung des Schalters während der Service-Arbeiten am Betätigungsmechanismus.

Zur Zeit gibt es einen Standardmechanismus für alle Decca-Doppelkanalschalter in Hohlleitergrössen 14, 15, 18, 20 und 22, der zwischen allen Grössen voll austauschbar ist. Ein demontierbarer Mechanismus für die grösseren Hohlleiter und für Dreikanalschalter ist im Entwicklungsstadium.

Bereits eingebaute Schalter können für den neuen Mechanismus modifiziert werden; Decca bietet den neuen Betätiger als Einzelbaugruppe und mit Unterstützung durch ihren Modifizier-Service an.

Die Abbildung zeigt einen Hohlleiter Nr. 14, von dem der demontierbare Betätigungsmechanismus entfernt ist.

EE 92 761 *für weitere Einzelheiten*

Statisches Dehnungsmessgerät

Vibro-Meter AG Fribourg, Schweiz, Englisches Büro: Haletop Civic Centre, Wythenshawe, Manchester, 22

(*Abbildung Seite 262*)

Ein volltransistorisiertes, tragbares Ablesegerät für statische Dehnungsmessungen mit Hilfe von Dehnmessstreifen in Halb- oder Vollbrückenschaltung. Die manuelle Kompensationsmethode wird angewendet, und das Messgerät ist von 5 ... 150 000 Mikrodehnungen geeicht. Die Genauigkeit ist besser als 0,5 Prozent und der K-Faktor von 1, 8 ... 2,2 kontinuierlich einstellbar. Die Trägerfrequenz ist 165 Hz.

Ein Ohmmeter zum Messen des Widerstandes der Dehnmessstreifen sowie des Isolationswiderstandes zwischen Dehnstreifen und Messoberfläche (Bereiche von 2 Ω ... 200 MΩ) ist eingebaut.

Das Gerät kann mit Batterien und am Netz betrieben werden.

EE 92 762 *für weitere Einzelheiten*

Welligkeitsmesser

Hewlett-Packard, Dallas Road, Bedford

(*Abbildung Seite 263*)

Der neue Hewlett-Packard Welligkeitsmesser 415E kann in HF- sowie Mikrowellensystemen Verwendung finden; er misst nicht nur das Stehwellenverhältnis, sondern auch Dämpfung, Verstärkung und jeden anderen Parameter, der durch die Differenz zwischen zwei Signalpegeln bestimmt werden kann. Modell 415E ist—wie andere Messgeräte dieses Types—ein abgestimmter Verstärker + Voltmeter mit Eichung in Dezibel und Stehwellenverhältnis und für Einsatz mit quadratischen Detektoren ausgelegt. Seine niedrige Rauschzahl von unter 4 dB gestattet Durchführung genauer Messungen selbst bei niedrigen Signalpegeln.

In das Instrument ist ein hochgenauer Abschwächer eingebaut; eine Dehn- und Verschiebeeinrichtung gestattet, jeden 2-dB-Abschnitt des Messumfangs von 70 dB für Höchstauflösung über die ganze Skala zu dehnen, und zwar mit einer spezifischen Linearität von ± 0,02dB.

Modell 415E kann entweder mit Kristall- oder Bolometerdetektoren, mit niedriger (100 Ω) oder hoher (5 kΩ) Kristall - Quellenimpedanz betrieben werden. Zur Aktivierung aller Standardbolometer wird ein auf der Frontplatte einstellbarer Vorspannungsstrom von 4,5 oder 8,7 mA abgegeben. Zum Schutz des Bolometers ist der Spitzenstrom der Vorspannung begrenzt.

Das Gerät hat isolierte Ausgangsklemmen für Schreiber und Verstärker. Es ist volltransistorisiert, wiegt weniger als 227 g und hat 2 W Leistungsaufnahme. Für Tragbarkeit oder Isolierung von Erdschleifeneinwirkungen ist als Zubehör eine intern untergebrachte, aufladbare Batterie lieferbar.

EE 92 763 *für weitere Einzelheiten*

Integratorverstärker

Vertrieb: General Test Instruments Ltd, Station Point, Wokingham, Berkshire

(*Abbildung Seite 263*)

Die neuen Burr-Brown-Modelle 1663 und 1666 haben als Abtast- und Halteverstärker und Schleusen-Integratorverstärker eine Doppelfunktion. Bei Einsatz als Abtast- und Halteeinheiten hat Modell 1663 eine Erfassungszeit von 10 μs und eine Nennhaltezeit von 100 ms für eine Genauigkeit von 0,1 Prozent des Skalenendwertes, während Modell 1666—das Gerät mit der längeren Haltezeit—eine Erfassungszeit von 100 μs und ein Haltezeit von 1 s für 0,1 Prozent Genauigkeit hat. Bei Einsatz als Integratoren integriert Modell 1663 mit 10^4 oder 10^3 V/V Sek und Modell 1666 mti 10^2 und 10 V/V Sek.

Bis zu 16 dieser Verstärker können in ein 90 mm hohes Feld eines 19″-Gestells eingebaut werden.

EE 92 764 *für weitere Einzelheiten*

Ultraschallgerät für Echo-Encephalographie

Ultrasonoscope Co. (London) Ltd, Sudbourne Road, London, S.W.2

(*Abbildung Seite 263*)

Das Ultrasonoscope Baumuster 3CM ist ein diagnostisches Ultraschallgerät, das speziell für Echo-Encephalographie entwickelt wurde.

Das Instrument gestattet Beobachtung jeder Verschiebung des Mittel-Echos vom Gehirn, was für die Diagnose von intercraniellen Verletzungen herangezogen werden kann.

Durch Anlegen von Prüfköpfen an gegenüberliegenden Seiten des Kopfes und Übertragung eines hochfrequenten Tonimpulses von einem zum anderen lässt sich die normale Lage der Mittellinie bestimmen.

Einer der Prüfköpfe wird dann als Sender-Empfänger verwendet. Das Echo von einer symmetrischen Mittellinienstruktur erscheint auf dem Schirm in derselben Position wie das direkte Übertragungssignal, da der Impuls für den Weg bis zur Mittellinie und zurück dieselbe Zeit benötigt wie zur Fortpflanzung durch den Schädel.

Auf dem 13-cm-Schirm der Oszillografenröhre ist jede Verschiebung der Mittellinie deutlich sichtbar. Die äusserst kurzen Impuls-Prüfköpfe haben ein ausgezeichnetes Auflösungsvermögen, und die Darstellung ist leicht auswertbar. Für Erwachsene finden Prüfköpfe für 1,25 MHz, für Kinder solche für 2,5 MHz Anwendung.

EE 92 765 *für weitere Einzelheiten*

Analogrechner

A. M. Lock & Co. Ltd. Prudential Buildings, Oldham, Lancashire

(Abbildung Seite 263)

Der preiswerte, transistorisierte Analogrechner "Teachaid" ("Ausbildungshilfe") wurde in erster Linie für die Experimente einzelner Studenten entwickelt. Die vier Funktionsverstärker sind klar in grafischer Form auf der Frontplatte dargestellt. Berechnungen können entweder einmalig oder wiederholt für Oszillografendarstellung durchgeführt werden. Lösungen werden 25mal je Sekunde wiederholt; die Rechenzeit ist ungefähr 35 ms, die Rückstellzeit 5 ms. Zur Synchronisierung der Zeitablenkung des Oszillografen wird ein 10-V-Impuls abgegeben. Einrichtungen zur Massstabänderung der Aufgaben und Regelung der Schleifenverstärkung sind vorhanden. "Teachaid" kann durch Einstecken von Widerständen und Kondensatoren in den Rückkopplungsweg des Funktionsverstärkers Differentialgleichungen viel höherer Ordnung mit Hilfe der Übertragungsfunktionsmethode und Anwendung der Simulationstechnik lösen. Nach dieser Methode wird statt nur R oder C ein komplexes Netzwerk in den Rückkopplungsweg des Funktionsverstärkers eingesteckt.

Bis zu drei "Teachaids" können mit Hilfe der Klemmen für Synchronisierungs-Eingang und -Ausgang zusammengeschaltet werden. Sie sind völlig gefahrlos, da die Höchstspannung an der Frontplatte 12 V beträgt.

"Teachaid" wird komplett mit Traggriff, Klappstand, Kabelhaltern und einem Steckersortiment zum Einstecken von Elementen in den Rückkopplungsweg geliefert.

EE 92 766 *für weitere Einzelheiten*

Phasenmesser

Dawe Instruments Ltd. Western Avenue, Acton, London, W.3

(Abbildung Seite 263)

Dawe Instruments Ltd hat einen neuen transistorisierten Phasenmesser Typ 632 angekündigt, der einen Vergleich zwischen symmetrischen Eingangssignalen über einen breiten Frequenzbereich (50 Hz ... 100 kHz) gestattet. Eingangsabschwächer erlauben ein hohes Verhältnis von Signalpegeln (10 mV bis zu 10 V, d.h. 60 dB), die beide mittels eines eingebauten Messgerätes gemessen werden können. Genauer Abgleich des Eingangspegels ist überflüssig, und keins der Bedienelemente ist frequenzempfindlich. Die Phasenmesserskala ist gedehnt und gibt für jeden Quadrantbereich Vollausschlag, wodurch eine bessere Auflösung erzielt wird.

Das Instrument besteht aus einem Bezugs- und einem Signalkanal, die beide vollkompensierte Abschwächer haben (von 30 mV bis zu 10 V Endwert in sechs Stufen). Das Voltmeter an der Frontplatte kann in jeden der Kanäle geschaltet werden, die beide Begrenzungsverstärker enthalten und die bistabile Schaltung des Ausgangsbausteins speisen. Der Ausgangsbaustein wird im Spannungsnullpunkt des Verstärkersignals getriggert und beaufschlagt den Phasenmesser mit einem Impuls-Ausgangssignal, dessen Tastverhältnis der Phasendifferenz zwischen den beiden Eingangssignalen proportional ist. Die Phasendifferenz ist in den vier Quadrantbereichen (0° ... 90°, 90° ... 180°, 180° ... 270° und 270° ... 360°) und den beiden Hilfsbereichen 0° ... 360°) und 180°-0°-180° direkt ablesbar.

Die Eingangsimpedanz jedes Kanals ist 1 MΩ parallel zu etwa 40 pF. Die Unsicherheit bei Phasenmessungen ist ±1,5 Prozent zwischen 50 Hz und 25 kHz, ±5 Prozent zwischen 25 kHz und 100 kHz und die der Spannung ±5 Prozent des Skalenendwertes. Der Verstärker ist zur Sicherung der Temperaturbeständigkeit durchweg mit Silizium-Epitaxial-Planar-Transistoren bestückt.

EE 92 767 *für weitere Einzelheiten*

Temperaturgeregeltes Normalelement

Muirhead & Co. Ltd, Beckenham, Kent

(Abbildung Seite 264)

Zur Befriedigung des Bedarfs an einer hochgenauen und konstanten EMK-Quelle für Vergleichszwecke hat Muirhead & Co. Ltd ein Normalelement angekündigt, das in einem kleinen Thermostat untergebracht ist. Die mit diesem Instrument erreichbare Konstanz ist 1×10^{-6}. Es wiegt nur 709 g, ist 165 mm lang und hat einen Durchmesser von 89 mm, kann sowohl in Schreiber wie Messgeräte eingebaut oder als freistehendes Tischgerät geliefert werden. Es ist robust genug, um Transport mit allen üblichen Mitteln ohne Beeinflussung der hochkonstanten Kenndaten auszuhalten.

EE 92 768 *für weitere Einzelheiten*

Digitaluhr

Racal Instruments Ltd. Western Road, Bracknell, Berkshire

(Abbildung Seite 264)

Racal Instruments Ltd stellt ein vielseitiges, volltransistorisiertes Digitaluhrsystem SA.7100 her. Diese als 24stündiger Tageszeitanzeiger oder für Anwendung in der Verfahrenstechnik und Datenerfassung entwickelte System gibt die Tageszeit in Ziffern als Stunden, Minuten und Sekunden in sechsstelliger Spalten- oder Zeilenanzeige und hat Einrichtungen zum Treiben eines Digital-Registriergerätes.

Verschiedene Ausführungen sind lieferbar. Die Genauigkeit des Typs SA. 7100A wird durch das 50-Hz-Netz bestimmt, während sie im Typ SA.7100C auf einen Präzisions-Quarzoszillator bezogen wird, der dem System eine Genauigkeit von besser als 2×10^{-9} je Tag gibt. Für Anwendungszwecke, die höhere Genauigkeit erfordern, kann ein externes Normal Verwendung finden.

Die Digitaluhr ist für Einbau in 19"-Standardgestelle und Betrieb in Umgebungstemperaturen von 0°C bis zu 45°C lieferbar. Vorgesehene Einrichtungen gestatten Synchronisieren der Anzeige in Stufen von 0,01, 0,1 und 1 s. Die Stromversorgung kann für 115 ... 230 V, 50 Hz oder 115 V, 400 Hz oder externe Batterien ausgelegt werden.

EE 92 769 *für weitere Einzelheiten*

Millivoltmeter

Marconi Instruments Ltd, St. Albans, Hertfordshire

(Abbildung Seite 264)

Das volltransistorisierte Instrument Typ TF2603 hat im Frequenzbereich 50 kHz ... 1,5 GHz einen direkten Messumfang von 300 μV ... 3V.

Der Messkopf hat 12,7 mm Durchmesser und enthält ein Paar schnelle Dioden in Zweiwegschaltung; bei Eingangssignalen unter 30 mV spricht er in fast echten Effektivwerten und im Bereich 0,5 ... 3 V in doppelten Spitzenwerten an. Durch die Zweiwegschaltung werden Fehler beim Messen von Signalspannungen mit komplexen Wellenformen verringert. Ein in den Messkopf eingebauter Heizer reduziert den Einfluss von Schwankungen in der Umgebungstemperatur.

Die leicht lesbare Skala des Messgerätes ist 127 mm lang und in Effektivwerten einer Sinuswellenform geeicht. Die Bestückung mit Halbleitern anstelle von Röhren ermöglicht Batteriebetrieb des Instruments anstelle des üblichen Netzanschlusses.

Ein Vorsteckteiler von 100:1 Typ TM7947 wird mitgeliefert und ermöglicht Spannungsmessungen von 30 mV...300 V im Frequenzbereich 500 kHz...500MHz. Die Eingangsimpedanz ist bedeutend höher als die, die ein mit heissen Dioden bestücktes Röhrenvoltmeter im selben Spannungs- und Frequenzbereich bieten kann. Als wahlweiser Zubehör kann ein koaxiales T-Zwischenstück für Spannungsmessungen an 50-Ω-Koaxialsystemen geliefert werden.

EE 92 770 *für weitere Einzelheiten*

Schutzkontaktrelais

Telefonbau und Normalzeit GmbH, 6 Frankfurt/Main 7, Mainzer Landstrasse, Deutschland

(*Abbildung Seite 264*)

Schutzkontaktrelais TN geben ausser allen Vorteilen der Zungenrelais noch 50 Prozent Raumersparnis.

Die patentierten Flachkontakte, die in ein mit Edelgas gefülltes flaches Glasgefäss eingeschmolzen sind, haben konstruktionseigene Anpassungsfähigkeit und Kontaktoberfläche, aus denen sich eine gleitende Betätigung mit schnellem Schliessen und Öffnen ergibt. Diese Relais sind vor allem für elektronische Schaltungen geeignet, in denen eine sehr zuverlässige, preiswerte und einfache Relaisfunktion erforderlich ist. Eigenschaften sind u.a. niedriger Kontaktwiderstand, hoher Isolationswiderstand, niedrige Kapazität, kurze Schaltzeit, Unempfindlichkeit gegen atmosphärische Einflüsse und lange Lebensdauer.

EE 92 771 *für weitere Einzelheiten*

Dekaden-Induktivitätskasten

Lionmount & Co. Ltd, Bellevue Road, New Southgate, London, N.11

(*Abbildung Seite 264*)

Der Induktivitätskasten Typ LD1 ist ein Vierdekaden-Instrument mit einer in 1-mH-Stufen erreichbaren Höchstinduktivität von 11,11 H. Die Genauigkeit ist bei 1 000 Hz 2 Prozent, aber der nutzbare Frequenzbereich liegt für die besten Q-Werte im Band 3 kHz ... 300 kHz.

Jede Dekade besteht aus einem Ferrittopfkern mit zehn Abgriffen; mit dieser Anordnung kann man eine langfristige Stabilität von 0,2 Prozent bei Q-Werten von 50 ... 200 erwarten.

Wie bei allen Spulen mit Magnetkern hängt auch hier die angelegte Spannung für eine gegebene Wicklung weitgehend von der Frequenz ab, und in diesen Instrumenten muss die Spannung auf einige hundert Millivolt begrenzt werden, um Sättigung des Kerns zu vermeiden.

Die Restinduktivität ist 1,6 μH; weitere Information über zusätzliche Induktion und Änderung von Q und Induktivität mit Frequenz wird noch bekanntgegeben.

Es werden durchweg keramische Scheibenschalter verwendet, und der Mahagoniekasten ist mit Abschirmmaterial ausgelegt.

EE 92 772 *für weitere Einzelheiten*

Modulares Gestell

Vero Electronics Ltd, South Mill Road, Regent's Park, Southampton

(*Abbildung Seite 265*)

Das neuste Erzeugnis der Vero Electronics Ltd ist ein 178 mm hohes, extra geräumiges, modulares Gestell, in dem die volle Höhe ausgenutzt wird und Veroboards mit 152,4 × 203,8 mm oder 152,4 × 279,4 mm Abmessungen untergebracht werden können. Das modulare Gestell passt in das Standard-19″-Gestell und kann Moduln von 279,4 oder 355 mm Tiefe aufnehmen. Modulare Frontplatten von 25,4 mm, 50,8 mm, 101,6 mm 203,8 mm Breite können Verwendung finden.

EE 92 773 *für weitere Einzelheiten*

Ätzmaschine

Lee-Smith Photomechanics Ltd, Lyon Way, Hatfield Road, St. Albans, Hertfordshire

(*Abbildung Seite 265*)

Eine neue, grössere Ausführung der Präzisions-Ätzmaschine Rota-Etch wurde von Lee-Smith Photomechanics Ltd angekündigt. Diese neuste Rota-Etch ist eine Weiterentwicklung der 23-cm-Maschine und mit einem runden Arbeitstisch ausgerüstet, auf den man Werkstücke mit einer höchsten Diagonalabmessung von 46 cm aufspannen kann.

Rota-Etch-Maschinen wurden besonders für das Präzisionsätzen von Standard-, Subminiatur- und Mikrodruckschaltungsplatten sowie die Fertigung von Aufdampfmasken und ähnlichen Erzeugnissen mittels chemischen Fräsens entwickelt.

Die zu ätzenden Werkstücke werden auf den runden Arbeitstisch im Klappdeckel der Wanne der Maschine gespannt. Während des Ätzens rotiert der Tisch mit konstanter Geschwindigkeit von 10 UPM, und die Ätzflüssigkeit wird durch drei umlaufende Zerstäubertrommeln aus geriffeltem Kunststoff nach oben gegen das Werkstück gespritzt. Auf diese Weise werden alle Teile des Werkstücks gleichmässig mit dem Ätzmittel getränkt.

Die Intensität des Ätzens lässt sich durch Änderung der Umlaufgeschwindigkeit der Zerstäubertrommeln regeln. Die Umlaufgeschwindigkeit der Trommeln ist von 0 ... 2 000 UPM kontinuierlich regelbar.

Zur Erzielung gleichbleibender Resultate ist Aufrechterhaltung einer konstanten Temperatur der Ätzlösung unbedingt erforderlich, und die Wanne ist für diesen Zweck mit Quarzheizelement und Kühlwasserröhren ausgerüstet. Die Ätzlösung wird kontinuierlich umgewälzt und kann bei jeder vorgewählten Temperatur im Bereich 10°C ... 54°C konstant gehalten werden.

Die Verfahrenszeit ist auf einer Schaltuhr einstellbar, und die Maschine wird nach Ablauf der gewählten Zeit automatisch ausgeschaltet.

Bei Anheben des Deckels schaltet ein Schutzschalter automatisch die elektrische Stromversorgung ab.

EE 92 774 *für weitere Einzelheiten*

Linearitätstester für Bauelemente

Vertrieb: Livingston Laboratories Ltd, Greycaines Estate, Bushey Mill Lane, North Watford, Hertfordshire

(*Abbildung Seite 265*)

Es wurde festgestellt, dass zwischen der Zuverläsigkeit von Kondensatoren und Widerständen und ihrer Linearität eine Beziehung besteht. Radiometer, Kopenhagen, hat jetzt ein Instrument eingeführt, das diese Technik für eine Zuverläsigkeitsanzeige von Bauelementen auswertet.

Der Linearitätstester für Bauelemente Modell CLT1 ist in Grossbritannien von Livingston Laboratories zu beziehen. Er misst die dritten Harmonischen der Spannungen, die durch die Nichtlinearität der Bauelemente erzeugt werden und kann bis zu 20 Bauelemente je Sekunde mit Impedanzen von 1 Ω ... 100 MΩ prüfen.

Ein interner Oszillator erzeugt eine sehr reine Grundfrequenz von 10 kHz mit bis zu 560 V Amplitude und Unterdrückung der dritten Harmonischen von 180 dB. Die dritte Harmonische von 30 kHz, die als Resultat der Nichtlinearität des Bauelement-Prüflings entsteht, wird auf einem Messgerät angezeigt, das Signalpegel bis zu −160 dB herunter nachweisen kann.

Messgeräte sind mit linearer oder logarithmischer Skala und 60-dB-Bereich für schnelle Fertigungskontrolle lieferbar.

EE 92 775 *für weitere Einzelheiten*

Solarzellen

The Plessey Co. Ltd, Dielectric and Magnetic Division, Towcester, Northamptonshire

(*Abbildung Seite 265*)

Silizium - Sperrschicht - Fotozellen in integrierter Batterieanordnung zur Umwandlung von Sonnenenergie auf Bodenhöhe in Stromversorgungen wurden von der Dielektrischen und Magnetischen Abteilung der Plessey-Bauelemente-Gruppe angekündigt.

Die Zellenfelder stellen eine hochzuverlässige Stromversorgung langer Lebensdauer dar, die Minimumwartung erfordert, und sind daher besonders für schwer zugängliche Installationen geeignet. Umfangreiche Erhebungen über die durchschnittliche Jahresinsolation (auffallende Sonnenenergie) in der ganzen Welt liegen nunmehr vor, und praktische Versuche haben Daten für Feldkonstruktionen für die verschiedensten erforderlichen Stromversorgungen ergeben.

Zur Aufrechterhaltung kontinuierlicher Leistungsabgabe sind die Zellenfelder so ausgelegt, dass sie Nickel-Kadmium-Akkumulatoren laden. Ein Spannungsregler verhindert das Erreichen des Dissoziationspotentials der Batterie, reduziert die elektrolytischen Verluste und damit die Wartungserfordernisse auf ein Minimum. Nunmehr lieferbare Einzelzellenfelder von ca. 930 cm^2 können in günstiger Lage Batteriespeisung von bis zu 50 mA bei 12 V für unbegrenzte Zeit aufrechterhalten. Selbst in heissen Klimas ist Wartung wahrscheinlich nur einmal alle vier bis fünf Jahre erforderlich.

Durch Zusammenschalten mehrerer Felder lassen sich höhere Stromstärken oder Spannungen erreichen.

Korrosion wird durch Vergiessen der Zellen in Epoxydharz unter einer Glasscheibe, die gegen windgetragenen Sand besonders abriebbeständig ist, verhindert. Diese Konstruktion gibt den Feldern fast unbegrenzte Lebensdauer, wodurch eine wesentlich zuverlässigere und langlebigere Stromversorgung als von der gespeisten Ausrüstung erwartet werden kann.

Anwendungsmöglichkeiten bestehen u.a. im Nachrichtenverkehr sowie meteorologischen oder navigatorischen Ausrüstungen in abgelegenen Gegenden. Theoretisch kann jeder Leistungsforderung genügt werden, praktische Überlegungen ergeben jedoch optimalen Einsatz für Dauerabgabe von 10 W.

EE 92 776 *für weitere Einzelheiten*

Zusammenfassung der wichtigsten Beiträge

Phasenfehlerkorrektur einer PAL-Farbfernsehübertragung von W. Bruch

Zusammenfassung des Beitrages auf Seite 212-217

Der Beitrag beschreibt ein neues Verfahren zur Korrektur von Fehlern in einem PAL-Farbfernsehsignal. Das Farbbild-Austast-Synchron-Signal wird durch eine Farbphasenlagenkorrektur ergänzt, die die unerwünschte Phasenmodulation ausgleicht. Die Kompensationsspannung wird von der Differenz zwischen zwei Farbsignalen abgeleitet; eins der Signale erhält man durch den direkten Kanal und das andere durch eine "Farbträger-Umsteuergrösse" in Kombination mit einer Verzögerungseinrichtung. Zusätzliche Amplitudenkorrektur beseitigt den resultierenden Kosinusfehler. Die gewählte Kompensationsform hat auf das Luminanzsignal keinen Einfluss.

Erzielung eines hohen Gesamtunterdrückungsfaktors in Differenzverstärkern von S. Salmons

Zusammenfassung des Beitrages auf Seite 218-221

Die Leistung eines symmetrischen Differenzverstärkers wird durch Abweichungen von der Symmetrie beeinträchtigt, besonders wenn sie durch nicht übereinstimmende Kennlinien eines Röhrenpaares hervorgerufen werden. In dem Beitrag wird eine Eingangsstufe beschrieben, in der diese Schwierigkeit überkommen wird, ohne dass Röhren in Spezialqualität oder ausgesuchte Bauelemente erforderlich sind. Mit einer einfachen Kompensationsregelung können Unterdrückungsfaktoren von über 300 000 erreicht werden. Diese Regelung kann ausserdem auch die Wirkung von Unsymmetrie an anderen Stellen des Verstärkers ausgleichen und eine entsprechende Verbesserung der gesamten Unterdrückung erreichen.

Der Entwurf von Eingangsschaltungen für rauscharme Transistor-ZF-Verstärker von R. H. Frater

Zusammenfassung des Beitrages auf Seite 222-229

In diesem Beitrag wird das Entwurfsverfahren für ein Eingangsnetzwerk für einen Transistorverstärker beschrieben, der gleichzeitig den Anforderungen nach maximaler Bandbreite, optimaler Quellenimpedanz für geringes Rauschen, und Phasen- sowie Amplitudengang, die für eine Anzahl von Verstärkern stark miteinander übereinstimmen, genügt. Das Verfahren berücksichtigt die breite Streuung der Transistor-Eingangsimpedanz. Mit der Kopplungsschaltung einer 408-MHz-Mischstufe zu einem 11-MHz-Verstärker erzielte Ergebnisse werden gegeben. Die Methode umfasst ein Entwurfsverfahren für eine Zweikreisschaltung beliebiger Bandbreite, in dem die Pole der Übertragungsfunktion gleiche Hinterglieder haben.

Kritische Induktivität für halbgesteuerte Thyristor-Gleichrichter von J. L. Storr-Best

Zusammenfassung des Beitrages auf Seite 230-233

Dieser Beitrag analysiert die kritischen Induktivitätsanforderungen von Filtern mit Drosseleingang für "halbgesteuerte" Ein- und Dreiphasen-Thyristorgleichrichter, in denen nur eine Hälfte der Elemente aus Thyristoren besteht, die andere aus einfachen Dioden. Die wichtigsten Unterschiede zwischen diesen Ergebnissen und den bekannteren der vollgesteuerten Gleichrichter werden besprochen. In einer Tabelle werden die Werte für das Verhältnis Thyristor-Spitzenstrom zu Ausgangsgleichstrom für die verschiedenen Zündwinkel bei kritischer Induktivität gegeben. Auch für den Spitzen- und Mittelwertstrom in der Nebenwegdiode werden in bezug auf den Ausgangsgleichstrom bei verschiedenen Zündwinkeln Kurven gegeben.

Ein Lochkarten-Lochstreifen-Umsetzer für indirekte Bearbeitung von D. W. W. Rogers

Zusammenfassung des Beitrages auf Seite 234-241

Dieser Beitrag behandelt den Entwurf eines Lochkarten-Lochstreifen-Umsetzers. Ein kommerzieller Lochkartenleser mit einer Kapazität von 22 Karten je Minute überträgt die in zwölf Löchern der Lochkarte gespeicherte Information über geeignete logische Netzwerke in einen Zwischenspeicher. Die in diesem Zwischenspeicher gehaltene Information wird mittels eines Streifenlochers Teletype 110 auf einen 8-Kanal-Lochstreifen übertragen. Eigenanpassungsfähigkeit wird der Ausrüstung durch ein dem Zwischenspeicher vorgeschaltetes 64-Zeichen-Rangierfeld gegeben, das Neuordnung der Information, Auslassungen und Einfügungen auf dem Lochstreifen gestattet. Durch Anwendung direktgekoppelter Widerstandslogik, einfache Schaltungen und sparsame Bauelementverwendung wird hohe Zuverlässigkeit erzeugt. Selbstkontrollierende Fehlererkennung für die Lochkarten und eine geradzahlige Paritätskontrolle KDF9 sind in das logische Netzwerk eingebaut. Es werden durchgehend Halbleiter angewendet.

Zusammengesetzte Kenndaten seriengeschalteter Tunneldioden von J. B. Earnshaw und Z. C. Tan

Zusammenfassung des Beitrages auf Seite 242-245

Zwei Verfahren zur Ableitung zusammengesetzter Kenndaten von Ketten seriengeschalteter Tunneldioden werden beschrieben. Einer kritischen Untersuchung dieser Eigenschaften folgt eine Stellungnahme zu Schaltungen mit Tunneldiodenketten.

Eine Präzisions-Diodentorschaltung für Analogrechner von F. Fallside und N. Thedchanamoorthy

Zusammenfassung des Beitrages auf Seite 246-250

In Analogrechnern, die mit mittelmässigen oder hohen Folgefrequenzen arbeiten, werden Halbleiterdioden-Torschaltungen in umfangreichem Masse für die Steuerung von Verstärkern eingesetzt, die als Integratoren betrieben werden. Wegen ihrer Empfindlichkeit auf Hochspannungsschwankungen sind sie für sehr langsames Rechnen weniger geeignet, und Relais werden oft vorgezogen. Eine beschriebene neue Torschaltung ist gegenüber Hochspannungsschwankungen sehr unempfindlich. Ausserdem wird eine sehr einfache, aber genaue Analyse der Übertragungsfunktion torgesteuerter Integratoren durchgeführt, die mit den Experimenten gut übereinstimmt.

Ein elektromechanischer Verdrehungstreiber mit elektrisch regelbarer Beharrungskraft von J. G. Thomas und V. Zakian

Zusammenfassung des Beitrages auf Seite 251-253

Ein elektromechanischer Verdrehungstreiber und die zugehörigen elektronischen Einrichtungen werden beschrieben. Der Treiber hat einen Winkeldurchlaufbereich von über 100° und kann ein maximales Drehmoment von 14, 1×10^4 Dyn·cm abgeben. Die Trägheit der beweglichen Teile ist 7 g·cm² und kann durch Anwendung einer elektronischen Rückführungsschaltung effektiv auf Null reduziert werden.